Regulation of ornibactin synthesis and utilisation in *Burkholderia cenocepacia*.

Kirsty Agnoli

Thesis submitted for the degree
of Doctor of Philosophy

Department of Medicine

May, 2007

Acknowledgements

Firstly, I would like to thank my supervisor, Dr. Mark Thomas, for his time, support and patience over the last few years.

Thanks also to Dr. Jon Shaw and Professor Jon Sayers, for all their help throughout this work, and to the MRC for funding my project.

I am especially grateful to Matt and Seed, who have prevented me from wasting away whilst writing this and helped me with my reference list and abbreviations, but most importantly have been the best friends a girl could have.

I would also like to thank Dr. Imran, who has taught me many things, including how to do a mean β-gal, and everyone from the lab, past and present, especially Michaela, Tomble, Dave, Mike, Penny, Sravanthi, Sarb, Anne, Guta and Eddie, for making work days a pleasure. Also, many thanks to 'Tea-Break' Matt, for the beautiful transporter images.

Thanks to my MS Word support crew, Matt A. and Eddie S., for copious help in formatting this thesis.

Finally, I am indebted to my parents, for their constant support and encouragement throughout my lengthy education.

Summary

Production of the siderophore ornibactin increases the virulence of the opportunistic pathogen *Burkholderia cenocepacia*. Siderophores are iron-scavenging molecules important for bacterial colonisation of iron-limited environments, such as within the human host. Ornibactin production and utilisation is specified by a cluster of 15 genes. The product of one of these genes, *orbS*, exhibits strong homology to an ECF σ factor of *Pseudomonas aeruginosa*, PvdS, which specifies the transcription of the pyoverdine siderophore biosynthesis and utilisation genes.

Three putative OrbS-dependent promoters were identified within the ornibactin gene cluster by homology to the PvdS-dependent promoter consensus sequence. Two candidate σ^{70}-dependent promoters were identified upstream of *orbS* itself. A combination of reverse-transcriptase PCR, ribonuclease protection assays, primer extension and reporter gene analysis demonstrated that the ornibactin gene cluster consists of four transcriptional units, allowed identification of the functional *orbS* promoter, and confirmed the status of the three putative OrbS-dependent promoters. Reporter gene analysis of these promoters, in the presence and absence of functional *orbS*, showed that OrbS is required for the iron-regulated activity of the three putative OrbS-dependent promoters, but not for its own activity.

Iron-regulation of the ornibactin gene cluster was found to be mediated by regulation of *orbS* transcription by Fur. Evidence was obtained suggesting that OrbS activity is also directly regulated by iron availability. The translational initiation codon of *orbS* was determined, and OrbS was found to possess a 29 bp N-terminal extension relative to PvdS. This extension was essential for full activity of OrbS, although its function remains unclear.

The sequence requirements for efficient promoter utilisation by OrbS were investigated, and compared to those of PvdS, leading to the identification of key differences between these apparently similar promoters. The precise -35 and -10 elements required for recognition by OrbS and PvdS were also established

Table of Contents

Abbreviations **8**
Chapter 1: Introduction **10**
1.1: The taxonomy of the *Burkholderia cepacia* complex 11
1.2: The Bcc as phytopathogens and biocontrol agents 14
1.3: The Bcc as pathogens of humans 15
1.3.1: Implications of the Bcc for chronic granulomatous disease patients 15
1.3.2: Bcc infection of cystic fibrosis patients 17
1.3.3: Virulence determinants of the Bcc 19
1.4: The importance of iron for bacterial growth 26
1.4.1: Iron acquisition using siderophores 27
1.5: Siderophores of the Bcc 28
1.5.1: The structure and iron-binding stoichiometry of the Bcc siderophores 28
1.6: Work leading up to this study 35
1.6.1: Isolation of ornibactin-negative mutants of *B. cenocepacia* 35
1.6.2: Identification of genes involved in ornibactin biosynthesis and transport in *B. cenocepacia* 35
1.7: RNA polymerase and σ factors 38
1.7.1: The RNAP core enzyme 38
1.7.2: The σ subunit 40
1.7.3: Transcription in bacteria 44
1.8: Siderophore-mediated transport systems 45
1.8.1: Outer membrane siderophore receptors 45
1.8.2: ATP-binding cassette transporters 50
1.9: The role of the ferric uptake regulator in iron homeostasis 52
1.10: The ornibactin operon 55
1.10.1: Ornibactin synthesis 55
1.10.2: Ornibactin transport 59
1.11: The siderophore malleobactin of *Burkholderia pseudomallei* 62
1.12: Main aims of this study 65
Chapter 2: Materials and Methods **66**
2.1: Bacteriological techniques 73
2.1.1: Bacteriological media 73
2.1.2: Media supplements 75
2.1.3: Agar plate-based phenotypic tests 78
2.1.4: Determination of bacterial growth rate 78
2.1.5: Techniques for plasmid transfer 79
2.1.6: Maintenance of bacterial strains 82
2.2: Techniques for DNA purification and analysis 82
2.2.1: PCR techniques 82
2.2.2: DNA preparation and manipulation techniques 86
2.3: Techniques for the preparation and analysis of RNA 92
2.3.1: RNA purification techniques 92
2.3.2: RNA analysis techniques 93
2.4: Protein purification and enzyme assays 100
2.4.1: Enzyme assays 100
2.4.2: Protein purification techniques 102

Chapter 3: The effect of siderophore deficiency on growth of *B. cenocepacia*....106
3.1: Introduction....107
3.1.1: Objectives....109
3.2: The ability of *B. cenocepacia* strains to grow on solid media containing EDDHA....110
3.3: Growth rates of *B. cenocepacia* 715j and siderophore deficient derivatives in response to iron availability....112
3.3.1: Determination of a suitable concentration of 2'2-dipyridyl to induce iron limited conditions....112
3.3.2: Analysis of the effect of iron limitation and sufficiency on growth rate..112
3.4: Discussion....116
Chapter 4: Construction of *lacZ* reporter vectors for use in *Burkholderia* spp..118
4.1: Introduction....119
4.1.1: Objectives....121
4.2: Construction and analysis of improved pRW50 derivatives....122
4.3: Construction and analysis of pTZ110 derivatives....129
4.4: Construction and analysis of pPR9TT derivatives....133
4.5: Discussion....141
Chapter 5: Organisation and regulation of the ornibactin gene cluster....142
5.1: Introduction....143
5.1.1: Objectives....145
5.2: Investigation of the transcriptional organisation of the ornibactin gene cluster....146
5.2.1: Analysis of ornibactin gene transcripts by RT-PCR....146
5.2.2: Analysis of ornibactin gene transcription by RNAse protection assay....150
5.3: Localisation and regulation of the ornibactin gene cluster promoters....154
5.4: Deletion analysis of the *orbS* promoter....159
5.5: Location of the transcription start sites of the ornibactin gene promoters....167
5.6: Discussion....172
Chapter 6: Determination of the DNA sequence requirements for promoter utilisation by OrbS....175
6.1: Introduction....176
6.1.1: Objectives....180
6.2: Investigation of the utilisation of OrbS- and PvdS-dependent promoters by PvdS and OrbS, respectively....181
6.2.1: Construction of pKAGd4-ppvdEfl and pKAGd4-ppvdFfl....181
6.2.2: Analysis of *pvdE* and *pvdF* promoter activity in *P. aeruginosa*....181
6.2.3: Activity of the *orbH* promoter in *P. aeruginosa*....184
6.2.4: Activities of the *pvdE* and *pvdF* promoters in *B. cenocepacia*....184
6.3: Investigation of the ability of OrbS and PvdS to functionally substitute for one another in *P. aeruginosa* and *B. cenocepacia*, respectively....186
6.3.1: Construction of *orbS* and *pvdS* expression plasmids....186
6.3.2: Activity of PvdS in *B. cenocepacia*....190
6.3.3: Activity of OrbS in *P. aeruginosa*....191
6.4: Analysis of DNA sequence requirements for promoter recognition by OrbS and PvdS....192
6.4.1: Construction of *porbH-lacZ* fusion plasmids....192
6.4.2: Determination of a 'minimal' *orbH* promoter for utilisation by OrbS and PvdS....193
6.4.3: Investigation of low *porbHfl* activity in *E. coli*....199

6.4.4: Investigation of the promoter sequence requirements of OrbS by construction of *orbH-pvdE* hybrid promoters 199
6.4.5: Investigation of OrbS and PvdS promoter recognition by single base substitution analysis of the *orbH* promoter 203
6.4.6: Investigation of the role of the G+C-rich spacer block and the A+G-rich block in promoter utilisation by OrbS and PvdS 206
6.4.7: Investigation of the role of the extended A+T tract in promoter utilisation by OrbS and PvdS 210
6.5: Bioinformatic analysis of the OrbS regulon 215
6.6: Discussion 221
Chapter 7: Investigation of the mechanisms of iron-dependent regulation of the ornibactin gene cluster 228
7.1: Introduction 229
7.1.1: Objectives 230
7.2: Investigation of the transcriptional regulation of *orbS* 231
7.2.1: Iron-dependent regulation of *porbS* in *E. coli* 231
7.2.2: Investigation of the role of Fur in the regulation of *porbS* 231
7.2.3: Determination of the location of the Fur binding site at *porbS* by FURTA 237
7.2.4: Analysis of Fur binding to *porbS* by EMSA 240
7.3: Investigation of possible mechanisms for the modulation of OrbS activity 244
7.3.1: Construction of a constitutive *orbS* expression vector 244
7.3.2: Investigation of the role of the C-terminal cysteines of OrbS in iron-dependent regulation of OrbS activity 250
7.3.3: Investigation of iron-dependent regulation by OrbS in the absence of Fur 256
7.3.4: Development of a system for purification of OrbS 261
7.4: Investigation of the N-terminal region of OrbS 269
7.4.1: Identification of the *orbS* translation initiation codon 269
7.4.2: Investigation of the importance of the N-terminal extension of OrbS 274
7.4.3: Detection of OrbSΔX activity using an *orbH-lacZ* fusion. 277
7.5: Discussion 279
Chapter 8: Final discussion and future directions 284
8.1: Final discussion 285
8.2: Future directions 288
References 290
Appendix: Primers used in this study 301

List of Figures

Figure 1.1: Scanning electron micrograph showing *B. vietnamiensis*, a member of the Bcc....12
Figure 1.2: An onion bulb infected with *Burkholderia cepacia*....12
Figure 1.3: Taxonomy of the Bcc....13
Figure 1.4: X-ray image showing the chest of a 12 year old boy suffering from CGD and infected with *B. vietnamiensis*....16
Figure 1.5: Transmission electron micrograph showing the cable-pilus produced by the B. cenocepacia ET-12 lineage....20
Figure 1.6: The structure of cepabactin....30
Figure 1.7: The structure of cepaciachelin....30
Figure 1.8: The structure of pyochelin....32
Figure 1.9: The structure of ornibactin....34
Figure 1.10: Identification of *B. cenocepacia* ornibactin-negative mutants....36
Figure 1.11: Locations of transposon insertions within the *B. cenocepacia* ornibactin gene cluster....37
Figure 1.12: Alignment of PvdS and OrbS....39
Figure 1.13: Structure of the *E. coli* $E\sigma^{70}$ holoenzyme....41
Figure 1.14: Alignment of *E. coli* RpoD (σ^{70}) with 4 known ECF σ factors and the putative ECF σ factor, OrbS....43
Figure 1.15: Mechanism of ferric citrate transport....46
Figure 1.16: The crystal structure of unloaded FecA....47
Figure 1.17: The structure of the $ModB_2C_2A$ ABC transporter....53
Figure 1.18: General mechanism of repression by Fur....54
Figure 1.19: The amino acids of ornibactin and the putative mechanisms for their derivatisation....57
Figure 1.20: Model for the non-ribosomal synthesis of ornibactin....58
Figure 1.21: Alignment of the N-terminal regions of TonB-dependent receptors....61
Figure 1.22: Model for ornibactin transport in *B. cenocepacia*....63
Figure 1.23: Aligment of OrbS and MbaS....64
Figure 3.1: The structure of EDDHA....108
Figure 3.2: The structure of 2'2-dipyridyl....108
Figure 3.3: Growth of *B. cenocepacia* strains on media with and without EDDHA..111
Figure 3.4: Cross-feeding of ornibactin between 715j and ornibactin-negative derivatives....111
Figure 3.5: Growth curves for 715j and siderophore-deficient strains under iron limited and iron replete conditions....113
Figure 3.6: Growth curves for siderophore-deficient strains of *B. cenocepacia* supplied with *orbS in trans*....115
Figure 4.1: Scheme for construction of pKAGc1 and pKAGc2....123
Figure 4.2: General scheme for the construction of pKAGc1-pbfd, pKAGc2-pbfd and pRW50-pbfd....126
Figure 4.3: Activities of pRW50 derivatives bearing a test promoter fragment....127
Figure 4.4: General scheme for the construction of pKAGb1(+) and pKAGb1(-)....130
Figure 4.5: General scheme for the construction of pKAGb2(+) and pKAGb2(-)....131
Figure 4.6: General scheme for the construction of pKAGd2....134

Figure 4.7: β-galactosidase activities specified by the *tac* promoter cloned into pKAGd2 and pKAGd4.....135
Figure 4.8: General scheme for the construction of pKAGd4.....137
Figure 4.9: Growth medium iron concentration does not affect the activity of non iron-dependently regulated promoters cloned into pKAGd4.....139
Figure 5.1: Putative promoter sequences for *orbS*.....144
Figure 5.2: Putative OrbS-dependent promoters identified *in silico*.....144
Figure 5.3: RT-PCR analysis of the ornibactin gene cluster.....148
Figure 5.4: Transcriptional organisation of the *B. cenocepacia* ornibactin gene cluster.....149
Figure 5.5: RPA analysis of the organisation of the ornibactin gene cluster.....153
Figure 5.6: Scheme for cloning DNA fragments bearing ornibactin gene promoters into pBluescript II KS.....155
Figure 5.7: Scheme for cloning the ornibactin gene cluster promoter fragments into pKAGd4.....156
Figure 5.8: Ornibactin gene promoter activity in response to iron availability and the presence or absence of functional *orbS*.....157
Figure 5.9: Deletion analysis of the *orbS* promoter region.....160
Figure 5.10: Scheme for the construction of pBBR-orbS-69 and pBBR-orbS-40.....161
Figure 5.11: CAS plate analysis of *B. cenocepacia* OM3 containing pBBR1MCS derivatives bearing *orbS* with different upstream endpoints.....162
Figure 5.12: Scheme for the construction of *porbS-lacZ* fusion plasmids.....164
Figure 5.13: Localisation of the *orbS* promoter.....165
Figure 5.14: Determination of the transcription start sites for of *orbS, orbI* and *orbH* by primer extension.....169
Figure 5.15: Transcription start sites of the *orbS* and the OrbS-dependent promoters.....170
Figure 6.1: Alignment of the OrbS, MbaS and PvdS-dependent promoters.....177
Figure 6.2: Alignment of the PvdS-dependent promoters of the *pvd* gene clusters....179
Figure 6.3: General scheme for construction of pKAGd4-ppvdEfl and pKAGd4-ppvdFfl.....182
Figure 6.4: Promoter activity in response to OrbS and PvdS.....183
Figure 6.5: Scheme for the construction of pBBR-2-pvdS.....187
Figure 6.6: Scheme for the construction of pBBR-2-orbS.....188
Figure 6.7: OrbS and PvdS activity in *B. cenocepacia* and *P. aeruginosa*.....189
Figure 6.8: General scheme for insertion of double-stranded oligonucleotides containing *porbH* and *ppvdE* promoter derivatives into pKAGd4.....194
Figure 6.9: Promoter deletion derivatives for the determination of a minimal *orbH* promoter.....195
Figure 6.10: Activities of *orbH* promoter deletion derivatives in *E. coli*.....197
Figure 6.11: Activity of *orbH* promoter deletion derivatives in *B. cenocepacia* and *P. aeruginosa*.....197
Figure 6.12: Role of downstream sequences in inhibition of *porbHfl* activity in *E. coli*.....200
Figure 6.13: *ppvdE-porbH* hybrid promoters constructed to determine the contribution of four conserved regions of *porbH* to OrbS promoter specificity.....202
Figure 6.14: Activities of *ppvdE-porbH* hybrid promoters.....202
Figure 6.15. Effects of single-base substitutions on the activity of the *orbH* promoter.....204

Figure 6.16: Sequences of *orbH* promoter derivatives altered in the A+G-rich block 207
Figure 6.17: Activities of *orbH* promoter derivatives with substitutions within the A+G-rich block. 208
Figure 6.18: Promoter derivatives constructed to test the importance of the length of the -35 region extended A+T tract. 212
Figure 6.19: Activities of *orbH* promoter derivatives with substitutions within the extended A+T-tract. 212
Figure 6.20: Alignment of the candidate promoters of the OrbS regulon 216
Figure 6.21: Localities of putative promoters of the OrbS regulon found on chromosome 1 218
Figure 6.22: Localities of putative promoters of the OrbS regulon found on chromosomes 2 and 3 219
Figure 6.23: Alignment of PvdS-dependent promoters 226
Figure 7.1: Activity of *porbS* and the OrbS-dependent promoters in *E. coli* 232
Figure 7.2: Scheme for the construction of pKAGd4ΔAp 234
Figure 7.3: Scheme for the construction of pKAGd4ΔAp-porbSfl 235
Figure 7.4: Activity of the *orbS* promoter is dependent on Fur. 236
Figure 7.5: The Fur titration assay (FURTA). 238
Figure 7.6: Analysis of promoters for the presence of Fur binding sites using the Fur titration assay 239
Figure 7.7: Scheme for the construction of pBluescript II KS derivatives containing *porbS* fragments with different upstream endpoints. 241
Figure 7.8: EMSA analysis of Fur binding to *porbS* and OrbS-dependent promoters. 242
Figure 7.9: Amino acid sequence alignment of PvdS and OrbS. 245
Figure 7.10: The structure of cysteine and the geometry of iron co-ordination by cysteine thiols. 245
Figure 7.11: Proposed model for iron-dependent regulation of ornibactin synthesis .246
Figure 7.12: Scheme for the construction of pBBR-orbSΔP2. 248
Figure 7.13: pBBR-orbSΔP2 fails to complement OM3 for ornibactin production ...249
Figure 7.14: Scheme for the construction of pBBR-orbSΔP-ptac. 251
Figure 7.15: pBBR-orbSΔP-ptac fails to complement OM3 for ornibactin production. 252
Figure 7.16: Analysis of ornibactin production by OM3 following introduction of plasmids containing cysteine-alanine codon substitutions. 253
Figure 7.17: Scheme for the construction of alanine for cysteine substitution plasmids by SOE. 255
Figure 7.18: Scheme for the construction of pBBR-5-orbS and pBBR-5-orbSCtetraA. 258
Figure 7.19: Scheme for the construction of pBBR-5-pvdS 259
Figure 7.20: Iron-dependent regulation of *porbH* by OrbS in the absence of Fur. 260
Figure 7.21: The construction of pET-orbS 262
Figure 7.22: The construction of pGEX-orbS 263
Figure 7.23: Polyacrylamide gel electrophoretic analysis of OrbS overexproduction. 265
Figure 7.24: The construction of pGEX-orbSNT and pGEX-orbSCT 267
Figure 7.25: Polyacrylamide gel electrophoretic analysis of OrbS C-terminal and N-terminal fragment overexpression. *E. coli* BL21λDE3 cells containing pGEX-orbSCT or pGEX-orbSNT were grown 268

Figure 7.26: The *orbS* coding sequence. 270
Figure 7.27: Scheme for the construction of pBBR-orbS bearing mutations within the possible *orbS* translation initiation codons....272
Figure 7.28: identification of the *orbS* translational initiation codon. 273
Figure 7.29: Scheme for the construction of pBBR-orbSΔX....275
Figure 7.30: The N-terminal amino acid sequence of OrbSΔX. 276
Figure 7.31: pBBR-orbSΔX fails to complement OM3 for ornibactin production 276
Figure 7.32: Detection of OrbSΔX-dependent transcriptional activity in *E. coli*. 278
Figure 7.33: Location of the Fur box at the *orbS* promoter region of *B. cenocepacia* 715j....280
Figure 7.34: Iron-sulphur clusters involving four cysteines 282

List of Tables

Table 2.1: Bacterial Strains used in this study 67
Table 2.2: Plasmids used in this study 68
Table 2.3: Final concentration of media supplements 77
Table 3.1: Growth rates of 715j and derivative strains 113
Table 3.2: Growth rates of siderophore-deficient strains of *B. cenocepacia* supplied with *orbS in trans*. 115
Table 4.1: β-galactosidase activities specified by novel *lacZ* fusion vectors 124
Table 4.2: Activities of pRW50 derivatives bearing a test promoter fragment 127
Table 5.1: Primer pairs used for RT-PCR analysis 147
Table 5.2: Primers used to construct probes for RPA, and resultant probe sizes. 151
Table 6.1: Activity of *porbH* promoter derivatives bearing substitutions in the G+C-rich spacer block....207
Table 6.2: Activity of *pvdE* promoter derivatives bearing substitutions in the extended A+T tract region. 214
Appendix: Primers used in this study....302

Abbreviations

ABC	ATP-binding cassette
AFLP	Amplified fragment length polymorphism
AHL	Acyl homoserine lactone
Ap	Ampicillin
ATP	Adenosine triphosphate
Bcc	*Burkholderia cepacia* complex
BCESM	*Burkholderia cepacia* epidemic strain marker
BHI	Brain-heart infusion medium
BHR	Broad host range
cAMP	Cyclic adenosine monophosphate
CAS	Chrome-azurol sulphonate
CF	Cystic fibrosis
CFTR	Cystic fibrosis transmembrane conductance regulator
CGD	Chronic granulomatous disease
CIP	Calf intestinal alkaline phosphatase
Cm	Chloramphenicol
CODP	Candidate OrbS-dependent promoter
CRP	cAMP receptor protein
CTD	C-terminal domain
DMF	Dimethylformamide
DMSO	Dimethylsulphoxide
ds	Double stranded
ECF	Extracytoplasmic function
EDDHA	ethylenediaminedi(o-hydroxyphenylacetic) acid
EDTA	ethylenediamine tetraacetic acid
EMSA	Electromobility shift assay
EPS	exopolysaccharide
$E\sigma^{OrbS}$	RNA polymerase holoenzyme with OrbS σ factor
$E\sigma^{PvdS}$	RNA polymerase holoenzyme with PvdS σ factor
FURTA	Fur titration assay
Gm	Gentamycin
HNP	Human neutrophil peptide
IM	Inner membrane
IPTG	Isopropyl β-D-thiogalactoside
IRR	Iron responsive regulator
IS	Insertion sequence
Km	Kanamycin
LB	Luria-Bertani
LPS	lipopolysaccharide
MCS	Multiple cloning site
MOPS	3-(N-morpholino)propanesulphonic acid
Mu	Miller units
NMR	Nuclear magnetic resonance
NRPS	Non-ribosomal peptide synthetase
NT	Not tested

NTD	N-terminal domain
NTP	Nucleoside triphosphate
OD	Optical density
OM	Outer membrane
Orb^-	Ornibactin negative phenotype
ORF	Open reading frame
PAGE	Polyacrylamide gel electrophoresis
Pch^-	Pyochelin negative phenotype
PCR	Polymerase chain reaction
PIC	Putative initiation codon
PMF	Proton motive force
Pvd^-	Pyoverdine negative phenotype
QS	Quorum sensing
RACE	Rapid amplification of cDNA ends
RAPD	Random amplified polymorphic DNA
RBS	Ribosome binding site
Rf	Rifampicin
RPA	Ribonuclease protection assay
RT-PCR	Reverse-transcription PCR
SDS	Sodium dodecyl sulphate
Sm	Streptomycin
SOE	Synthesis by overlap extension
ss	Single stranded
Tc	Tetracycline
TEMED	Tetramethylethylenediamine
TNF	Tumour necrosis factor
Tp	Trimethoprim
TSS	Transcriptional start site
UTP	Uridine triphosphate
X-gal	5-bromo-4-chloro-3-indolyl-β-D-galactoside

Chapter 1

Introduction

1.1: The taxonomy of the *Burkholderia cepacia* complex

Burkholderia cenocepacia cells are Gram-negative motile rods, 1-2 μm in length and 0.6-0.9 μm wide (Vandamme *et al.*, 2003). *Burkholderia cenocepacia* is a member of a complex of closely related bacterial species known as the *Burkholderia cepacia* Complex (Bcc). The first isolate of the Bcc was identified as the organism responsible for causing 'sour skin' in onion bulbs (Figures 1.1 and 1.2). The name *Pseudomonas cepacia* was proposed, although it was noted that the new species differed from the plant pathogens of the genus *Pseudomonas*, having a higher maximum growth temperature (42°C), and also being capable of metabolising a broader range of substrates (Burkholder, 1950). The genus *Burkholderia* was subsequently proposed to house a number of related bacteria that were originally classified as *Pseudomonas spp.*, but were later found to have distinct differences in their 16 S ribosomal RNA sequences from the pseudomonads *sensu stricto* (Yabuuchi *et al.*, 1992). The newly named genus *Burkholderia* was assigned to the β subdivision of the proteobacteria by 16 S rRNA typing, whereas the true pseudomonads fall within the γ proteobacteria (Coenye *et al.*, 2001). Isolates previously defined as *Burkholderia cepacia* were later found to constitute a number of phenotypically similar, but genotypically distinct, genomovars, and these were collectively referred to as the Bcc. These genomovars were reclassified as species upon determination of suitable phenotypic tests to distinguish them (Coenye *et al.*, 2001; Vandamme *et al.*, 2003). The Bcc currently comprises 10 distinct bacterial species (Figure 1.3). Bcc members share a high degree of similarity, including 98 %-99 % 16 S rRNA identity (Coenye *et al.*, 2001). *Burkholderia cenocepacia* was previously classified as *Burkholderia cepacia* genomovar III, and can be distinguished amongst other Bcc isolates using a polyphasic approach in which several tests, including amplified fragment length polymorphism (AFLP) analysis and rRNA typing, are carried out (Vandamme *et al.*, 2003). The original isolate described by Burkholder was assigned the name *B. cepacia*.

Members of the Bcc are found throughout the environment, especially within the rhizosphere. The Bcc species *B. cepacia*, *B. cenocepacia* and *B. vietnamiensis* are capable of fixing nitrogen (Perin *et al.*, 2006). However, the Bcc can also cause serious opportunistic infections in humans. The Bcc are well documented as life-

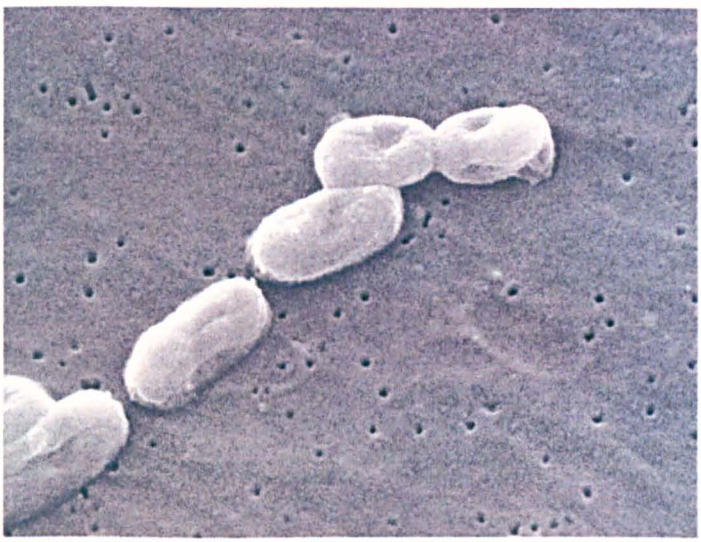

Figure 1.1: Scanning electron micrograph showing *B. vietnamiensis*, a member of the Bcc. Reproduced from http://web.umr.edu/~microbio/BIO221_2000/Burkholderia_cepacia.html

Figure 1.2: An onion bulb infected with *Burkholderia cepacia*. The outer scales of the bulb have succumbed to 'sour skin', whereas the inner scales remain unharmed, typical of this infection. Reproduced from http://www.apsnet.org/education/feature/BurkholderiaCepacia/

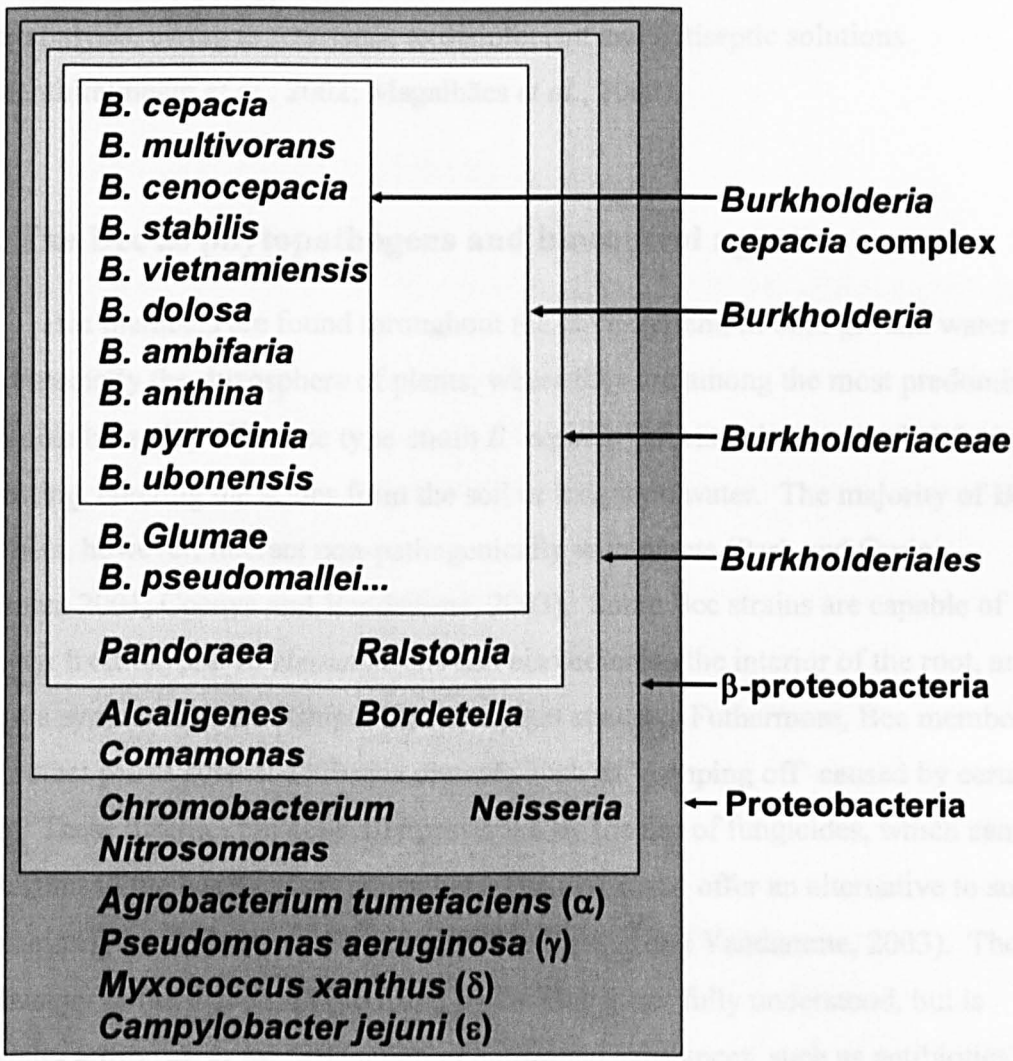

Figure 1.3: Taxonomy of the Bcc. The phylum 'proteobacteria' contains 5 sub-phyla entitled α through ε. One species representative of each sub-phylum is shown, except for the β proteobacteria, of which the genus *Burkholderia* is part. The Bcc currently consists of 10 members, all of which are shown (Adapted from Thomas, 2007).

threatening pathogens of cystic fibrosis (CF) and chronic granulomatous disease (CGD) patients, their inherent resistance to antimicrobials making treatment difficult. They are also prevalent as nosocomial pathogens, for example in patients requiring haemodialysis, owing to resistance to disinfectant and antiseptic solutions (Mahenthiralingam *et al.*, 2002; Magalhães *et al.*, 2003).

1.2: The Bcc as phytopathogens and biocontrol agents

Bcc members are found throughout the environment, in both ground water and soil (especially the rhizosphere of plants, where they are among the most predominant culturable bacteria). The Bcc type-strain *B. cepacia* infects onions wounded during harvesting, entering the scales from the soil or irrigation water. The majority of Bcc members, however, interact non-pathogenically with plants (Park and Gurian-Sherman, 2001; Coenye and Vandamme, 2003). Some Bcc strains are capable of nitrogen fixation, and *B. vietnamiensis* can also colonise the interior of the root, and live in a symbiotic relationship with some plant species. Futhermore, Bcc members can protect plants against soilborne diseases such as 'damping off' caused by certain fungi. These diseases are generally prevented by the use of fungicides, which can be deleterious to the health of the consumer. The Bcc could offer an alternative to such treatments (Park and Gurian-Sherman, 2001; Coenye and Vandamme, 2003). The mechanism of the biocontrol mediated by the Bcc is not fully understood, but is generally attributed to the production of antifungal substances, such as antibiotics and siderophores. The Bcc produce a number of antibiotics, including cepacin and cepamide. Strains also produce up to 4 siderophores, and can utilise others (so-called 'xenosiderophores'), allowing them to compete with fungi for iron, which is essential for cell growth (Park and Gurian-Sherman, 2001). The importance of iron for cell growth and its acquisition through siderophores are discussed later (Section 1.4).

Bcc members can metabolise a broad range of substrates, allowing their use in bioremediation of soil and groundwater containing various contaminants. These include the polycyclic aromatic hydrocarbons found in crude oil and a range of herbicides, such as 2,4,5-trichlorophenoxyacetic acid, the principal component of Agent Orange (Park and Gurian-Sherman, 2001).

The use of the Bcc in biocontrol of fungal diseases and bioremediation has thus far been hampered by safety concerns, owing to the ability of these organisms to cause opportunistic infections in humans, especially in patients suffering from chronic granulomatous disease or cystic fibrosis (Speert, 2002).

1.3: The Bcc as pathogens of humans

1.3.1: Implications of the Bcc for chronic granulomatous disease patients

Chronic granulomatous disease (CGD) is an autosomal recessive disorder with an incidence of ~1 in 250,000 live births. Patients have a mutation within 1 of 4 genes encoding subunits of NADPH oxidase present in phagocytes, rendering this enzyme inactive.

NADPH oxidase transfers electrons from NADPH to oxygen, resulting in O_2^- and O_2^{2-}. These reactive oxygen species (ROS) become protonated, resulting in a rise in pH, despite the influx of acidic granule contents from lysosomal fusion. The gradient across the vacuole membrane produced by proton consumption is balanced by an influx of H^+ and K^+ ions. If this charge were compensated for by H^+ influx alone, the net pH in the vacuole would not change as a result of these processes, but owing to the partial compensation by K^+ influx, the net pH within the phagolysosome rises. The phagolysosome granules contain a strongly anionic sulphated proteoglycan matrix, to which the cationic proteases responsible for bacterial killing (eg neutrophil elastase and cathepsin G) are tightly bound. These proteases must be solubilised to become active. The combination of increased pH and K^+ concentration solubilises these proteases, leading to bacterial killing. Hence, in individuals suffering from CGD, these proteases are inactive (Reeves *et al.*, 2002; Ahluwalia *et al.*, 2004).

CGD patients are susceptible to infections by a fairly narrow range of bacteria, of which members of the genus *Burkholderia*, including Bcc members, are the most virulent of the Gram-negative pathogens. Normal phagocytes can kill ingested cells by both oxidative and non-oxidative means. However, Bcc members are highly resistant to non-oxidative killing, which is mediated by antimicrobial cationic peptides. *Burkholderia* infection of CGD patients most commonly manifests itself as an aggressive respiratory infection, with the potential for bacteraemia (Speert, 2002). Figure 1.4 shows the accumulation of fluid in the lungs as a result of pneumonia in a

CGD patient infected with a Bcc member. The prognosis for CGD patients has improved dramatically since the disease was first described in the 1950s, when death invariably occurred in early childhood, with improvements in antibiotics for treatment of infections and prophylaxis. However, the highly antimicrobial resistant *Burkholderia* genus remains an important cause of infection (Speert, 2002).

1.3.2: Bcc infection of cystic fibrosis patients

Cystic fibrosis (CF) is the most common autosomal recessive disease amongst the Caucasian population, with an incidence of 1 in 2,500 live births. CF is caused by mutation of the gene encoding the CFTR (cystic fibrosis transmembrane conductance regulator), an ABC (ATP-binding cassette) transporter protein responsible for the transport (both import and export) of chloride ions through epithelia such as those lining the airways.

Healthy airways are sterile below the first bronchial division, despite constant challenge from inhaled micro-organisms. There are two main mechanisms by which this sterility is maintained. The first is mediated by co-ordinated ciliary beating, which propels the thin film (~30 μm) of the airway surface liquid (ASL) towards the mouth. The second involves a mixture of antimicrobial agents present within the ASL, including proteases, oxidants and antibiotics (Wine, 1999).

Two hypotheses have been suggested to explain CF lung disease. These are generally known as the 'high salt' and 'low volume' (or 'dehydration') hypotheses. Briefly, in the high salt hypothesis, the absence of CFTR function results in reduced Cl^- movement from the ASL through the epithelium and into the blood plasma. This results in increased salt concentration in the ASL, which interferes with the activity of host-produced antibiotic agents, such as lysozyme and defensins (Goldman *et al.*, 1997; Wine 1999).

In contrast, the low volume hypothesis suggests that 'too little salt' is present in the ASL. CFTR conductance is known to down-regulate the activity of a number of other types of ion channel, including the amiloride-sensitive epithelial Na^+ channel (ENaC). In CF, ENaC is derepressed, resulting in increased transport of Na^+ into the plasma, accompanied by increased chloride transport into the plasma through alternative chloride channels. This ion movement creates an osmotic gradient,

resulting in water movement into the plasma, and hence reducing the volume of the ASL. The decrease in ASL volume leads to ciliar collapse, preventing mechanical clearance of the ASL (Matsui *et al.*, 1998; Wine 1999; Boucher, 2007).

Evidence has been presented to support both hypotheses, however recent studies support the low volume hypothesis. For example, human clinical studies of the effects of inhaled hypertonic saline (containing 7 % NaCl, as opposed to the blood plasma concentration of 0.9 %) on CF lung disease, found that quality of life and lung function increased with this treatment, with no elevation in numbers of lung bacteria. If the high salt hypothesis were true, then hypertonic saline would be expected to exacerbate, rather than alleviate, CF lung disease (Donaldson *et al.*, 2006; Boucher, 2007). It should be noted that neither of these hypotheses take into account Cl^- secretion by CFTR, to which many symptoms of the CF syndrome such as loss of pancreatic function and degeneration of the vas deferens, have been attributed (Wine, 1999).

In CF infants, *Staphylococcus aureus, Haemophilus influenzae* and *Pseudomonas aeruginosa* are the predominant pathogens, however among adults the predominance of the former two bacteria decreases. Amongst adults *P. aeruginosa* and Bcc members are some of the most important pathogens (Gadsby *et al.*, 2006). It should be noted that CF affects all exocrine epithelia. However, the majority of deaths amongst CF patients are due to pneumonia, as a result of bacterial colonisation of the lung.

The incidence of Bcc infections of CF patients varies between centres, from ~3 % to 40 % (Ledson *et al.*, 1998; Hodson and Geddes, 2000). The most prevalent Bcc member among CF patients is *B. cenocepacia*, which causes over 50 % of infections across the USA, Canada and Italy. *B. multivorans* is also highly prevalent, and infections with this strain and *B. cenocepacia* account for >90 % of total Bcc infections of CF patients, although all Bcc members are capable of causing infections (Mahenthiralingham *et al.*, 2002). When infected with a Bcc pathogen, CF patients generally follow one of three clinical trends; chronic asymptomatic carriage, progressive deterioration over many months that eventually stabilises at a low level, or rapid, usually fatal deterioration of lung function known as 'cepacia syndrome' (Ledson *et al.*, 1998). Cepacia syndrome is characterised by severe pneumonia and septicaemia (Hodson and Geddes, 2000). ~20 % of CF patients colonised by Bcc members develop this syndrome (Ledson *et al.*, 1998).

Members of the Bcc are transmissable between CF patients, leading to the segregation of Bcc-infected CF patients in many treatment centres. One particular *B. cenocepacia* strain was found to be highly infectious, and spread through Canada and into the UK through patient to patient contact at CF summer camps. This 'epidemic strain' was designated as the ET-12 (electrophoretic type 12) or cable-pilus encoding strain (Mahenthiralingham *et al.*, 2002). It was found to produce peritrichously arranged, cable-like pilus fibres (Figure 1.5), which would be expected to aid adhesion to eukaryotic cell surfaces (Goldstein *et al.*, 1995). *B. cenocepacia* has been shown to be capable of replacing other Bcc isolates in the CF lung. A study of a CF treatment centre in which all Bcc-infected patients were allowed to mix freely showed that the range of Bcc members initially present were replaced over time by a *B. cenocepacia* ET-12 (cable-pilus producing) strain, associated with a poor prognosis.

1.3.3: Virulence determinants of the Bcc

Many putative virulence factors have thus far been described for this group of organisms. However, few have been demonstrated to play a role in pathogenicity. The following is a discussion of a selection of putative and confirmed virulence determinants of the Bcc:

Pili (fimbriae) - Pili are responsible for attachment to epithelial surfaces and to mucin, a protein found in mucus, which is abundant in the CF lung. The presence of the laterally expressed cable-pilus in *B. cenocepacia* correlates with increased transmissibility, although apparently not with increased virulence (Sun *et al.*, 1995). The Bcc have been found to produce five morphologically distinct types of pilus. These are the cable pilus (mentioned above); the filamentous pilus (isolated from non-epidemic clinical strains infecting CF patients); the spine pilus (isolated from clinical strains infecting non-CF patients); the spike pilus (isolated from environmental strains); and finally the mesh pilus, which forms a dense mat of peritrichously arranged pili, using one of the previously described pilus types (excluding spine-type) as a structural framework (Goldstein *et al.*, 1995).

Haemolysin - *B. cenocepacia* produces a lipopeptide haemolysin which has been implicated in evasion of the host immune response through induction of neutrophil

apoptosis and degranulation of phagocytes, which was demonstrated in human cell lines (Hutchison *et al.*, 1998). The structure of this haemolysin has not been reported.

Lipopolysaccharide (LPS) - The production of LPS has been shown to induce pro-inflammatory cytokines TNFα and IL-6 in human cell lines. Chronic infection of the CF lung leads to long-term stimulation of pro-inflammatory cytokines by LPS, resulting in chronic inflammation and tissue damage by reactive oxygen species, released as a result of the inflammatory response (Bamford *et al.*, 2007; Silipo *et al.*, 2007). Production of LPS is known to be an important factor in resistance to cationic peptides produced as part of the innate immune response, through which non-oxidative killing is mediated. A *B. cenocepacia* mutant producing a truncated LPS was unable to survive in the rat agar bead model of infection (Loutet *et al.*, 2006). This model was developed for the investigation of chronic respiratory infection, and involves the intratracheal inoculation of bacteria enmeshed in agar beads, leading to the beads being deposited within the lungs (Cash *et al.*, 1979). Furthermore, this mutant was sensitive to three cationic peptides, including human neutrophil peptide 1 (HNP-1), produced during the innate immune response, while the parent strain was resistant to these three peptides (Loutet *et al.*, 2006).

Epidemic *B. cenocepacia* isolates commonly exhibit a rough colony morphotype, while environmental and other clinical isolates tend to exhibit a smooth colony morphotype. This difference in appearance is due to the structure of the LPS produced. The smooth morphotype results from production of LPS with a complete O side-chain, whereas the rough morphotype is due to loss of the O side-chain. Bacteria producing smooth LPS tend to be resistant to the bactericidal activity of serum, whereas those producing rough LPS tend to be serum-sensitive. However, strains belonging to either morphotype are capable of persistent infection of CF patients.

Exopolysaccharide (EPS) - The production of excessive EPS results in mucoid colonies. Mucoid strains of *P. aeruginosa* producing the EPS alginate have long been established as having greater persistence in the CF lung than non-mucoid strains. Most Bcc strains produce an exopolysaccharide known as cepacian, which appears to be essential for the formation of thick, mature biofilms (Govan and Deretic, 1996). The ability of Bcc strains to persist within the CF lung and to produce biofilms, however, was found not to be highly influenced by the production of cepacian,

probably owing to strain differences and other factors influencing the formation of biofilms (Cunha *et al*, 2004). A different type of exopolysaccharide was produced by a *B. cenocepacia* strain isolated from a CF patient. This isolate had developed from a non-mucoid strain into a mucoid, EPS overproducing strain in this patient. This EPS-overproducing strain was found to be more persistent in a mouse model of pulmonary infection than its non-mucoid parent strain. Recognition of the non-mucoid parent strain by leucocytes was found to be 2.5-3 fold higher than its mucoid derivative, showing the importance of EPS in this case (Conway *et al.*, 2004).

Biofilm production - The ability to produce biofilms is the major factor conferring the ability to colonise medical devices such as catheters, a trait for which the Bcc is well known (Isles *et al.*, 1984). Biofilms are also known for their antibiotic resistance; strains sensitive to a certain antibiotic tend to persist within biofilms, even when treated with several thousand fold more of this antibiotic than would normally be required to kill the same strain when growing planktonically (Stewart and Costerton, 2001). It is hardly surprising then, that the already multiple antibiotic resistant Bcc are often impossible to eliminate following colonisation of the CF lung. Three hypotheses exist regarding the mechanism of antibiotic resistance in biofilms; that antibiotic penetration is slowed by resistant bacteria within the biofilm, allowing them to deal with far greater concentrations than would ordinarily be possible; that changes in the biofilm microenvironment, such as alterations in pH or aeration could reduce antibiotic effectiveness (for example aminoglycosides are known to be less effective under anaerobic conditions); and finally, it has been speculated that a proportion of bacteria within the biofilm might enter a spore-like state, allowing re-establishment of the biofilm even if all other bacteria within it have been destroyed (Stewart and Costerton, 2001). *In vitro* experiments have shown that the presence of PAO1, even when inactivated by irradiation, increases the binding of Bcc isolates to epithelial monolayers (Saiman *et al.*, 1990), suggesting that these bacteria might form mixed biofilms, to the benefit of the Bcc member involved.

Metalloproteases- Two zinc metalloproteases, ZmpA and ZmpB, have been associated with virulence in *B. cenocepacia*, and are present in most Bcc members. ZmpA and ZmpB are broad-spectrum proteases, and cleave, among others, type IV collagen and fibronectin. Thus they may directly damage the tissue of the CF lung.

ZmpA and ZmpB have been found to cleave α-1 protease inhibitor. α-1 protease inhibitor inactivates neutrophil elastase, preventing damage to tissue components. It has not yet been established whether cleavage of α-1 protease inhibitor by ZmpA or ZmpB inactivates this inhibitor, but if it does, tissue damage would be expected to result.

ZmpA has been shown to be important for persistent infection in the rat agar bead model in *B. cenocepacia* strain K56-2, whereas *zmpB* mutants showed similar persistence to K56-2. Infection in the rat agar bead model with K56-2 *zmpA* and *zmpB* single mutants and a *zmpAB* double mutant resulted in significantly less histopathology than wild type, and the histopathology caused by all three mutants was similar, suggesting that the activity of these enzymes is not additive. The virulence of a strain 715j *zmpA* mutant was similar to the parent (a CF isolate), suggesting that ZmpA metalloprotease may only act as a virulence factor in some strains of *B. cenocepacia* (Corbett *et al.*, 2003). It has been found that in some strains expression of the *zmpA* gene is reduced or lacking, and this is perhaps the case for 715j (Gingues *et al.*, 2005). The effect of a *zmpB* mutation on the virulence of strain 715j has not been characterised (Corbett *et al.*, 2003; Kooi *et al.*, 2006).

The Bcc epidemic strain marker (BCESM) - Another contributing factor in the virulence of *B. cenocepacia* is the presence of the BCESM. The BCESM was discovered during RAPD (random amplified polymorphic DNA) typing of Bcc isolates from CF patients. It was identified as a conserved amplification product amongst the otherwise distinct patterns of strain fingerprints, and has been widely used to identify isolates with an increased risk of patient to patient transmission. The 1.4 kb BCESM was found to encode a putative negative transcriptional regulator, *esmR*, and to be exclusive to *B. cenocepacia*. Investigation of the phylogeny of the *B. cenocepacia recA* gene showed that four differing strain lineages are present, known as III-A, -B, -C and -D (as *B. cenocepacia* was originally entitled *B. cepacia* genomovar III). The BCESM is found in over 77 % of III-A strains. It is absent from the majority of III-B strains isolated from CF patients, and has not been found within strains of the other two lineages (Mahenthiralingam *et al.*, 2001; Manno *et al.*, 2004). BCESM strains are generally associated with increased transmissibility, virulence and mortality (Mahenthiralingam *et al.*, 2001; Speert *et al.*, 2002). Further study of the BCESM showed that it was part of a pathogenicity island unique to *B.*

cenocepacia, which was named the cenocepacia island (*cci*) (Baldwin *et al.*, 2004). Preliminary annotation of this island revealed 47 predicted coding sequences, including an N-acyl homoserine lactone (AHL) synthase gene and its transcriptional regulator (*cciI* and *cciR*, the components of a quorum sensing system, described below), a cluster of fatty acid biosynthesis genes, a decarboxylase gene and a cluster of amino acid transport and metabolism genes. The *cci* also contained a cluster of 7 coding sequences with homology to genes of unknown function. Mutation of the putative AHL synthase and porin genes of this island was found to significantly reduce virulence in the rat agar bead model of respiratory tract infection. This demonstrates that the *cci* contains genes important for the virulence of *B. cenocepacia*. The *cci* is not essential for pathogenicity, however, since many *B. cenocepacia* strains isolated from CF patients lack this island (Baldwin *et al.*, 2004).

Intracellular pathogenicity- It has been suggested that the Bcc are intracellular pathogens, owing to their genetic similarity to *Burkholderia mallei*, an intracellular pathogen of humans and horses. The Bcc can invade epithelial cells (Sajjan, 1992), and can be isolated from within the cells of infected mice, supporting this hypothesis (Speert, 2002). The growth of *B. cenocepacia* is primarily extracellular (Marolda *et al.*, 1999). However, a recent study has shown that *B. cenocepacia* can remain intact for a number of hours within macrophages, and that the presence of *B. cenocepacia* within a phagosome delays lysosome fusion for ~6 hours, potentially allowing for the expression of genes necessary for survival within the phagolysosome. Macrophages infected with *B. cenocepacia* were found to progressively lose viability after this ~6 hour delay, by unknown mechanisms (Lamothe *et al.*, 2007).

Siderophores- Another factor associated with bacterial virulence is the production of siderophores. Siderophores are low molecular weight molecules with a high binding affinity for iron, responsible for the acquisition of iron from low iron environments. The pyoverdine siderophores produced by *P. aeruginosa* are well-known virulence factors of this organism. Pyoverdine-deficient *P. aeruginosa* has been shown to be avirulent when injected into burned mice; however, virulence was restored when mice were co-injected with pure pyoverdine. In *B. cenocepacia*, production of the siderophore ornibactin, discussed later, has been shown to increase virulence. The colonisation and pathology of 2 *B. cenocepacia* strains, a wild type ornibactin-

producing CF isolate and a mutant of this strain defective in ornibactin production, were tested for virulence using the rat agar bead model of respiratory tract infection. The ornibactin mutant was rapidly cleared from the rat lung, whereas the wild type strain effectively colonised the lung. Furthermore, significantly lesser pathology was noted as a result of the ornibactin mutant strain compared to wild type before clearance of this organism (Sokol *et al.*, 1999).

Quorum sensing as a mechanism for regulation of *B. cenocepacia* virulence factor production - As previously mentioned, the cenocepacia pathogenicity island (*cci*) contains a predicted acyl homoserine lactone (AHL) synthase gene (*cciI*), and a putative response regulator, *cciR*, important for *B. cenocepacia* virulence (Baldwin *et al.*, 2004). Such genes are the basis of quorum sensing (QS) in Gram-negative bacteria. This is a mechanism for gene regulation in response to the density of a bacterial population. QS in Gram-negative bacteria typically involves an AHL produced by a LuxI-type AHL synthase, and a sensor/response regulator encoded by a *luxR*-type gene. The Lux nomenclature hails from the initial identification of QS in *Vibrio fischeri*, responsible for luminescence when a bacterial population reaches a threshold density, or quorum (Fuqua *et al.*, 1996; Williams *et al.*, 2007). AHL molecules can freely diffuse across bacterial membranes, resulting in the intracellular and extracellular concentrations being equal (Parsek and Greenberg, 2000). When intracellular concentrations reach the required threshold, the AHL binds the response regulator, which can then bind specific promoter motifs known as *lux* boxes to regulate gene activity (usually by activating transcription). This threshold concentration is often modelled as the Kd of the regulator for the AHL in question (Fuqua *et al.*, 1996). The AHLs of different QS systems differ in acyl-chain length and modification at the C3 position of the acyl side-chain. LuxR-type regulators preferentially bind the AHL produced by their cognate LuxI-type synthase, resulting in selectivity of the QS system (Steindler and Venturi, 2007).

Two QS systems have been identified in *B. cenocepacia*: the previously mentioned *cciIR* system, and the *cepIR* system. The *cepIR* system is widely distributed throughout the Bcc. CepI is an AHL synthase, responsible for synthesis of *N*-octanoyl-L-homoserine lactone (OHL) and also of *N*-hexanoyl-L-homoserine lactone (HHL). CepR is the response regulator of this system, and appears to be

involved in the regulation of numerous genes. This was determined by proteomic analysis involving reporter fusions of genomic DNA fragments from a *B. cepacia* strain, which identified 28 putative CepR-regulated promoters (Aguilar *et al.*, 2003). In *B. cenocepacia*, CepR is involved in the regulation of a number of virulence factors, such as the development of mature biofilms, extracellular protease production, zinc metalloprotease (ZmpA) production, and ornibactin production. A *cepR* mutant of *B. cenocepacia* was found to over-produce ornibactin in dense cultures by approximately 2 fold, compared to its parent strain, suggesting that CepR would normally negatively regulate production of this siderophore (Lewenza and Sokol, 2001). *cepIR* mutants have been shown to be significantly less virulent than wild type strains in various models of infection, including the rat agar bead model, in which such mutants gave rise to a significantly decreased pathology compared to wild type (Sokol *et al.*, 2003). QS is known to be important in the regulation of virulence in a number of pathogens, including *P. aeruginosa*, and owing to the large number of genes apparently regulated by QS in *B. cenocepacia*, and the known virulence factors that have been shown to be regulated by QS, this could constitute an important mechanism for the regulation of *B. cenocepacia* virulence.

1.4: The importance of iron for bacterial growth

Iron is essential for cell growth. Its ability to undergo reversible changes of oxidation state has led to it being used by almost all micro-organisms (members of the *Lactobacillus* family are the only exceptions to date). It is used as a cofactor for a wide variety of enzymes, such as cytochromes and ribonucleotide reductase. The acquisition of iron has been implicated as the major determinant of bacterial survival within the animal host, as all other necessary nutrients, such as carbon, nitrogen, phosphates and sulphates, are freely available within the host. Bacteria unable to acquire iron within the host will cease to grow, and will be eliminated from the host either by the immune response or by iron starvation. Under aerobic conditions, such as those found both within the host and in the external environment, iron is largely found in the oxidised form, Fe^{3+}. This is unavailable to micro-organisms owing to its low solubility (the maximum concentration of free Fe^{3+} in solution at pH 7.0 is 1.4×10^{-9} M), which is 1 to 3 orders of magnitude lower than the level required for normal

bacterial growth. The importance of iron for bacterial growth has led to the suggestion that iron uptake could constitute an effective target for the design of new drugs (Guerinot, 1994; Ratledge and Dover, 2000).

In the human host, iron, having entered the bloodstream following assimilation from the diet, is bound by transferrins. The transferrins are a class of glycoproteins able to bind iron with high affinity at two similar sites, and are present throughout the vertebrates. There are three classes of transferrin: that found in the serum (serotransferrin); lactotransferrin (or lactoferrin), which is found in many extracellular fluids; and ovotransferrin, found in the albumin of eggs. In order to ensure that any surplus iron is bound, thus limiting its availability to infecting micro-organisms, an excess of unsaturated transferrin must be present at all times (Ratledge and Dover, 2000).

The major iron storage protein of most organisms is ferritin. Ferritins are hollow, roughly spherical proteins capable of holding ~4,500 Fe^{3+} atoms, which can enter and exit the ferritin protein through numerous pores within the surface (Theil *et al.*, 2002). Ferritin levels in the CF lung are significantly higher than in the lungs of healthy humans. One study found a 70 fold increase in ferritin levels in the CF lung, while transferrin levels remained constant.

In order to survive within animal hosts and iron-poor natural environments, bacteria have developed iron acquisition mechanisms enabling them to scavenge iron from the various iron-binding proteins of the host, such as ferritin and the transferrins. *B. cenocepacia* produces a protease that can degrade ferritin, allowing it to utilise this iron source (Whitby *et al.*, 2006).

1.4.1: Iron acquisition using siderophores

Bacteria use two principal systems to acquire iron. In one of these systems the bacterium directly contacts the iron source (usually transferrin), and reduces the bound Fe^{3+} for uptake. The alternative and apparently most common system involves the synthesis of siderophores (from the Greek terms '*sideros*' (iron) and '*phoros*' (carriers)). Siderophores are low molecular weight (generally <1000 Da) compounds which possess high affinity for iron (Escolar *et al.*, 1999). The majority of siderophores are classified either as catecholates or hydroxamates, after the iron-

binding ligands present within them (Ankenbauer *et al.*, 1988). They facilitate iron solubilisation and transport by chelating ferric iron (Fe^{3+}), before being taken up as ferric siderophore complexes, via specific transport systems. The iron is then freed from the ferric siderophore, often by an iron reductase (Guerinot, 1994; Escolar *et al.*, 1999). This is discussed in greater detail later in this chapter. Some siderophores have a higher affinity for iron than host iron-binding proteins, allowing them to 'rob' iron from the host. Siderophores are invariably produced only under conditions of iron limitation. The mechanisms involved in iron-dependent regulation of iron acquisition are discussed later in this chapter.

1.5: Siderophores of the Bcc

Members of the Bcc produce up to four siderophores; cepabactin, cepaciachelin, pyochelin and ornibactin, the latter two of which are predominant in *B. cenocepacia* strains. Salicylic acid, a precursor of pyochelin (as well as several other siderophores), is also widely produced by clinical isolates, and has been classified as a siderophore in *Pseudomonas fluorescens* (Meyer *et al.*, 1992). However, the iron-binding constant of salicylate is too low to allow it to effectively compete with ions such as phosphate present within the blood, which cause free iron to precipitate. Salicylate has been shown to have little effect on the concentration of soluble Fe^{3+} *in vitro*, and furthermore cannot sequester iron from a complex with chrome azurol sulphonate (CAS), the standard test for a siderophore (discussed later). This suggests that salicylate does not in truth act as a siderophore (Ratledge and Dover, 2000; Chipperfield and Ratledge, 2000). As a result, salicylate will not be regarded as a siderophore throughout this work.

1.5.1: The structure and iron-binding stoichiometry of the Bcc siderophores

Iron co-ordination by chelating agents

The co-ordination of iron by iron-chelating agents requires the formation of six ligands. These form an octahedral arrangement around the central iron atom.

Cepabactin

Cepabactin can be considered as a cyclic hydroxamate, and a heterocyclic analogue of catechol. As such it belongs to both of the two most common groups of siderophore molecules, the hydroxamates and the catecholates. ^{1}H-NMR (nuclear magnetic resonance) has shown that the structure of cepabactin is 1-hydroxy-5-methoxy-6-methyl-2(1H)-pyridinone (Figure 1.6), which has also been described as an antibiotic produced by *Pseudomonas alcaligenes* and *Pseudomonas* strain BN227, suggesting that cepabactin acts as a siderophore in these organisms also. Cepabactin has the characteristics of a siderophore: it is synthesised only under iron limitation, can stimulate the growth of the parent strain *in vitro* when added to iron limited media, and promotes iron uptake (Meyer *et al.*, 1989). However, it has not yet been shown that cepabactin acts as a siderophore *in vivo*.

Cepabactin binds Fe^{3+} with a stoichiometry of three bidentate molecules to one metal ion, forming an orange complex. In the presence of the Bcc siderophore pyochelin (discussed later), a purple complex forms, comprising Fe^{3+}, cepabactin and pyochelin, in a 1:1:1 ratio (Klumpp *et al.*, 2005). In this case four of the necessary ligands are provided by pyochelin and two by cepabactin.

Cepabactin is produced only by certain members of the Bcc. However, it is possible that Bcc strains that do not produce cepabactin can still utilise it. For example, the addition of cepabactin to cultures of *P. aeruginosa* PAO1 (which does not produce this siderophore) promotes iron uptake, suggesting that cepabactin might be utilised by strains other than those that produce this siderophore.

Cepaciachelin

Cepaciachelin is a catecholate siderophore, with the structure 1-*N*-[2-*N'*,6-*N'*-di(2,3-dihydroxybenzoyl)-L-lysyl]-1,4-diaminobutane (Figure 1.7), which was determined by ^{1}H and ^{13}C NMR and mass spectrometry. It was first isolated from an environmental isolate of the Bcc species *Burkholderia ambifaria.* Its status as a siderophore has not been confirmed experimentally, but rather inferred from its structural similarity to known siderophores, such as protochelin of *Azotobacter vinelandii* (Barelmann *et al.*, 1996).

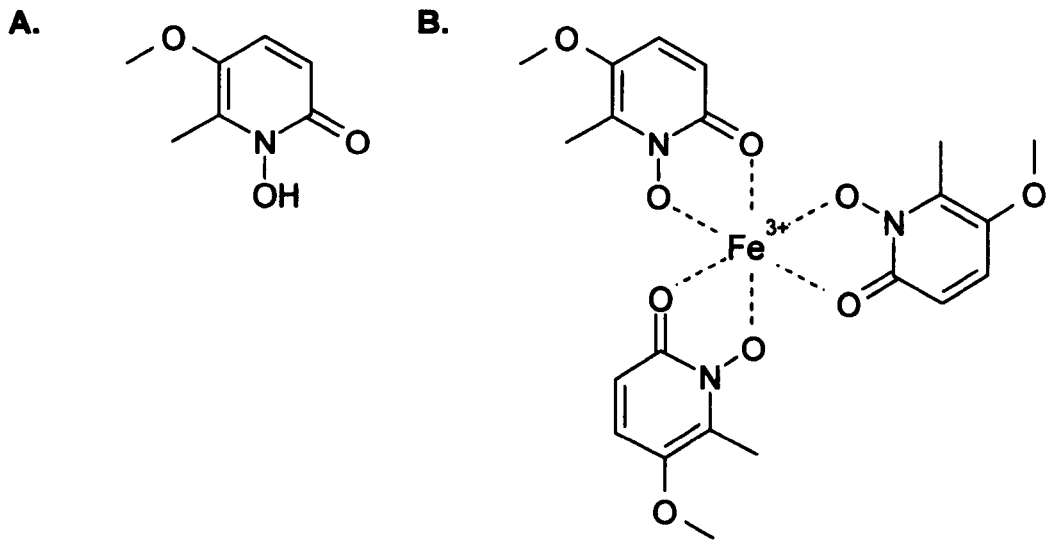

Figure 1.6: The structure of cepabactin. **A**: Cepabactin. **B**: Ferric cepabactin; three cepabactin molecules combine to bind to Fe^{3+} (Meyer *et al.*, 1989; Klumpp *et al.*, 2005; Thomas, 2007).

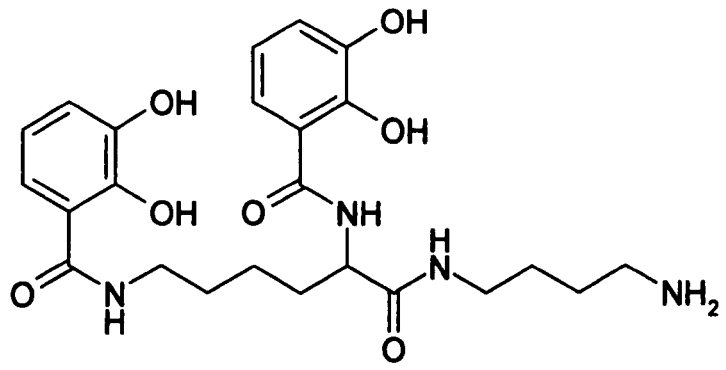

Figure 1.7: The structure of cepaciachelin (Barelmann et al., 1996)

Pyochelin

The siderophore pyochelin (Figure 1.8) was first isolated from *Pseudomonas aeruginosa,* but has also been found to be produced by some Bcc species, including strains belonging to *B. cepacia* and *B. cenocepacia.* ~ 50 % of clinical Bcc isolates from CF patients were found to produce little or no pyochelin in two studies (Sokol, 1986; Darling *et al.*, 1998), showing that while this siderophore is common amongst pathogenic strains, it is by no means essential for infection of the CF lung. Furthermore, in the rat agar bead model of infection, a pyochelin negative mutant of a CF clinical isolate of *B. cenocepacia* showed little difference in persistence in comparison to its parent strain (Visser *et al.*, 2004).

The structure of pyochelin has been determined by ^{1}H and ^{13}C NMR as 2-(2-o-hydroxyphenol-2-thiazolin-4-yl)-3-methylthiazolidine-4-carboxylic acid (Cox *et al.*, 1981).

Each molecule of pyochelin is synthesised from one salicylic acid molecule and two cysteine residues (Tseng *et al.*, 2006). The biosynthetic pathway for pyochelin has been recently reviewed by M. Thomas (2007). Pyochelin is fluorescent, appearing a yellow-green colour under ultra-violet light (Cox and Graham, 1979). When complexed with Fe^{3+}, pyochelin loses its fluorescence, and imparts a wine red or orange colour to solutions at a pH of 2.5 or a pH range of 4-7, respectively. Pyochelin contains three chiral centres, and exists as an equilibrium mixture of 2 spontaneously interconvertible stereoisomers dependent upon the configuration of the chiral centre adjacent to the free carboxyl group in the thiazolidine ring (see Figure 1.8 A). Only one of these stereoisomers, known as pyochelin I, can form a complex with Fe^{3+}. Pyochelin has four co-ordinating groups for iron-binding, and binds ferric iron at a 1:1 or 2:1 stoichiometric ratio (pyochelin:iron) in solution, dependent upon the relative concentrations of iron and pyochelin (Tseng *et al.*, 2006). Pyochelin appears to be less efficient at binding iron than most other siderophores, including ornibactin, having an iron-binding coefficient of 5×10^{5} M^{-1} (Cox and Graham, 1979). However, this was determined in ethanol, and might not therefore be a true representation of the iron-binding efficiency *in vivo*. Pyochelin has a higher affinity for iron than transferrin, allowing it to scavenge iron from this host iron-binding protein (Ankenbauer *et al.*, 1988). It has been shown that when both iron and sulphur are depleted, pyochelin is not produced, suggesting that cysteine is conserved for other

A.

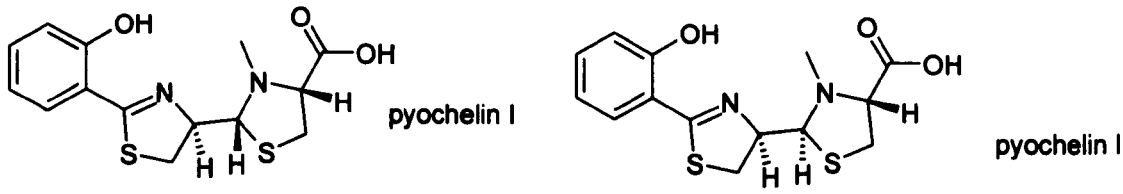

B.

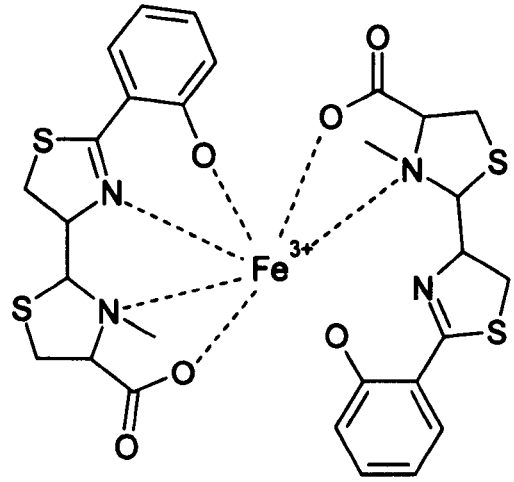

Figure 1.8: The structure of pyochelin. **A**: The pyochelin stereoisomers. The two stereoisomers of pyochelin shown occur as an equilibrium mixture, with only the pyochelin I configuration being capable of binding Fe^{3+} (Zamri and Abdallah, 2000). **B:** Stoichiometry of Fe^{3+} binding by pyochelin I (Tseng *et al.*, 2006).

purposes, rather than incorporation into pyochelin (Farmer and Thomas, 2004). Pyochelin has been shown to bind other transition metals besides iron, for example Cu^{2+}, Co^{2+}, Mo^{6+} and Ni^{2+}, and might also play a role in the delivery of these metal ions to the cell (Visca *et al.*, 1992).

Ornibactin

Ornibactin is a tetrapeptide composed of 2 L-ornithines, flanking single D-aspartate and L-serine residues, with the structure L-Orn[1] (N^5-OH, N^5-acyl)-D-*threo*-Asp(β-OH)-L-Ser-L-Orn[4](N^5-OH, N^5-formyl)-1,4-diaminobutane (see Figure 1.9 A). The sidechain nitrogen of the N-terminal ornithine is modified with a 3-hydroxy acid. The C-terminal ornithine is modified at the sidechain nitrogen with formic acid, and at the carboxyl group with putrescine. The sidechain nitrogens of both ornithines are also hydroxylated. Ornibactin has three bidentate ligands, the outer two of which are hydroxamates and the inner a hydroxycarboxylate, each of which are modifications to the sidechains of three amino acids of the tetrapeptide backbone. The serine residue does not participate in iron-binding, and essentially serves as a spacer. Ornibactin binds ferric iron with a 1:1 stoichiometric ratio, probably with a higher association constant than the other siderophores of the Bcc, as predicted through structural similarities of the iron-binding ligands of ornibactin to those of the pyoverdines, produced by the pseudomonads (the peptide backbone of the pyoverdines varies amongst the pseudomonads, but in each case one bidentate ligand is provided by a chromophore, while the remaining two are formed in some pyoverdines by the modification of two ornithine residues, as occurs in ornibactin (Stephan *et al.*, 1993; Ravel and Cornelis, 2003; Thomas 2007)).

There are three structurally different ornibactins; ornibactins $-C_4$, $-C_6$ and $-C_8$ (Figure 1.9). These differ at the N-terminus of the tetrapeptide according to the carbon chain length of the 3-hydroxy acid, and are present in the Bcc as a microheterogeneous population (Stephan *et al.*, 1993). Ornibactin is apparently the most widely produced siderophore of the Bcc, and was isolated from culture supernatants of 60 out of 63 strains (mostly clinical isolates) tested in one study (Darling *et al.*, 1998). Strong evidence points to the siderophore malleobactin produced by the non-Bcc member *Burkholderia pseudomallei* being structurally very similar to ornibactin. This is discussed in greater detail at the end of this chapter (Alice *et al.*, 2006).

A.

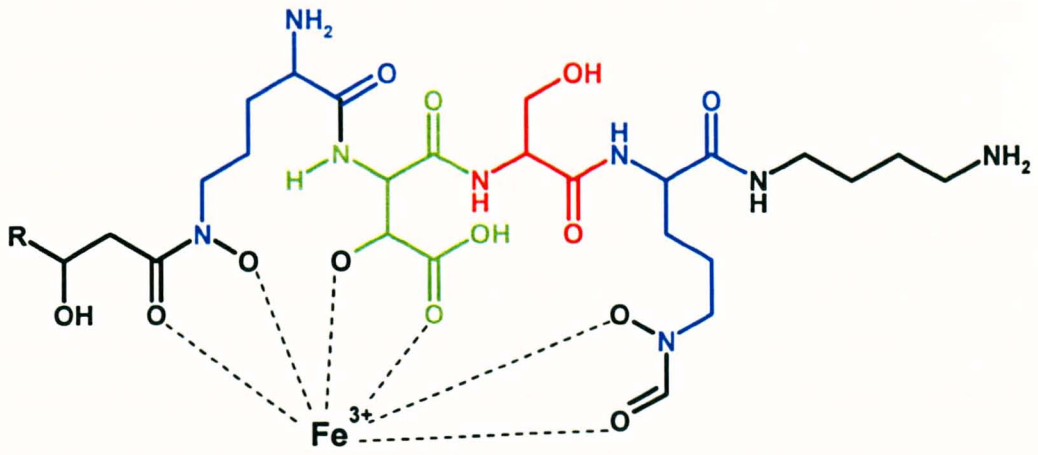

B.

Ornibactin-C4	R= -CH_3
Ornibactin-C6	R= -$CH_2CH_2CH_3$
Ornibactin-C8	R= -$CH_2CH_2CH_2CH_2CH_3$

Figure 1.9: The structure of ornibactin. A: Ferric ornibactin. The amino acid residues of the ornibactin backbone have been coloured, L-ornithine in blue, D-aspartate in green and L-serine in red. The sidechain nitrogen of one L-ornithine derivative has been derivatised with a 3-hydroxy acid (which contributes a ligand), and the other L-ornithine has been derivatised at the amino nitrogen with putrescine. Apart from the sidechain carboxyl group of the D-aspartate residue, all of the iron-binding ligands are contributed by modifications to the amino acid sidechains. **B:** The different alkyl groups of the 3-hydroxy acid present in the three ornibactins. The ornibactins are named ornibactin-C4, -C6 and –C8, according to the chain length of the acid bound to the sidechain nitrogen of the N-terminal ornithine. (Adapted from Stephan *et al,* 1993)

1.6: Work leading up to this study

1.6.1: Isolation of ornibactin-negative mutants of *B. cenocepacia*

B.cenocepacia strain 715j, a clinical isolate from a CF patient, produces the siderophores ornibactin and pyochelin, and is resistant to all antibiotics commonly used within the laboratory for selection of plasmids and transposons, excepting chloramphenicol (Cm) and trimethoprim (Tp). A spontaneous mutant of 715j was previously isolated that produced only one siderophore, ornibactin. This was termed KLF1 (Farmer, 1998; Agnoli *et al.*, 2006). The transposon mini-Tn*5*Tp was subsequently used in a second round of mutagenesis, and ornibactin-negative mutants were selected by plating cells onto chrome azurol sulphonate (CAS) agar. Mini-Tn*5*-Tp is a small (0.74 kb) transposon encoding resistance to trimethoprim, and lacking the flanking transcription and translation terminators that are present in the progenitor mini-transposon, mini-Tn*5*Cm (de Lorenzo *et al.*, 1990). This reduces the occurrence of polar effects on the expression of genes downstream of the integrated transposon when the *dfrB2* (Tp^R) gene is in the same orientation as the inactivated gene (Agnoli *et al.*, 2006). CAS is a dye capable of binding Fe^{3+}, resulting in a blue complex. The CAS assay is based on the higher affinity for Fe^{3+} of siderophores compared to this dye. The scavenging of Fe^{3+} from the dye, by siderophores, results in a colour change from blue to orange. This gives rise to an orange halo surrounding siderophore-producing colonies plated onto CAS agar (Schwyn and Neilands, 1987). Ten mutants of strain KLF1 were isolated, nine of which exhibited a complete absence of ornibactin production, while the remaining one (OM14) showed reduced ornibactin production (Figure 1.10). For further information see Agnoli *et al.*, 2006.

1.6.2: Identification of genes involved in ornibactin biosynthesis and transport in *B. cenocepacia*

In order to determine which gene had been disrupted in each mutant, the DNA flanking the inserted transposon was sequenced (Lowe, 2001; Agnoli *et al.*, 2006). The genome sequence of *B.cenocepacia* strain J2315 has been determined, allowing identification of the complete sequences of the genes into which the transposons had inserted. Figure 1.11 shows the locations of the inserted transposons that resulted in a

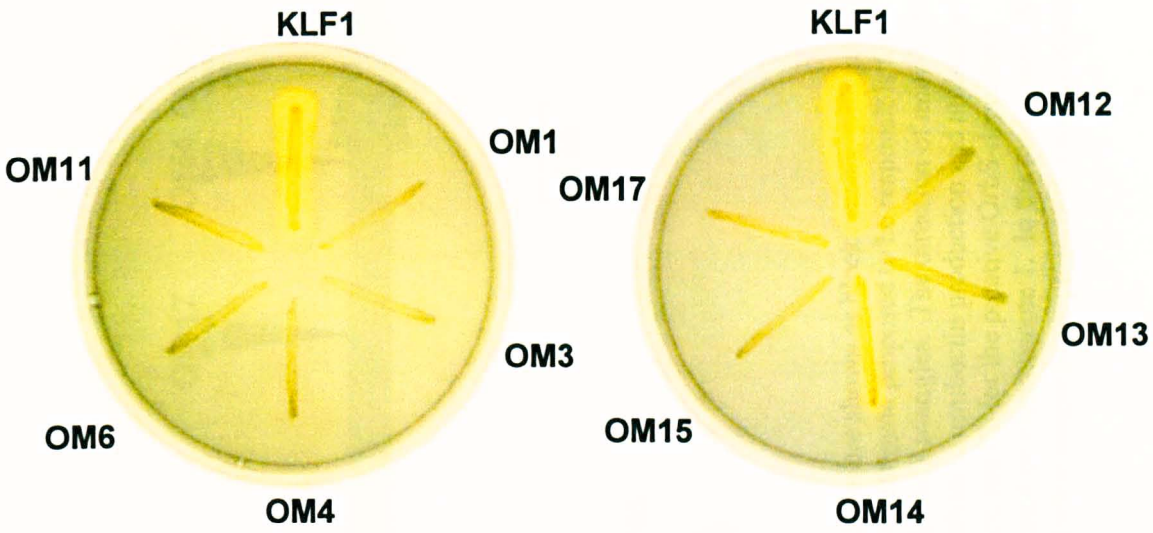

Figure 1.10: Identification of *B. cenocepacia* ornibactin-negative mutants. The pyochelin-negative *B. cenocepacia* strain KLF1 was mutagenised with mini-Tn*5*Tp and ornibactin-deficient mutants (OM) were identified on CAS agar (reproduced from Agnoli *et al.*, 2006). CAS, when bound to iron, gives a blue/green colouration to agar plates. When a siderophore removes the iron from the dye, the colour changes to orange, providing a simple indicator test for siderophore presence. As ornibactin was the only siderophore produced by the parent strain KLF1, any colonies that did not produce orange halos on CAS were ornibactin mutants (Schwyn and Neilands, 1987).

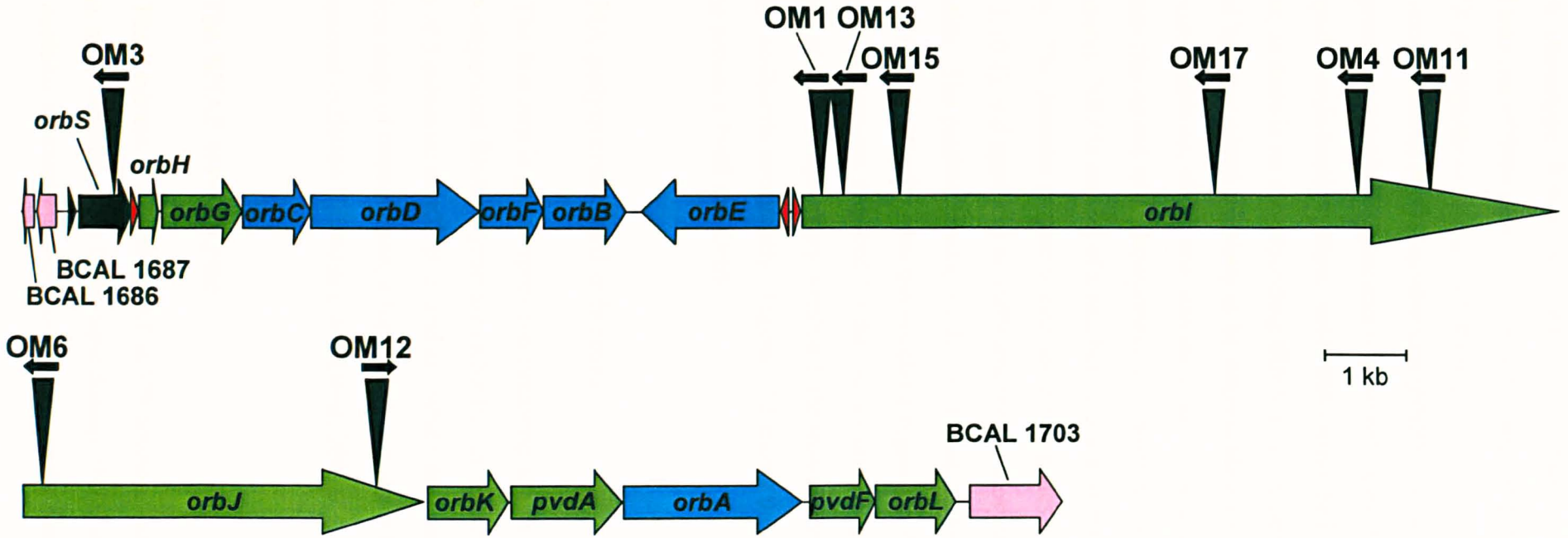

Figure 1.11: Locations of transposon insertions within the *B. cenocepacia* ornibactin gene cluster. Genes are shown as block arrows, with putative ornibactin biosynthetic genes depicted in green, transport and utilisation genes in blue, and the putative σ-factor gene proposed to be responsible for transcription of the ornibactin operon shown in black. Transposon insertion sites have been indicated with black triangles. The direction of mini-Tn*5*Tp insertion has been indicated above. Genes flanking the ornibactin gene cluster and believed not to be involved in ornibactin production and utilisation have been shown in pink. Promoter regions within the ornibactin gene cluster have been indicated with triangles: red fill for the putative OrbS-dependent promoters and black fill for the putative σ^{70}-type *orbS* promoter region. The ornibactin gene cluster is located on chromosome 1. In the preliminary *B. cenocepacia* J2315 sequence annotation, genes *orbS-orbL* have been designated BCAL1688-BCAL1702 (www.sanger.ac.uk/projects/B_cenocepacia/).

fully Orb$^-$ phenotype. It was found that in each of these mutants, the transposon had inserted into one of three genes. These were assigned putative functions using the BLASTX programme to search for homology. Two of the genes were predicted to encode non-ribosomal peptide synthetases (NRPS) owing to their similarity with NRPS genes involved in the synthesis of pyoverdine by the pseudomonads. NRPSs form peptide bonds between amino acids that cannot be joined together by the ribosome, as there is no corresponding tRNA, to form peptides. The proteins produced by these genes are likely to be responsible for the assembly of the ornibactin tetrapeptide backbone, which contains three novel amino acids; two L-ornithines and a D-aspartate (the amino acids incorporated into proteins by the ribosome are all L-enantiomers). NRPSs consist of a number of domains responsible for peptide assembly. The domains present within these two genes were investigated *in silico* (see Section 1.10.1), and appear to be sufficient for the biosynthesis of the ornibactin tetrapeptide. The putative product of the third gene, termed *orbS,* showed closest homology (36.5 % identity over the matching region) to PvdS, an alternative sigma (σ) factor of *P. aeruginosa,* required for the transcription of genes for the biosynthesis and utilisation of the siderophore pyoverdine I, the iron-binding moiety of which resembles ornibactin structurally. Figure 1.12 shows the similarity in amino acid sequence between PvdS and OrbS.

1.7: RNA polymerase and σ factors

The first step in gene expression (transcription) in living organisms is mediated by DNA-dependent RNA polymerase (RNAP). In bacteria, the RNAP core enzyme consists of 5 subunits; αI, αII, β, β' and ω. While the core enzyme is capable of the elongation stage of transcription, a further subunit, the σ factor, is required for transcriptional initiation (Murakami and Darst, 2003).

1.7.1: The RNAP core enzyme

The α subunit of *E. coli* RNAP is 329 amino acids in length, and consists of 2 domains, an N-terminal and a C-terminal domain (NTD and CTD, respectively). The α NTD contains a dimerisation region resulting in the formation of an α_2 dimer. The α

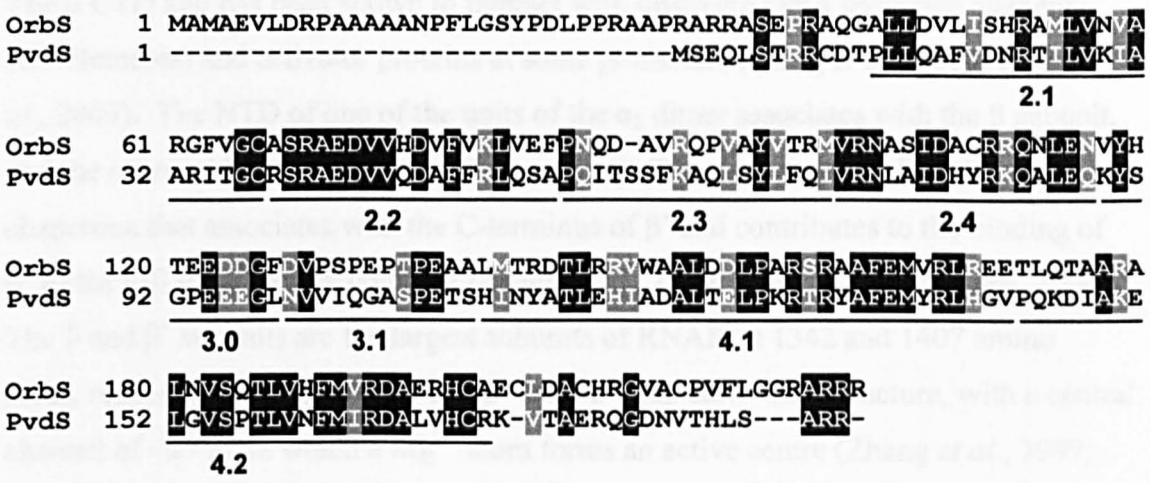

Figure 1.12: Alignment of PvdS and OrbS. Important regions for σ factor function are underlined in black and labelled accordingly. Identical residues at the corresponding position are shown in white font and shaded black, and similar residues are shown in white font and shaded grey. Alignment was carried out using ClustalW, using the longest possible translated product encoded by *orbS*. The important regions of PvdS had been previously identified in an extensive alignment (Gruber and Gross, 2003), and from this the corresponding regions of OrbS were inferred.

CTD is disordered in crystal structures, suggesting that the position of this domain is not fixed, due to the flexible linker that connects it to the α NTD (Meng *et al.*, 2000). The α CTD and has been shown to interact with upstream DNA sequence elements (UP elements) and activator proteins at some promoters (Meng *et al.*, 2000; Ross *et al.*, 2003). The NTD of one of the units of the α_2 dimer associates with the β subunit, and the other with the β' subunit. The ω subunit (91 amino acids in *E. coli*) is a chaperone that associates with the C-terminus of β' and contributes to the binding of β' to the $\alpha_2\beta$ subassembly complex (Zhang *et al.*, 1999; Mathew and Chatterji, 2006). The β and β' subunits are the largest subunits of RNAP, at 1342 and 1407 amino acids, respectively, in *E. coli*. β and β' form a 'crab claw'-like structure, with a central channel of ~27 Å, in which a Mg^{2+} atom forms an active centre (Zhang *et al.*, 1999; Ebright, 2000).

1.7.2: The σ subunit

Core RNAP forms a complex with a σ factor to form a holoenzyme, which is capable of initiating transcription from specific promoter sequences (Figure 1.13) (Borukhov and Nudler, 2003). Two distinct σ factor families exist, based on sequence similarity. These are known as the σ^{54} and σ^{70} families, and they differ from one another almost entirely in amino acid sequence. Most eubacterial σ factors are of the σ^{70} family, which was named after the primary σ factor of *E. coli*. σ factors recognise specific DNA sequences known as 'promoters' located upstream of genes. σ^{70}-dependent promoters generally consist of two hexameric DNA sequence elements, located at approximately positions -35 to -30 and -12 to -7, with regards to the transcription start site of the downstream gene, and hence known as -35 and -10 regions, respectively (Wösten, 1998). The -10 region is also known as the Pribnow box, after David Pribnow, who first described this consensus element (Pribnow, 1975). The 17 bp (±1) separating these two hexameric DNA sequences, known as the spacer, is required to place the centres of the -35 and -10 elements on the same face of the DNA helix, ~2 turns apart (Auble *et al.*, 1986; Schulzaberger *et al.*, 2006). Some σ^{70}-dependent promoters do not have a -35 region, but have a 2 bp 'extended -10 region', located 1 bp upstream of the -10 element (Ponnambalam *et al.*, 1986).

Most bacteria contain one primary σ factor (known as σ^{70} or RpoD in *E. coli*) which is responsible for directing transcription of the majority of genes in the

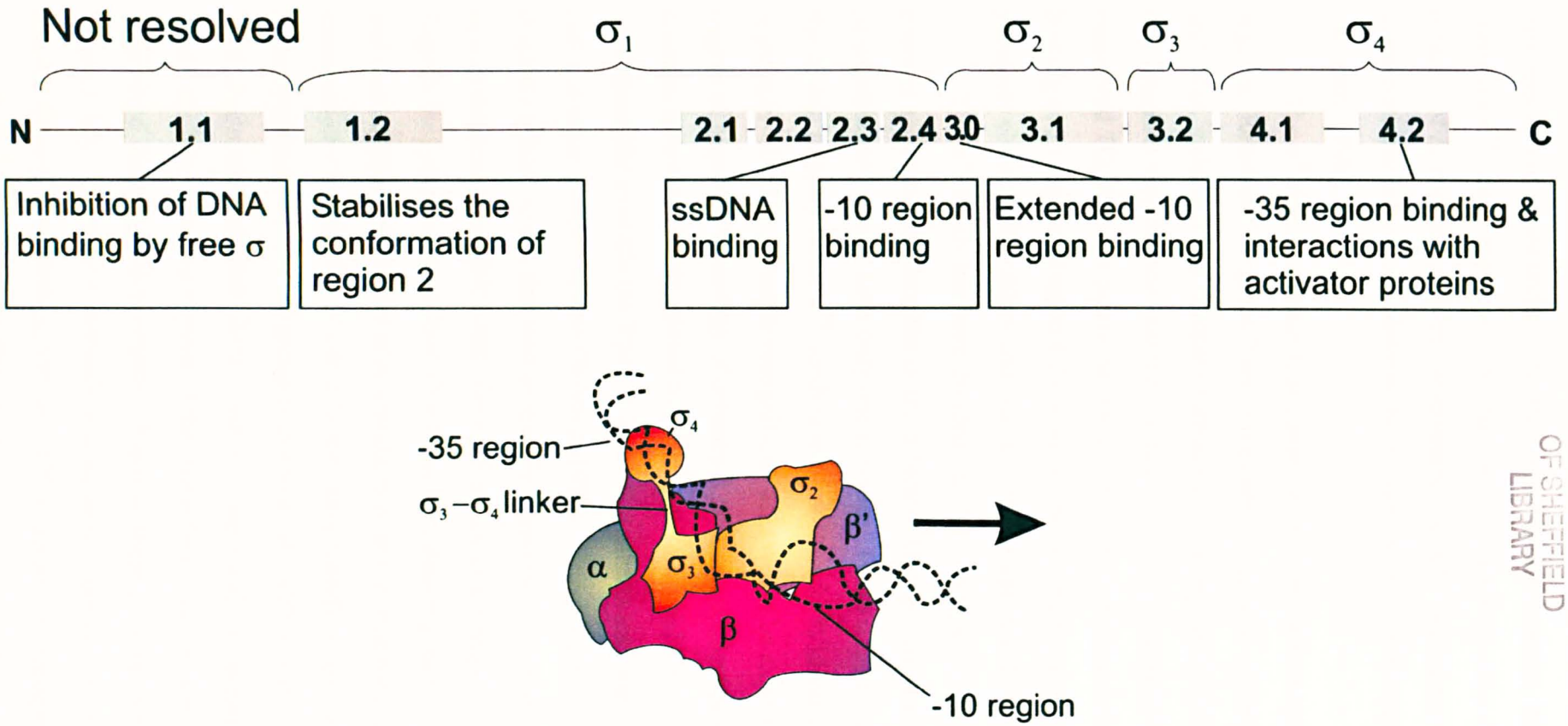

Figure 1.13: Structure of the *E. coli* Eσ^{70} holoenzyme. The amino acid sequence of σ^{70} has been divided into sections based on structure and sequence conservation with other σ^{70} family members. Regions encoding the four domains of σ^{70} are indicated at the top of the diagram, as are the functions of some of these regions (ssDNA is single-stranded DNA). Region 3.0 was formerly known as region 2.5, but was reclassified owing to its location within the same domain as region 3.1. A schematic representation of Eσ^{70} RNAP is depicted below, in which the αII subunit is occluded by αI. The α-CTD is not shown as its structure has not been resolved, owing to its mobile nature. ω is also occluded in this diagram. This subunit interacts with β'. The path of DNA through the holoenzyme has been shown throughout, and the direction of transcription has been indicated by an arrow. (Adapted from Borukhov and Nudler, 2003; Gruber and Gross, 2003; Paget and Helmann, 2003; Zenkin *et al.*, 2007).

bacterium, and a number of alternative σ factors, which allow the transcription of different sets of genes under different environmental stresses. Many bacteria also contain a σ^{54} family member. This family was named after the σ^{54} nitrogen regulation σ factor of *E. coli*, and require the assistance of ATP-dependent activator proteins for transcriptional activation, whereas the σ^{70} family tend not to require such activators (Wösten, 1998).

The σ^{70} family contain four conserved regions, which are divided into sub-regions. Residues in regions 2 and 3 mediate recognition of the promoter -10 element and DNA melting (open complex formation). Subregions 2.3 and 2.4 form an α-helix that interacts with the non-template strand of the -10 element. Region 3.0 contacts the conserved TG, found at positions -14 to -15, in the extended -10 element of promoters lacking a -35 region. Region 4.2 contains a helix-turn-helix motif that contacts the -35 promoter element (Borukhov and Nudler, 2003; Paget and Helmann, 2003).

The σ^{70} family has been divided into four categories based on the amino acid primary sequence and function of the σ factor. Group 1 contains the primary σ factors, of which most bacteria have only one member. These σ factors are closely related to the *E. coli* primary factor σ^{70}, tending to be at least 51 % identical, especially at regions involved in promoter recognition. This would be expected given the high degree of sequence homology of primary σ factor-dependent promoters. Group 2 contains σ factors closely related to σ^{70}, but not essential for cell growth under normal conditions, for example the RpoS σ factor that directs stationary phase growth in *E. coli* and other enteric bacteria (Wösten, 1998). Group 3 contains σ factors more distantly related to σ^{70}, that tend to specify transcription in response to a signal, such as a developmental check point. Group 3 σ factors are responsible for transcription of flagella biosynthesis, some heat shock and sporulation genes. Group 4 is the largest and most diverse group, and accommodates σ factors that mediate responses to extracytoplasmic signals. These σ factors have therefore been termed the ECF (extracytoplasmic function) group (Lonetto *et al*, 1992; Lonetto *et al*, 1994; Helmann, 2002; Paget and Helmann, 2003). Many group 3 and 4 σ factors lack region 1, which masks the DNA-binding regions of the free σ factor, and as a result such free σ factors might bind their cognate promoters. Many of these σ factors also lack region 3.2 (see Figure 1.14). This region normally maintains the correct spacing between regions 2.4 and 4.2 for promoter binding, and yet ECF σ factors still recognise -35 and -10 promoter elements, implying that the distance between regions 2.4 and 4.2 is

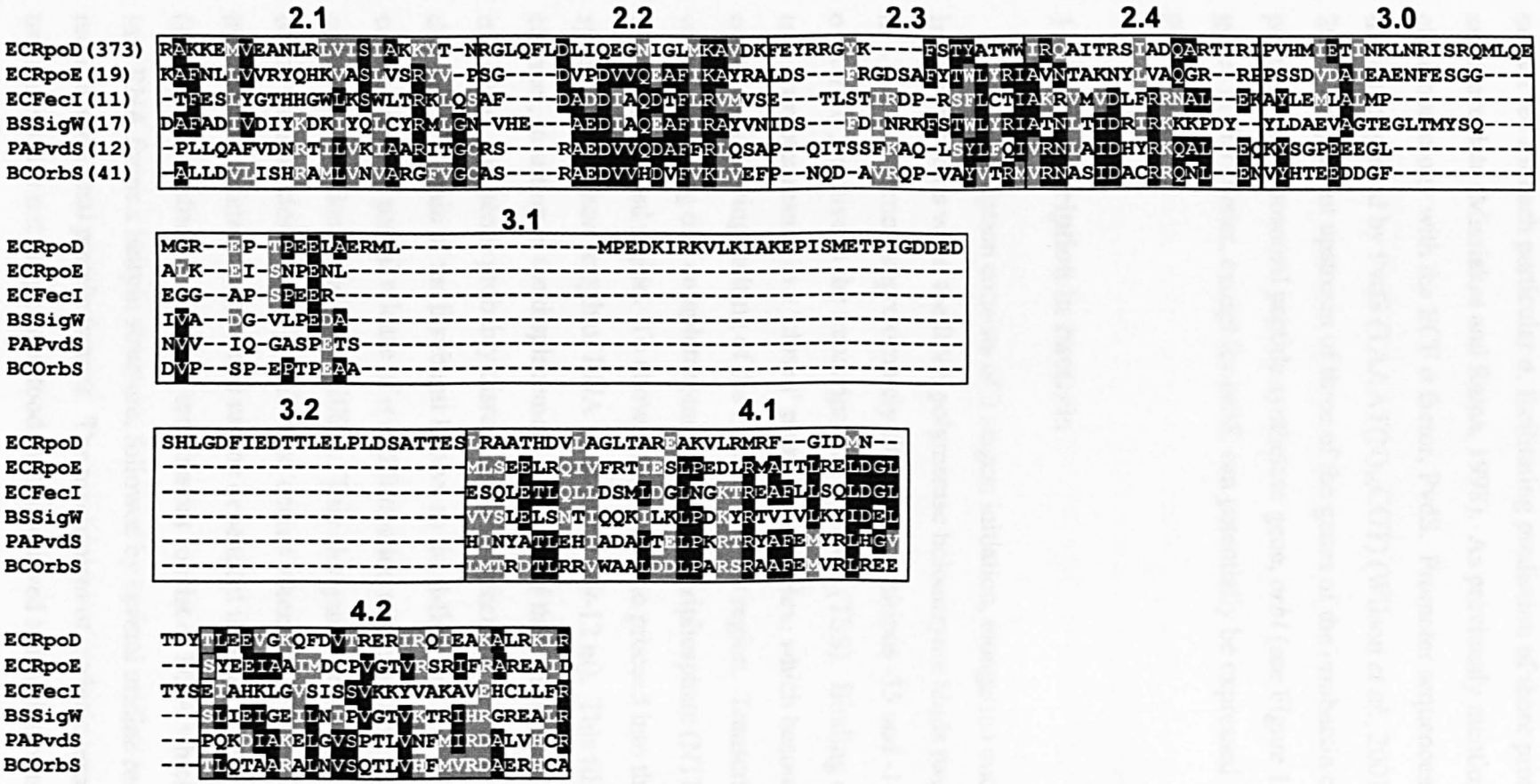

Figure 1.14: Alignment of *E. coli* RpoD (σ^{70}) with 4 known ECF σ factors and the putative ECF σ factor, OrbS. The alignment shows regions 2.1-4.1 of the following σ factors: *E. coli* RpoD (ECRpoD), *E. coli* RpoE (ECRpoE), *E. coli* FecI (ECFecI), *Bacillus subtilis* σ^{W} (BSSigW), *P. aeruginosa* PvdS (PAPvdS), and *B. cenocepacia* OrbS (BCOrbS). Numbers in brackets refer to the position of the first amino acid shown within each σ factor, and illustrate the additional N-terminal amino acids of RpoD, constituting region 1. Alignment was constructed using a ClustalW alignment of OrbS and PvdS (Figure 1.12) and the extensive alignment carried out by Gruber and Gross (2003), to ensure accuracy. The alignment was then shaded manually, with similar residues at a position in 50 % of polypeptides shown in white font and shaded grey, and identical residues at a position in 50 % of polypeptides shown in white font and shaded black.

maintained in such σ factors. The mechanism of this spacing has yet to be determined (Borukhov and Nudler, 2003).

The consensus promoter sequences recognised by ECF σ factors are highly conserved for each particular σ, facilitating prediction of these promoters from raw sequence data (Missiakas and Raina, 1998). As previously mentioned, OrbS shares close homology with the ECF σ factor, PvdS. Promoter sequences closely resembling those recognised by PvdS ($TAAAT(N)_{16}CGT$) (Wilson *et al.*, 2001; Ochsner *et al.*, 2002) are present upstream of three of the genes of the ornibactin cluster, including the putative non-ribosomal peptide synthetase gene, *orbI* (see Figure 1.11). All of the genes in this cluster, except for *orbS*, can potentially be expressed from these three promoters.

1.7.3: Transcription in bacteria

Transcription consists of 3 stages; initiation, elongation and termination. Initiation occurs when the RNA polymerase holoenzyme binds two conserved regions in a DNA sequence, approximately situated at positions -35 and -10 (in the case of the σ^{70} family) relative to the transcriptional start site (TSS). Binding of the holoenzyme to a promoter results in a 'closed' promoter complex, which becomes an 'open' complex following melting of the DNA at the -10 region. Transcription then begins, with the binding of a complementary nucleoside triphosphate (NTP) at the TSS (+1) within the melted region. To allow transcription to proceed into the elongation phase, synthesis of a short length of RNA must occur (~9-12 nt). This fills the RNA exit channel, resulting in the displacement of a loop of the σ factor within the channel (the $\sigma_{3.2}$ loop), and hence probably disrupting the interactions between the σ_4 globular domain, a domain of the β subunit known as the β-flap, and the -35 promoter element, causing at least partial release of σ and formation of the highly processive elongation complex (Murakami and Darst, 2003). This elongation complex proceeds to the end of the transcriptional unit. Termination occurs when RNAP encounters a transcriptional terminator, which can be dependent upon a protein factor, such as Rho (ρ), or can be intrinsic. Intrinsic terminators consist of DNA which when transcribed into RNA forms a hairpin structure, followed by several uridine residues, and do not require additional protein factors. The mechanism of intrinsic termination of transcription is not fully understood, but is believed to involve removal of the RNA

from the RNA binding site of the elongation complex by hairpin formation, and release of the complex as a result of weak hydrogen bonding between A and U residues (Yarnell and Roberts, 1999; Borukhov and Nudler, 2003; Murakami and Darst, 2003).

1.8: Siderophore-mediated transport systems

Each siderophore or class of siderophores requires its own specific receptor and other transport proteins that recognise the ferric siderophore complex but not the free siderophore, thereby ensuring iron uptake. *E. coli* produces one siderophore, enterochelin, but can utilise six others, including dicitrate, which is discussed further below. Clearly, in the absence of iron starvation or the specific ferric siderophore for each receptor, the production of the transport proteins required for each siderophore would be an unnecessary burden upon the cell. As a result, siderophore biosynthesis and transport pathways are carefully regulated, and σ factors may play an important role in this regulation. The transport systems for the siderophores ferrichrome and dicitrate have been extensively studied in *E. coli*. The general mechanisms involved in these and other ferric siderophore transport systems appear to be conserved, and are discussed below with particular reference to the ferric citrate and ferrichrome uptake systems.

1.8.1: Outer membrane siderophore receptors

Figure 1.15 illustrates the mechanism of ferric citrate transport. The outer membrane (OM) surface receptor for diferric dicitrate (the actual composition of this ferric siderophore complex), FecA, consists of a 22-strand β-barrel spanning the OM. Loops extend from this barrel out of the cell, which are involved in binding and recognition of ferric citrate. At the base of the barrel, where it contacts the periplasm, the β-strands are connected by much shorter turns that barely extend into the periplasm. A 'plug' domain (also known as a cork or hatch) is formed from approximately the first 150 residues at the N-terminus (Ferguson *et al.*, 2002; Yue *et al.*, 2003). This structure appears to be conserved throughout the transport receptors for the uptake of macromolecules too large to diffuse through OM porins, such as siderophores and vitamin B12 (Wiener, 2005), and is illustrated in Figure 1.16.

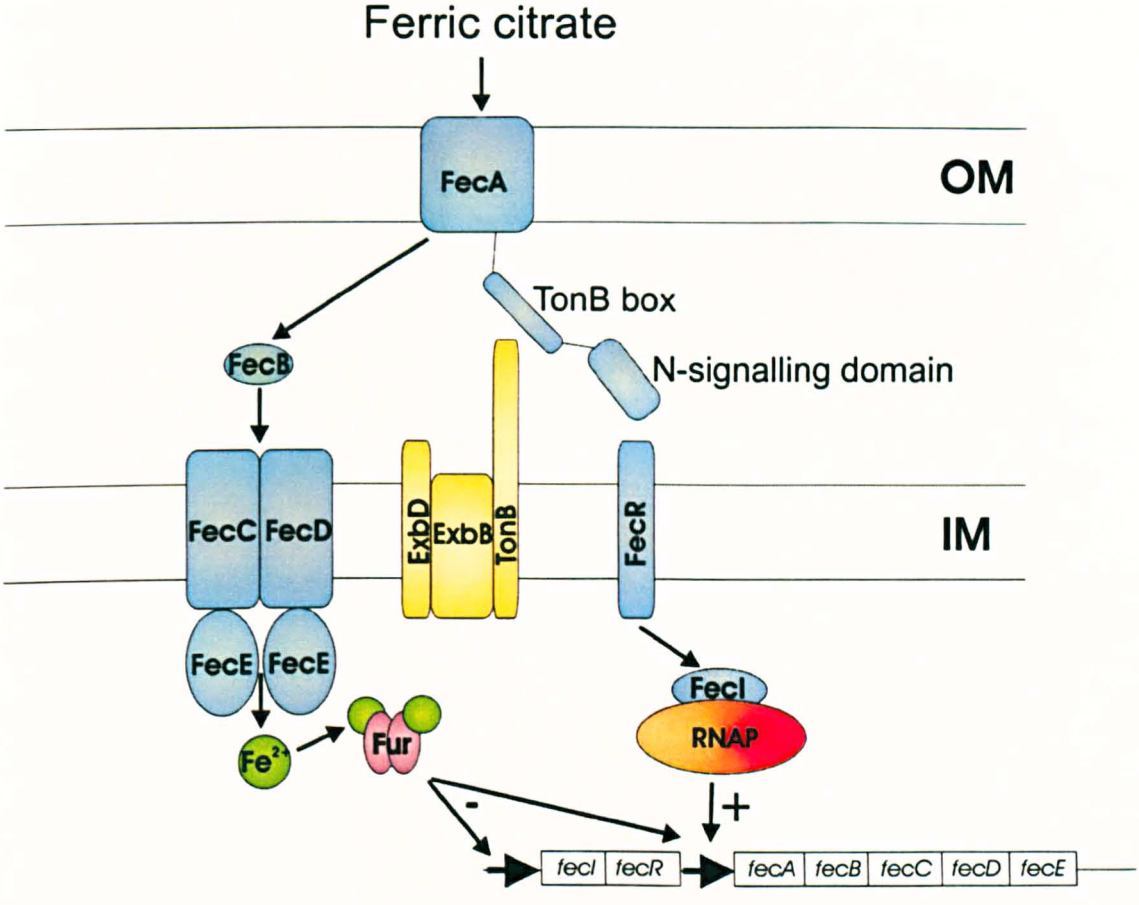

Figure 1.15: Mechanism of ferric citrate transport. The FecA receptor recognises diferric dicitrate, and transports it into the periplasm, utilising the proton motive force (PMF) generated at the inner membrane and transduced to the outer membrane by the TonB complex (shown in yellow). Fe^{3+} is transported from the periplasm into the cytoplasm (whether it is still part of a complex with citrate at this point is unknown) via the FecBCDE proteins. FecB is a periplasmic binding protein, and the FecCDE complex is an ABC transporter. The binding of ferric citrate by FecA also signals, via its N-terminal domain, for the activation of FecI (σ factor), via contact with the integral membrane regulator, FecR. FecI then directs transcription of the *fec* operon, resulting in increased concentration of the ferric citrate transport system. When intracellular iron levels become high, free Fe^{2+} binds the Fur aporepressor, activating it. Fur then negatively regulates transcription of the *fec* operon.

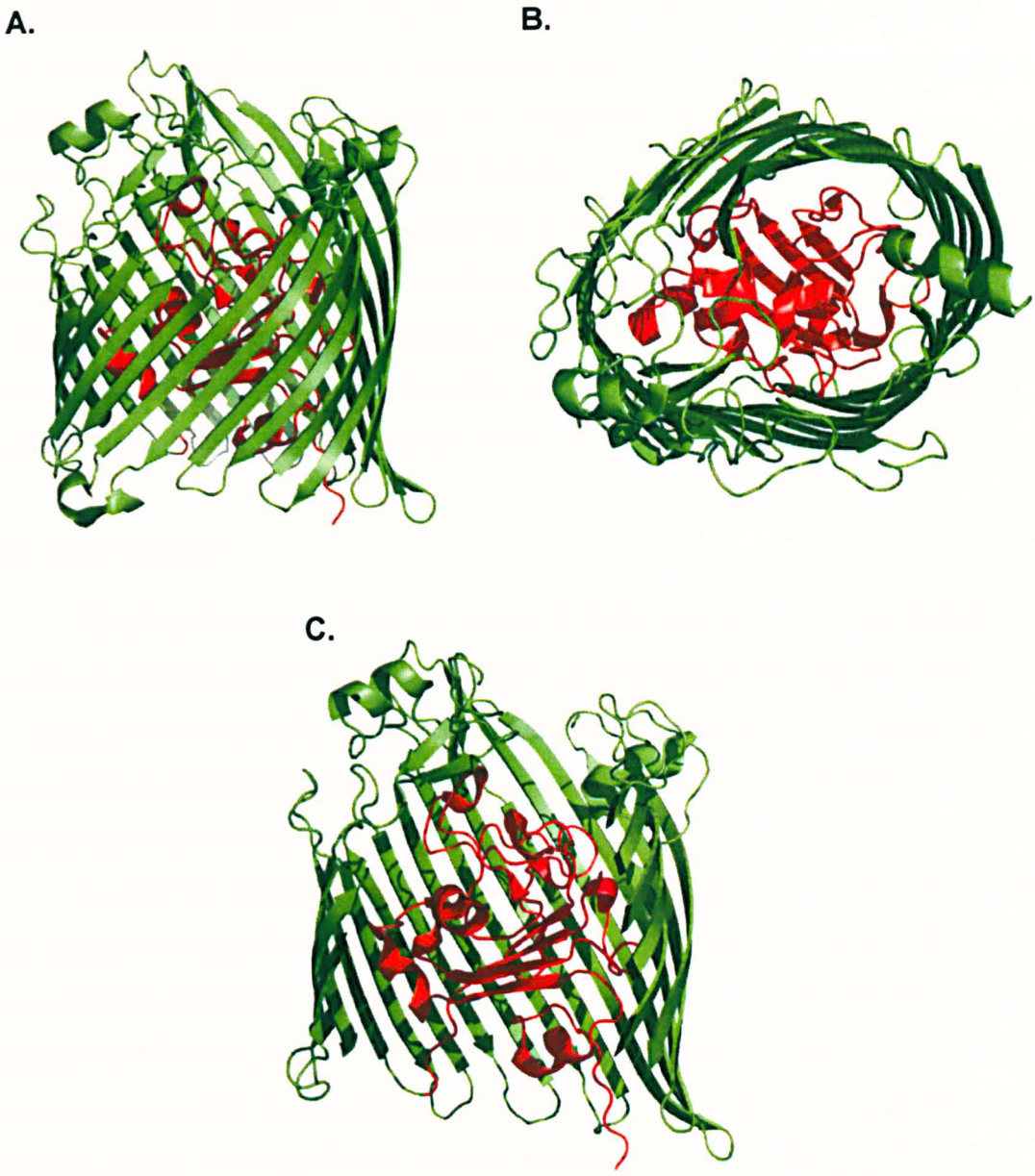

Figure 1.16: The crystal structure of unloaded FecA. Illustrations show FecA in the absence of bound substrate. The 22-strand β-barrel has been shown in green, whereas the plug domain has been shown in red. **A.** Side view of FecA showing the large extracellular loops and short periplasmic turns. The top of the β-barrel would extrude from the cell, and the bottom would contact the periplasm. **B.** Top view showing the lumen of the β-barrel occluded by the plug domain. **C.** Structure (shown in A) has been shown as if a section through the β-barrel had been taken, so as to better show the 'plug' domain. (PDB ID: 1KMO, Ferguson *et al.*, 2002).

Siderophore outer membrane receptors can constitute important targets for bacteriophages and antibiotics. For example, FhuA, the *E. coli* OM receptor for hydroxamate siderophores such as ferrichrome and its analogue ferricrocin, is also a receptor for the antibiotics albomycin and rifamycin CGP 4832, and for bacteriophages T5, T1, UC-1 and φ80. Initially, 2 genes were identified, the disruption of which resulted in resistance of *E. coli* to bacteriophage T1. These genes were named *tonA* and *tonB* (for T-one A and T-one B) (Hantke and Braun, 1978; Koebnik, 2005). Following elucidation of the role of TonA as the OM transporter for ferrichrome and analogues, it was renamed FhuA (for ferric hydroxamate uptake) (Kadner *et al.*, 1980). *tonB*, discussed further below, retained its name.

The 'plug' domain

The plug domain occludes the lumen of the β-barrel, and contains further loops which extend extracellularly, forming part of the siderophore binding site (Braun *et al.*, 2003; Buchanan, 2005). On binding of the ferric siderophore concerned, the extracellular loops of the receptor and plug domain close around the ferric siderophore, sequestering it.

In order for the ferric siderophore to pass across the OM, it is necessary for the plug domain to either change conformation or to be either partially or completely removed from the barrel. For ferric siderophore transport to be possible through the lumen of the β-barrel, a clear channel of ~15 Å in diameter is necessary, which is not apparent in any of the TonB-dependent transporters whose structures have been solved (Wiener, 2005). The available evidence is mixed as to whether the plug domain is removed from the lumen of the transporter. The results of one study suggest that the cork domain undergoes subtle rearrangements, facilitating ferric siderophore transport, as point mutations that led to disulphide bond formation between the barrel and cork domains of the ferrichrome receptor, FhuA, thus inhibiting its removal from the β-barrel, did not inhibit transport of a ferrichrome analogue (Eisenhauer *et al.*, 2005). However, a molecular dynamics study suggested that in order for a ferric siderophore to pass through the β-barrel structure, the plug domain would need to be at least partially removed from the barrel, mediated by solvation of the plug by a large number of water molecules present within the lumen of the barrel (Chimento *et al.*, 2005).

TonB and TonB-dependent transducers

An N-terminal extension of the FecA receptor protein is located within the periplasm. This consists of 2 domains, a TonB box, which interacts with TonB in response to ferric citrate binding, and a signalling domain which interacts with FecR. On binding of the ferric siderophore at the receptor, the TonB box undergoes a conformational change and becomes disordered, and therefore not visible to X-ray crystallography. This signals the presence of ferric citrate to TonB (Koebnik, 2005).

The storage of energy via an ion gradient, as occurs at the inner, cytoplasmic membrane (IM), results in a potential difference across this membrane. Such a gradient cannot be established across the OM, since small solutes may freely diffuse through the porins of this membrane. Futhermore, periplasmic phosphatases prevent energy production through ATP hydrolysis (Larsen *et al.*, 1996). Therefore the purpose of TonB is to transduce energy to the OM, for example to facilitate active transport. Energy from the ion gradient across the IM is probably harvested by a complex of proteins ExbB and ExbD (Postle and Larson, 2007).

The TonB protein is conserved throughout Gram-negative bacteria (Larsen *et al.*, 1996). *E. coli* TonB is 239 amino acids in length, and comprises an amino-terminal domain (residues 2-65) and a carboxy-terminal domain (residues 103-239), separated by a 36 amino acid proline-rich spacer. The structure of the entire TonB protein has not yet been solved. However, structures have been reported for the carboxy-terminal domain (Pawelek *et al.*, 2006).

The amino terminus contains a signal sequence for the export of TonB to the IM. However, the majority of the protein, including the entire linker region and C-terminal domain, is located in the periplasmic space. The spacer region is predicted to extend TonB, allowing it to reach across the periplasmic space to the OM. The importance of this region is unclear, however, since its deletion *in vivo* has little impact on TonB activity (Seliger *et al.*, 2001). The carboxy-terminal domain of TonB is responsible for interaction with OM transporters and energy transfer through as yet unknown conformational changes, resulting in disruption of the receptor's plug domain, allowing release of the ferric siderophore complex into the periplasm (Pawelek *et al.*, 2006).

A sub-group of the TonB-dependent transporters are the TonB-dependent transducers. These are involved not only in the transport of macromolecules across

the OM, but also in signal transduction. This sub-group is characterised by the presence of a signalling domain within the N-terminal extension, in addition to the TonB box, such as that present in FecA (see Figure 1.15). In the case of FecA, which is constitutively present at a low concentration, the binding of ferric citrate results in transcription of *fecA*, and hence an increase in the number of ferric citrate receptors present (Koebnik, 2005). This is mediated by a change in the N-terminal signalling domain of FecA, which signals to FecR, which is anchored within the CM. FecR is a regulator, and activates the FecI σ factor, allowing it to complex with core RNAP and direct transcription of the *fec* operon (Braun *et al.*, 2003; Buchanan, 2005; Garcia-Herrero and Vogel, 2005). This general mechanism appears to be common in siderophore transport systems that rely on ECF σ factors for transcription. However, in most such systems, instead of the regulator FecR, an anti-σ factor is involved. Like FecR, anti-σ factors involved in TonB-dependent transduction are anchored in the cytoplasmic membrane, and ordinarily bind their cognate σ factor. In response to the signal transmitted by the siderophore receptor signalling domain, the anti-σ releases its cognate σ, allowing it to function (Helmann, 1999; Koebnig 2005).

The OM receptor for ferric pyoverdine transport (FpvA) is an example of such a transducer. The binding of ferric pyoverdine to FpvA causes conformational changes resulting in interactions between the N-terminal domain of the receptor (including both the TonB box and signalling domain) and TonB and FpvR. FpvR is an anti-σ factor, and ordinarily binds the σ factors PvdS (responsible for transcription of the pyoverdine biosynthesis and transport genes) and FpvI (responsible for transcription of *fpvA*). In response to the binding of ferric pyoverdine to FpvA, these σ factors are released by FpvR, resulting in the transcription of their cognate gene sets (Redly and Poole, 2005; Wirth *et al.*, 2007).

A further aspect of regulation of transcription of the *fec* genes is mediated by the ferric uptake regulator, Fur. This is also a common factor involved in regulation of iron transport mechanisms, and is discussed in greater detail in Section 1.9.

1.8.2: ATP-binding cassette transporters

Import of ferric siderophore complexes into the cytoplasm, across the IM, and export of siderophores across this membrane into the periplasm, is mediated by a family of transporters known as the ATP-binding cassette (ABC) transporters. The

proteins FecB, FecD and FecE of the *fec* operon (Figure 1.15), are subunits of the ABC transporter responsible for the import into the cytoplasm of ferric citrate.

ABC transporters are present in both prokaryotes and eukaryotes. They consist of two similar or identical transmembrane domains (TMDs), each of which is formed by a series of membrane spanning α-helices. ATP is hydrolysed by a two domain ATPase component (ABC), providing the energy required to drive transport. ABC transporters span the IM, and are involved in the transport of numerous substrates in addition to siderophores and ferric siderophores, such as amino acids, sugars and vitamin B_{12}. The OM siderophore receptors display higher substrate specificity than the ABC transporters that mediate transport through the IM, and as a result there tend to be a greater number of different TonB-dependent OM receptors than ABC transporters. For example, 34 putative TonB-dependent transporters have been identified in the *P. aeruginosa* genome, most of which would be expected to be involved in ferric siderophore uptake, while only four ABC transporters have been identified to complete iron transport into the cell. Thus, one ABC transporter may be responsible for the uptake of several ferric siderophore complexes across the IM.

In eukaryotes, ABC transporters are involved in the transport of many different substrates. Most pertinent to this work, the cystic fibrosis transmembrane regulator (CFTR) is an ABC transporter responsible for chloride ion transport across the epithelium. Mutations in CFTR lead to CF (Section 1.3.2). The two TMDs and two ABC domains may be present in prokaryotic ABC transporters as up to 4 separate subunits, whereas those of the eukaryotes generally consist of only a single polypeptide (Locher *et al.*, 2002).

ABC transporters that function as importers in bacteria generally utilise a periplasmic binding protein to deliver the substrate to the periplasmic entrance to the transporter, while exporters tend to bind substrate directly from the cytoplasm (Locher *et al.*, 2002). On substrate binding to the entrance of the transporter, the ABC component (ATPase) carries out the 'power stroke' in which ATP binding and hydrolysis occur, concurrent with a conformational change resulting in substrate transport. Following substrate translocation, the products of ATP hydrolysis dissociate from the ABC component, and the transporter returns to a resting state (Locher *et al.*, 2002).

The structure of an ABC importer complex, including its periplasmic binding protein, has recently been solved. The archaeal putative molybdate transporter is

composed of two TMDs, each consisting of six membrane spanning α helices (ModB), two ABC domains (ModC), and the periplasmic binding protein, ModA. The general structure and mode of operation of ABC transporters is believed to be conserved throughout this family, and therefore this structure can be considered as a model for other ABC transporters (Hollenstein *et al.*, 2007). The structure of $ModB_2C_2A$ is illustrated in Figure 1.17.

1.9: The role of the ferric uptake regulator in iron homeostasis

As previously mentioned, iron is essential for bacterial cell growth. However, excess iron can catalyse the formation of toxic superoxides. A potential mechanism for Fe^{2+} efflux, involving the FieF antiporter, has recently been described for *E. coli* (Grass *et al.*, 2005), and furthermore iron uptake is tightly regulated to maintain intracellular concentrations within acceptable limits.

Iron-dependent regulation is achieved at the transcriptional level in a multitude of bacterial species by the ferric uptake regulator, Fur (Escolar *et al.*, 1999). Fur was originally identified as a 17 kDa zinc metalloprotein in *E. coli* (Schaffer *et al.*, 1985). Fur is a global regulator, and exhibits a high level of homology (>50% identity) throughout bacteria (Ochsner *et al.*, 1996). As a result, functional substitution with *E. coli* Fur can be used to confirm the status of putative Fur proteins in other bacteria (Lowe *et al.*, 2001). Fur binds free Fe^{2+}, causing a conformational change that allows the protein to bind as a dimer to specific motifs called Fur boxes located at iron-regulated promoters. The sequence of the Fur box consists of two overlapping inverted repeat sequences, each of which is bound by a Fur dimer (Baichoo and Helmann, 2002; Lavrrar and McIntosh, 2003). Binding of the Fur-Fe^{2+} complex to a Fur box overlapping a promoter prevents the binding of RNA polymerase at the promoter. When iron concentrations are low, the equilibrium of bound and unbound iron is displaced, and so iron is released from Fur, causing it to dissociate from the Fur boxes and allowing transcription to take place (Escolar *et al.*, 1999). This process is illustrated in Figure 1.18. It has been hypothesized that two Fur dimers bind to the Fur box, with one Fur dimer positioned on either DNA strand of the site. This was postulated because a single Fur dimer would be expected to protect at most 20 bp in a DNAse I protection assay, while the observed protection in such assays spans 27-30 bp. Pohl and colleagues have solved the crystal structure of *P. aeruginosa* Fur, and

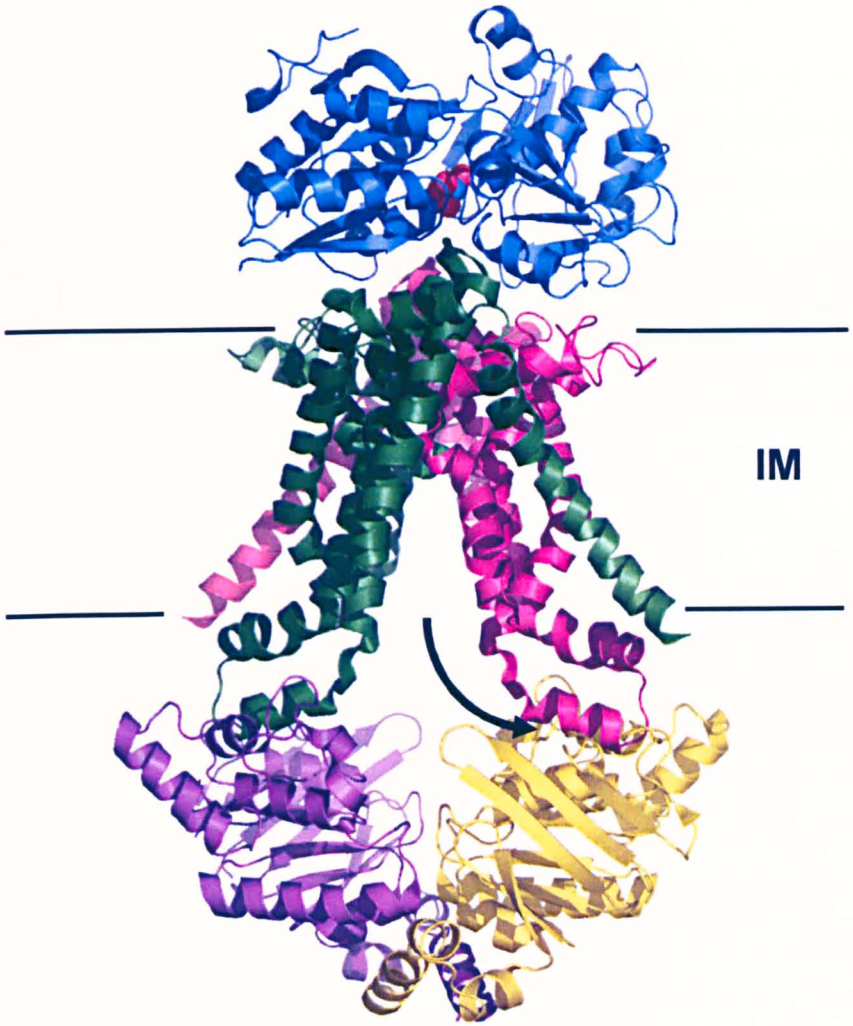

Figure 1.17: The structure of the $ModB_2C_2A$ ABC transporter. Each protein subunit is shown in a different colour; the two transmembrane subunits (ModB) are shown in pink and green, and the ABC cassette subunits (ModC) in yellow and purple. Molybdate (represented as a cluster of red spheres attached to a light-blue central sphere) is presented at the periplasmic entrance to the transporter (top) by a periplasmic binding protein, ModA (blue). The ABC (ATPase) component carries out the 'power stroke' in which ATP binding and hydrolysis occur, concurrent with a conformational change resulting in substrate transport through the transmembrane domain. The substrate exits the transporter via a large water-filled space at the cytoplasmic end of the transporter. This is indicated with a bold arrow. The inner membrane (IM) is also indicated. (PDB ID: 2ONK; Hollenstein *et al.*, 2007).

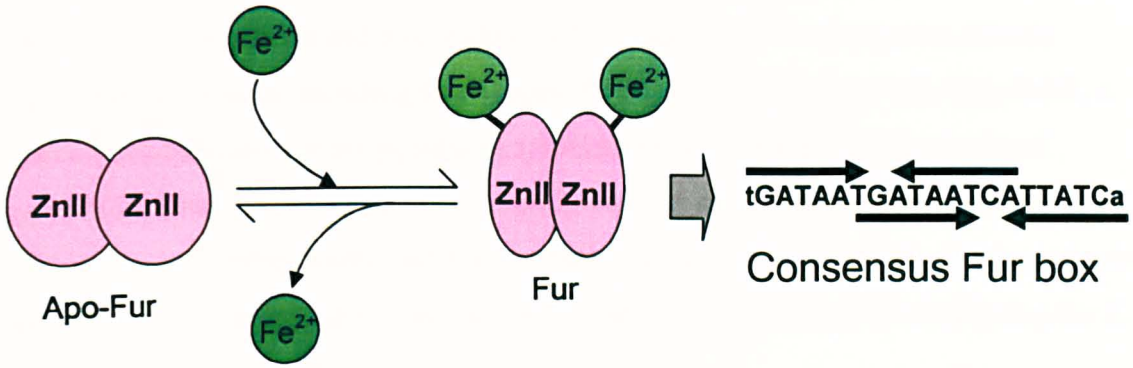

Figure 1.18: General mechanism of repression by Fur. Free Fe^{2+} ions bind the Fur aporepressor, changing its conformation. The resultant Fur repressor can then bind to 'Fur box' sequences located in the promoter regions of iron-dependently regulated genes, blocking RNAP binding. Each Fur monomer contains a ZnII metallocentre, as indicated. Bold arrows illustrate the overlapping inverted repeat sequences postulated by Baichoo and Helmann, 2002.

produced a potential model showing the binding of two Fur dimers to the *pvdS* Fur box (Pohl *et al.*, 2003).

Fur has been shown to negatively regulate the production of the two siderophores pyochelin and pyoverdine in *P. aeruginosa*. Fur boxes are present upstream of the gene encoding the σ factor PvdS, and of the genes encoding PchR, a transcriptional activator for pyochelin synthesis required for the biosynthesis of pyochelin, *pchE* (an NRPS-encoding gene), and the pyochelin receptor gene, *fptA* (Ochsner *et al.*, 1996; Redly and Poole, 2003; Thomas, 2007). The *B. cenocepacia fur* gene has been cloned and sequenced, and is capable of functionally substituting for *E. coli fur* (Lowe *et al.*, 2001).

1.10: The ornibactin operon

Transposon mutagenesis identified three genes that were essential for ornibactin biosynthesis and utilisation (Section 1.6.). By BLAST searches, these genes were found to be part of a larger cluster of genes, exhibiting homology to genes required for the biosynthesis and utilisation of siderophores in other bacteria (Figure 1.11). Therefore, it was hypothesised that this cluster is responsible for the biosynthesis and utilisation of ornibactin. Three other genes in the ornibactin cluster had been previously characterised: *pvdA*, *orbA*, and *pvdF* (Sokol *et al.*, 1999; Sokol *et al.*, 2000). The names for the remaining ornibactin cluster genes were assigned as shown in Figure 1.11.

The putative mechanism of ornibactin synthesis and transport has been determined by *in silico* study of the similarity of the ornibactin cluster genes with genes of known function, and using experimentally determined information about *pvdA, orbA* and *pvdF*.

1.10.1: Ornibactin synthesis

Ornibactin is made up of four amino acids, of which only L-serine is one of the 22 amino acids that can be incorporated into proteins by the ribosome. The remaining three amino acids consist of an aspartate and two ornithine residues, all of which have been derivatised: β-hydroxyaspartate, N^5-3-hydroxyacyl, N^5-hydroxyornithine and N^5-formyl-N^5-hydroxyornithine. The aspartic acid is also in the D form, rather than the L

enantiomer incorporated into ribosomally synthesised proteins. The modification processes of these amino acids, described below, are illustrated in Figure 1.19. β-hydroxyaspartate is formed by the addition of a hydroxyl group to C3 of the L-aspartate. This is probably mediated by OrbG, which is homologous to α-ketoglutarate-dependent hydroxylases. These enzymes are responsible for similar modifications to a number of amino acids, including aspartate (Hausinger, 2004). Genes exhibiting homology to OrbG are present in those pseudomonads that incorporate β-hydroxyaspartate into their pyoverdines, such as *P. syringae* and *P. putida*, but are absent from *P. aeruginosa*, which does not utilise this amino acid in pyoverdine synthesis (Meyer, 2000). During incorporation into the ornibactin peptide, the β-hydroxyaspartate is epimerised to the D form by a domain within OrbI.

To make N^5-3-hydroxyacyl, N^5-hydroxyornithine and N^5-formyl-, N^5-hydroxyornithine, PvdA (L-ornithine N^5-oxygenase), first adds a hydroxyl group to the side-chain nitrogen of ornithine, which is produced as an intermediate of arginine synthesis (Visca *et al.*, 1994). N^5-formyl-, N^5-hydroxyornithine is then formed by addition of a formyl group by PvdF (N^5-hydroxyornithine transformylase) (McMorran *et* al., 2001; Thomas, 2007). PvdA and PvdF are so named because their products are similar to the two genes of the same name involved in pyoverdine synthesis in *P. aeruginosa,* and are predicted to carry out the same reactions. Pyoverdine also contains ornithine derivatised with a hydroxyl and formyl group at the side-chain nitrogen. Following addition of a hydroxyl group to ornithine by PvdA, N^5-3-hydroxyacyl, N^5-hydroxyornithine is made by derivatisation with a β-hydroxy acid, also at the side-chain nitrogen. This is probably carried out by either OrbK or OrbL, which are homologous to N-acetyl transferases.

It is not clear at which point the modifications to the constituent amino acids of ornibactin occur. Figure 1.20 illustrates the assembly of ornibactin by the two NRPS units of ornibactin synthetase, OrbI and OrbJ. The adenylation domains present in the NRPSs are responsible for activating the α-carboxyl group of the amino acids, allowing the phosphopantetheine (P-pant) arms attached to the peptidyl carrier domains to form thioester bonds with the activated amino acids. The condensation domains present in the NRPSs promote the formation of peptide bonds between the amino group of each amino acid as it becomes positioned within one of these domains, and the activated carboxyl group linked to the adjacent P-pant arm. This results in displacement of the more N-terminal amino acid (or growing peptide) from the P-pant

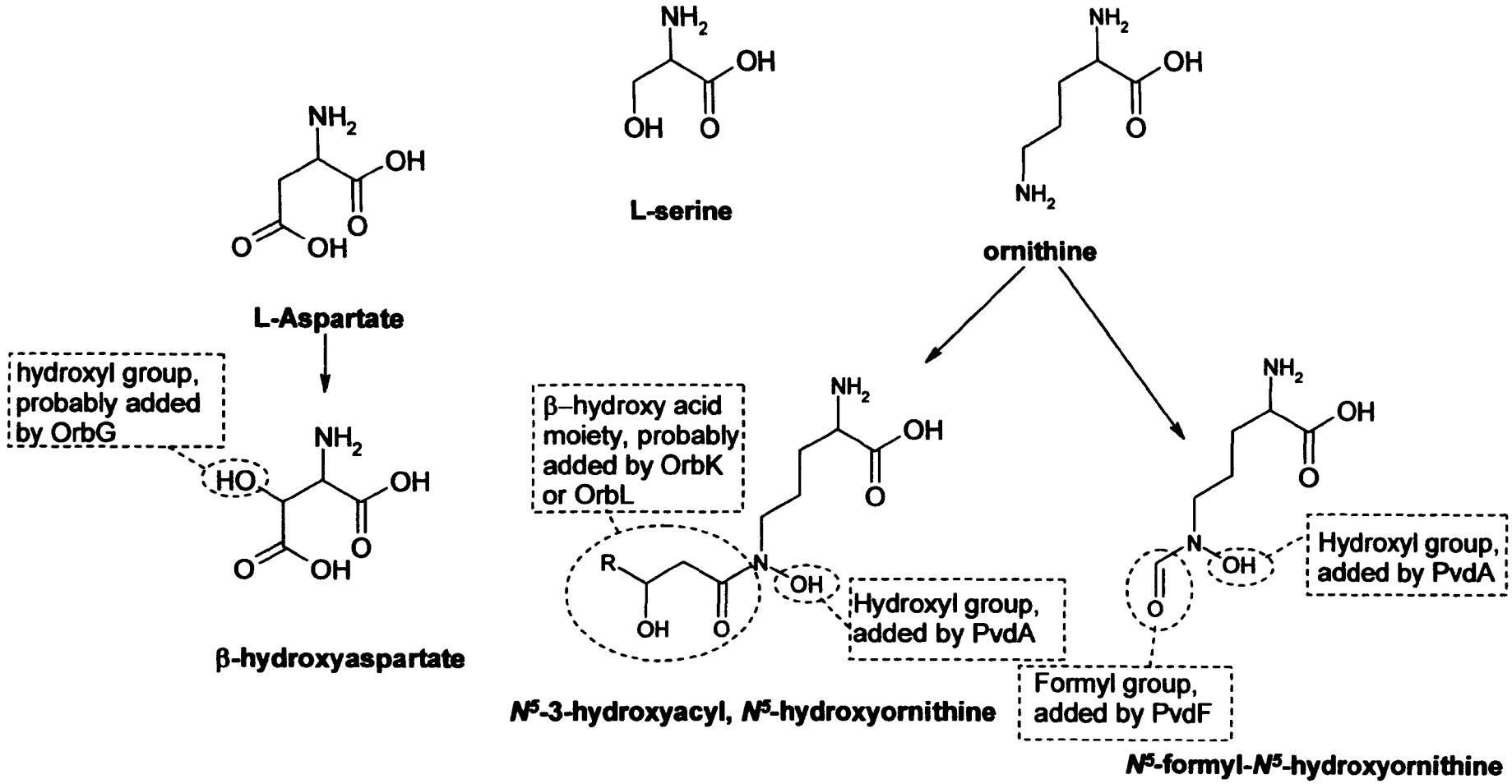

Figure 1.19: The amino acids of ornibactin and the putative mechanisms for their derivatisation. R= C_4, C_6 or C_8, and this variability in carbon chain length is probably a result of the different putative acyltransferases (OrbK and OrbL).

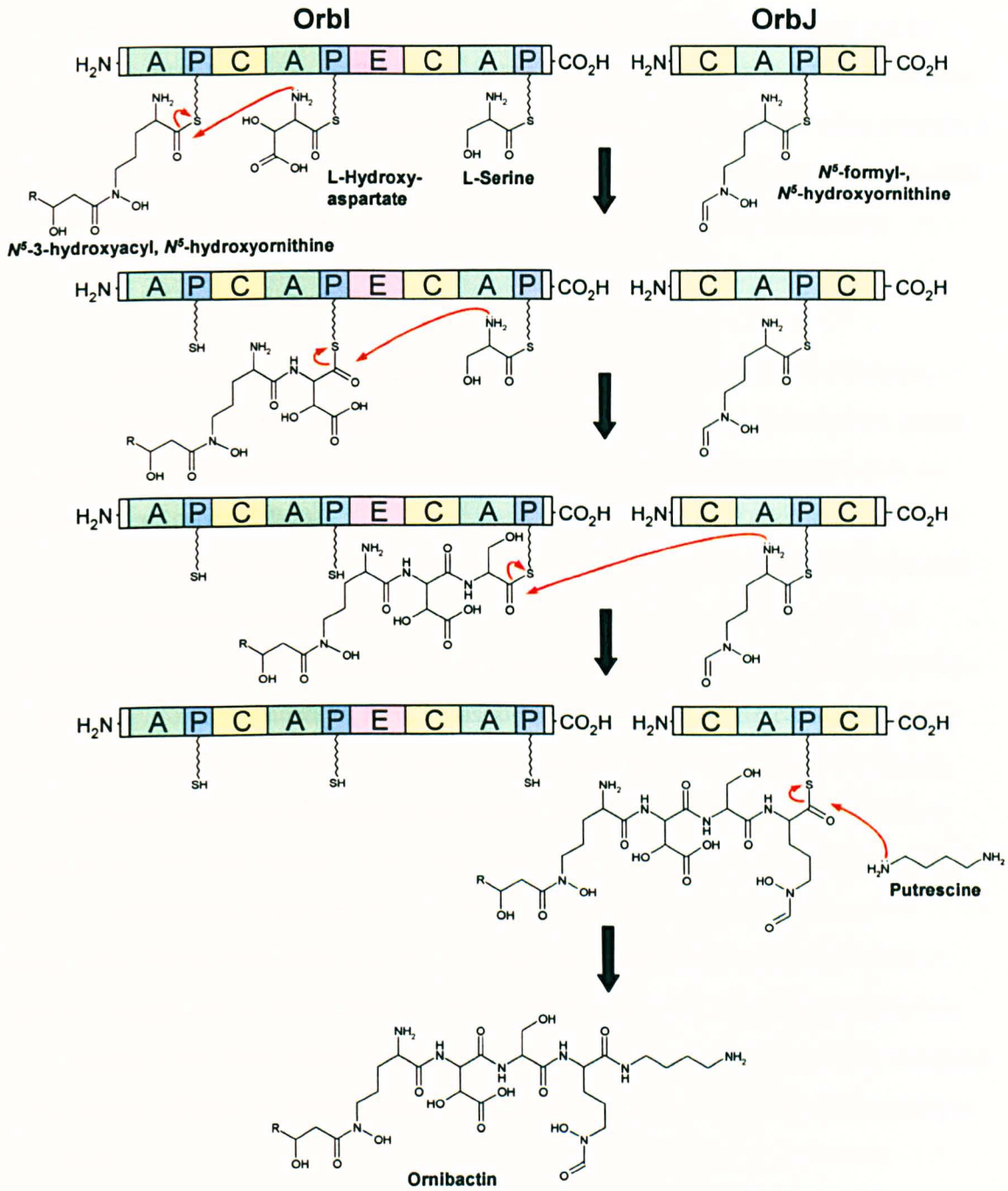

Figure 1.20: Model for the non-ribosomal synthesis of ornibactin. The NRPSs OrbI and OrbJ consist of adenylation (A), peptidyl carrier (P) and condensation (C) domains. OrbI also contains a predicted epimerase (E) domain for the conversion of L-hydroxyaspartate to D-hydroxyaspartate. The phosphopantetheine arms to which the amino acids are bound are shown as zig-zag lines. Curved arrows represent the formation of peptide bonds, catalysed by the condensation domains of the NRPSs. In this figure it is assumed that the modifications carried out to the constituent ornithine and aspartate amino acids (apart from the epimerisation of hydroxyaspartate) have taken place prior to their incorporation into the growing peptide chain, although it is not known if this is the case (adapted from Thomas, 2007).

arm, and causes the growing peptide to move towards the C-terminus of the NRPS. The final step is displacement of ornibactin from the NRPS. This is carried out by putrescine, which displaces ornibactin from the final P-pant arm in OrbJ by formation of an amide bond, in a similar manner to earlier displacements. NRPSs often contain a thioesterase domain, or else a free thioesterase is required, for the cleavage of the final thioester bond, but in this case such an enzyme is predicted to be unnecessary.

1.10.2: Ornibactin transport

In most cases, those genes not implicated in the biosynthesis of ornibactin, described above, were also assigned putative functions by homology to known genes. Amongst the predicted products of these genes were two ABC-type transporters (described in Section 1.8.2).

Of the two putative ABC transporters involved in ornibactin utilisation, one is a predicted importer and one an exporter. The putative importer is comprised of subunits encoded by *orbC* and *orbD*. These subunits were assigned putative functions by homology to components of ABC transporters involved in ferric citrate and ferric hydroxamate uptake in *E. coli*. The two TMDs of the transporter comprise a single OrbD subunit, unlike the situation in the molybdate transporter, where they are two separate subunits (see Figure 1.17). Two OrbC subunits comprise the two domains of the ABC component, analogous to the two ModC subunits of the molybdate transporter. Ferric ornibactin is probably delivered to the periplasmic face of the $OrbC_2D$ transporter by the product of *orbB*. OrbB is homologous to the periplasmic components of the ferric citrate and ferric hydroxamate ABC importers, and analogous to the ModA subunit of the molybdate transporter (Agnoli *et al.*, 2006; Hollenstein *et al.*, 2007).

The remaining putative ABC transporter is the product of *orbE*. This transporter was identified by homology to the PvdE protein of the *P. aeruginosa* pyoverdine gene cluster. Both OrbE and PvdE have the characteristics of ABC transporters. However, in these cases both the transmembrane and ATP cassette region are located within a single subunit. OrbE and PvdE also share homology with a number of exporters for antibiotics, such as the SyrD syringomycin efflux pump of *Pseudomonas syringae* (Quigley *et al.*, 1993), and since no other candidate exporter is encoded within the gene clusters for ornibactin and pyoverdine utilisation, they are

likely to be responsible for export of unloaded siderophore across the IM (Agnoli *et al.*, 2006).

A further transporter-encoding gene has been identified, known as *orbA*. The OrbA protein was found to be located in the OM, and is necessary for ornibactin utilisation in *B. cenocepacia* (Sokol *et al.*, 2000). The predicted amino acid sequence of OrbA contains a TonB box near its N-terminus, as would be expected, as all active OM ferric siderophore transporters characterised thus far are TonB-dependent, as discussed in Section 1.8.1. The predicted amino acid sequence of mature (i.e. processed) OrbA lacks the N-terminal signalling domain present in the transducer sub-group of TonB-dependent receptors, previously discussed (Section 1.8.1), as illustrated in Figure 1.21 (Koebnik, 2005). This suggests that this receptor does not interact with an anti-σ factor. This is supported by the lack of a putative anti-σ factor-encoding gene within the ornibactin cluster. Such a gene would normally be situated adjacent to the gene encoding the σ factor responsible for transcription of the siderophore synthesis and utilisation genes (Koebnik, 2005). In this case the putative σ factor responsible for transcription of the ornibactin operon is OrbS, as previously discussed. Rather than a putative anti-σ factor-encoding gene, *orbS* is adjacent to *orbH* (see Figure 1.11). The putative product of *orbH* is an 80 amino acid protein exhibiting homology to MbtH of *Mycobacterium tuberculosis*, a protein required for the production of the siderophore mycobactin. Homologues of *mbtH* are present in the clusters for biosynthesis and utilisation of a number of other non-ribosomal peptides, including the pyoverdine cluster of *P. aeruginosa*, however the function of these *mbtH*-like genes remains unknown (Quadri *et al.*, 1998; Agnoli *et al.*, 2006).

A single gene of the ornibactin cluster remains to be discussed. This gene is *orbF*, which encodes a putative reductase, homologous to a putative reductase of *E. coli*, FhuF. FhuF has been shown to increase removal of iron from the siderophores coprogen, ferrichrome and ferrioxamine B. Siderophores have a much lower affinity for Fe^{2+} than Fe^{3+}, and therefore reduction of iron complexed with a siderophore, followed by binding of that iron by another ligand, constitutes an efficient mechanism for removal of iron from ferric siderophore complexes. FhuF contains a C-terminal motif consisting of four cysteines (organised as $CC(X)_{10}C(X)_2C$), constituting an iron-sulphur cluster. This motif is proposed to constitute the alternative iron-binding ligand mentioned above (Muller *et al.*, 1998). OrbF contains a similar motif, organised as

Figure 1.21: Alignment of the N-terminal regions of TonB-dependent receptors. Shown are the N-termini of the following TonB-dependent siderophore receptors; *P. aeruginosa* FoxA, FiuA and FpvA (PAFoxA, PAFiuA, PAFpvA); *E. coli* FecA, FhuA and FepA (ECFecA, ECFhuA, ECFepA) and *B. cenocepacia* OrbA and FptA (BCOrbA, BCFptA). Predicted signal leader sequences have been shown in red. The putative TonB box regions have been highlighted in yellow. Between the TonB box and signal cleavage site in the FoxA, FiuA, FpvA and FecA proteins is the conserved N-terminal signalling region present in TonB-dependent transducers. The remaining TonB-dependent receptors lack this region. Alignment was performed using ClustalW. The N-terminal TonB-dependent transducer regions have been shown in white font and highlighted black for identical and grey for similar residues, using a matching threshold for shading of 50 % (adapted from Thomas, 2007).

$CC(X)_{11}C(X)_2C$, indicating that this protein too is likely to contain an iron-sulphur cluster.

The genes described above with putative functions in ornibactin utilisation have been used to construct a model of ornibactin utilisation, illustrated in Figure 1.22. In this model, ornibactin, as assembled in the biosynthetic pathway already described, is exported via the OrbE ABC transporter through the IM. The mechanism by which ornibactin crosses the outer membrane is unclear. Outside the cell, ornibactin chelates Fe^{3+}, and crosses the OM into the periplasm via the TonB-dependent OrbA receptor. Ferric ornibactin is then bound by OrbB and translocated through the IM by the OrbCD ABC transporter. Once in the cytoplasm, complexed iron is removed from the ornibactin siderophore by the OrbF reductase, potentially readying the siderophore for export once more.

1.11: The siderophore malleobactin of *Burkholderia pseudomallei*

The non-Bcc pathogen *B. pseudomallei* elaborates the siderophore malleobactin in response to iron-limitation (Yang *et al.*, 1991). Recent work has shown that malleobactin consists of a mixture of at least 3 compounds, as is the case with ornibactin. Malleobactin biosynthesis and utilisation is encoded by a gene cluster similar to the ornibactin cluster of *B. cenocepacia*, but lacking homologues of genes OrbK and OrbL, and containing an additional ORF (BSPL1782) with no homologue in the *B. cenocepacia* ornibactin cluster. It has been shown that the OM receptor for ferric malleobactin (FmtA) is capable of transporting ornibactin, and that the ornibactin receptor, OrbA, can transport malleobactin, restoring growth to biosynthetic mutants of *B. pseudomallei* and *B. cenocepacia*. This suggests that these siderophores are similar in structure, and this is supported by mass spectrometry analysis of malleobactin (Alice *et al.*, 2006). The absence of OrbK and OrbL homologues in the *mba* gene cluster, which are believed to be responsible for derivatisation of nascent ornibactin with a 3-hydroxy acid, suggests that while similar, these siderophores may not be identical. Transcription of the malleobactin gene cluster is specified by a putative ECF σ factor, MbaS, which is highly homologous (73 % identity) to *B. cenocepacia* OrbS (Figure 1.23) (Alice *et al.*, 2006).

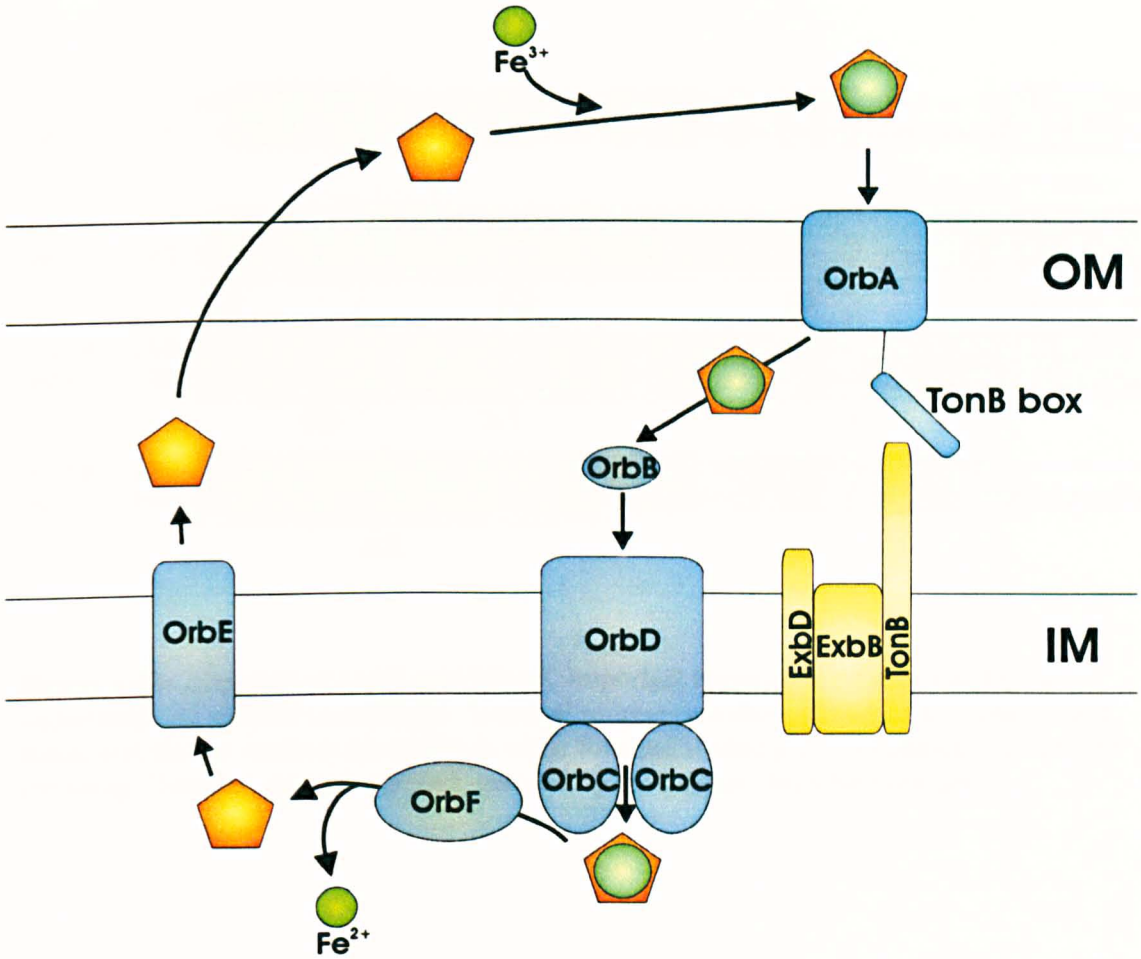

Figure 1.22: Model for ornibactin transport in *B. cenocepacia*. Proteins encoded by ornibactin cluster genes have been shown in blue. Proteins involved in the TonB complex have been shown as yellow oblongs. Ornibactin is represented as an orange pentagon, and iron is represented as a green circle. Ornibactin is exported across the inner, cytoplasmic membrane (IM) by the ABC transporter OrbE. The mechanism for transport of ornibactin across the outer membrane (OM) is unclear. Outside the cell, ornibactin forms a complex with Fe^{3+}, and is transported across the OM by the TonB-dependent OrbA transporter. An ABC transporter comprising OrbB, OrbD and OrbC is responsible for import of ferric ornibactin into the cytoplasm, where it is released from the siderophore by OrbF reductase. It has been suggested that following removal of iron, siderophores might be ready for export once more, and this has been reflected in the model (adapted from Thomas, 2007).

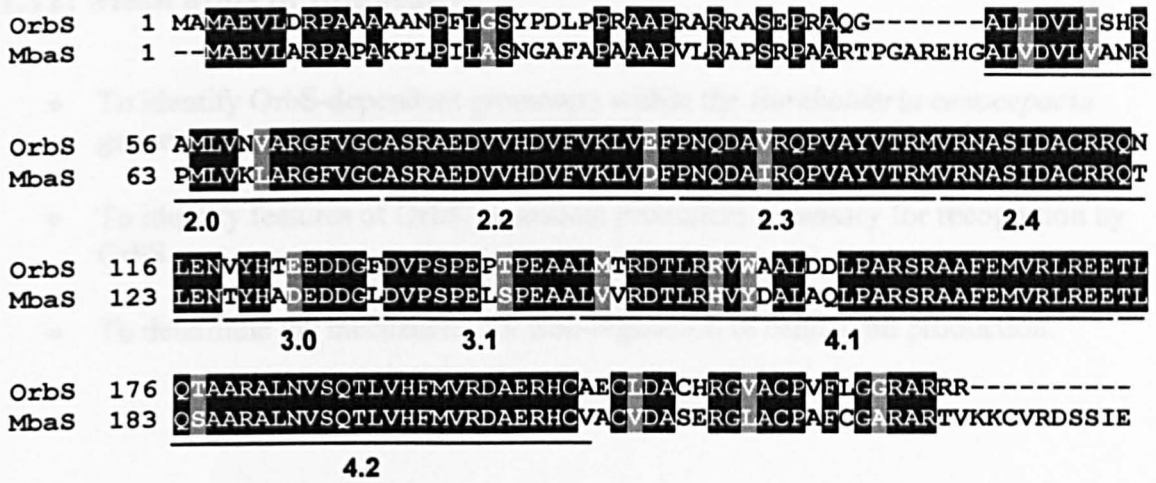

Figure 1.23: Aligment of OrbS and MbaS. Important regions for σ factor function are underlined and labelled accordingly. Identical residues are shown in white font and shaded black, and similar residues are shown in white font and shaded grey. Alignment was carried out using ClustalW, using the protein encoded by the longest ORFs for each gene.

1.12: Main aims of this study

- To identify OrbS-dependent promoters within the *Burkholderia cenocepacia* genome.
- To identify features of OrbS-dependent promoters necessary for recognition by OrbS.
- To determine the mechanism for iron-regulation of ornibactin production.

Chapter 2

Materials and Methods

Table 2.1: Bacterial Strains used in this study

Bacterial strain	Genotype/description	Source/reference
B. cenocepacia		
715j	CF isolate, prototroph	McKevitt *et al.*, 1989; Darling *et al.*, 1998
KLF1	spontaneous Pch$^-$ mutant of 715j	Farmer, 1998
OM1	KLF1-*orbI*::mini-Tn*5*Tp (Orb$^-$ Pch$^-$ Tp^R)^c	Agnoli *et al.*, 2006
OM3	KLF1-*orbS*::mini-Tn*5*Tp (Orb$^-$ Pch$^-$ Tp^R)	Agnoli *et al.*, 2006
715j-orbS::Tp	715j with *dfrB2* cassette inserted in *orbS* (Orb$^-$ Pch$^+$ Tp^R)	Agnoli *et al.*, 2006
H111	CF isolate, prototroph	Romling *et al.*, 1994; Gotschlich *et al.*, 2001
H111-orbS::Tp	H111 with *dfr* cassette inserted in *orbS* (Orb$^-$ Pch$^+$ Tp^R)	Agnoli *et al.*, 2006
P. aeruginosa		
PAO1	prototroph	Stover *et al.*, 2000
PAO1-pvdS::Gm	PAO1 *aac1* cassette inserted in *pvdS* (Pvd$^-$ Gm^R)	Ochsner *et al.*, 1996
E. coli		
MC1061	*hsdR araD139* Δ(*ara-leu*)7697 Δ*lacX74 galU galK rpsL* (Sm^R)	Casadaban and Cohen, 1980
JM83	F$^-$ *ara* Δ(*lac-proAB*) *rpsL* ϕ80d*lacZΔM15* (Sm^R)	Yanisch-Perron *et al.*, 1985
NM522	Δ(*lac-proAB*) *thi* Δ(*hsdMS-mcrB*)5 (r_K^-, m_K^-) *supE*/F' *lacI^q lacZΔM15 proAB*$^+$	Gough and Murray, 1983
H1717	*aroB fhuF*::λp*lac*Mu53	Hantke, 1987
QC1732	F$^-$ Δ(*argF-lac*)*U169 rpsL* Δ*fur*::*kan* (Sm^R Km^R)	Touati *et al.*, 1995
S17-1	*thi proA hsdR recA* RP4-2-*tet*::Mu-1 *kan*::Tn*7* integrant (Tp^R Sm^R)	Simon *et al.*, 1983
DH5α	F$^-$ Φ80d*lacZΔM15* Δ(*lacZYA-argF*)$_{U169}$ *recA1 endA1 hsdR17*(r_K^-, m_K^+) *supE44 thi-1 relA1 gyrA96*	Hanahan *et al.*, 1983

Abbreviations used within this table: Ap^R, encodes ampicillin resistance; Gm^R, gentamycin resistant; Rf^R, rifampicin resistant; Sm^R, streptomycin resistant; Tp^R, trimethoprim resistant; Pch$^-$, pyochelin-negative phenotype; Orb$^-$, ornibactin-negative phenotype; Pvd$^-$, pyoverdine-negative phenotype.

Table 2.2: Plasmids used in this study

Plasmid	Description	Source/reference
pBBR1MCS	mobilisable BHR cloning vector. IncP- and ColE1-compatible (Cm^R)	Kovach *et al.*, 1994
pBBR1MCS-2	mobilisable BHR cloning vector. IncP- and ColE1-compatible (Km^R)	Kovach *et al.*, 1995
pBBR1MCS-5	mobilisable BHR cloning vector. IncP- and ColE1-compatible (Gm^R)	Kovach *et al.*, 1995
pBBR-orbS	pBBR1MCS containing the *B. cenocepacia* 715j *orbS* gene (Cm^R)	Agnoli *et al.*, 2006
pBBR-orbSΔX	pBBR1MCS containing ~900bp *orbS* gene minus sequence for N-terminal extension (Cm^R)	This study
pBBR-orbSC196A	pBBR-orbS containing mutations in *orbS* codon 196 resulting in a C → A substitution (Cm^R)	Agnoli, 2003
pBBR-orbSC2199A	pBBR-orbS containing mutations in *orbS* codon 199 resulting in a C → A substitution (Cm^R)	Agnoli, 2003
pBBR-orbSC203A	pBBR-orbS containing mutations in *orbS* codon 203 resulting in a C → A substitution (Cm^R)	This study
pBBR-orbSC209A	pBBR-orbS containing mutations in *orbS* codon 209 resulting in a C → A substitution (Cm^R)	This study
pBBR-orbSC196+203A	pBBR-orbS containing mutations in *orbS* codons 196 and 203 resulting in 2 C → A substitutions (Cm^R)	This study
pBBR-orbSC196+209A	pBBR-orbS containing mutations in *orbS* codons 196 and 209 resulting in 2 C → A substitutions (Cm^R)	This study
pBBR-orbSCtetraA	pBBR-orbS containing mutations in *orbS* codons 196, 199, 203 and 209 resulting in 4 C → A substitutions (Cm^R)	This study
pBBR-orbSΔP	pBBR1MCS containing *orbS* coding sequence and Shine-Dalgarno but minus promoter (Cm^R)	Agnoli, 2003
pBBR-orbSΔP2	pBBR-orbSΔP cut with *Asp*718 and *Xho*I, end-filled and religated to produce a nonsense codon in frame with *lacZα* (Cm^R)	This study
pBBR-orbSΔP-ptac	pBBR-orbSΔP containing *ptac* upstream of MCS (Cm^R)	This study
pBBR-orbS-69	pBBR1MCS containing *orbS* with upstream endpoint at -69 relative to TSS (Cm^R)	This study

pBBR-orbS-40	pBBR1MCS containing *orbS* with upstream endpoint at -40 relative to TSS (Cm^R)	This study
pBBR-orbSi1-TAA	pBBR1MCS containing *orbS* with first potential translation initiation codon (ATG) substituted with TAA (stop) (Cm^R)	This study
pBBR-orbSi2-TAA	pBBR1MCS containing *orbS* with second potential translation initiation codon (ATG) substituted with TAA (stop) (Cm^R)	This study
pBBR-orbSi3-TAA	pBBR1MCS containing *orbS* with third potential translation initiation codon (GTG) substituted with TAA (stop) (Cm^R)	This study
pBBR-orbSi2-GCC	pBBR1MCS containing *orbS* with second potential translation initiation codon (ATG) substituted with GCC (ala) (Cm^R)	This study
pBBR-orbSi3-GTC	pBBR1MCS containing *orbS* with third potential translation initiation codon (ATG) substituted with GTC (val) (Cm^R)	This study
pBBR-pvdS	pBBR1MCS containing *P. aeruginosa pvdS* gene (Cm^R)	
pBBR-2-orbS	pBBR1MCS-2 containing *B. cenocepacia* 715j *orbS* (Km^R)	This study
pBBR-2-pvdS	pBBR1MCS-2 containing *P. aeruginosa* PAO1 *pvdS* gene (Km^R)	This study
pBBR-5-orbS	pBBR1MCS-5 containing *B. cenocepacia orbS* (Gm^R)	This study
pBBR-5-orbSCtetraA	pBBR1MCS-5 containing *orbS* gene from pBBR-orbSCtetraA (Cm^R)	This study
pBBR-5-pvdS	pBBR1MCS-5 containing *P. aeruginosa PvdS* gene (Gm^R)	This study
pBR328	Cloning vector. IncP-compatible (Cm^R, Tc^R, Ap^R)	Soberon *et al.*, 1980
pUCP22	pRO1600-based BHR cloning vector (Ap^R)	West *et al.*, 1994
pUCP22-pvdS	pUCP22 containing 1.8 kb *Pst*I fragment harbouring *P. aeruginosa pvdS* gene without its native promoter (Ap^R)	I. Lamont (Otago)
pUC18rrnBT1T2b	pUC18 containing *E. coli rrnB*T1T2 terminators (Ap^R)	M.S. Thomas, unpublished
pUC18NotlacZYA	pUC18Not containing 5.90 kb promoterless *lacZYA* cassette (Ap^R)	E. Dave and M.S. Thomas, unpublished
pUTmini-Tn5CmlacZYA	pUT containing mini-Tn5 bearing *cat lacZYA* (Ap^R, Cm^R)	M.S. Thomas, unpublished

pTZ110	Mobilisable BHR *lac* reporter vector (Ap^R)	Schweizer and Chuanchuen, 2001.
pKAGb1(+)	pTZ110 harbouring *cat* cassette from pUTminiTn5CmlacZYA inserted into *bla* gene in same orientation as *lacZ* (Cm^R)	This study
pKAGb1(-)	pTZ110 harbouring *cat* cassette from pUTminiTn5CmlacZYA inserted into *bla* gene in opposite orientation to *lacZ* (Cm^R)	This study
pKAGb2(+)	pTZ110 harbouring PCR amplified *cat* gene of pBR328 inserted into *bla* gene in same orientation as *lacZ* (Cm^R)	This study
pKAGb2(-)	pTZ110 harbouring PCR amplified *cat* gene of pBR328 inserted into *bla* gene in opposite orientation to *lacZ* (Cm^R)	This study
pRW50	BHR *lacZ* reporter vector with pUC18 MCS (Tc^R)	Lodge *et al.*, 1992
pRW50-pbfd	pRW50 containing *pbfd-lacZ* fusion (Tc^R)	This study
pRW500	pRW50, with *Bam*HI-*Sac*I *lacZ* fragment from pTL61T in place of 5' half of *lacZ* and *trpBA* (Tc^R)	M.S. Thomas, unpublished
pKAGc1	pRW500 with *Hin*dIII site in MCS (Tc^R)	This study
pKAGc1-pbfd	pKAGc1 containing *pbfd-lacZ* fusion (Tc^R)	This study
pKAGc2	pKAGc1 with *rrnB*T1T2 terminators from pUC18rrnBT1T2b inserted upstream of MCS (Tc^R)	This study
pKAGc2-pbfd	pKAGc2 containing *pbfd-lacZ* fusion (Tc^R)	This study
pPR9TT	mobilisable BHR *lacZ* translational fusion vector, IncP (Cm^R, Ap^R)	Santos *et al.*, 2001
pKAGd2	transcriptional fusion vector derived from pPR9TT (Cm^R, Ap^R)	This study
pKAGd2-ptac	pKAGd2 bearing *ptac-lacZ* fusion (Cm^R, Ap^R)	This study
pKAGd4	pKAGd2 containing *lacZ* gene and RNAse III processing site from pUC18NotlacZYA (Cm^R, Ap^R)	This study
pKAGd4-ptac	pKAGd4 bearing *ptac-lacZ* fusion (Cm^R, Ap^R)	This study
pKAGd4-cysI	pKAGd4 bearing *B. cenocepacia cysI-lacZ* fusion (Cm^R, Ap^R)	M.S. Thomas, unpublished
pKAGd4-cysD	pKAGd4 bearing *B. cenocepacia cysD-lacZ* fusion (Cm^R, Ap^R)	M.S. Thomas, unpublished

pKAGd4-porbSfl	pKAGd4 containing *porbSfl-lacZ* fusion (Cm^R, Ap^R)	This study
pKAGd4-porbHfl	pKAGd4 containing *porbHfl-lacZ* fusion (Cm^R, Ap^R)	This study
pKAGd4-porbEfl	pKAGd4 containing *porbEfl-lacZ* fusion (Cm^R, Ap^R)	This study
pKAGd4-porbIfl	pKAGd4 containing *porbIfl-lacZ* fusion (Cm^R, Ap^R)	This study
pKAGd4-porbS-69	pKAGd4 containing *porbS* with upstream endpoint at -69 (Cm^R, Ap^R)	This study
pKAGd4-porbS-40	pKAGd4 containing *porbS* with upstream endpoint at -40 (Cm^R, Ap^R)	This study
pKAGd4-porbS+5	pKAGd4 containing *porbS* with upstream endpoint at +5 (Cm^R, Ap^R)	This study
pKAGd4-ppvdEfl	pKAGd4 containing *P. aeruginosa ppvdEfl-lacZ* fusion (Cm^R, Ap^R)	This study
pKAGd4-ppvdFfl	pKAGd4 containing *P. aeruginosa ppvdFfl-lacZ* fusion (Cm^R, Ap^R)	This study
pKAGd4-ppvdEds(1-7)	pKAGd4 containing minimal *ppvdE* promoter-*lacZ* fusions, containing corresponding ds oligonucleotide (see Appendix 1) (Cm^R, Ap^R)	This study
pKAGd4-porbHds(1-51)	pKAGd4 containing *porbH* promoter-*lacZ* fusions, containing corresponding ds oligonucleotide (see Appendix 1) (Cm^R, Ap^R)	This study
pKAGd4ΔAp	pKAGd4 containing *nptII* cassette from p34E-Km inserted in *bla* gene (Cm^R, Km^R)	This study
pKAGd4ΔAp-porbSfl	pKAGd4ΔAp containing *porbSfl-lacZ* fusion (Cm^R, Km^R)	This study
p34E-Tp	p34E containing *dfr* gene (Tp^R, Ap^R)	DeShazer and Woods, 1996
p34E-Km	p34E containing *nptII* cassette from pKNOCK-Km (Km^R, Ap^R)	E. Bull and M.S.T., unpublished
pTrc99A	pBR322-derived expression vector containing strong inducible *trc* promoter and $lacI^q$ gene (Ap^R)	Amann *et al.*, 1988
pAHA21	pTrc99A containing *B. cenocepacia fur* gene (Ap^R)	Lowe *et al.*, 2001
pUC18	*E. coli*-specific cloning vector (Ap^R)	Yanisch-Perron *et al.*, 1985
pAHA18	pUC18 containing *B. cenocepacia pbfd* (Ap^R)	Asghar, 2002
p3ZFBS	pGEM3Z containing consensus *E. coli* Fur binding site (Ap^R)	Vanderpool and Armstrong, 2001
pBluescript II KS	*E. coli*-specific cloning vector (Ap^R)	Alting-Mees and Short, 1989
pBS-porbSfl	pBluescript II KS containing full-length *orbS* promoter (Ap^R)	This study

pBS-porbS-69	pBluescript II KS containing *porbS* with upstream endpoint -69 (Ap^R)	This study
pBS-porbS-40	pBluescript II KS containing *porbS* with upstream endpoint -40 (Ap^R)	This study
pBS-porbS+5	pBluescript II KS containing *porbS* with upstream endpoint +5 (Ap^R)	This study
pBS-porbHfl	pBluescript KS II containing *orbHfl* promoter (Ap^R)	This study
pBS-porbEfl	pBluescript KS II containing *orbEfl* promoter (Ap^R)	This study
pBS-porbIfl	pBluescript KS II containing *orbIfl* promoter (Ap^R)	This study
pBS-ptac	pBluescript KS II containing *tac* promoter (Ap^R)	This study
pET-14b	*E. coli*-specific expression vector for producing N-terminally His-tagged protein	Novagen
pET-porbS	pET-14b containing *orbS*	This study
pGEX-KG	*E. coli*-specific expression vector for producing N-terminally GST-tagged protein	Guan and Dixon, 1991
pGEX-orbS	pGEX-KG containing *orbS*	This study
pGEX-orbSNT	pGEX-KG containing N-terminal of *orbS*	This study
pGEX-orbSCT	pGEX-KG containing C-terminal of *orbS*	This study

Abbreviations used within this table: Ap^R, encodes ampicillin resistance; Cm^R, encodes chloramphenicol resistance; Km^R, encodes kanamycin resistance; Gm^R, encodes gentamycin resistance, Tp^R, encodes trimethoprim resistance; Tc^R, encodes tetracycline resistance; MCS, multiple cloning site; BHR, broad host-range; ds, double-stranded; TSS, transcriptional start site,

2.1: Bacteriological techniques

2.1.1: Bacteriological media

All media were stored at room temperature, or at 4 °C if not sterilised, unless otherwise stated.

LB broth and LB agar

The following were dissolved in 1000 ml H_2O (>18 MΩ).

- 10 g tryptone
- 5 g yeast extract
- 10 g NaCl

The resultant LB broth was then distributed into 10 ml and 100 ml aliquots and autoclaved.

LB agar was made by solidifying LB broth with 1.5 % (w/v) agar (Oxoid).

Minimal salts medium and minimal salts agar

Glucose was dissolved in 90 ml H_2O (>18 MΩ). A final concentration of 0.2 % glucose was used for *E. coli* growth, or 0.5 % for *B. cenocepacia*. To make agar plates, 1.5 g agar (Oxoid) was added to 90 ml minimal salts medium. The medium was then autoclaved and cooled to ~60 °C prior to addition of the salts below:

- 10 ml X10 M9 salts
- 0.1 ml 1M $MgSO_4$, filter sterilised using a 0.22 μm membrane
- 0.1 ml 0.1M $CaCl_2$, filter sterilised using a 0.22 μm membrane

X10 M9 salts

- 60 g Na_2HPO_4 anhydrous
- 30 g KH_2PO_4 anhydrous
- 5 g NaCl
- 10 g NH_4Cl

H_2O (>18 MΩ) was added to a total volume of 1 L, and the salts solution autoclaved.

Chrome azurol S (CAS) agar

CAS agar was prepared using the method of Schwyn and Neilands, 1987. CAS mix and Y minimal agar were prepared and autoclaved separately. Following cooling to ~45 °C, 10 ml CAS mix was slowly poured into 90 ml Y minimal agar, and mixed thoroughly but slowly until homogeneous.

CAS mix

For 90 ml CAS mix, the following were mixed in 50 ml H_2O (>18 MΩ) until the CAS powder was dissolved. 1 mM $FeCl_3.6H_2O$ was prepared by dissolution in 10 mM HCl.

- 10 ml 1 mM $FeCl_3.6H_2O$
- 60.5 mg CAS powder

72.9 mg hexadecyltrimethylammonium bromide (HDTMA) was dissolved in 40 ml H_2O (>18 MΩ), which was then added to the CAS/$FeCl_3$ mixture with constant stirring. CAS mix was stored at room temperature in the dark.

Y minimal agar

- 0.169 g glutamic acid (sodium salt)
- 0.3 g Tris base
- 0.1 ml $MgSO_4.7H_2O$ (10 % w/v)
- 0.1 ml $CaCl_2.6H_2O$ (22 % w/v)
- 0.1 ml $K_2HPO_4.3H_2O$ (22 % w/v)

The above components were dissolved in H_2O (>18 MΩ), and after adjusting the pH to 6.8, the final volume was adjusted to 90 ml. 1.5 g agar (Oxoid) was added prior to autoclaving.

On combining the CAS mix with Y minimal agar, the resultant CAS agar contained 10 μM $FeCl_3$. For CAS agar containing excess iron, 50 μM additional $FeCl_3.6H_2O$ was added to the medium prior to pouring, to give a final concentration of 60 μM Fe^{3+}.

CAS plates were streaked as described in Section 2.1.3.

2.1.2: Media supplements

Stock solutions of media supplements were made up as described below. They were incorporated into media at the concentrations indicated in Table 2.3.

$FeCl_3$

$FeCl_3$ was dissolved in 10 mM HCl to a concentration of 0.1 M. It was then filter sterilised and stored at room temperature in the dark.

2'2-dipyridyl

2'2-dipyridyl was dissolved in 100% ethanol to a concentration of 0.1 M. Stored at -20 °C.

Ethylenediaminedi(o-hydroxyphenylacetic) acid (EDDHA)

EDDHA was dissolved in 1M NaOH to a concentration of 30 mg ml^{-1}. This was added to M9 salts agar following the addition of the other components. This was stored at 4 °C for up to two days. EDDHA was not sterilised before use.

IPTG

Isopropyl β-D-thiogalactoside was dissolved to a concentration of 100 mM in H_2O (>18 MΩ), after which it was filter sterilised and stored at –20 °C.

X-gal

5-bromo-4-chloro-3-indolyl-β-D-galactoside was dissolved to 20 mg ml^{-1} in dimethylformamide (DMF), and stored at –20 °C.

Chloramphenicol (Cm)

Cm was dissolved to 25 mg ml^{-1} in absolute ethanol, and stored at –20 °C.

Ampicillin (Ap)

Ap was dissolved to 100 mg ml^{-1} in H_2O (>18 MΩ). The solution was then filter sterilised and stored at –20 °C.

Kanamycin (Km)

Km was dissolved to 25 mg ml^{-1} in H_2O (>18 MΩ), filter sterilised and stored at –20 °C.

Tetracycline (Tc)

Tc was dissolved to 40 mg ml^{-1} in H_2O (>18 MΩ). An equal volume of absolute ethanol was added to give a final concentration of 20 mg ml^{-1}. The solution was stored at -20 °C.

Table 2.3: Final concentration of media supplements

Supplement (medium)[a]	Bacterium		
	E. coli	*B. cenocepacia*	*P. aeruginosa*
Antibiotics			
Cm (LB)	25 μg ml^{-1}	50 μg ml^{-1}	60 μg ml^{-1}
Cm (M9)	N/A	100 μg ml^{-1} to select for pKAGd4. 50 μg ml^{-1} for other plasmids and for β-galactosidase assays.	100 μg ml^{-1}
Km (M9)	N/A	100 μg ml^{-1} (H111)	600 μg ml^{-1}
Km (LB)	25 μg ml^{-1}	N/A	400 μg ml^{-1}
Ap (LB)	100 μg ml^{-1}	N/A	N/A
Gm (LB)	20 μg ml^{-1}	N/A	N/A
Antibiotic combinations			
Cm, Km (M9)	N/A	Cm 50 μg ml^{-1}, Km 50 μg ml^{-1}	Cm 100 μg ml^{-1}, Km 400 μg ml^{-1}
Cm, Km (LB)	Cm 25 μg ml^{-1} Km 25 μg ml^{-1}	N/A	N/A
Cm, Gm (LB)	Cm 25 μg ml^{-1}, Gm 20 μg ml^{-1}	N/A	N/A
Others			
Casamino acids (M9)	0.1 % (w/v)	0.1 % (w/v)	0.1 % (w/v)
2'2- dipyridyl (LB)	175 μM	N/A	N/A
2'2- dipyridyl (M9)	N/A	100 μM	100μM
$FeCl_3$ (all media)	50 μM	50 μM	50 μM

[a]The medium given in parentheses indicates the medium in which the concentration of supplement given was used.

2.1.3: Agar plate-based phenotypic tests

Testing bacterial cultures on CAS agar

To ensure that approximately equal numbers of bacteria were streaked, 5 ml BHI cultures containing antibiotics as appropriate for plasmid maintenance (see Table 2.3), were grown overnight to saturation at 37 °C with shaking. Bacteria were transferred to the agar using a sterile loop, and plates were incubated at 37 °C for ~12 hours to allow diffusion of siderophores.

Fur titration Assay (FURTA)

FURTA was carried out using *E. coli* strain H1717, into which high copy number plasmids bearing the DNA sequence to be analysed for the presence of Fur binding sites were introduced by transformation. MacConkey agar base (Difco) was made as per the manufacturer's guidelines, and sterilised by autoclaving. 1 % (w/v) lactose and 40 μM $Fe(NH_4)_2(SO_4)_2$ (from a filter sterilised 30 mM stock solution (dissolved in H_2O (>18 MΩ)) were added following cooling of the agar to ~50 °C, whereupon the agar was poured into Petri-dishes and allowed to set. Cells to be analysed by FURTA were grown overnight at 37 °C in LB broth, and sreaked onto the agar using a sterile wire loop. Inoculated Petri-dishes were incubated overnight at 37 °C to allow colony formation.

2.1.4: Determination of bacterial growth rate

In order to determine the growth rate of bacterial strains in a particular medium, the strains to be analysed were grown overnight at 37 °C with shaking. The overnight cultures were then diluted in the same medium to a standard OD_{600} (0.5), and 1 ml used to inoculate 50 ml aliquots of the desired medium. Growth was monitored by taking 1 ml samples immediately following inoculation, and at 30 minute intervals thereafter, while the cultures were incubated at 37 °C with shaking. The OD_{600} of each sample was determined at the time of sampling. Growth curves were plotted using Microsoft Excel from the data obtained, using a logarithmic scale for the optical density measurements, and a line of best fit calculated using the 'exponential trendline' facility for the exponential growth phase (characterised by a linear progression). The

equation of each line of best fit was used in conjunction with the following equations to determine growth rate.

The equation of each line was in the following format:

$$y = me^{cx}$$

The elements of this equation were inserted into the following:

$$T_n = (\ln n - \ln m)/c$$

$$T_{2n} = (\ln 2n - \ln m)/c$$

Where T_n = time (hours) to reach OD_{600} of n
Growth rate (doublings per hour) was calculated as:

$$1/(T_{2n} - T_n)$$

2.1.5: Techniques for plasmid transfer

Transformation of *E. coli* cells

Preparation of competent cells for transformation: Hanahan's method

The method of Hanahan (1985) was used to transform *E. coli* cells with plasmid DNA. 5 ml of LB broth or BHI broth was inoculated with the appropriate *E. coli* strain, which was then grown overnight at 37 °C with shaking. 0.5 ml of the overnight culture was used to inoculate 50 ml LB broth, and this was incubated at 37 °C with shaking until the cells reached exponential phase (OD_{600} 0.3-0.5). The culture was then chilled on ice for 15 minutes, and the cells were harvested by centrifugation at 4,000 rpm for 10 minutes at 4 °C in a refrigerated bench top centrifuge. The supernatant was discarded and the cell pellets were resuspended by moderate vortexing in 16 ml ice cold RF1 solution. The cells were incubated on ice for 30 minutes prior to centrifugation for 10 minutes at 4,000 rpm, at 4 °C. The supernatant was discarded and the cell pellets were gently resuspended in 4 ml RF2 solution and chilled on ice for 15 minutes. The competent cells were then aliquoted (in 200 µl or 400 µl aliquots) into 1.5 ml microcentrifuge tubes and stored frozen at –80 °C.

RF1

- 7.46 g KCl
- 9.90 g $MnCl_2.4H_2O$
- 2.94 g potassium acetate
- 1.50 g $CaCl_2.2H_2O$
- 150 ml glycerol

The above were dissolved in ~750 ml H_2O (>18 MΩ), and the resultant solution was adjusted to pH 5.8 using 0.2 M acetic acid. The final volume was then made up to 1 L. The solution was filter sterilised through a 0.22 μm membrane, and stored at 4 °C.

RF2

- Solution A: 0.5 M MOPS, pH 6.8
- Solution B: 10 mM KCl
  75 mM $CaCl_2.2H_2O$
  15% (w/v) glycerol

Both solutions A and B were made up in >18 MΩ H_2O, and stored at 4 °C. 0.2 ml of solution A and 9.8 ml of Solution B were mixed together on the day of use.

Transformation

DNA to be used for transformation (1-30 μl) was chilled on ice for ~5 minutes prior to addition of 100 μl competent cells to each sample. A "cell only" control was also prepared. The tubes were then incubated on ice for 30 minutes. The mixtures were then heat-shocked at 42° C for 2.5 minutes. Following heat-shock, the mixtures were returned to ice for 5 minutes. 1 ml LB broth was added to each mixture and the tubes were incubated at 37 °C for 1 hr to allow expression of antibiotic resistance genes carried by the plasmid.

100 μl of each transformed culture was spread on selective medium, and the remainder of the culture was harvested by centrifugation at 13,000 rpm for 5 minutes in a microcentrifuge. The majority of the supernatant was drained from each tube, leaving ~100 μl broth, and the cell pellets were resuspended in the remaining broth. This was then spread onto a separate agar plate. Plates were incubated at 37 °C overnight.

Conjugation of plasmid DNA into *B. cenocepacia* and *P. aeruginosa*

Plasmids harbouring an origin of transfer (*oriT*) were mobilised into *B. cenocepacia* or *P. aeruginosa* ('recipient'), using *E. coli* strain S17-1 as the 'donor'. 10 ml LB broth or BHI was inoculated with donor and recipient strains (antibiotics were included in the donor culture for plasmid maintenance), and cultures were grown overnight at 37 °C with shaking. 1 ml of each overnight culture was harvested by centrifugation at 13,000 rpm for 5 minutes using a microcentrifuge. The supernatants were discarded and the cell pellets were each resuspended in 0.85 % (w/v) sterile saline. The volume of sterile saline used was normally 125 µl, except for when >4 donor strains were being used, when the volume (in µl) used was equal to the number of donor strains, multiplied by 25, plus 25 µl to allow for pipetting error. Using sterile forceps, 0.45 µm nitrocellulose membrane filters were placed on nutrient rich plates (blood agar or MacConkey-lactose agar). 25 µl of the donor and recipient cultures were pipetted, separately and in combination, directly onto the membranes. For the conjugation plate, 25 µl of donor culture was pipetted onto the membrane, followed by 25 µl of the recipient. The cultures were spread across the membrane using a pipette tip. The plates were inverted and incubated at 37 °C for 8-16 hours. Using sterile forceps, the filters were transferred to sterile universal bottles containing 3 ml sterile 0.85 % (w/v) saline, and the bottles were vortexed to resuspend the bacteria in the saline. 10^{-1}, 10^{-2} and 10^{-3} dilutions of the resultant cell suspension were prepared in 0.85 % (w/v) sterile saline for trabsfer of broad host range plasmids. 100 µl of each dilution and the undiluted suspension plated onto selective media and incubated at 37 °C.

Two ex-conjugants were restreaked from each conjugation onto the same medium, to purify them from the background of donor and recipient cells. Isolated colonies located far away from the origin of the streak were restreaked once again onto minimal salts agar supplemented with appropriate selective antibiotics, and were then considered free from this background.

2.1.6: Maintenance of bacterial strains

Maintenance of *E. coli* and *P. aeruginosa* strains

E. coli and *P. aeruginosa* strains were maintained long-term as glycerol stocks and short-term on LB or minimal salts agar plates containing appropriate antibiotics at 4 °C. Agar plates were sealed with Parafilm prior to storage. Strains maintained on agar plates were restreaked onto fresh plates every four weeks, and the freshly streaked plates incubated at 37 °C overnight before storage at 4 °C.

Maintenance of *B. cenocepacia* strains

B. cenocepacia loses viability at 4 °C, and dies rapidly on rich medium. *B. cenocepacia* strains were therefore maintained as glycerol stocks or on minimal salts agar plates stored at room temperature and sealed with Parafilm.

Glycerol stocks

A BHI or LB culture was grown overnight at 37 °C with shaking. 0.7 ml of this culture was mixed with 0.3 ml sterile 50% glycerol in a cryogenic vial, to give a final concentration of ~15 % glycerol. The vial containing the culture was vortexed briefly and stored frozen at –80 °C.

2.2: Techniques for DNA purification and analysis

2.2.1: PCR techniques

Where PCR products were to be used for cloning, a proof-reading DNA polymerase, Accuzyme (Bioline), or *Pfu* Turbo (Strategene) was used for amplification. Where a PCR was for diagnostic purposes only, Taq polymerase (Yorkshire Biosciences) was used.

Where the template was *B. cenocepacia* DNA, DMSO was always included and the hotstart procedure followed.

PCR using purified plasmid DNA as a template

The following were added to a 0.5 ml PCR tube for each reaction:

- ~100 ng template DNA
- 1 µl 10 mM dNTP (2.5 mM each dNTP)
- 3 µl 10 µM forward primer
- 3 µl 10 µM reverse primer
- 5 µl X10 buffer (Taq/Accuzyme buffer/ *Pfu* Turbo buffer)
- 3 µl $MgCl_2$ (only added when Taq was used, as $MgCl_2$ included in Accuzyme buffer)
- 2.5 µl DMSO
- 1 µl polymerase (Taq/Accuzyme/ *Pfu* Turbo)

Sterile H_2O (>18 MΩ) was added to each reaction to a total volume of 50 µl.

Thermocycling was as below:

PCR regime

95 °C	4 minutes	
95 °C	30 seconds	25 cycles.
T_A	30 seconds	
72 °C	1 minute per kb of amplicon	

T_A = annealing temperature of primers.

T_A was determined by taking 5 °C from the primer melting temperature, as determined by the computer programme Gene Jockey.

Where *B. cenocepacia* DNA was to be amplified, the hotstart procedure was followed. In this procedure, DNA polymerase was omitted from the reactions, and added subsequent to the initial denaturation step (95 °C, 4 minutes), to prevent the formation of non-specific DNA.

PCR using purified *B. cenocepacia* chromosomal/boiled lysate DNA as a template

The following were added to a 0.5 ml PCR tube for each reaction.

- ~200 ng purified DNA/5µl boiled lysate (Section 2.2.2)
- 1 µl 10mM dNTP (2.5 mM each dNTP)
- 3 µl 10µM forward primer
- 3 µl 10µM reverse primer
- 5 µl X10 buffer (Taq/Accuzyme)
- 3 µl $MgCl_2$ (only added when Taq was used, as $MgCl_2$ included in Accuzyme buffer)
- 2.5 µl DMSO

Sterile H_2O (>18 MΩ) was added to each reaction to a total volume of 50 µl.

Thermocycling was as below:

PCR regime

95 °C	4 minutes	
95 °C	30 seconds	} 30 cycles.
T_A	30 seconds	
72 °C	1 minute per kb of amplicon	

T_A = annealing temperature of primers.

PCR screening for inserts cloned in pKAGd4

Single *E. coli* colonies on agar plates were picked and a small quantity of material transferred into the bottom of 0.25 ml PCR tubes, using a sterile wooden toothpick. The following were added to these tubes for each reaction:

- 0.5 µl 10 mM dNTP (2.5 mM each dNTP)
- 1.5 µl 10 µM AP10 primer
- 1.5 µl 10 µM AP11 primer
- 2.5 µl X10 Taq buffer
- 1.5 µl $MgCl_2$

Sterile H_2O (>18 MΩ) was added to each reaction to a total volume of 25 µl. Thermocycling was as below:

PCR regime

95 °C	4 minutes	
95 °C	30 seconds	} 30 cycles.
55 °C	30 seconds	
72 °C	1 minute	

Synthesis by Overlap Extension (SOE) PCR

A three primer (i.e. 'megaprimer') variation of SOE PCR was employed as the mutagenesis method for production of cysteine-to-alanine codon substitutions and putative translation start codon mutations in *orbS*. In the first step, the central, mutagenic primer and either orbSrev2 (for cysteine-to-alanine codon substitutions) or orbSfor (for putative translational start codon mutations) were used for amplification of a 'megaprimer'. Template DNA used was: for the single cysteine substitutions (i.e. to make pBBR-orbSC205A and pBBR-orbSC211A) and translational start codon mutations, pBBR-orbS; for the double and quadruple cysteine substitutions (i.e. to make pBBR-orbSC198+205A, pBBR-orbSC198+211A and pBBR-orbSCtetraA), pBBR-*orbS*C198A. In the second step,10 pmol of either orbSfor (for cysteine-to-alanine codon substitutions), or orbSrev2 (for translational start mutations), and ~30 pmol of the product from the first step, i.e. the 'megaprimer', were used to amplify the complete product. The proofreading DNA polymerase *Pfu* Turbo (Stratagene) was

used to amplify the template in both steps. PCR was carried out for 25 cycles in each case, with an annealing temperature of 55 °C for the first SOE step, and 50 °C for the second step. The introduction of the correct mutations were checked by sequencing the entire *orbS* gene.

DNA sequencing

As DNA polymerases can introduce errors during PCR, all plasmid constructs containing PCR-amplified inserts were sequenced with appropriate primers to allow the sequence of the entire insert to be checked.

DNA sequencing was carried out by Lark Technologies, Inc., or by the Sheffield University Medical School Core Sequencing Facility. Plasmid DNA for sequencing was prepared using the QIAprep Spin Miniprep Kit (Qiagen).

2.2.2: DNA preparation and manipulation techniques

The following protocols were used to prepare plasmid DNA from *E. coli*.

Large scale plasmid preparation

Large scale plasmid preparation was carried out using the QIAfilter Plasmid Midi Kit (Qiagen), as per the manufacturer's instructions. Pure plasmid DNA was dissolved in 200 µl EB.

QIAprep Spin Miniprep Kit

The QIAprep Spin Miniprep Kit (Qiagen) was used as per the manufacturer's guidelines to prepare small quantities of plasmid DNA for sequencing. pKAGd4 and its derivatives that were required for restriction digestion analysis was also prepared using this kit, as DNA prepared by this method was cut more efficiently. An additional step was added to the protocol as follows: following the centrifugation to remove any remaining ethanol from the spin column, the column was placed in a collection tube as normal, but left open for ~5 mins to allow any traces of ethanol to evaporate.

pKAGd4 is a large (~10 kb), low copy number plasmid, and therefore the following measures were taken to increase yields: culture volume was increased from 3 to 5 ml; the optional PB wash step mentioned in the manufacturer's instructions was included; elution was carried out in buffer EB, pre-warmed to 70 °C.

Small scale preparation of plasmid DNA by alkaline lysis ("miniprep")

2 ml bacterial cultures were grown overnight with aeration at 37 °C in LB broth or BHI broth containing antibiotics as appropriate. ~1.9 ml of each culture was poured into 1.5 ml microcentrifuge tubes, and the cells were harvested by centrifugation at 13,000 rpm for 5 minutes in a bench top microcentrifuge. The supernatant was discarded, and the cell pellet was resuspended thoroughly in 100 µl Solution I. 200 µl Solution II was added, and the tubes were inverted gently 4-6 times. Following 5 minutes incubation on ice, 150 µl Solution III was added, and the tubes were gently shaken 6-8 times before being returned to ice for a further 5 minutes. The protein and chromosomal DNA were then harvested by centrifugation in a bench top microcentrifuge at 13,000 rpm for 5 minutes. The supernatants, containing plasmid DNA and contaminating RNA, were transferred to fresh microcentrifuge tubes. 400 µl phenol:chloroform:isoamyl alcohol (25:24:1) was added to extract any remaining protein. The tubes were vortexed briefly and then centrifuged for 3 minutes at 13,000 rpm in a bench top microcentrifuge. The upper, aqueous, phase was then transferred to microcentrifuge tubes, and the nucleic acids were precipitated using 2 volumes (~800 µl) absolute ethanol. The tubes were vortexed briefly and incubated at room temperature for at least 5 minutes to allow complete precipitation. The DNA was recovered by centrifugation for 5 minutes at 13,000 rpm using a microcentrifuge, and the supernatant was discarded. 1 ml 70 % ethanol was added to wash the pellet. Following brief vortexing, the DNA was harvested once more by centrifugation for 5 minutes at 13,000 rpm. The supernatant was discarded, and the pellet allowed to air dry. The purified plasmid DNA was then dissolved in 50 µl DNAse-free H_2O (>18 MΩ).

Solution I

- 50 mM glucose
- 25 mM Tris-HCl (pH 8.0)
- 10 mM EDTA (pH 8.0)

This was autoclaved and stored at 4 °C. This solution was prepared using sterile (autoclaved) stock solutions of 1 M Tris-HCl (pH 8.0) and 0.5 M EDTA (pH 8.0).

Solution II

- 0.2 M NaOH
- 1 % (w/v) SDS

This solution was stored at room temperature without autoclaving, and replaced every 6 months.

Solution III

- 60 ml 5M potassium acetate
- 11.5 ml acetic acid, glacial
- 28.5 ml H_2O (>18 MΩ)

The solution was autoclaved and stored at 4 °C.

Crude boiled lysate preparation of chromosomal DNA

To prepare crude chromosomal DNA, 200 µl TE buffer was inoculated with a bacterial colony. The cells were resuspended by vortexing and boiled for four minutes.
TE buffer consisted of 10 mM Tris and 1 mM EDTA, with the pH adjusted to 8.0.

Digestion of contaminating RNA using RNAse A

Miniprep DNA was incubated with RNAse A if an inserted DNA fragment was to be released by restriction digestion and visualised on an agarose gel. RNA would otherwise obscure this band. 1 µl 1 mg ml^{-1} RNAse A was added to the preparation, which was then incubated for 30 mins at 37 °C.

Oligonucleotide annealing to produce double-stranded fragments for cloning

The following were combined in a 0.5 ml PCR tube:

- 45 µl each of 100 pmol μl^{-1} (100 µM) primer in H_2O (>18 MΩ)
- 10 µl annealing buffer (10 mM $MgCl_2$, 200 mM Tris-Cl (pH 8.0) in >18 MΩ H_2O)

This mixture was incubated for 10 minutes at 90 °C in a thermal block, before being removed to the bench-top to cool for 1 hour.

Restriction digestion

Restriction digestions were carried out at 37 °C for 2 hours, using enzymes purchased from either NEB or Promega. The following reagents were mixed by pipetting in a 1.5 ml microcentrifuge tube prior to addition of 10 u enzyme. Where a double digest was carried out, an appropriate buffer was chosen to gain optimum efficiency for both enzymes, and 10 u of each enzyme was added to the digestion.

- 5 µl 10X restriction enzyme buffer
- ~1000 ng DNA

Sterile H_2O (>18 MΩ) was then added to a total volume of 30 µl for diagnostic purposes or 50 µl where products were to be inserted into a plasmid.

Where the digestion products were to be ligated for cloning, the reaction was 'cleaned' using the QIAquick Spin PCR Purification Kit (Qiagen), following the manufacturer's guidelines. In cases where other products of digestion besides the desired product might have interfered with a ligation, the digested products were fractionated by electrophoresis through an agarose gel and the required DNA fragment was excised. The Qiagen QIAquick gel extraction kit was used to extract and purify the desired fragment, as per the manufacturer's guidelines.

Use of calf intestinal alkaline phosphatase (CIP)

CIP (Promega) was added directly to restriction endonuclease-digested DNA without prior purification of the DNA. 5 µl CIP 10X reaction buffer (supplied by the manufacturer) was mixed with 0.01 u CIP per pmol of DNA ends and added to the 50 µl DNA digest. The mixture was incubated at 37 °C for 30 minutes, and another

equivalent aliquot of diluted CIP added, mixed as before. The mixture was incubated at 37 °C for a further 30 minutes. The CIP was removed using the QIAquick PCR Purification Kit (Qiagen), following the manufacturer's guidelines.

Agarose gel electrophoresis of DNA

A mixture of TAE X1 buffer and agarose was prepared within a conical flask and boiled using a microwave oven until completely homogeneous (normally 0.8 % w/v agarose was used. However, a higher percentage (1-1.5 %) was used to resolve bands of <500 bp, and 0.4% was used to visualise large plasmids (≥10 kb) such as pKAGd4). The agarose solution was allowed to cool to ~50 °C before pouring into a gel tray (Biorad minigel system). Once set, the gel was placed in a Biorad gel tank, the comb removed and the gel submerged in TAE buffer. The samples to be separated were mixed with X 10 loading buffer (composition 50 % (v/v) glycerol in H_2O (>18 MΩ), 0.1 % (w/v) bromophenol blue). 2 µl loading buffer was added to each sample, except for DNA fragment extraction from the gel, where 25 µl samples were used with 5 µl loading buffer. DNA ladders were used to allow approximation of band sizes. Ladders used were as follows: Promega Supercoiled DNA ladder, Bioline Hyperladder I and Hyperladder IV and Yorkshire Biosciences Q-step 4 ladder. Ladders were prepared for loading as per the manufacturer's guidelines.

A voltage of 60 V was applied to the system (4 V cm^{-1}) until the loading dyes had migrated from the wells into the gel, at which point the voltage was increased in to 80 V. Following separation of the samples, the gel was removed from the tray and immersed in a 5 µg ml^{-1} solution of ethidium bromide for 20 minutes to allow intercalation of the ethidium bromide into the DNA within the gel. After rinsing the gel with tap water, the fluorescent bands were visualised under an ultraviolet transilluminator.

<u>50 X TAE buffer</u>

- 242 g Tris-base
- 57.1 ml glacial acetic acid
- 37.2 g di-sodium EDTA dihydrate

- H_2O (>18 MΩ) to 1 L

The final pH of 50 X TAE is 8.

DNA ligation

The DNA fragment to be cloned and recipient plasmid were digested with appropriate restriction endonucleases and either purified by extraction from an agarose gel or by the QIAquick PCR Purification Kit (Qiagen). For gel extraction the Qiagen QIAquick Gel Extraction Kit was used, according to the manufacturer's guidelines. Ligation was carried out using Promega T4 DNA ligase in a total volume of 30 µl, containing 3 µl X 10 ligase buffer (supplied by the manufacturer), and 1 µl ligase. Approximately a 3:1 molar ratio of insert:vector was used, with a vector concentration of ~0.5 µg ml^{-1}. Two control reactions were also set up: a vector control, containing cut vector but no insert or ligase, and a ligation control, containing cut vector and ligase but no DNA insert. The Ligation mixture and controls were incubated at room temperature overnight prior to transformation of *E. coli* competent cells.

Phenol:chloroform extraction

H_2O (>18 MΩ) was added to samples for extraction to a volume of 200 µl. 200 µl phenol:chloroform:isomayl alcohol (25:24:1) was added and samples were vortexed vigorously for 10 secs, before centrifugation for 3 mins at 13,000 rpm in a microcentrifuge, to separate the DNA-containing aqueous and protein-containing organic phases. 180 µl of the upper, aqueous phase was removed with a pipette, without disturbing the interface between the phases. DNA was precipitated by the addition of 0.1 volumes sodium acetate (pH 5.2), 1 µl glycogen (as a carrier), and 2.5 X the final volume (including the volume of the 3 M sodium acetate) of absolute ethanol. Samples were incubated on dry ice for 10 mins, before centrifugation for 10 mins at 13,000 rpm using a microcentrifuge. The supernatant was removed, and the DNA pellets were washed in 0.5 ml 70 % ethanol and briefly vortexed before repeating the centrifugation. The supernatant was once again removed, and the pellets were resuspended in 30-50 µl buffer EB (Qiagen), or H_2O as required.

Determination of proper insertion of a fragment into a plasmid vector following ligation

All plasmid constructs were verified by restriction digestion and/or sequencing. The proper integration of fragments was verified by digestion with suitable restriction enzymes, usually those that were used to digest the plasmid and insert prior to ligation. This was carried out for all constructs, except where small (<200 bp) fragments were

inserted into pKAGd4, as, owing to the low copy number and large size of this plasmid, neither inserts nor alterations to the parent plasmid's size could be readily visualised on a gel following digestion. In this case, clones were screened by PCR (Section 2.2.1) and the products were analysed on a 1.2 % agarose gel.

Sequencing was used to ensure that no errors were present in cloned PCR amplified DNA fragments, and where two oligonucleotides had been annealed and inserted into a plasmid vector. M13 forward and/or reverse primers were used when sequencing products cloned into pBBR1MCS, pBBR-2-MCS and pBluescript II KS. Primer AP10 was used to sequence inserts cloned into the low copy number vector pKAGd4, following amplification of the inserted fragment using primers AP10 and AP11.

2.3: Techniques for the preparation and analysis of RNA

2.3.1: RNA purification techniques

Small scale RNA purification

Small scale RNA purification for RT-PCR was carried out using the Ribopure Bacteria Kit (Ambion). A *B. cenocepacia* 715j starter culture was grown overnight at 37 °C in M9 salts medium containing casamino acids (0.1 %). Sub-cultures were set up at 100 fold dilution in 10 ml of the same medium supplemented with 50 μM $FeCl_3$ for iron replete and 100 μM 2'2-dipyridyl for iron limited conditions which were grown to OD_{600} ~0.5. RNA was then extracted as per the manufacturer's instructions, and eluted from the column using two aliquots of 25 μl of the elution buffer provided to maximise recovery. The resultant RNA solution was treated with the DNAse I provided in the kit, according to the manufacturer's instructions. However, the recommended 30 minute incubation at 37 °C with the DNAse I enzyme was found to be insufficient, and was therefore increased to 1 hr. Typical yield was ~50 ng RNA per 10 ml of sub-culture.

Large scale RNA purification

Large scale RNA purification for primer extension was carried out using the RNAqueous Midi kit (Ambion). This kit has been optimised for the isolation of RNA from eukaryotic cells, and therefore a number of modifications were made to the

manufacturer's protocol, as follows. A *B. cenocepacia* 715j starter culture was grown overnight at 37 °C in M9 salts medium containing casamino acids (0.1 %). Sub-cultures were set up at 100 fold dilution in 100 ml of the same medium supplemented with 50 μM $FeCl_3$ for iron replete and 100 μM 2'2-dipyridyl for iron limited conditions and were grown to OD_{600} ~0.8. The collected cells from these cultures were resuspended in 15 ml of lysis/binding solution, and vortexed at high speed for 5 minutes to ensure thorough disruption of the cell membranes. All 'optional' steps within the manufacturer's protocol were followed. Most important of these was the clarifying centrifugation, which was carried out after lysis for 15 mins at 10,000 g. 20 ml of Solution 1 was passed through the filter unit, followed by a total of 30 ml of Solution 2/3. RNA was eluted using two aliquots, each of ~1.5 ml, Elution Solution at 100 °C (boiled over a Bunsen burner). The concentration of the eluted RNA was determined by spectrophotometry, as described in Section 2.3.2. RNA was then precipitated using the lithium chloride solution provided in the RNAqueous Midi kit, as per the manufacturer's protocol, and resuspended in RNAse-free H_2O (Molecular Biology Grade, Sigma) to a concentration of ~5,000 ng ml^{-1} (on the assumption that LiCl precipitation is quantitative for the mRNA concerned).

2.3.2: RNA analysis techniques

Determination of RNA concentration and purity

RNA concentration and purity was determined by spectrophotometry at 260 nm and 280 nm using a quartz cuvette, as plastic absorbs light at these wavelengths. Usually, 2 μl RNA was added to 98 μl RNAse free H_2O, in a cuvette with 100 μl capacity. The following calculations were applied to the results:

RNA concentration

$$OD_{260} \text{ X Dilution factor X } 40 = \text{RNA concentration } (\mu g\ ml^{-1})$$

This is based on the observation that nucleic acid absorbs light at 260 nm, and that 40 μg ml^{-1} RNA has an approximate OD_{260} of 1.0.

RNA purity

The purity of RNA can be measured by its OD_{260}:OD_{280} ratio. For highly pure RNA, this value falls between 1.8 and 2.1.

Reverse transcription PCR (RT-PCR)

RT-PCR was carried out using RNA purified via the Ribopure Bacteria Kit (Ambion) (see Section 2.3.1). 1 µg template RNA was used in each reaction. Optimum annealing temperatures for each primer pair were determined by performing standard PCR on genomic DNA prior to RT-PCR. $MgSO_4$ concentration used was 1mM for every reaction. Reactions were carried out as per the manufacturer's guidelines, with the addition of 2.5 µl DMSO to each 50 µl reaction, as *B. cenocepacia* DNA is G+C-rich. RT-PCR products were analysed by electrophoresis through a 1.6 % agarose gel.

RNAse protection assay (RPA)

RPA was carried out using the RPA III Kit (Ambion), with RNA purified via the Ribopure Bacteria Kit (Ambion) (See 2.6.1) as template. Template DNA for production of RNA probes was generated by PCR, and purified by phenol:chloroform:isoamyl alcohol extraction to remove contaminating RNAse as follows.

Phenol chloroform extraction

RNAse-free water (Molecular Biology Grade, Sigma) was added to each PCR to a total volume of 200 µl. 200 µl of phenol:chloroform:isoamyl alcohol (pH 8, 25:24:1) was then added and the tubes were vortexed for 20 seconds, before centrifugation at 13,000 rpm using a microcentrifuge. ~175 µl of the upper, aqueous phase was extracted from each tube, ensuring that the interface between the phases was not disturbed. DNA was precipitated by the addition of 2.1 volumes RNAse-free Precipitation Solution (95 % (v/v) ethanol, 1 % (w/v) potassium acetate) and 1 µl RNAse free glycogen was added as a carrier. The samples were gently mixed, and the DNA was allowed to precipitate for 10 minutes at room temperature, before centrifugation for 10 minutes at 13,000 rpm. The supernatant was removed and the pellets were air dried before resuspension in 30 µl RNAse-free Elution Buffer (Qiagen).

In vitro transcription and purification of RNA probes

The following reagents were combined in a microcentrifuge tube. All reagents were RNAse-free:

- 5 µl 5X T7 RNA polymerase buffer (Promega)
- 2.5 µl 100 mM DTT (Ambion)
- 1 µl RNAsin (Promega) (22 units μl^{-1})
- 4 µl 2.5 mM (of each ribonucleotide) rATP, rCTP, rGTP mix
- 2.4 µl 100 µM rUTP
- 4 µl DNA template (PCR product)
- 3 µl [α^{32}P] rUTP, (10 mCi ml^{-1};800 Ci $mMol^{-1}$)
- 20 Units T7 RNA polymerase (Promega)

- Water (Molecular Biology Grade, Sigma) to 25 µl.

Samples were incubated for 1 hr at 37 °C, before treatment with 2 units of DNAse I per sample and incubation for 15 mins at 37 °C. RNA probes were purified from unincorporated label and shorter *in vitro* transcription products as follows: samples were diluted 1:1 in Gel Loading Buffer (provided in the RPA III kit), and incubated at 95 °C for 3 mins, before loading on to a 1.5 mm thick 8 M urea, 5 % acrylamide gel. The stock acrylamide solution was prepared as follows:

- 16.7 ml 30% Acrylamide/Bis-acrylamide Solution, 19:1 (Biorad)
- 48 g urea
- 10 ml 10X TBE (Section 2.3.2)

- H_2O (>18 MΩ) to 100 ml

This stock was filter sterilised and stored in the dark at 4 °C.

Before pouring a gel, 10 ml of the stock solution was mixed with 40 µl ammomium persulphate (10 % w/v) and 10 µl TEMED. Gels were cast using the Biorad MiniProtean gel system. Samples were electrophoresed at 120 V until the bromophenol blue in the loading buffer had run out from the bottom of the gel. The gel was removed from the plates and sealed within a polypropylene pouch. Photographic film (Hyperfilm, Amersham Biosciences) was then exposed to the gel for 5 minutes in the dark and developed. Markings were drawn upon the film to allow re-positioning upon the gel. The full length labelled transcript was excised from the gel using a new, sterile scalpel, and the probe was eluted using the probe elution buffer provided in the RPA III kit, as per the manufacturer's instructions. The gel was re-exposed to ensure successful excision of the probes.

The probe was approximately quantitated as follows: probes were diluted 100 X in EB buffer (Qiagen) and 1 µl was taken up by pipette and held near to a Geiger counter. Accurate quantitation was not deemed necessary. RPA was then carried out using the RPA III kit as per the manufacturer's intructions for the standard hybridisation procedure, using 0.6 µg RNA and ~2000 counts min^{-1} probe. RPA products were analysed using PAGE (gel prepared as above). A radiolabelled DNA ladder, prepared as described below, was included as an approximate size standard. The samples were electrophoresed at 200 V (using the Biorad MiniProtean gel system) until the bromophenol blue had migrated to the bottom of the gel (~30 minutes). The gel was mounted on Whatman filter paper (3 MM) and dried for 3 hours at 80 °C using a Biorad Model 583 gel drier. The gel was exposed overnight to a phosphorimager screen, and then scanned using a Fujifilm FLA-3000 phosphorimager.

Polynucleotide kinase labelling of 50 bp DNA ladder

An end-labelled 50 bp DNA ladder was used as a size standard for determining the sizes of protected RNA probes in the RPA. In order to allow incorporation of [γ-^{32}P] ATP at the 5' ends of the DNA fragments, they were first 5' dephosphorylated using calf intestinal alkaline phosphatase (CIP). The following were mixed in a microfuge tube:

- 2 µl 50 bp DNA ladder (Amersham)
- 1 µl CIP (Promega) (diluted to 0.24 U μl^{-1} in CIP dilution buffer)
- 5 µl 10 X CIP buffer (Promega)
- H_2O (>18 MΩ) to 50 µl.

This was incubated at 37 °C for 30 min, before addition of a further 1 µl of diluted CIP and incubation for 30 min more at 37 °C. The ladder DNA was then purified by phenol:chloroform:isoamyl alcohol extraction (25:24:1) (Section 2.2.2), and resuspended in 30 µl Elution Buffer (Qiagen).

To carry out the 5' end labelling reaction, the following were mixed in a microcentrifuge tube:

- 15 µl dephosphorylated 50 bp ladder (Amersham)
- 2 µl T4 polynucleotide kinase (10 u µlP-1) (Promega)
- 5 µl 10 X T4 PNK reaction buffer (Promega)
- 1 µl [γ-^{32}P]-ATP (10 mCi ml^{-1};3000 Ci mMol^{-1})

- H_2O (>18 MΩ) to 50 µl.

The reaction mixture was incubated for 30 mins at 37 °C, before extraction with phenol:chloroform:isomayl alcohol (25:24:1) (Section 2.2.2). For PAGE, 5 µl labelled DNA ladder and 5 µl loading buffer (from the RPA III kit (Ambion)) were mixed and incubated at 95 °C for 4 mins to denature the double-stranded ladder. The ladder was then stored on ice until loading.

Primer Extension

Primer extension was used to determine the 5' end of mRNAs and was carried out with RNA isolated using the RNAqueous Midi kit (Ambion) (see Section 2.3.1).

Primer labelling

The following were combined in a microcentrifuge tube, all components were RNAse-free.

- 1 µl reverse primer (10 µM)
- 2 µl 10 X kinase buffer (Promega)
- 5 µl [γ-^{32}P]-ATP (10 mCi ml^{-1}; 3000 Ci mMol^{-1})
- 11.4 µl H_2O (Sigma)
- 1 µl T4 polynucleotide kinase (10 u µl^{-1}) (Promega)

Samples were incubated at 37 °C for 45 minutes, and then at 70 °C for 10 minutes to inactivate the enzyme. Primers were purified using the Qiagen QIAquick Nucleotide Removal Kit, and eluted in 40 µl EB buffer.

Primer annealing and reverse transcription

~50 ng RNA, 2 µl labelled and purified primer and H_2O to 16.5 µl were combined in a microcentrifuge tube and incubated at 80 °C for 10 minutes, followed by cooling on ice for 5 minutes, to allow the primer to anneal to any complementary RNA. The following were then added to the annealing reaction .

- 6 µl — 5X reverse transcriptase buffer (Promega)
- 3 µl — dNTP mix (10 mM each dNTP) (Promega)
- 0.5 µl — RNAsin (22 u μl^{-1}) RNAse inhibitor (Promega)
- 3 µl — sodium pyrophosphate (Sigma), 40 mM solution in RNAse-free H_2O (Molecular Biology Grade, Sigma), pre-heated to 42 °C
- 1 µl — AMV reverse transcriptase (10 u μl^{-1}) (Promega)

- H_2O was added to a total of 30 µl.

The samples were incubated at 42 °C for 1 hour, before purification by phenol:chloroform extraction as described in Section 2.2.2. Following phenol:chloroform extraction, samples were resuspended in 3 µl formamide loading buffer (0.025 % bromophenol blue, 0.025 % xylene cyanol, 40 % (w/v) deionised formamide, 5 M urea, 5 mM NaOH, 1 mM EDTA) and 3 µl 0.1 M NaOH. Samples were incubated at 90 °C for 2 minutes and 4 µl was loaded on a pre-heated denaturing 8 % polyacrylamide gel (formula below) alongside a DNA sequencing sequencing ladder, which was prepared using the same primer as described below.

Generation of the sequencing ladder

Primer-extended products were sized against a DNA sequencing ladder generated with the extended primer. A high copy number plasmid bearing the DNA encoding the mRNA to which the primer anneals, together with the upstream sequences containing the predicted promoter region, was used as the template for construction of the sequencing ladder. Pure plasmid DNA was isolated using the Qiagen QIAprep Spin Miniprep Kit, and was denatured by incubation for 20 minutes at 37 °C with 0.1 volumes 2 M NaOH and 2 mM EDTA. 0.1 volumes of 3 M sodium actetate solution (pH 5.5) was then added to neutralise the reaction, and denatured DNA was precipitated by the addition of 2.5 volumes of absolute ethanol, followed by incubation of the samples on dry ice for 15 minutes. The DNA was harvested by centrifugation at 13,000 rpm for 10 minutes in a microcentrifuge, the supernatant removed, and the DNA pellet washed with 0.5 ml 70 % ethanol. DNA was collected by centrifugation once again, and the supernatant thoroughly removed. Pellets were air-dried and resuspended in H_2O (>18 MΩ) to a concentration of ~600 µg ml^{-1}.

The sequencing ladder was generated using the Sequenase Version 2.0 kit (USB). The protocol was adapted as follows to utilise the radioloabelled primer used in the primer extension experiment. The following were combined in a microfuge tube:

- 7 µl denatured template DNA
- 2 µl Sequenase reaction buffer
- 1 µl radiolabelled primer

Samples were incubated at 65 °C for 2 minutes, before cooling on ice for 30 minutes to allow the primer to anneal to the template DNA. 1 µl 0.1 M dithiothreitol (DTT) and 2 µl diluted polymerase (1 µl sequenase, 0.5 µl pyrophosphatase, 6.5 µl H_2O) was added to the annealing reaction. Samples were incubated at room temperature for 5 minutes. 2.8 µl aliquots of this reaction mixture were then added to the termination mix tubes, prepared as described in the manufacturer's protocol, and extension was allowed to continue for 5 minutes. Ractions were stopped with 4 µl stop solution provided in the kit. Samples were heated to 75 °C for 2 minutes before loading onto an 8 % polyacrylamide DNA sequencing gel alongside the products of the primer extension reaction.

Preparation of the polyacrylamide sequencing gel

Acrylamide stock was prepared by mixing the following:

- 126.126 g urea (BDH)
- 30 ml 10 X TBE
- 60 ml 40 % acrylamide, 19: 1 acrylamide:bis-acrylamide (Biorad)

- H_2O (>18 MΩ) to 300 ml.

The stock solution was deionised by the addition of a small spatula-full of Amberlite mixed bed exchanger MB-150 (Sigma), and stirred for 10 minutes. The stock solution was then degassed by filtration through a 0.2 µm membrane under vacuum, and stored at 4 °C in the dark.

The Biorad Sequi-Gen gel system was used for running a 0.4 mm thick sequencing gel, as per the manufacturer's instructions. To a 50 ml aliquot of stock gel solution, 50 µl TEMED and 250µl APS were added before pouring to initiate polymerisation. After casting the gel, the sample wells were flushed with 10 X TBE prior to and after

pre-running, which was carried out at 50 W until the gel temperature reached 50 °C. The samples were rapidly loaded, and electrophoresed at 50 W until the bromophenol blue reached the bottom of the gel. Following electrophoresis, the urea was flushed from the gel using a solution of 10 % acetic acid 10 % methanol, which was layered onto the gel using a syringe, and the gel transferred to 3 mm Whatman filter paper for drying using a Biorad Model 583 gel drier. Drying was carried out for 2.5 hours at 80 °C. The gel was anaysed by autoradiography using a Fujifilm FLA-3000 phosphorimager.

10 X TBE

The following components were dissolved in H_2O to a total volume of 1 l:

- 108 g Tris base
- 55 g Boric acid
- 9.3 g disodium EDTA dehydrate

The resultant buffer was autoclaved to slow the rate of precipitation.

2.4: Protein purification and enzyme assays

2.4.1: Enzyme assays

β-galactosidase assay

β-galactosidase activity in bacterial cells was determined by the method of Miller (1972). 3 ml of the appropriate medium (minimal salts (with casamino acids, 0.1 %)/LB broth, with antibiotics as appropriate) was inoculated with the relevant bacterial strain and incubated at 37 °C for ~24 hours for *B. cenocepacia* cultures or ~14 hours for *E. coli* and *P. aeruginosa* cultures. Fresh medium was prepared with the reagents used for the overnight cultures, but containing 50 μM $FeCl_3$ where iron-replete conditions were desired or 2,2-dipyridyl (Section 2.1.1) where iron-limited conditions were required. 3 X 3 ml aliquots of each medium were distributed into polypropylene universal bottles and were inoculated with the overnight culture to give 1:100 dilution. The cultures were incubated at 37 °C with shaking until the desired OD_{600} was reached. For *E. coli* cultures, this OD_{600} was ~0.4, whereas for *B. cenocepacia* and *P. aeruginosa* cultures this OD_{600} was ~0.6. Once at the appropriate

OD_{600}, the cultures were transferred to ice for at least 25 minutes before carrying out the assay.

Dependent on the projected strength of the promoter being tested under the growth conditions used, a culture volume for the assay was chosen, of between 25 µl and 200 µl. Z buffer (1 ml minus the chosen culture volume) was then added to 2 test tubes per culture, as each culture was assayed in duplicate. 30 µl chloroform was then pipetted directly into the Z buffer. 30 µl SDS was gently pipetted into the tube along its side (so as not to disturb the chloroform 'bead'), and the chosen volume of each culture was added in the same way. Two control tubes were also set up, containing sterile culture medium instead of bacterial culture. After bacterial culture was added to all of the tubes, the test-tubes were vortexed for 10 seconds, before being placed in a rack within a 30 °C waterbath. They were then incubated for 15 minutes to equilibrate to that temperature. 200 µl ONPG (from a 4 mg ml^{-1} stock solution in Z buffer containing 2-mercaptoethanol (see below)) was added to each tube at 30 second intervals to initiate the assay. Following addition of ONPG, each tube was vortexed for 1 second, before being returned to the waterbath. The reaction was stopped by the addition of 0.5 ml Na_2CO_3 solution, once an appropriate yellow colour had developed (between ~OD_{420} 0.2 and 0.7). Tubes were again vortexed for 1 second, and then placed in a rack at room temperature for ~10 minutes for the chloroform to settle. The times at which ONPG and Na_2CO_3 were added were recorded for each tube, so as to allow calculation of the reaction time. Na_2CO_3 was added to the control tube last.

The OD_{420} (to measure the intensity of the yellow colour due to hydrolysis of ONPG) and OD_{550} (to measure the light-scattering effect of the cell debris) were measured for 1 ml of the reaction mixture from each tube, using the control reactions as blanks. The OD_{600} was measured for 1 ml of each bacterial culture (that had been maintained on ice), using sterile culture medium as a blank. The following equation was then applied:

$$\frac{OD_{420} - 1.75(OD_{550})}{\text{Time (min)} \times \text{culture volume added (ml)} \times OD_{600}} \times 1000 = \text{Miller units}$$

The mean value of each pair of duplicate assays was calculated. The average value for each set of three cultures was then calculated by taking the mean of these values. The standard deviation of these three values from the mean was also determined.

Z buffer

- 16.1 g $Na_2HPO4.7H_2O$
- 5.5 g $NaH_2PO4.H_2O$
- 0.75 g KCl
- 0.246 g $MgSO_4.7H_2O$

The above components were dissolved in H_2O (>18 MΩ). Z buffer was stored at 4 °C.

2.4.2: Protein purification techniques

Growth of bacterial cultures and induction of protein overproduction

E. coli BL21λDE3 cells harbouring plasmids expressing *orbS* were grown at 37 °C in LB broth to an OD_{600} of 0.5, in the presence of 100 μg ml^{-1} ampicillin. 2 mM IPTG was added to induce expression of the cloned *orbS* gene, and an additional 100 μg ml^{-1} ampicillin was added to compensate for any that had been hydrolysed by the plasmid encoded β-lactamase. Cells were incubated for a further period, previously ascertained by an induction test in which samples were taken and analysed by SDS-PAGE immediately before induction, and every hour thereafter for 5 hours. 1 ml samples were removed for SDS-PAGE analysis, as detailed in Section 2.4.1.

Protein purification by batch chromatography

500 ml LB broth containing induced BL21λDE3 cells was centrifuged at 9,000 rpm, and the supernatant decanted. The bacterial pellet was resuspended in 50 ml phosphate buffered saline (pH 7) per 10 g pellet. A solution of 40 mg ml^{-1} Phenylmethylsulphonyl fluoride (PMSF) (in >18 MΩ H_2O) was added slowly while stirring, to a final concentration of 40 μg ml^{-1}, and lysozyme was added to a final concentration of 200 μg ml^{-1}. The bacterial suspension was incubated on ice for 30 minutes, before the addition of dithiothreitol (DTT) to a final concentration of 2 mM and sodium deoxycholate, to a final concentration of 500 μg ml^{-1}. The suspension was incubated on ice with gentle stirring until its viscosity had increased, indicating that the cells had lysed. A 1 ml sample was removed for SDS-PAGE analysis, and the

remaining lysed bacteria were further disrupted by sonication. A 1 ml sample of the sonicated material was removed, before centrifugation of the lysate at 43,000 x g for 30 minutes at 4 °C to collect insoluble material. The supernatant was decanted and 1 ml taken for SDS-PAGE analysis. When attempting to purify His-tagged OrbS, imidazole was added to the supernatant, to a final concentration of 200 mM, from a 2 M stock solution (in >18 MΩ H_2O). A crude attempt was made to purify the protein by the addition of 200 µl resin (glutathione sepharose 4B (Amersham) for GST-tagged OrbS and Talon resin (Clontech) for His-tagged OrbS), prepared as per the manufacturer's guidelines. The mixtures were incubated at room temperature for 30 minutes with rotation in a 50 ml centrifuge tube to allow tagged protein to bind the resin. Suspensions were centrifuged at 500 x g for 5 minutes, the supernatant was collected for SDS-PAGE analysis, and pellets were washed with 1 ml phosphate buffered saline. This washing process was repeated 3 times, and each time the supernatant from centrifugation was collected for SDS-PAGE analysis. Bound protein was eluted by resuspension of the collected slurry pellet in 100 µl elution buffer, and incubation for 10 minutes at room temperature with rotation. This elution process was repeated three times. SDS-PAGE was used to analyse a 10 µl sample from each elution.

Elution buffer for GST-tagged proteins consisted of 50 mM Tris-Cl, pH 8.0 and 10 mM reduced glutathione dissolved in phosphate-buffered saline. Elution buffer for His-tagged proteins consisted of 200 mM imidazole dissolved in phosphate buffered saline.

Preparation of inclusion bodies

One litre of dense, induced bacterial culture was centrifuged at 9,000 rpm for 15 minutes, and the pellet resuspended in 20 ml HEPES solution (50 mM HEPES-NaOH, pH 7.5; 0.5 M NaCl; 1mM PMSF, 5mM DTT, 0.35 mg ml^{-1} lysozyme). The suspension was incubated at room temperature for 30 minutes with gentle shaking, before Triton X-100 (Sigma) was added to a final concentration of 1 % (v/v). The suspension was then sonicated until the viscosity had decreased. A 1 ml sample was extracted for SDS-PAGE analysis, before centrifugation of the sample at 30,000 x g for 30 minutes at 4 °C, to collect the inclusion bodies. The pellet, containing the inclusion bodies, was washed twice with phosphate-buffered saline containing 1 %

Triton-X 100. After each wash the inclusion bodies were collected by centrifugation at 30,000 x g for 30 minutes at 4 °C, and samples of each wash were taken for analysis by SDS-PAGE. The pellet was partially resuspended in a 2 ml solution containing 50 mM HEPES-NaOH (pH 7.5) and 1 M urea, and incubated for 1 hour at 4 °C with gentle shaking (it should be noted that the pellet was not fully soluble in this solution). The inclusion bodies were once again collected by centrifugation at 30,000 x g for 30 minutes at 4 °C, and the supernatant removed for SDS-PAGE analysis. The inclusion bodies were now solubilised using 2 ml 50 mM HEPES-NaOH (pH 7.5) containing 8 M urea, and incubated at 4 °C for 1 hour with gentle shaking. A final clarifying centrifugation was carried out at 30,000 x g, for 30 minutes at 4 °C, and the supernatant, containing the solubilised inclusion body protein, was removed, and a sample retained for SDS-PAGE analysis.

Sodium dodecyl sulphate polyacrylamide gel electrophoresis (SDS-PAGE) analysis

Sample preparation

Samples for SDS-PAGE analysis were resuspended in 2 X Laemmli sample buffer, and boiled for 10 minutes to denature and solubilise proteins.

2 X Laemmli sample buffer

- 60 mM Tris-Cl (pH 6.8)
- 2 % (w/v) sodium dodecyl sulphate (SDS)
- 20 % (w/v) glycerol
- 10 % (v/v) 2-mercaptoethanol
- 1 mg bromophenol blue

SDS-PAGE analysis of proteins was carried out using a 12 % resolving gel overlaid with a 5 % stacking gel, prepared as described below. The Biorad Mini-Protean II system was used for casting and running gels. Electrophoresis was carried out at 145 V until the bromophenol blue reached the bottom of the gel.

12 % resolving gel

- 3.3 ml H_2O (>18 MΩ)
- 4 ml 30 % acrylamide:bis-acrylamide (29:1) (Biorad)
- 2.5 ml 1.5 M Tris-Cl (pH 8.8)
- 100 µl 10 % (w/v) SDS
- 100 µl 10 % ammonium persulphate
- 4 µl TEMED

Sufficient resolving gel mix was prepared to cast two gels. Gels were poured to within ~2 cm from the top of the plate to allow for the stacking gel. Immediately following pouring, the resolving gel was overlaid with butanol, which is hydrophobic and results in a flat surface to the gel. After polymerisation, the butanol was decanted and rinsed from the plate cassette, the stacking gel poured and the comb inserted.

5 % stacking gel

- 2.7 ml H_2O (>18 MΩ)
- 670 µl 30 % acrylamide:bis-acrylamide (29:1) (Biorad)
- 500 µl 1 M Tris-Cl (pH 6.8)
- 40 µl 10 % (w/v) SDS
- 40 µl 10 % ammonium persulphate
- 4 µl TEMED

10 X running buffer

(used at 1 X)

- 30.3 g Tris base
- 144 g glycine
- 10 g SDS

- Made to 1 L with H_2O (>18 MΩ).

Chapter 3

The effect of siderophore deficiency on growth of *B. cenocepacia*

3.1: Introduction

In order to study the effect of iron on growth and gene expression in *B. cenocepacia*, conditions were required that were known to be 'iron limited' and 'iron replete'. In order to achieve iron replete conditions, iron must be added in sufficient quantity that the elaboration of siderophores is unnecessary. This is achieved for many bacterial species by the addition of 50 μM $FeCl_3$ to the growth medium. Iron-limiting conditions are more difficult to achieve, as even nutritionally poor media contain traces of iron (present as Fe^{3+} under aerobic conditions). This iron must be sequestered, preventing its uptake and necessitating induction of high affinity uptake systems such as siderophores. Several methods are used to produce iron limited conditions, such as pre-treatment of media with chelex resin, which allows removal of ions within media, or addition of a metal cation chelator to growth medium to sequester iron during bacterial growth. Two common chelators used for this purpose are ethylenediaminedi(*o*-hydroxyphenylacetic) acid (EDDHA) and 2'2-dipyridyl. EDDHA strongly chelates extracellular Fe^{3+}, while 2'2-dipyridyl (which is a small, hydrophobic molecule), is able to enter bacterial cells to chelate Fe^{2+}.

EDDHA binds Fe^{3+} with a 1:1 stoichiometry via two phenolic rings (see Figure 3.1). The resultant Fe^{3+}-EDDHA complex is stable (having an association constant for iron of $10^{33.9}$ M^{-1} (Rogers, 1973)), and only siderophores with high iron binding coefficients can scavenge the bound iron. EDDHA is commonly used to chelate Fe^{3+} in both solid and liquid media. In contrast, 2'2-dipyridyl binds Fe^{2+}, and shows very little reactivity towards Fe^{3+}. Each molecule of 2'2-dipyridyl has two co-ordinating groups, and therefore three 2'2-dipyridyl molecules are required to chelate each ferrous ion (See Figure 3.2). 2'2-dipyridyl was used in this work to chelate intracellular iron in liquid cultures for growth curves and β-galactosidase assays. The ability of *B. cenocepacia* 715j and derivative strains to grow in media containing different concentrations of these two chelators was tested, so as to determine suitable concentrations of these chelators to effect iron restriction. These agents are toxic to bacteria at certain concentrations, which must be determined empirically for each bacterial species and each medium. The aim of the work described in this chapter was to find the minimal concentration of each iron chelator that would limit iron for the different media used.

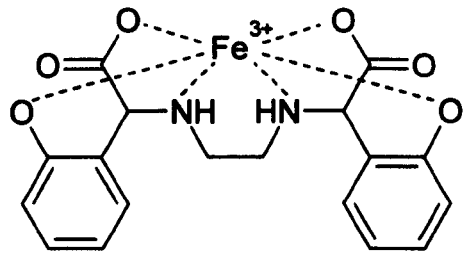

Figure 3.1: The structure of EDDHA (ethylenediaminedi(o-hydroxyphenylacetic)) acid, showing its iron-binding ligands.

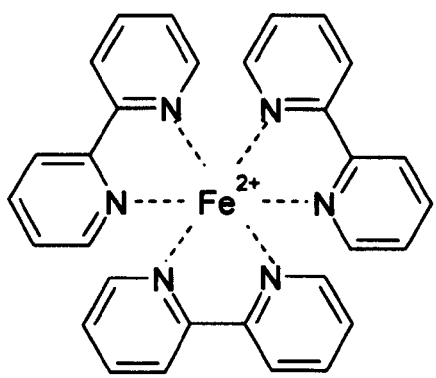

Figure 3.2: The structure of 2'2-dipyridyl. Three molecules of 2'2-dipyridyl are required to bind one Fe^{2+} atom, via the ligands shown.

3.1.1: Objectives

- To determine the optimum concentration of EDDHA and 2'2-dipyridyl to effect iron starvation in *B. cenocepacia.*
- To investigate the effect of siderophore production on the growth of *B. cenocepacia* strains under iron replete and iron limited conditions.

3.2: The ability of *B. cenocepacia* strains to grow on solid media containing EDDHA

As previously discussed, *B. cenocepacia* 715j produces two siderophores, ornibactin and pyochelin (and produces no other CAS-assay detectable siderophores). Growth of *B. cenocepacia* strain 715j (Orb^+, Pch^+) and its siderophore deficient mutants, KLF1 (Orb^+, Pch^-) (the parent strain of OM1 and OM3, see Section 1.6), OM1 (Orb^-, Pch^-), OM3 (Orb^-, Pch^-) and 715j-orbS::Tp (Orb^-, Pch^+), was examined on M9-salts agar containing casamino acids at 0.1%, and EDDHA (prepared as described in Section 2.1.2) at concentrations of 25-50 μg ml^{-1} in increments of 5 μg ml^{-1}. On media lacking EDDHA, all five strains grew well (see Figure 3.3). On media containing 25 μg ml^{-1} EDDHA, OM1, OM3 and 715j-orbS::Tp were unable to grow, while 715j and KLF1 grew at a similar rate as judged by colony size (not shown). At 35 μg ml^{-1} EDDHA 715j grew well, but produced smaller colonies than when EDDHA was not present in the medium. KLF1 grew more slowly than 715j at this concentration of EDDHA, and OM1, OM3 and 715j-orbS::Tp were unable to grow (see Figure 3.3).

There was evidence of some cross-feeding of siderophores from 715j to 715j-orbS::Tp, as bacteria streaked close to a confluent area of 715j growth showed some growth, whereas those further away did not (Figure 3.3 D). This would occur because siderophores are secreted, and can be taken up by other strains provided that the correct receptors are present. The *orbS* gene of 715j-orbS::Tp is disrupted by a trimethoprim resistance gene (Agnoli *et al.*, 2006), but there may still be low level expression of *orbA*, which encodes the ornibactin receptor, which may allow it to take up ferric ornibactin. A cross-feeding experiment was set up to examine this phenomenon in the ornibactin mutants OM1 (*orbI*::mini-Tn5-Tp) and OM3 (*orbS*::mini-Tn5-Tp), alongside 715j-orbS::Tp. M9 minimal salts agar plates containing casamino acids (0.1%) and either 0 or 35 μg ml^{-1} EDDHA were streaked vertically with 715j, and horizontally with OM1, OM3 and 715j-orbS::Tp as shown in Figure 3.4. OM3 was unable to grow in the region of the streak close to 715j, and hence unable to utilise ornibactin from 715j, whereas OM1 showed growth in the area closest to 715j, demonstrating its ability to take up ferric ornibactin produced by 715j. As before, 715j-orbS::Tp grew in the area closest to 715j, showing that this strain could also utilise ferric ornibactin from 715j.

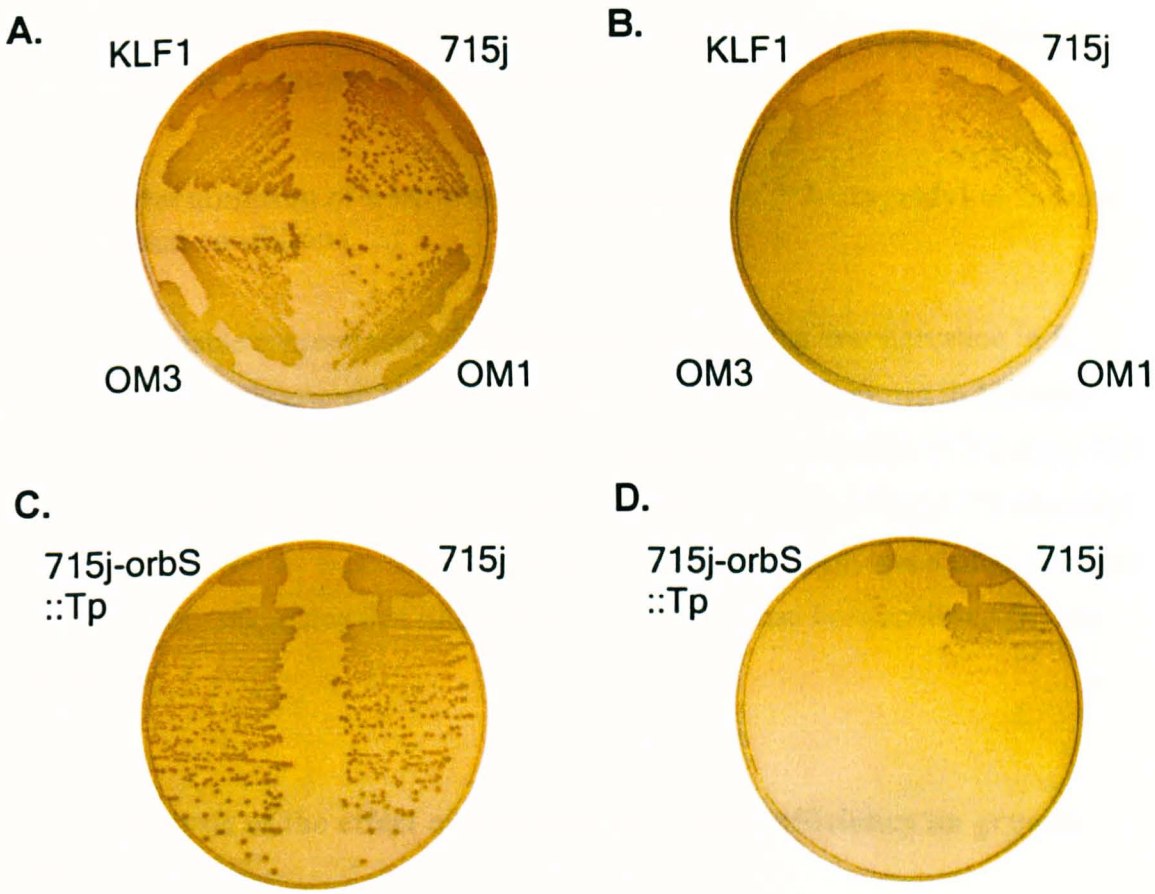

Figure 3.3: Growth of *B. cenocepacia* strains on media with and without EDDHA. **A** and **C**: strains indicated were streaked on M9 salts agar containing 0.1% casamino acids. **B** and **D**: strains indicated were streaked on M9 salts agar containing 0.1% casamino acids and 35 μg ml^{-1} EDDHA. Bacterial cultures were grown to saturation in BHI at 37 °C, before streaking with a loop to approximately standardise the number of bacteria plated. Plates were incubated for ~48 hrs at 37 °C.

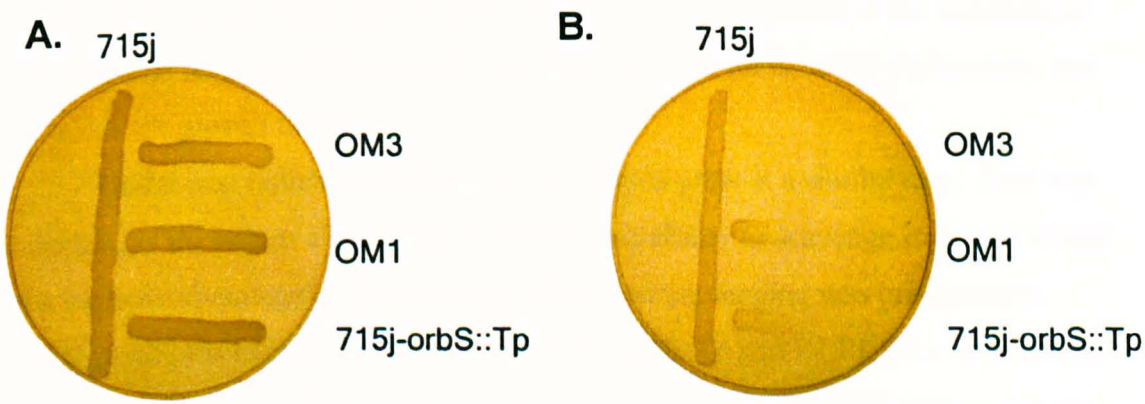

Figure 3.4: Cross-feeding of ornibactin between 715j and ornibactin-negative derivatives. Strains indicated were streaked onto M9 salts agar containing 0.1 % casamino acids. **A:** Medium did not contain EDDHA, **B:** Medium contained EDDHA at 35 μg ml^{-1}. Bacterial cultures were grown to saturation in BHI at 37 °C, before streaking with a loop to approximately standardise the number of bacteria plated. Plates were incubated at 37 °C for ~48 hrs.

3.3: Growth rates of *B. cenocepacia* 715j and siderophore deficient derivatives in response to iron availability

3.3.1: Determination of a suitable concentration of 2'2-dipyridyl to induce iron limited conditions

A suitable concentration of 2'2-dipyridyl for inducing iron starvation in *B. cenocepacia* was determined by plotting a growth curve of 715j grown in M9-salts medium containing 0.1% casamino acids with varying concentrations of 2'2-dypyridyl (0 μM, 100 μM, 120 μM, 140 μM, 160 μM, 180 μM, 200 μM). 100 μM 2'2-dipyridyl was chosen for further experiments, as at this concentration there was a small decrease in growth rate, suggesting that iron starvation conditions had been achieved (results not shown).

3.3.2: Analysis of the effect of iron limitation and sufficiency on growth rate

Growth curves were plotted for *B. cenocepacia* strains 715j, and the siderophore-deficient derivatives 715j-orbS::Tp, KLF1 and OM3, under conditions of iron limitation (100 μM 2'2-dipyridyl) and iron sufficency (medium contained 50 μM $FeCl_3$) (see Figure 3.5). Growth rates were calculated for each strain under each set of conditions using the linear part of each curve (which corresponds to the exponential growth phase on a logarithmic scale) (see Section 2.1.4 for detailed explanation, and Table 3.1 for growth rates).

Under iron replete conditions, all the strains grew at a similar rate. This was expected, as the strains should differ only in their ability to scavenge iron, and would thus have no advantage or disadvantage when iron scavenging was unnecessary. Under conditions of iron limitation, 715j, 715j-orbS::Tp and KLF1 grew at a similar rate, which was slower than under iron replete conditions. The final culture density was also lower than when iron was exogenously supplied (OD_{600} ~1.5 as opposed to 4.5 under iron replete conditions). Strain OM3, which does not produce any siderophores, grew 5 fold slower under iron-limiting conditions than strains that produced one or both siderophores, and had a longer lag phase, showing the

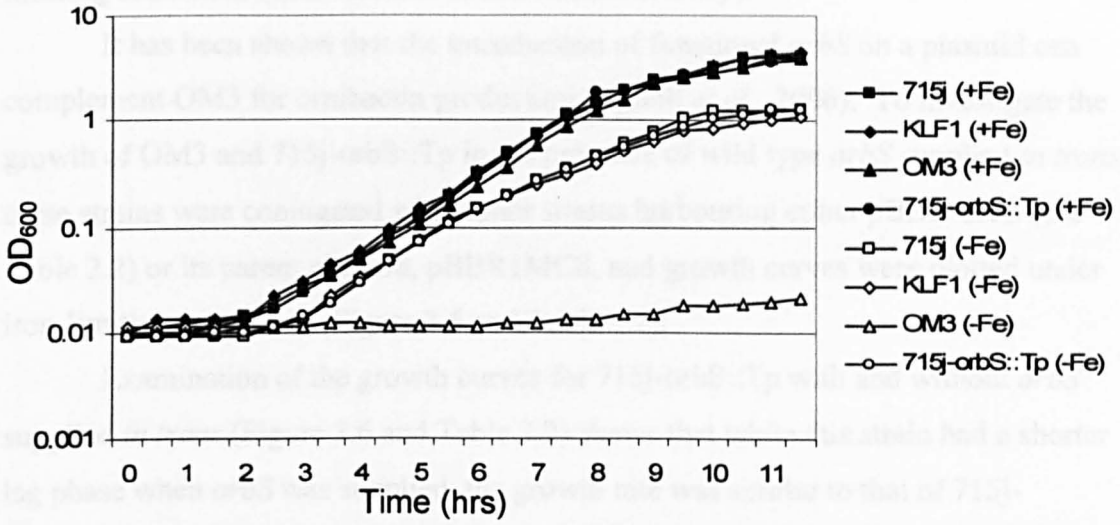

Figure 3.5: Growth curves for 715j and siderophore-deficient strains under iron limited and iron replete conditions. Growth curves were carried out at 37 °C in M9-salts medium containing 0.1 % casamino acids and 50 μM $FeCl_3$ for iron replete (+Fe) or 100 μM 2'2-dipyridyl for iron limiting (-Fe) conditions.

Table 3.1: Growth rates of 715j and derivative strains

Strain	Growth rate (doublings hr^{-1})[a]	
	Iron replete	Iron limited
715j	1.27	1.11
KLF1	1.19	1.07
OM3	1.14	0.18
715j-orbS::Tp	1.25	1.14

[a]Growth rates of the indicated strains were calculated as described in Section 2.1.4, using the curves shown in Figure 3.5.

importance of siderophore production for growth of *B. cenocepacia* under iron-limiting conditions (such as those found within the body).

It has been shown that the introduction of functional *orbS* on a plasmid can complement OM3 for ornibactin production (Agnoli *et al.*, 2006). To investigate the growth of OM3 and 715j-orbS::Tp in the presence of wild type *orbS* supplied *in trans*, these strains were conjugated with donor strains harbouring either pBBR-orbS (see Table 2.2) or its parent plasmid, pBBR1MCS, and growth curves were plotted under iron-limiting conditions (Figure 3.6 and Table 3.2).

Examination of the growth curves for 715j-orbS::Tp with and without *orbS* supplied *in trans* (Figure 3.6 and Table 3.2) shows that while this strain had a shorter lag phase when *orbS* was supplied, the growth rate was similar to that of 715j-orbS::Tp containing pBBR1MCS. This is consistent with the previous observation that 715j and 715j-orbS::Tp have similar growth rates under conditions of iron-limitation (see Figure 3.5). For OM3, however, which has a slower growth rate than 715j under iron-limiting conditions (see Figure 3.5), the introduction of *orbS* leads to an increase in growth rate of ~3 fold. This confirms that the transposon mutation present within *orbS* in OM3 can be complemented by the introduction of functional *orbS*, as was shown previously by CAS plate assay (Agnoli *et al.*, 2006). 715j-orbS::Tp carrying either plasmid grew at a similar rate and to a similar density compared with the corresponding plasmid-less strain from the previous experiment (see Figure 3.5 and Table 3.1), showing that the introduction of pBBR1MCS and its derivative pBBR-orbS were not overly burdening the strains.

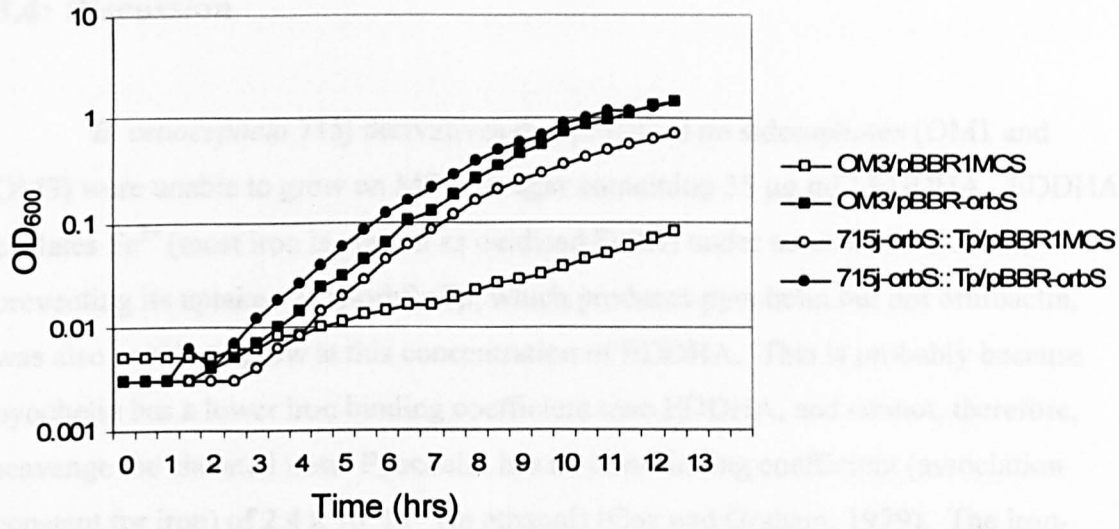

Figure 3.6: Growth curves for siderophore-deficient strains of *B. cenocepacia* supplied with *orbS in trans*. Growth curves carried out at 37 °C in M9-salts medium containing chloramphenicol, 0.1 % casamino acids and 100 μM 2'2-dipyridyl.

Table 3.2: Growth rates of siderophore-deficient strains of *B. cenocepacia* supplied with *orbS in trans*.

Strain	Growth rate (doublings hr^{-1})[a]	
	pBBR1MCS[b]	pBBR-orbS[b]
OM3	0.32	1.05
715j-orbS::Tp	1.09	1.00

[a]Growth rates for the indicated strains were calculated as described in Section 2.1.4, using the curves shown in Figure 3.6.
[b]Strains contained either pBBR1MCS or pBBR-orbS, as indicated.

3.4: Discussion

B. cenocepacia 715j derivatives that produced no siderophores (OM1 and OM3) were unable to grow on M9 salts agar containing 35 μg ml^{-1} EDDHA. EDDHA chelates Fe^{3+} (most iron is present as oxidised Fe(III) under aerobic conditions), preventing its uptake. 715j-orbS::Tp, which produces pyochelin but not ornibactin, was also unable to grow at this concentration of EDDHA. This is probably because pyochelin has a lower iron binding coefficient than EDDHA, and cannot, therefore, scavenge the chelated iron. Pyochelin has an iron-binding coefficient (association constant for iron) of 2.4×10^5 M^{-1} (in ethanol) (Cox and Graham, 1979). The iron-binding coefficient of ornibactin has not been reported, but is likely to be much higher than that of pyochelin, as the structure of ornibactin is similar to that of the iron-binding moiety of pyoverdine, which has a coefficient of 10^{33} M^{-1}. Furthermore, ornibactin can scavenge iron from EDDHA, which has an iron-binding coefficient approximately equal to that of pyoverdine (Rogers, 1973; Cox and Graham, 1979; Visser *et al.*, 2004). Those strains that produced ornibactin (715j and KLF1), were able to grow on media containing 35 μg ml^{-1} EDDHA, supporting the idea that ornibactin is a stronger siderophore than pyochelin.

Ornibactin mutant OM3 was found to be incapable of being cross-fed by 715j on iron-deficient solid medium, whereas 715j-orbS::Tp could be cross-fed. This difference was probably the result of the different orientation of the *dfr* (Tp^R) genes within *orbS* in the two strains. In OM3 it is in the opposite orientation to *orbS* and to the ornibactin operon downstream of *orbS*, and so would be expected to prevent transcription of the entire operon (see Figure 1.11). In 715j-orbS::Tp, the *dfr* cassette within *orbS* is orientated in the same direction as the genes of the operon, and this may drive the expression of the ornibactin uptake genes *orbC* to *orbE*, and also some expression of the *orbA* receptor. It is known that the *dfr* gene has a strong promoter (Levesque *et al.*, 1994; Deshazer and Woods, 1996). OM1 showed some cross-feeding, which was unexpected as the orientation of the *dfr* gene in the OM1 transposon is in the opposite direction to the downstream part of the operon, and therefore although OrbS should still be produced, and able to specify the transcription of the ornibactin uptake genes *orbC* to *orbB*, transcription of the *orbA* gene encoding the receptor would not be expected to occur (see Figure 1.11). Some read-through

transcription of *orbA* is evidently still occurring in this strain. It should be noted that only a low level of *orbA* expression would be expected to be required to allow ferric siderophore uptake, and hence relieve iron-starvation.

In liquid culture, under iron replete conditions, 715j and the siderophore-deficient derivatives tested all grew at the same rate. This shows that under iron-replete conditions these strains can acquire sufficient iron, demonstrating that some uptake mechanism that is not siderophore-dependent must be operating.

Under conditions of iron limitation, 715j (Orb^+, Pch^+), 715j-orbS::Tp (Orb^-, Pch^+) and KLF1 (Orb^+, Pch^-) were found to grow at similar rates. A similar phenomenon has been observed previously: an *orbA*$^-$ mutant of 715j grew similarly to 715j in iron limited liquid medium (where iron limitation was effected by the addition of 2'2-dipyridyl) (Visser *et al.*, 2004). OrbA is the receptor for ornibactin uptake, therefore this mutant produced both pyochelin and ornibactin, but lacked the ability to utilise ornibactin. In contrast, the previous experiments investigating growth on solid media containing EDDHA suggested that ornibactin is a more efficient siderophore than pyochelin. It would appear that mutants deficient in either pyochelin or ornibactin production can sufficiently over-produce the other siderophore to overcome the chelation of intracellular Fe^{2+} by 2'2-dipyridyl, but that pyochelin does not have a high enough affinity for Fe^{3+} to remove iron from EDDHA.

It should be noted that while pyochelin-deficient mutants of 715j have been shown to be similarly virulent to the parent strain in the rat agar bead model, ornibactin-deficient mutants are less virulent than the parent in the same model system (Visser *et al.*, 2004). This suggests that although the growth rate under iron-limiting conditions *in vitro* is similar for these strains, ornibactin is the more important siderophore *in vivo.*

The growth of OM3 was severely compromised under conditions of iron limitation. When *orbS* was supplied *in trans* to complement the disrupted *orbS* gene of OM3, the growth rate was restored to that of 715j, showing the importance of siderophore production for growth under conditions of iron limitation, and confirming that pBBR-orbS can complement the growth rate phenotype of OM3 under iron-limiting conditions.

Chapter 4

Construction of *lacZ* reporter vectors for use in *Burkholderia* spp.

4.1: Introduction

For investigation of the conditions under which the putative *orbS* and OrbS-dependent promoters (*porbH, porbI, porbE*) are expressed, it was decided to construct transcriptional *lacZ* fusions. Previously within our group, transcriptional reporter gene fusions were constructed by integration of the *lacZ* gene into *B. cenocepacia* chromosomal DNA, using either an integrative plasmid or a mini-transposon containing *lacZ*. In the integrative plasmid method the promoter under analysis is fused to a promoterless *lacZ* gene on a suicide vector, which is then introduced into the strain in question. Recombinants resulting from single crossover interaction of the plasmid at the corresponding genomic locus are selected, giving a promoter-*lacZ* fusion without disrupting the native gene. This system gives an accurate reflection of the activity of the promoter upstream of *lacZ*, at single copy and within the correct chromosomal context. However, such systems are time-consuming to construct, and the target range of bacterial species is limited, for example the single crossover method described above could only be used to integrate a fusion into bacteria bearing a homologous gene to that fused to *lacZ*.

Another commonly employed method involves use of a broad host-range plasmid vector bearing a promoterless *lacZ* gene with an MCS located upstream and a suitable selectable marker. The advantage of such systems is that DNA fragments to be assayed for activity can be rapidly cloned and introduced into a range of bacterial species without the need for lengthy screening procedures. However, the promoter-*lacZ* fusions generated have a copy number of greater than one, dictated by the plasmid's origin of replication. This copy number can be influenced by growth conditions and the activity of the fused promoter (Adams and Hatfield, 1984). Furthermore, constant antibiotic selection is required during growth of cells for maintenance of such reporter vectors. Such reporter gene fusions can be either 'transcriptional' or 'translational'. In translational fusions the gene of interest, complete with its own translation initiation codon, ribosome binding site and promoter, is fused to *lacZ*, such that a hybrid protein should result. This facilitates analysis of the combined effects of both transcriptional and translational regulation of the gene in question. Transcriptional fusions are used to assay only the transcriptional

regulation of a gene, by the fusion of the promoter for that gene to promoterless *lacZ* (with both its own ribosome binding site and start codon).

Owing to the large number of transcriptional *lacZ* fusions to be constructed during this project, both in *E. coli* and *B. cenocepacia*, it was desirable to use a reporter plasmid rather than making chromosomal fusions. An ideal plasmid would require not only the *lacZ* gene that specifies the production of β-galactosidase (including its translational initiation codon and ribosome binding site), but also a broad host-range origin of replication, an appropriate selectable marker, and an origin of transfer, to facilitate introduction into *B. cenocepacia* by conjugation. No plasmid with all of these properties was available, and so three existing *lacZ* reporter plasmids were chosen for modification. These plasmids were: pRW50 (derived from pRW2 (Lodge *et al.*, 1990) by removing a second *Hin*dIII site downstream of the *lac* operon (S. Busby, personal communication)); pTZ110 (Schweizer and Chuanchuen, 2001); and pPR9TT (Santos *et al.*, 2001). pRW50 and pTZ110 are transcriptional fusion vectors, whereas pPR9TT is a translational fusion vector. These three plasmids are all broad host-range vectors, but only pTZ110 and pPR9TT are mobilisable by conjugation. The proposed pRW50 derivative was to be used to assay promoter activity using *E. coli* as a model for *B. cenocepacia*, since it is a low copy number plasmid specifying a very low background level of β-galactosidase activity (<1.0 Miller unit). However, there are problems associated with the use of pRW50, which, owing to the presence of *trp* gene sequences upstream of *lacZ*, can be an ineffective reporter plasmid for promoters with low activity (see Section 4.2). To make pTZ110 suitable for use in *B. cenocepacia*, a new selectable marker was required. *B. cenocepacia* 715j is sensitive to only two antibiotics commonly used for plasmid selection in laboratories: chloramphenicol and trimethoprim. As the *orbS* gene had been disrupted using a trimethoprim resistance gene when constructing 715j-orbS::Tp, and this strain was to be used throughout this study, it was necessary for pTZ110 to confer chloramphenicol resistance, rather than ampicillin resistance. Finally, it was decided to convert pPR9TT, which already encodes resistance to chloramphenicol, from a translational fusion vector to a transcriptional fusion vector by supplying translation initiation signals and a start codon for *lacZ*.

4.1.1: Objectives

- To adapt two available broad host-range *lacZ* reporter plasmids as transcriptional fusion vectors for use in *B. cenocepacia.*

- To 'improve' the pRW50 *lacZ* reporter plasmid for use in *E. coli.*

4.2: Construction and analysis of improved pRW50 derivatives

pRW50 contains the *lacZYA* genes and specifies tetracycline resistance. Previously a derivative of pRW50 known as pRW500 had been constructed, in which the MCS and 5' end of *lacZ* (downstream of the internal *Sac*I site) was replaced with the corresponding region of pTL61T (E. Dave and M. Thomas, unpublished results). This also resulted in inclusion of an RNase III processing site between the MCS and *lacZ* (see Figure 4.1). The promoter-*lacZ* hybrid mRNA is cleaved at the RNAse III processing site, standardising the 5' end of the *lacZ* RNA, which otherwise can influence mRNA stability (Linn and St. Pierre, 1990). The insertion of the pTL61T fragment into pRW50 also eliminated the *trpBA* genes. These genes are translationally coupled with *lacZ* in pRW50, and can lead to 10 fold variability in the β-galactosidase activity observed from a cloned promoter fragment, depending on whether *trpB* is translated. This will occur if translation begins from within the cloned fragment and continues in frame with translation of the *trpB* gene. If *trpB* is translated in the wrong reading frame, it will significantly decrease the resultant β-galactosidase activity owing to polar effects on expression of the *trpB-lacZ* fusion (Aksoy *et al.*, 1984).

The insertion of the pTL61T fragment into pRW50 also resulted in the loss of two of the unique restriction endonuclease sites from the MCS (*Hin*dIII and *Pst*I), leaving only *Eco*RI and *Bam*HI. To make the vector more versatile, it was decided to expand the MCS of pRW500 by introducing a *Hin*dIII site. Two complementary oligonucleotides were designed (Hindfor and Hindrev) so as to have *Eco*RI and *Bam*HI cohesive ends and an internal *Hin*dIII site when annealed. The resultant double-stranded oligonucleotide was ligated with *Eco*RI and *Bam*HI-digested pRW500. Transformants were selected on LB agar containing tetracycline. Plasmid DNA was purified from a number of these transformants, and digested with *Eco*RI, *Bam*HI and *Hin*dIII to check that the double-stranded oligonucleotide had been successfully integrated. The resultant vector, pKAGc1, was assayed for background *lacZ* transcriptional activity. pRW50 and pRW500 were also assayed for comparison (Table 4.1).

The *trpBA* genes present in pRW50 contain transcriptional terminators, resulting in a near absence of background activity for this vector (Table 4.1). These

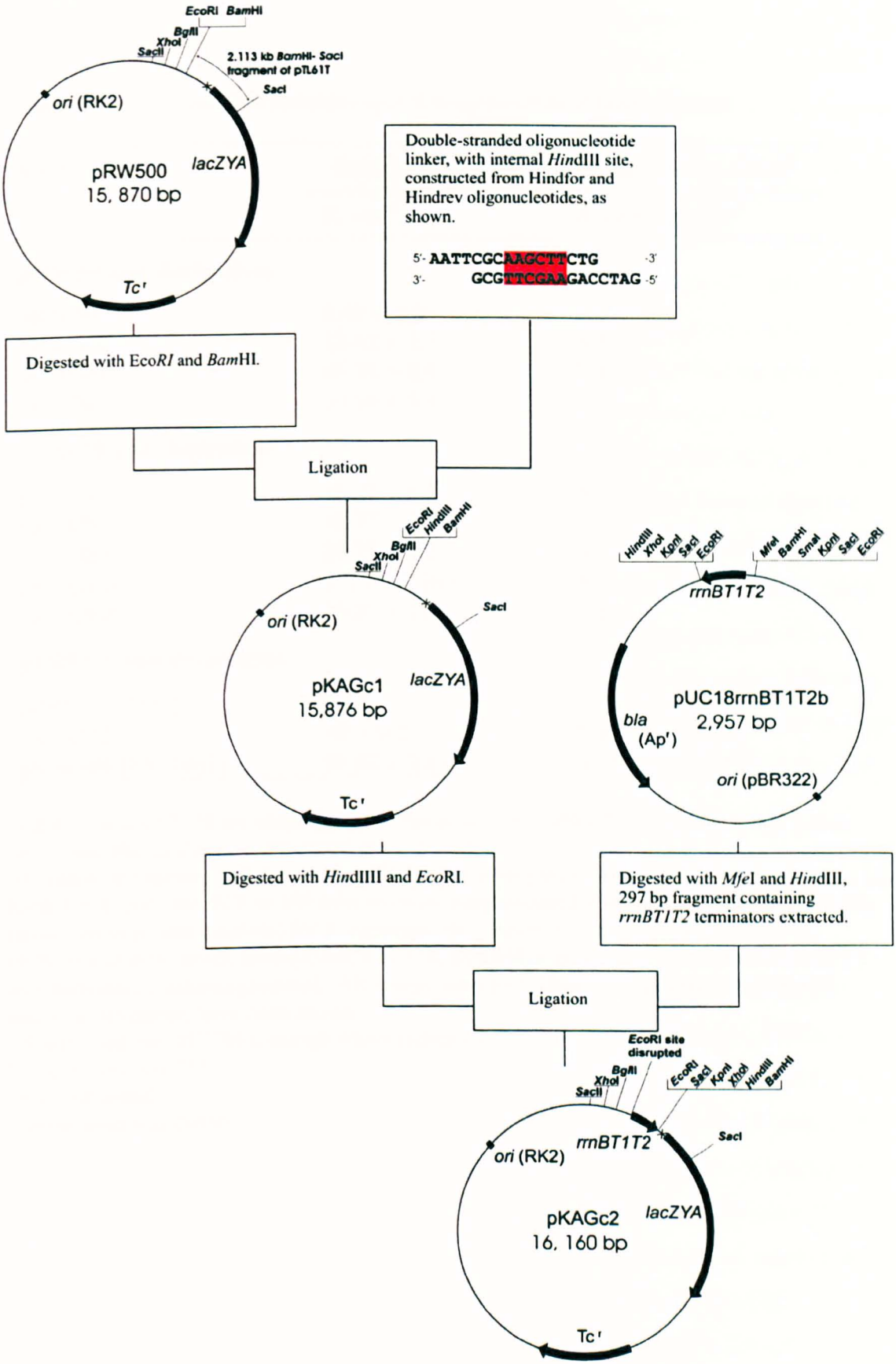

Figure 4.1: Scheme for construction of pKAGc1 and pKAGc2. Only pertinent restriction sites have been shown. Non-unique sites are underlined. *Hin*dIII site in linker insert has been highlighted in red. Cross represents the RNAse III processing site.

Table 4.1: β-galactosidase activities specified by novel *lacZ* fusion vectors

Vector[a]	Background β-galactosidase activity (Mu)[b]	
	E. coli[c]	*B. cenocepacia*[d]
pRW50 and derivatives		
pRW50	0.68 ± 0.0	NT[e]
pRW500	22.62 ± 2.0	NT
pKAGc1	66.74 ± 2.4	NT
pKAGc2	50.56 ± 0.9	NT
pTZ110 and derivatives		
pTZ110	16.23 ± 1.6[f]	NT
pKAGb1(+)	18.77 ± 1.3	NT
pKAGb1(-)	27.53 ± 4.2	NT
pKAGb2(+)	171.57 ± 10.0	NT
pKAGb2(-)	15.83 ± 1.5	NT
pPR9TT and derivatives		
pPR9TT [715j]	NT	<0 ± 0.2 [BHI]
pKAGd2	<0 ± 0.2	0.94 ± 0.3 [BHI]
pKAGd4 [MC1061]	55.02 ± 2.8	82.41 ± 1.7 [M9]

[a] pRW50 and pTZ110 are transcriptional fusion vectors. pPR9TT is a translational fusion vector and the *lacZ* gene is truncated at the 5' end.
[b] all values are means, and are expressed in Miller units (Mu). Activities were measured in LB broth for *E. coli,* and BHI or M9 salts medium supplemented with casamino acids and $FeCl_3$ (indicated in square brackets) for *B. cenocepacia.* Antibiotics were added as follows: pRW50 and derivatives, tetracycline; pTZ110, ampicillin; pTZ110 derivatives and pPR9TT and derivatives, chloramphenicol. All assays were performed on triplicate cultures, and standard deviations have been shown.
[c] Strain used was MC1061, except where indicated.
[d] Strain used was 715j
[e] NT, not tested
[f] Strain used was DH5α.

terminators, however, also lead to low levels of activity from cloned promoter fragments. pRW500 has a higher background activity of ~23 Miller units, which is acceptably low, especially considering the extra sensitivity engendered by the removal of *trpBA*. The increased activity may also be due to increased stability of the *lacZ* mRNA, owing to processing of the 5' end by RNAse III, and the presence of a different Shine-Dalgarno sequence for *lacZ* translation. However, the background activity unexpectedly rose to ~67 Miller units on insertion of the *Hin*dIII linker to make pKAGc1. It was decided that to attempt to reduce this background level, the rrnBT1T2 transcription terminators would be introduced into pKAGc1 upstream of the MCS, to prevent read-through from any upstream promoter-like sequences.

The plasmid pUC18rrnBT1T2b was digested with *Mfe*I and *Hin*dIII, and the 297 bp fragment bearing the tandem *rrnB* terminators was excised from an agarose gel. pKAGc1 was digested with *Eco*RI (which produces cohesive ends compatible with those produced by *Mfe*I) and *Hin*dIII, and then ligated with the *rrnB*T1T2 DNA fragment. Transformants were selected on LB agar containing tetracycline. Correct incorporation of the terminator fragment was checked by DNA sequencing following digestion with *Sac*II and *Bam*HI and cloning of the resultant fragment into pBluescript II KS. The background activity of pKAGc2 was tested by β-galactosidase assay and found to remain relatively high at ~51 Miller units (see Table 4.1).

In order to evaluate the suitability of pKAGc1 and pKAGc2 as reporter plasmids, a promoter known to have a high level of activity was cloned between the *Eco*RI and *Hin*dIII sites of these plasmids. The same fragment was also cloned into pRW50 for comparison. The promoter chosen was *pbfd*, an iron regulated promoter responsible for transcription of the *B. cenocepacia tonB* operon (Asghar, 2002). Figure 4.2 illustrates the method used in the construction of these three vectors, pKAGc1-pbfd, pKAGc2-pbfd and pRW50-pbfd. The transcriptional activities of the *lacZ* gene in the pKAGc1-pbfd and pKAGc2-pbfd constructs were determined in *E. coli* and were found to be many fold higher than that of pRW50-pbfd (Figure 4.3 and Table 4.2). This illustrates the activity dampening effects of *trpBA*, and might also be partially owed to increased transcript stability engendered by the RNAse III processing site, and perhaps to a more efficient ribosome binding site for *lacZ* translation. Unfortunately, whereas pRW50-pbfd showed 12 fold regulation of *pbfd* in response to iron availability, pKAGc1 and pKAGc2 showed only 5 and 6 fold

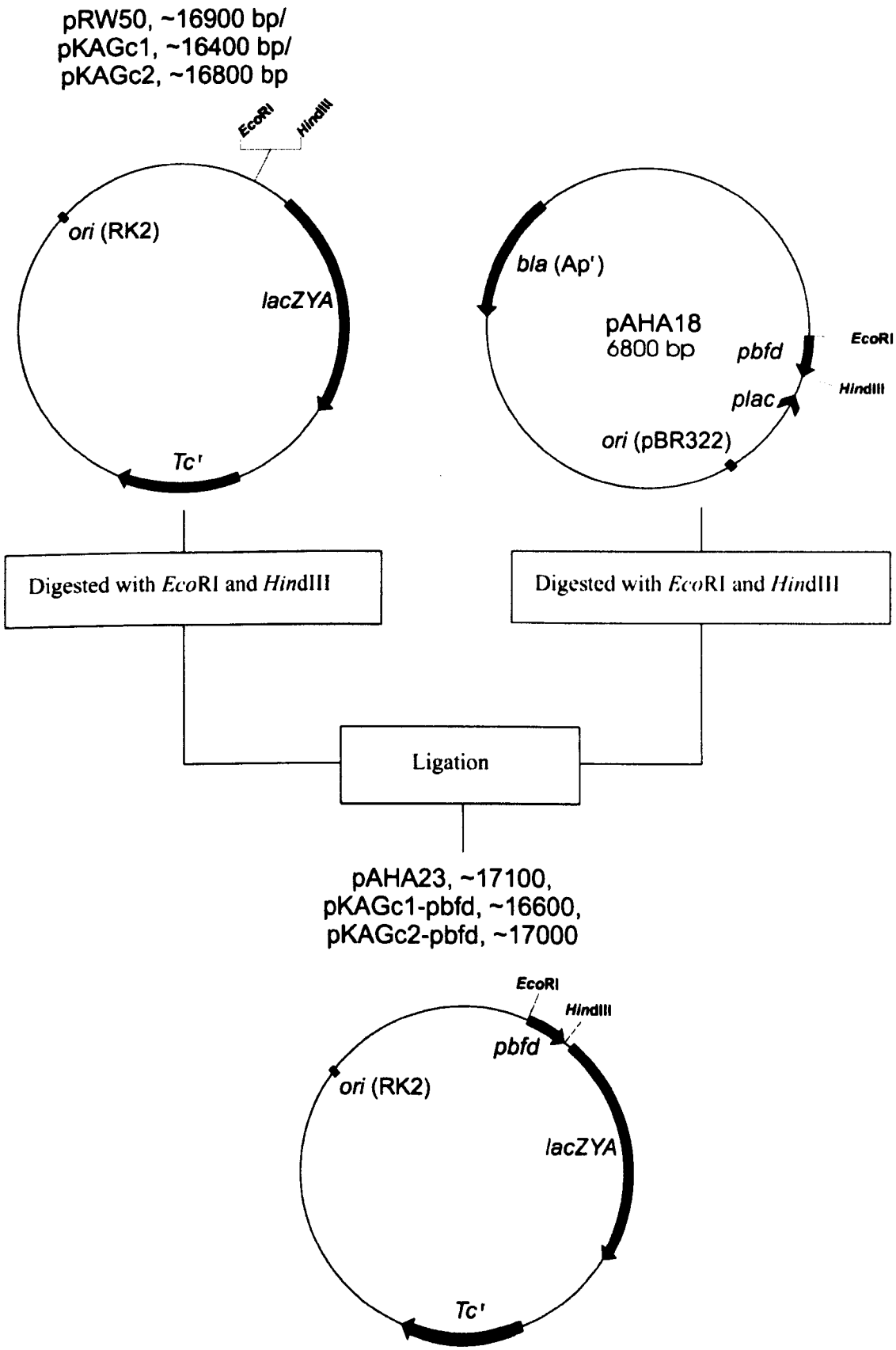

Figure 4.2: General scheme for the construction of pKAGc1-pbfd, pKAGc2-pbfd and pRW50-pbfd. Only pertinent restriction sites are shown.

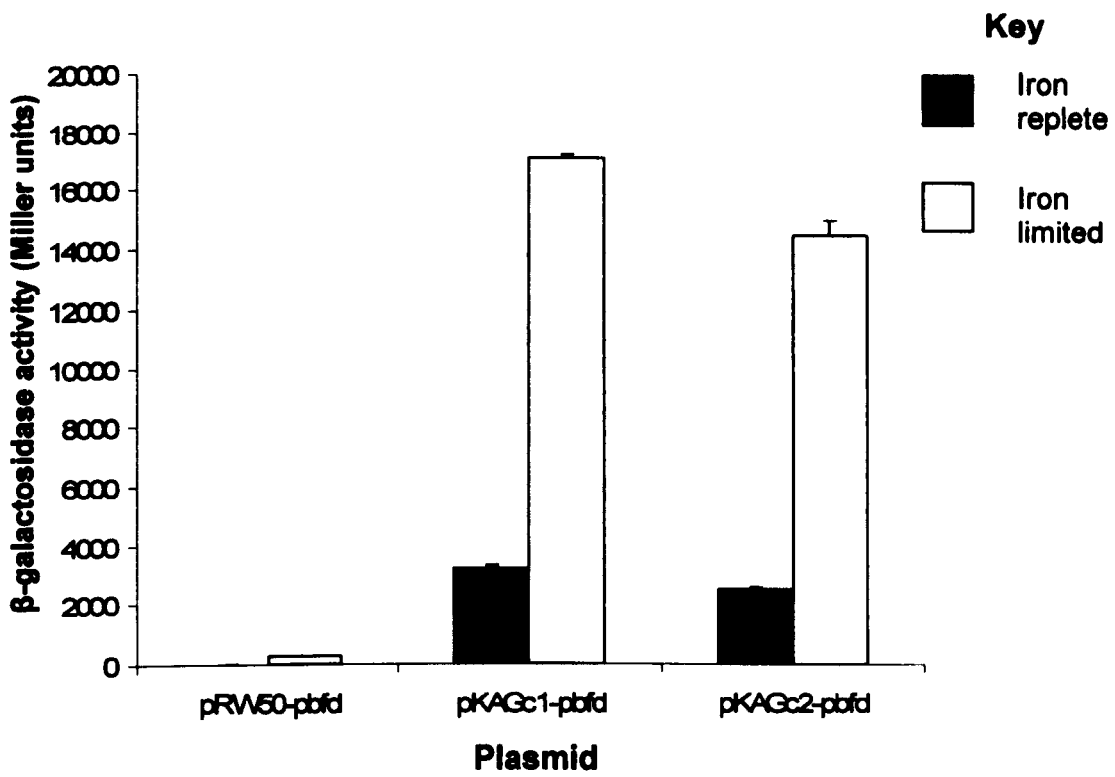

Figure 4.3: Activities of pRW50 derivatives bearing a test promoter fragment. β-galactosidase assays were carried out on *E. coli* MC1061 cells containing the plasmids indicated, grown under iron limiting or iron replete conditions as indicated. Activities were background corrected by subtracting the activity specified by each vector without inserted *pbfd* growing under the appropriate conditions. Assays were performed on triplicate cultures, and error bars represent the standard deviation. Growth medium was LB broth containing tetracycline.

Table 4.2: Activities of pRW50 derivatives bearing a test promoter fragment[a]

Plasmid	β-galactosidase activity[a]		Fold repression[b]
	Iron replete	Iron limited	
pRW50-pbfd	25	296	12
pKAGc1-pbfd	3233	17116	5
pKAGc2-pbfd	2553	14486	6

[a] Values shown are those used to draw Figure 4.3.
[b] Fold repression exhibited between cells grown under iron replete compared to iron limited conditions.

regulation, respectively. This apparent decrease in regulation might be the result of the high β-galactosidase activity observed in cells containing pKAGc1-pbfd or pKAGc2-pbfd under iron limited conditions. This high activity might be toxic for the cells, leading to an artificially low β-galactosidase activity under iron limited conditions. As the *rrnB*T1T2 terminators made only a small difference to the background activity of pKAGc2, there was little apparent advantage in using pKAGc2 over pKAGc1 apart from the presence of an additional unique restriction site (*Kpn*I) in the MCS of the former.

4.3: Construction and analysis of pTZ110 derivatives

To make pTZ110 suitable for use in *B. cenocepacia*, it was necessary to introduce a chloramphenicol resistance cassette as a selectable marker. Part of transposon mini-Tn*5*Cm, which bears the Ω-Cm interposon containing the *catA2* gene from plasmid pSa, flanked at both ends by transcriptional terminators (Fellay *et al.*, 1987; de Lorenzo *et al.*, 1990), was excised from pUTmini-Tn5CmlacZYA (Asghar, 2002) by digestion with *Hin*dIII. pTZ110 was digested with *Sca*I which cuts within the *bla* gene, and ligated with the chloramphenicol resistant interposon (see Figure 4.4). *E. coli* MC1061 transformants were selected using LB agar containing chloramphenicol, and purified plasmid DNA was digested with *Pvu*II to determine the orientation of the *cat* gene, as the interposon contains an asymmetrically positioned *Pvu*II site. Two clones were chosen, one with the *cat* and *lacZ* genes in the same orientation, pKAGb1(+), and one with these genes in opposite (i.e. divergent) orientations, pKAGb1(-). The background β-galactosidase activity specified by these plasmids was determined (see Table 4.1).

The results show that the background activity specified by pKAGb1(+) and pKAGb1(-) are sufficiently low for their use as reporter plasmids. However, when fragments bearing the putative promoters for *orbS* and the OrbS-dependent promoters (see Chapter 5) were cloned between the *Eco*RI and *Hin*dIII sites of pKAGb1(+) and pKAGb1(-) for analysis, the resultant plasmids appeared to be unstable in *E. coli* MC1061. This conclusion was reached by the appearance of white transformant colonies on LB agar containing X-gal, owing to the loss of β-galactosidase activity. As pTZ110 is stably maintained in *E. coli* (Schweizer and Chuanchuen, 2001), it was deemed likely that the ~3.7 kb interposon bearing the *catA2* gene (642 bp) was destabilizing the plasmid. Therefore, it was decided to PCR amplify the *cat* gene from pBR328 with primers catfor and catrev to allow incorporation of only the *cat* gene into pTZ110, without any extraneous DNA. This would reduce the size of the inserted Cm^R fragment from ~3.7 kb for the *catA2*-bearing interposon to ~920 bp. The PCR amplified *cat* gene was digested with *Pst*I, and ligated with the corresponding site within the *bla* gene of pTZ110, as shown in Figure 4.5, and *E. coli* MC1061 tranformants selected using LB agar containing chloramphenicol. The orientation of

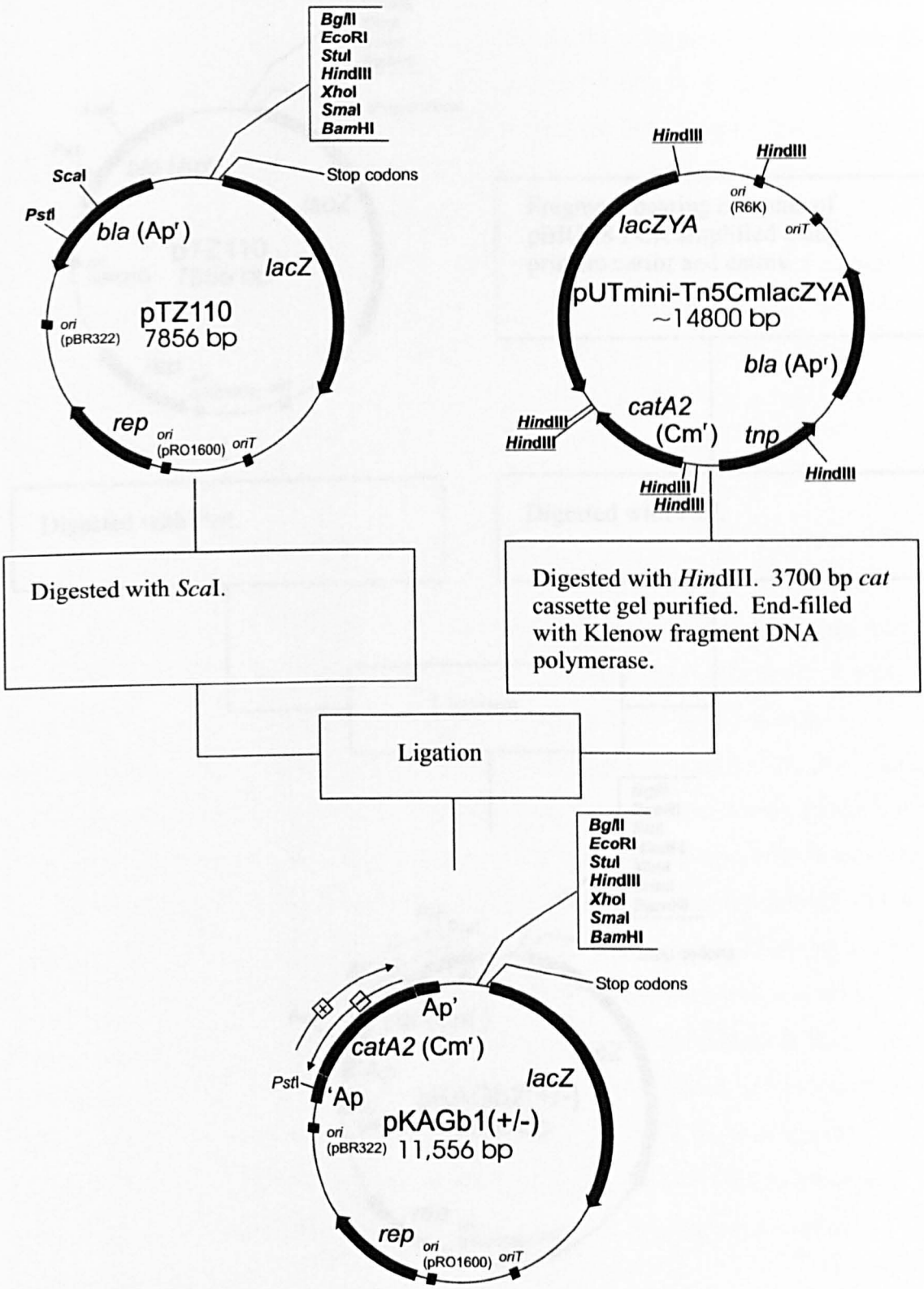

Figure 4.4: General scheme for the construction of pKAGb1(+) and pKAGb1(-). Only pertinent restriction sites are shown. Non-unique sites have been underlined.

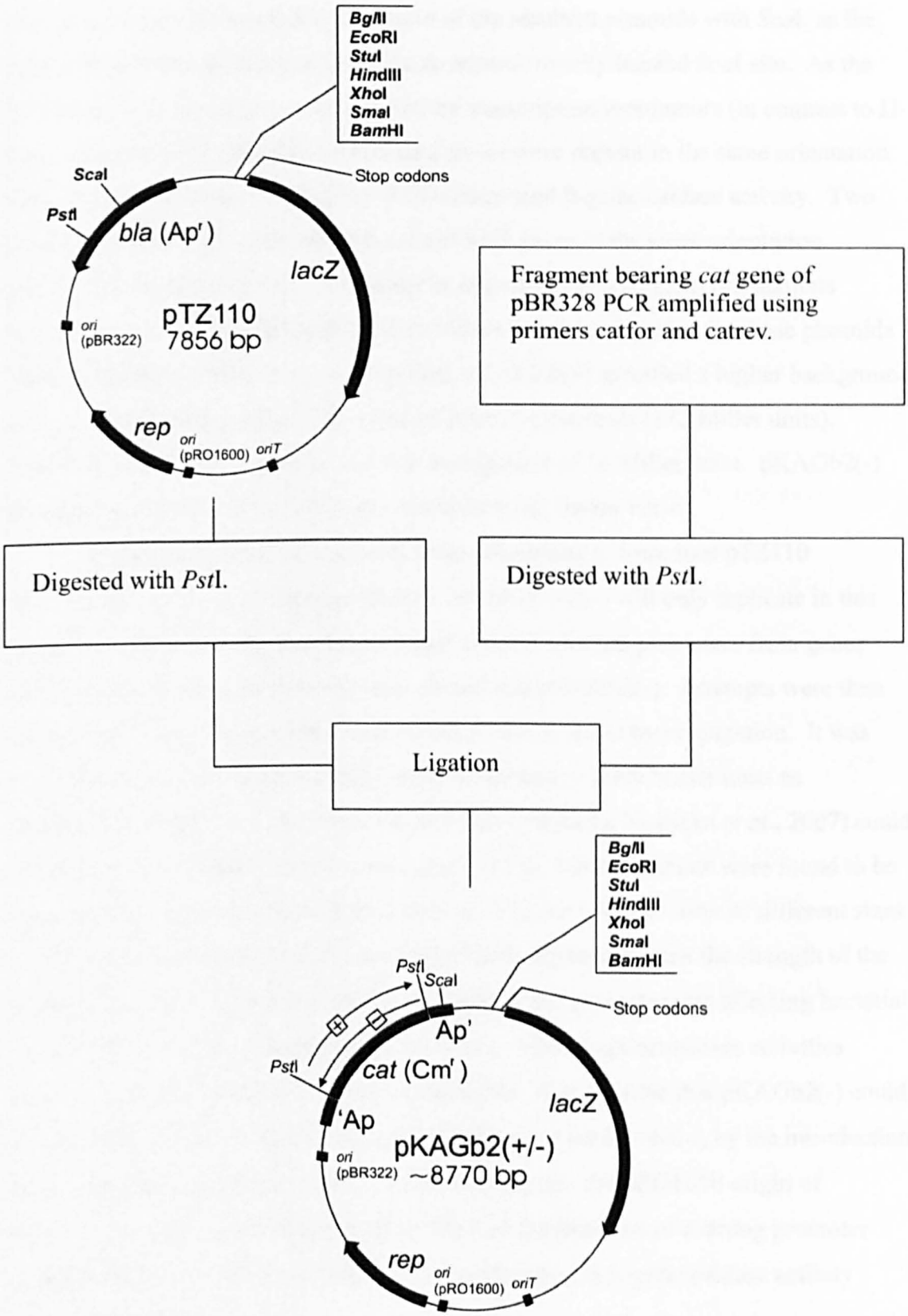

Figure 4.5: General scheme for the construction of pKAGb2(+) and pKAGb2(-). Only pertinent restriction sites are shown.

the *cat* gene was determined by digestion of the resultant plasmids with *Sca*I, as the pBR328-derived *cat* fragment contains an asymmetrically located *Sca*I site. As the PCR amplified *cat* gene was not flanked by transcription terminators (in contrast to Ω-Cm), constructs in which the *cat* and *lacZ* genes were present in the same orientation were likely to give rise to a high level of background β-galactosidase activity. Two plasmids were chosen, one with the *cat* and *lacZ* genes in the same orientation (pKAGb2(+)), and one with these genes in opposite (i.e. divergent) orientations (pKAGb2(-)). The background β-galactosidase activities specified by these plasmids were determined (Table 4.1). As expected, pKAGb2(+) specified a higher background activity level than the pKAGb1(+) and pKAGb1(-) plasmids (172 Miller units). However, pKAGb2(-) specified a lower background of 16 Miller units. pKAGb2(-) therefore appeared most suitable as a transcriptional fusion vector.

Subsequent observations made when attempting to introduce pTZ110 derivatives into *B. cenocepacia* indicated that pKAGb2(-) will only replicate in this bacterium when a strong promoter is fused to *lacZ*. Several promoters from genes involved in cysteine biosynthesis were cloned into pKAGb2(-). Attempts were then made to introduce the resultant vectors into *B. cenocepacia* by conjugation. It was found that only derivatives bearing strong promoters (~3,000 Miller units as determined by reporter analysis using pKAGd4 (Iwanicka-Nowicka *et al.*, 2007) could be efficiently conjugated into *B. cenocepacia* 715j. These plasmids were found to be more stable in *B. cenocepacia* K56-2 than in 715j, but colonies were of different sizes on M9 agar supplemented with chloramphenicol, dependent upon the strength of the inserted promoter, suggesting that the strength of this promoter was affecting bacterial growth (M. Thomas, personal communication). Thus, β-galactosidase activities derived from these plasmids would be unreliable. It is possible that pKAGb2(-) could be stabilised within *B. cenocepacia*, thus making it a useful vector, by the introduction of a strong promoter downstream of *lacZ*, reading into the pRO1600 origin of replication. This should have the same effect as the insertion of a strong promoter upstream of *lacZ*, but without increasing the background β-galactosidase activity specified by the vector.

4.4: Construction and analysis of pPR9TT derivatives

pPR9TT is a translational fusion vector, meaning that the *lacZ* gene it carries does not have its own translational start codon. Promoter fragments to be assayed using this system must therefore be cloned with the downstream gene in-frame with *lacZ*. As a result, β-galactosidase fusion proteins are generated. To convert pPR9TT into a transcriptional fusion vector, a double-stranded DNA linker was constructed, using oligonucleotides pPR9TTfor and pPR9TTrev. This linker was designed to have *Sma*I- and *Hin*dIII-compatible ends, and was inserted into pPR9TT that had also been digested with these enzymes (see Figure 4.6). The resultant plasmid was named pKAGd2, the successful insertion of the double-stranded oligonucleotide having been verified by DNA sequencing. Introduction of this linker sequence resulted in the incorporation of stop codons in all three reading frames (to prevent readthrough translation), followed by a Shine-Dalgarno sequence and an ATG (translational start) codon in frame with *lacZ*.

The background β-galactosidase activity specified by pKAGd2 was found to be very low, i.e. <1 Miller unit in both *E. coli* and *B. cenocepacia* (Table 4.1). To test the suitability of this vector for promoter analysis, the *tac* promoter was used. *ptac* is a hybrid promoter derived from the *E. coli trp* and *lac* promoters, which are responsible for transcription of the tryptophan biosynthesis and lactose utilisation genes, respectively (De Boer *et al.*, 1983). *ptac* is a strong promoter and its activity was predicted to be constitutive in *B. cenocepacia*, which does not have the *lac* repressor gene, and in *E. coli* Δ*lac* hosts such as MC1061.

The *tac* promoter was available within pBBR1MCS (Lowe, 2001). It was excised using *Kpn*I and *Xho*I, and inserted into the corresponding sites of pBluescript II KS, where its sequence was confirmed. The resultant plasmid was named pBS-ptac. The *tac* promoter was excised as a 146 bp fragment from pBS-ptac, using *Bam*HI and *Xho*I, and inserted into pKAGd2 cut with *Bgl*II and *Xho*I. β-galactosidase activity was then assayed with *E. coli* MC1061 and *B. cenocepacia* 715j as hosts. However, the activity level in both hosts was unexpectedly low: 48.15 Miller units in the *B. cenocepacia* host (see Figure 4.7), and 57.26 Miller units in the *E. coli* host, with both values having been corrected for background activity of the vector. This suggested that there was a mutation, either within *ptac*, or else within the *lacZ* gene on pKAGd2.

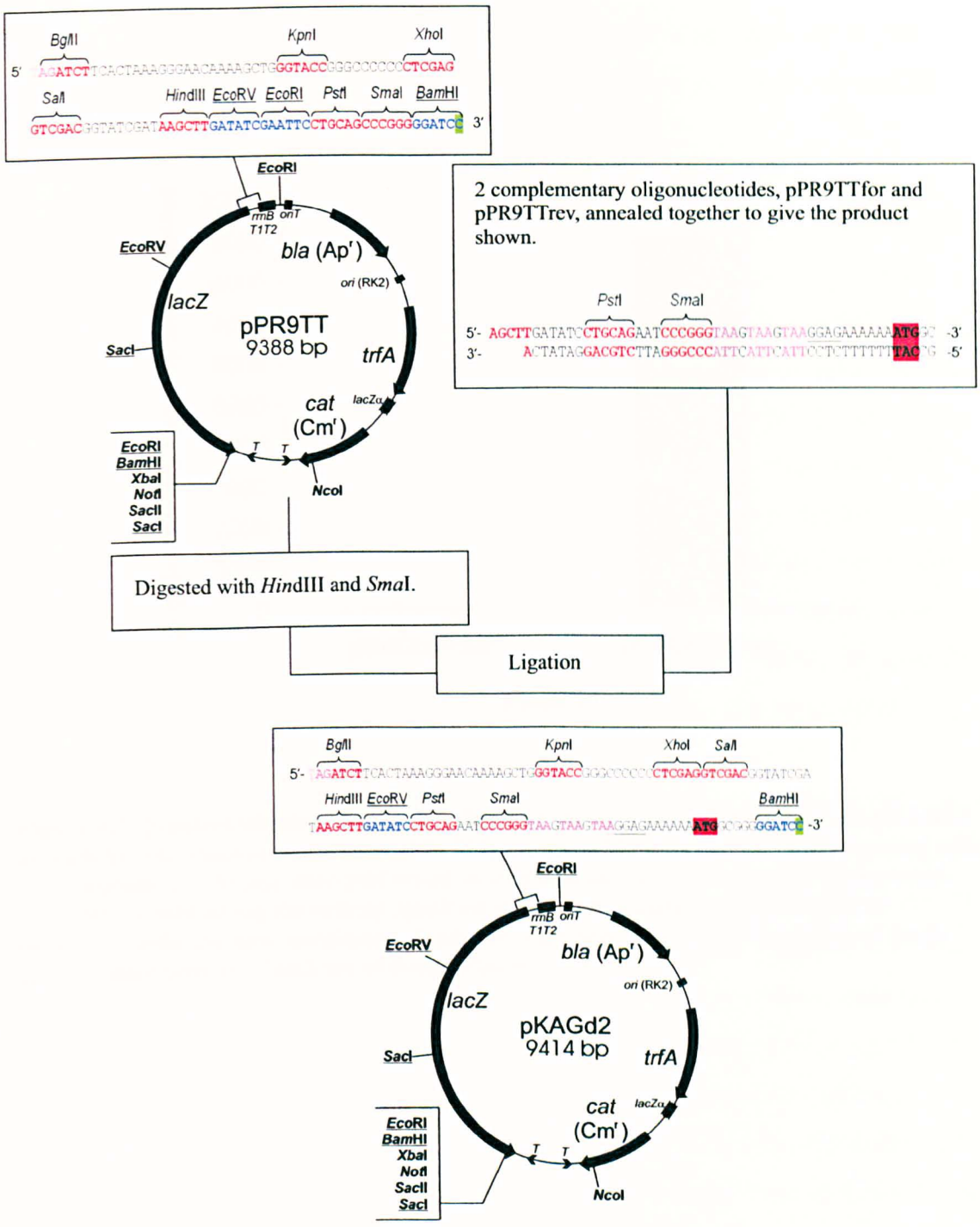

Figure 4.6: General scheme for the construction of pKAGd2. MCS and oligonucleotide linker sequences are shown. Restriction enzyme sites have been indicated, unique sites within the sequence shown are in red, and non-unique sites are shown in blue with their names underlined. Translational terminators are shown in magenta. The introduced ATG start codon for *lacZ* translation is highlighted in red. The first base of the native *lacZ* coding sequence is highlighted in green, and constitutes the second base of codon 9 of this sequence. Only the sense strand of the pPR9TT and pKAGd2 MCSs are shown, whereas both strands of the oligonucleotide linker are shown.

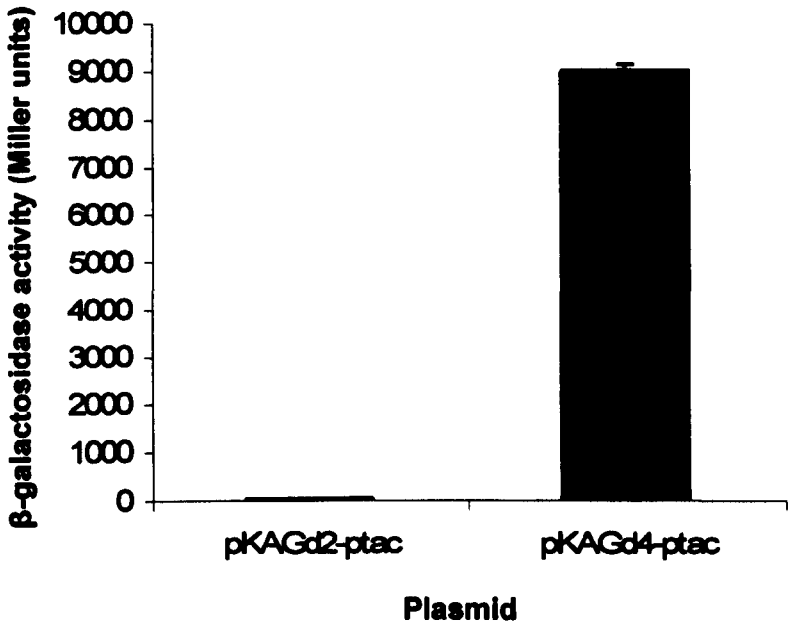

Figure 4.7: β-galactosidase activities specified by the *tac* promoter cloned into pKAGd2 and pKAGd4. Plasmids were assayed in 715j grown in M9 salts medium supplemented with chloramphenicol. Assays were performed on triplicate cultures. Values were background-corrected by subtracting the activity specified by the parent plasmid (i.e. pKAGd2 or pKAGd4) under the same conditions. Error bars represent the standard deviation of the β-galactosidase activity of each set of three cultures.

However, nucleotide sequence determination of *ptac* and of the whole of *lacZ* in pKAGd2 did not reveal any mutations, and therefore the cause of this low activity remained unknown.

One possible explanation for the observed lack of activity specified by pKAGd2-ptac was that the Shine-Dalgarno and/or *lacZ* initiation codon in the mRNA were sequestered in a region of secondary structure that might have formed. This would greatly decrease the efficiency of *lacZ* mRNA translation. It was therefore decided to substitute another *lacZ* gene for that of pKAGd2, and in so doing change the sequenceof the *lacZ* leader mRNA. This was obtained from pUC18NotlacZYA (Shalom, 2002). Thus, pKAGd2 was digested with *Not*I and end-filled with DNA polymerase Klenow fragment, prior to digestion with *Hin*dIII. pUC18NotlacZYA was digested with *Dra*I and *Hin*dIII, and the DNA fragment containing *lacZ* was purified from an agarose gel for ligation with pKAGd2 (Figure 4.8). Transformants were selected on LB agar containing chloramphenicol and X-gal, and purified plasmid DNA was analysed by restriction digestion to find a suitable clone. The resultant plasmid was named pKAGd4.

The *lacZ* gene in pUC18NotlacZYA was derived from pRW500, and therefore is preceded by an RNAse III processing site (discussed in Section 4.2). The fragment of pUC18NotlacZYA transferred into pKAGd2 contained the *lacZ* gene, and also its translational initiation codon and the upstream RNAse III processing site. As a result, the β-galactosidase transcripts specified following the insertion of promoters into pKAGd4 should have standardised 5' ends, and therefore equal stability, and the β-galactosidase activity specified by derivatives of pKAGd4 containing different promoters should be comparable. Furthermore, while the *Sma*I site within the MCS of pKAGd2 was lost in the construction of pKAGd4, usable *Sph*I, *Xba*I and *Bam*HI sites have been gained, increasing the versatility of this vector. pKAGd4 and derivatives were found to be unstable in *B. cenocepacia* 715j in the absence of antibiotic selection, with white (Lac^-) colonies appearing on agar supplemented with X-gal unless sufficient chloramphenicol was present.

The background β-galactosidase activity specified by pKAGd4 was measured in *E. coli* MC1061 and *B. cenocepacia* 715j (see Table 4.1). The background activity was higher than that of strains harbouring pKAGd2, but was within an acceptable limit, and therefore the *tac* promoter was cloned into the new vector for testing. Both pBS-ptac and pKAGd4 were digested with *Xho*I and *Kpn*I. The *tac* promoter

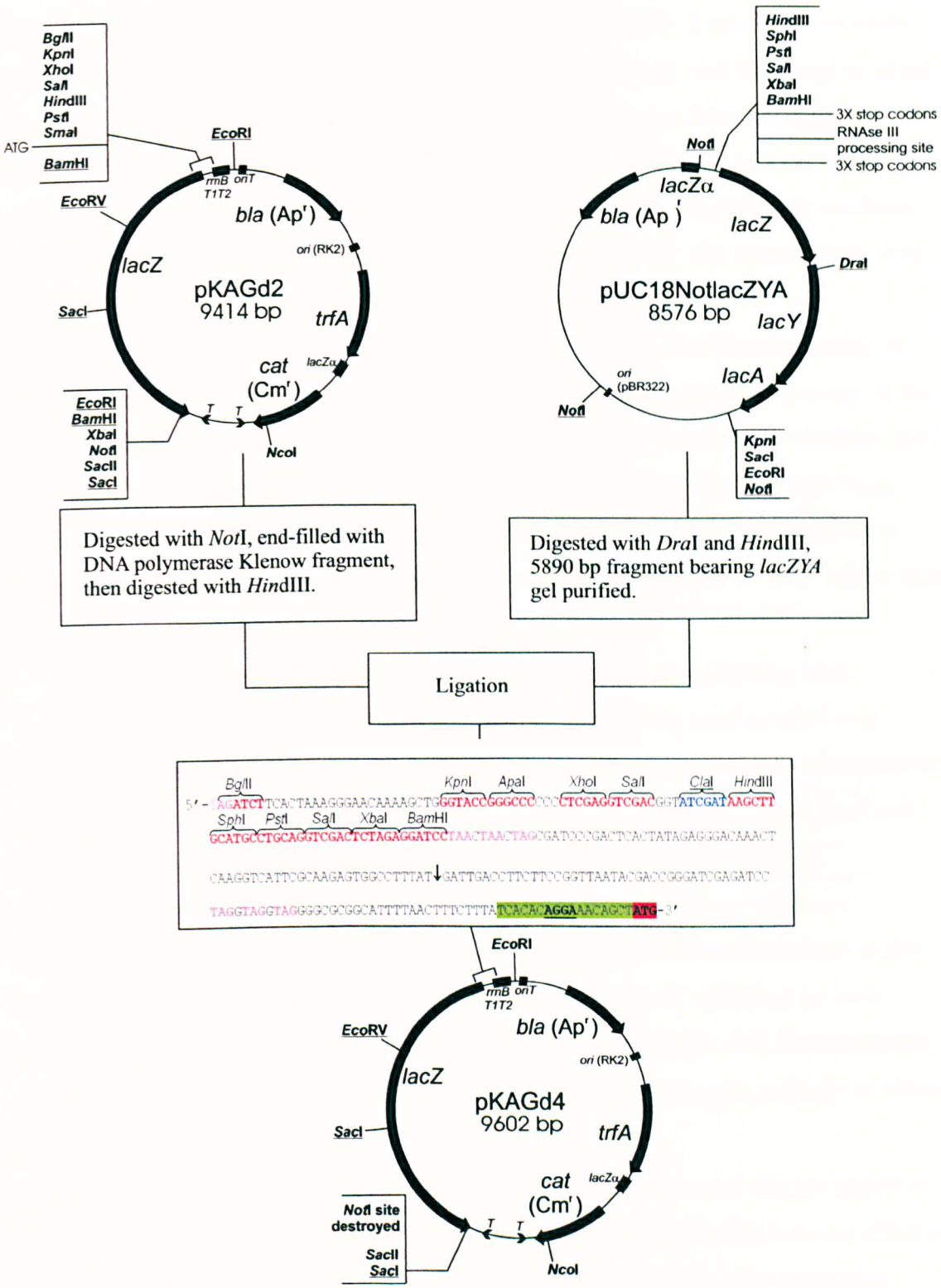

Figure 4.8: General scheme for the construction of pKAGd4. Sense strand sequence of the pKAGd4 MCS is given. Restriction enzyme sites have been indicated, unique sites within the sequence shown are in red, and non-unique sites are shown in blue with their names underlined. Translational terminators are shown in magenta. The RNAse III processing site is located between the two sets of three stop codons, and the precise cleavage site is indicated by an arrow. The native *lacZ* sequence is highlighted in green, with the Shine-Dalgarno site underlined, and the translational start codon is highlighted in red and emboldened.

was extracted from an agarose gel and ligated with pKAGd4. Transformants were selected using LB agar containing chloramphenicol and X-gal, and the integrity of the recombinant plasmid was analysed by restriction digestion and DNA sequencing. The resultant plasmid, pKAGd4-ptac, was introduced into *B. cenocepacia* 715j by conjugation, and the β-galactosidase activity of cultures grown in M9 salts medium containing casamino acids and chloramphenicol was assayed. The *tac* promoter was found to specify an activity of ~9,000 Miller units (see Figure 4.7). The *B. cenocepacia* genome does not encode the Lac repressor, and therefore induction of *ptac* with IPTG was expected to be unnecessary. This was confirmed by assay of the β-galactosidase activity specified by pKAGd4-ptac in 715j grown in the medium used above, but supplemented with 1 mM IPTG and induced for 1 hour. No significant difference was observed between the *ptac* activity specifed under these conditions ('induced' cells gave rise to 9013 Miller units activity, as opposed to 8983 Miller units for 'uninduced' cells).

Before using pKAGd4 as a *lacZ*-reporter vector for investigating iron-regulated promoters, the effect of iron availability on plasmid copy number was indirectly assessed by measuring the activity of iron-independent promoters cloned in pKAGd4. Two pKAGd4 derivatives bearing iron-independent promoters, *cysI* and *cysD*, which are involved in cysteine biosynthesis (pMH609 and pMH612, respectively) (Iwanicka-Nowicka *et al.*, 2007) were introduced into 715j by conjugation, and β-galactosidase assays were carried out in M9 salts medium under conditions of iron sufficiency and iron limitation. The activity specified by both promoters was found to be similar under both conditions (Figure 4.9), demonstrating that growth of 715j under iron limited and iron replete conditions is unlikely to affect the copy number of pKAGd4.

Although the iron replete and iron limited conditions tested did not appear to affect the copy number of pKAGd4 derivatives, these conditions did have an effect on the background activity specified by pKAGd4. *E. coli* MC1061 cells containing pKAGd4 grown in iron limited LB broth (containing 175 μM 2'2-dipyridyl), had a background activity of 53 Miller units, compared to 42 units for iron replete LB broth (containing 50 μM $FeCl_3$). *B. cenocepacia* 715j cells containing pKAGd4 grown in iron limited M9 salts broth (containing 100 μM 2'2-dipyridyl) had a background activity of 111 Miller units, compared to 82 Miller units when grown in iron replete medium (containing 50 μM $FeCl_3$). These differences are insignificant when

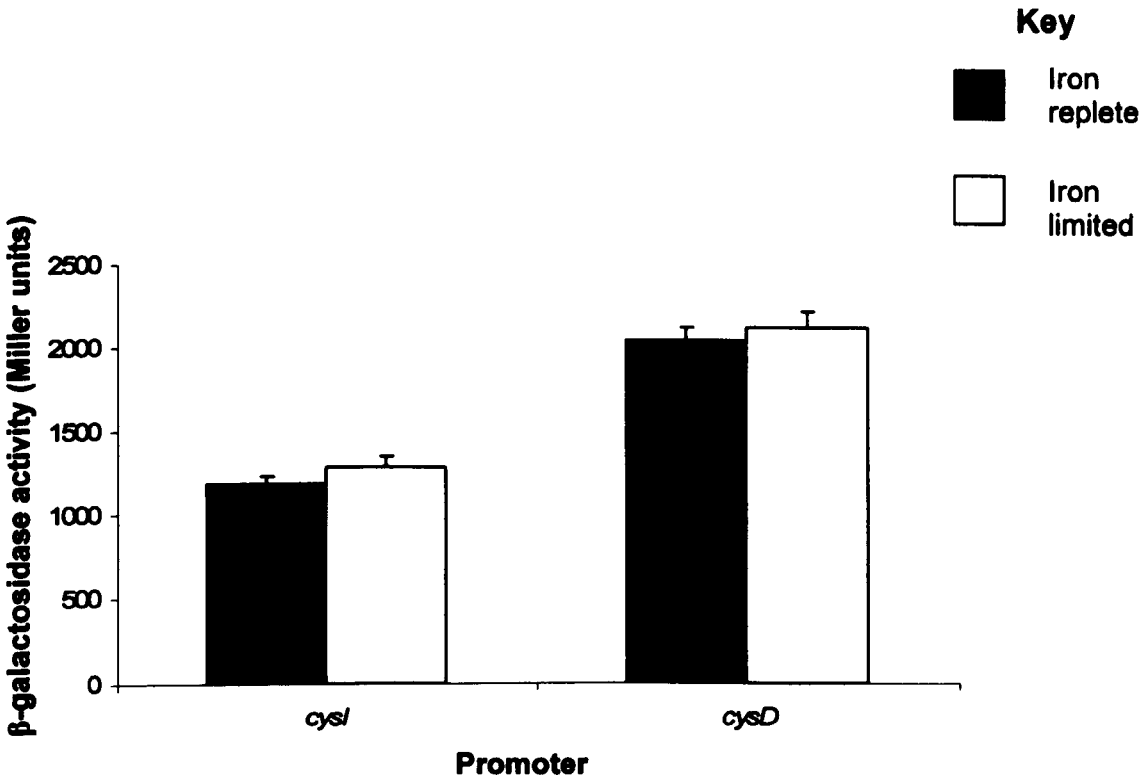

Figure 4.9: Growth medium iron concentration does not affect the activity of non iron-dependently regulated promoters cloned into pKAGd4. Plasmids pMh609 (*pcysI*) and pMh612 (*pcysD*) were assayed in triplicate in 715j, grown in M9 salts medium with chloramphenicol, under conditions of iron limitation and repletion. Activities were background corrected by subtracting the activity specified by pKAGd4 under the same conditions. Error bars represent the standard deviation of the activities of each set of three cultures.

compared to the high level of β-galactosidase activity specified by pKAGd4 bearing a promoter, and therefore were not deemed important. Furthermore, no trend was observed for the background β-galactosidase activity specified by pKAGd4 in cells grown in the presence of $FeCl_3$ or 2'2-dipyridyl: the *E. coli* background value was highest in cells grown in the presence of 2'2-dipyridyl, whereas the *B. cenocepacia* value was highest when cells were grown in the presence of $FeCl_3$. As the iron limited and iron replete conditions used did not appear to affect the copy number of pKAGd4, or to have a large effect on the background activity specified by this vector, pKAGd4 was deemed suitable for further use in characterising iron-regulated promoters.

4.5: Discussion

A number of *lacZ* transcriptional fusion vectors were modified for potential use. Of these, pKAGd4 was deemed the most suitable, as this vector could be mobilised into *B. cenocepacia* and maintained within this bacterium. However, pKAGd4 was found to be unstable in *B. cenocepacia* 715j in the absence of antibiotic selection, with white (Lac^-) colonies appearing on X-gal-containing agar unless sufficient chloramphenicol was present. This instability has been observed with other RK2-based plasmids in the Bcc (V. Venturi, personal communication), but with suitable selection conditions does not prevent their use. This vector specifies a fairly high background β-galactosidase activity (~80 Miller units in 715j grown in M9 salts broth). However, this activity was still low in comparison to the activity specified by three test promoters (*tac, cysI, cysD*), and therefore the vector was deemed suitable for use.

The pTZ110 derivatives were found to be unreliable. From observations made when attempting to introduce pKAGb2(-) into *B. cenocepacia* 715j, it appears that this plasmid will only replicate in this bacterium when a strong promoter is fused to *lacZ*. pKAGb2(-) does appear to replicate in strain K56-2, but colony sizes are proportional to promoter strength, indicating variable copy number and stability. For these reasons the pTZ110 derivatives constructed were not used within this study.

The pRW50 derivatives are potentially useful vectors, although they were not used extensively in this study, as pKAGd4 was found to work well in *E. coli*. These vectors specified a higher background β-galactosidase activity than their direct progenitor pRW500, and therefore would be most useful when the additional *Hin*dIII site inserted into plasmids pKAGc1 and pKAGc2 was required. *B. cenocepacia* is resistant to the majority of antibiotics commonly used for plasmid selection, including tetracycline. For this reason pRW50 and the derivatives produced cannot be stably introduced into *B. cenocepacia*. Furthermore, despite being broad host-range plasmids, pRW50 and the derivatives produced lack origins of transfer, and therefore are not mobilisable for conjugative transfer.

Chapter 5

Organisation and regulation of the ornibactin gene cluster

5.1: Introduction

The genes of the ornibactin operon were identified *in silico*, and their upstream regions were inspected for sequences resembling promoters. Two candidate promoters were identified upstream of *orbS* by their similarity to promoters recognised by the *B. cenocepacia* primary σ factor, σ^{70} (see Section 1.7.2 and Figure 5.1).

As previously mentioned (Section 1.6.2), OrbS and PvdS have similar amino acid sequences, showing 37 % identity over the matching region. The PvdS-dependent promoter consensus is TAAAT $(N)_{16}$ CGT (Wilson *et al.*, 2001; Ochsner *et al.*, 2002; Visca *et al.*, 2002). Sequences highly homologous to the PvdS-dependent promoter consensus were found upstream of *orbH*, *orbE* and *orbI* (see Section 1.6.2 and Figure 5.2). The putative *orbE* promoter sequence was identical to the PvdS-dependent promoter consensus, while the two other putative promoters differed at the fifth position of the -35 region, having an A residue rather than a T.

The two candidate σ^{70}-dependent promoters identified upstream of *orbS* (Figure 5.1) are good matches for the σ^{70}–dependent consensus sequence (TTGACA $(N)_{17}$ TATAAT (Wösten, 1998)), which they match at 5/6 positions of both the -35 and -10 elements. The furthest from *orbS* of the two candidate promoters has a sub-optimal spacer region between the -35 and -10 elements of only 16 bases, whereas the closer of the two sequences to *orbS* has a spacer region of optimal length (17 bp). However, some promoters with a 16 bp spacer, such as *ptac*, can be highly active (De Boer *et al.*, 1983).

In the work presented in this chapter, reverse transcriptase PCR (RT-PCR) was used to determine the transcriptional organisation of the operon, and thereby to identify intergenic regions which are likely to contain promoters. The location of the promoters within the ornibactin gene cluster was determined by a combination of *lacZ*-fusion analysis and primer extension. The response of the promoters to iron availability was also investigated.

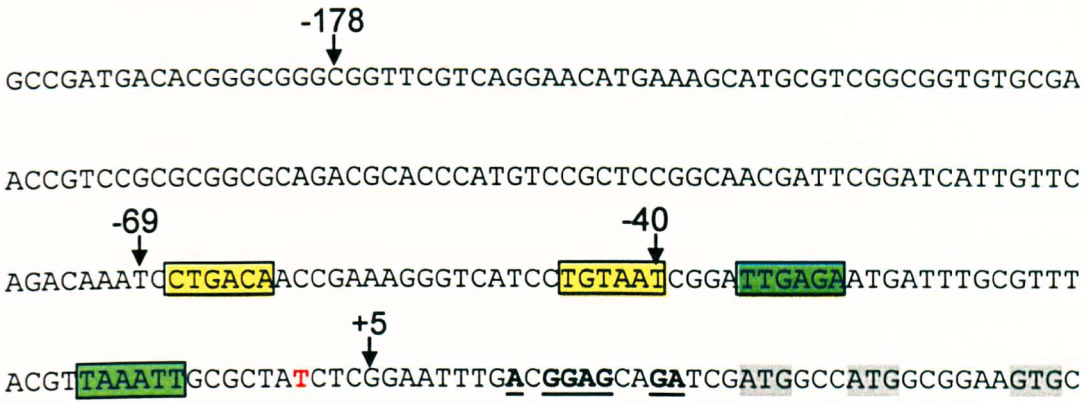

Figure 5.1: Putative promoter sequences for *orbS*. The -35 and -10 regions of two putative σ^{70}-type promoters located upstream of *orbS* are shown in boxes, one highlighted in yellow and one in green. The putative ribosome binding site has been emboldened and underlined, and the three putative start codons for translation of *orbS* mRNA have been highlighted in grey. The putative transcription start site (TSS) for the downstream promoter-like sequence is shown in red font. The promoter deletion endpoints used in Section 5.4 were measured from this putative TSS, and are indicated.

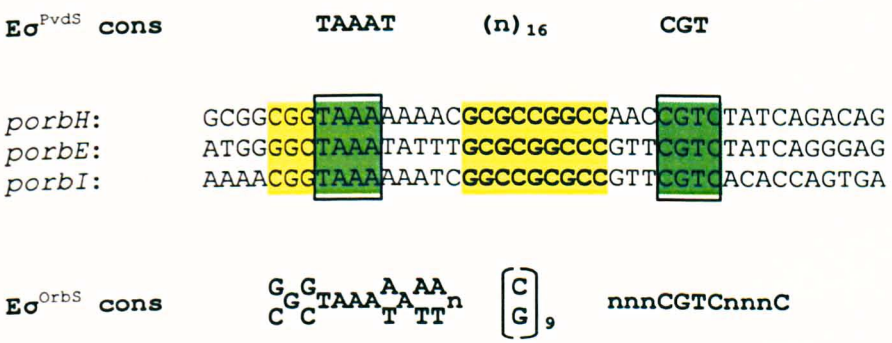

Figure 5.2: Putative OrbS-dependent promoters identified *in silico*. The three putative OrbS-dependent promoters, which have been named after the first gene downstream of each promoter, have been aligned. The predicted -35 and -10 regions have been boxed, highlighted in green, and labelled accordingly. Conserved G+C-rich regions have been highlighted in yellow. The PvdS-dependent promoter consensus is shown above the alignment, and the consensus sequence of the putative OrbS-dependent promoters is shown below (Adapted from Agnoli *et al.*, 2006).

5.1.1: Objectives

- To determine the transcriptional unit organisation within the ornibactin gene cluster.
- To locate the promoter elements responsible for transcription of the ornibactin gene cluster, and demonstrate iron-dependent regulation.

5.2: Investigation of the transcriptional organisation of the ornibactin gene cluster

5.2.1: Analysis of ornibactin gene transcripts by RT-PCR

Reverse transcriptase PCR (RT-PCR) was used to examine the transcriptional units within the ornibactin gene cluster. Primer pairs were designed that could amplify DNA spanning each intergenic region (determined by *in silico* analysis). Reverse transcription of *B. cenocepacia* 715j RNA was used to produce cDNA for amplification using these primers. RNA was isolated from *B. cenocepacia* cultures grown under conditions of both iron starvation and iron sufficiency, to allow comparison of transcription of the gene cluster under both of these conditions. RT-PCR was carried out using the Access RT-PCR kit (Promega), which, it should be noted, is a one-stage RT-PCR kit, and therefore RNA can be reverse-transcribed using either primer included for the PCR stage, depending on the polarity of the mRNA. Primer pairs used are indicated in Table 5.1. PCR products obtained from *B. cenocepacia* chromosomal DNA using the RT-PCR primer pairs were used as size controls, and to confirm that the primers were specific. Negative control PCR reactions were also carried out in the absence of reverse transcriptase on RNA isolated under iron limited conditions.

Figure 5.3 shows the agarose gel electrophoretic analysis of the RT-PCR products obtained. When RT-PCR was carried out on RNA purified from cells grown under iron starvation conditions, products of the expected size for the primer pairs used were generated for each of the predicted intergenic regions within the ornibactin gene cluster, apart from the regions between *orbE* and *orbI,* and *orbJ* and *orbK.* No product of the correct size was produced for the predicted intergenic regions at each end of the gene cluster, i.e. the regions between ORF BCAL1687 and *orbS*, and between *orbL* and BCAL1703 (Figure 5.4). However, several products, all of incorrect size, were generated by RT-PCR of the intergenic region between BCAL1687 and *orbS* (Figure 5.3). Bands of incorrect size were probably the products of non-specific primer annealing, and were also produced by RT-PCR across the *orbH-orbG* and *orbD-orbF* intergenic regions, in addition to a band of the expected

Table 5.1: Primer pairs used for RT-PCR analysis

Intergenic region	Primer[a]		cDNA product[b]	
	Forward	Reverse	-Fe	+Fe
BCAL1687-*orbS*	SKorbSFor2	SKorbSRev2	-	-
orbS-orbH	orbSmbtHFor	orbSmbtHRev	+	-
orbH-orbG	mbtHsyrPFor	mbtHsyrPRev	+	-
orbG-orbC	syrPfecEFor	syrPfecERev	+	-
orbC-orbD	fecEfecDFor	fecEfecDRev	+	-
orbD-orbF	FecDfhuFFor	FecDfhuFRev	+	-
orbF-orbB	fhuFfecBFor	fhuFfecBrev	+	-
orbB-orbE	fecBpvdEFor	fecBpvdERev	+	-
orbE-orbI	pvdEpvdIFor	pvdEpvdIRev	-	-
orbI-orbJ	pvdIpvdDFor	pvdIpvdDRev	+	-
orbJ-orbK	pvdDpvdZ1For	pvdDpvdZ1rev	-	-
orbK-pvdA	pvdZ1pvdAFor	pvdZ1pvdARev	+	-
pvdA-orbA	pvdAorbAFor	pvdAorbARev	+	-
orbA-pvdF	orbApvdFFor	orbApvdFRev	+	-
pvdF-orbL	pvdFpvdZ2For3	pvdFpvdZ2Rev3	+	-
orbL-BCAL1703	pvdZ2hipOFor	pvdZ2hipORev	-	-

[a]Primers extended across the indicated intergenic regions.
[b]The results of RT-PCR analysis are shown. + indicates that an RT-PCR product of the expected size was generated, - indicates that no RT-PCR product of the correct size was generated.

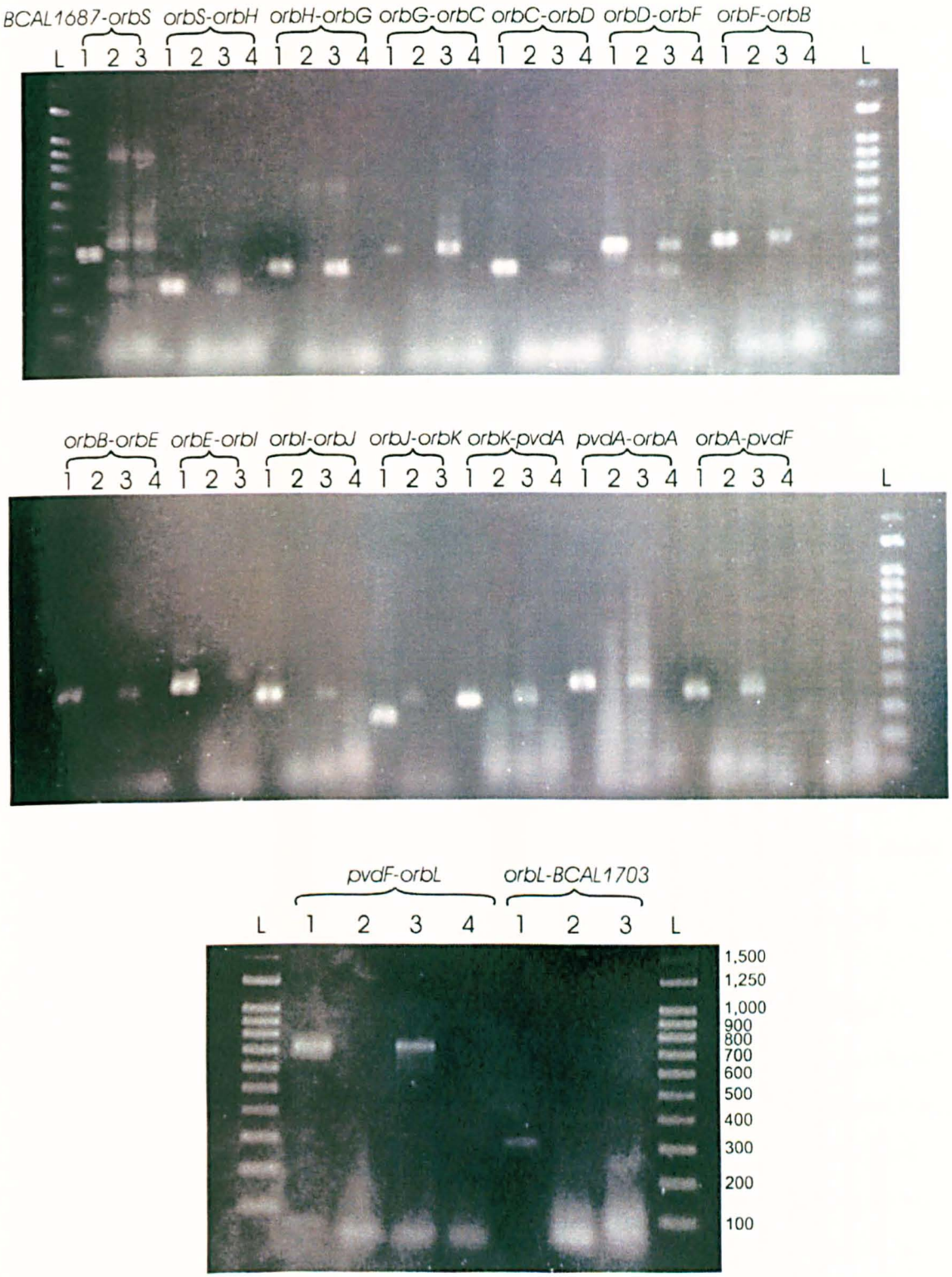

Figure 5.3: RT-PCR analysis of the ornibactin gene cluster. RT-PCR was carried out on *B. cenocepacia* RNA isolated under iron limited and iron replete conditions, using the Access RT-PCR kit (Promega). Amplification products were analysed by electrophoresis using 1.6 % agarose gels. The intergenic region spanned by each pair of primers is indicated above the gels. Lane contents were as follows; L, Q-step 4 ladder (York Biosciences) (size standards (bp) have been indicated next to the lower gel); 1, size marker, produced by PCR using *B. cenocepacia* genomic DNA as template; 2, RT-PCR using RNA isolated under iron replete conditions; 3, RT-PCR using RNA isolated under iron limited conditions; 4, negative control performed in the absence of reverse transcriptase (only shown where RT-PCR gave a positive result under iron-limited conditions).

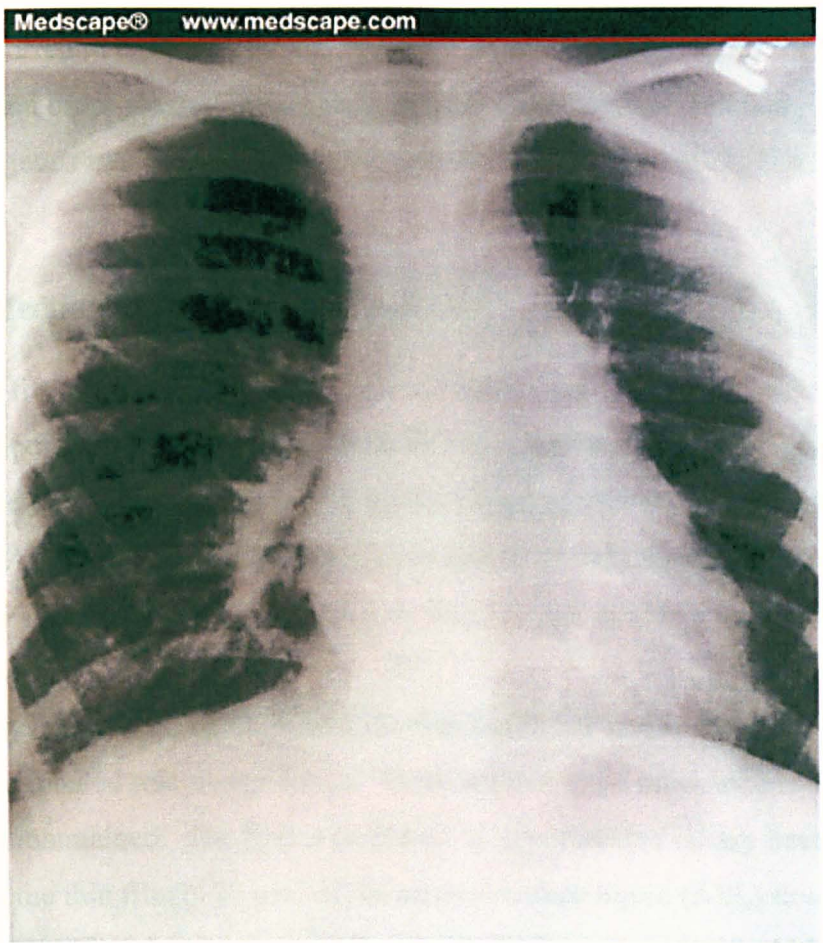

Figure 1.4: X-ray image showing the chest of a 12 year old boy suffering from CGD and infected with *B. vietnamiensis*. The patient's right lung (to the left of the image) contains white, cotton wool-like tendrils, representing the accumulation of fluid as a result of pneumonia. Reproduced from Speert *et al.*, 2002.

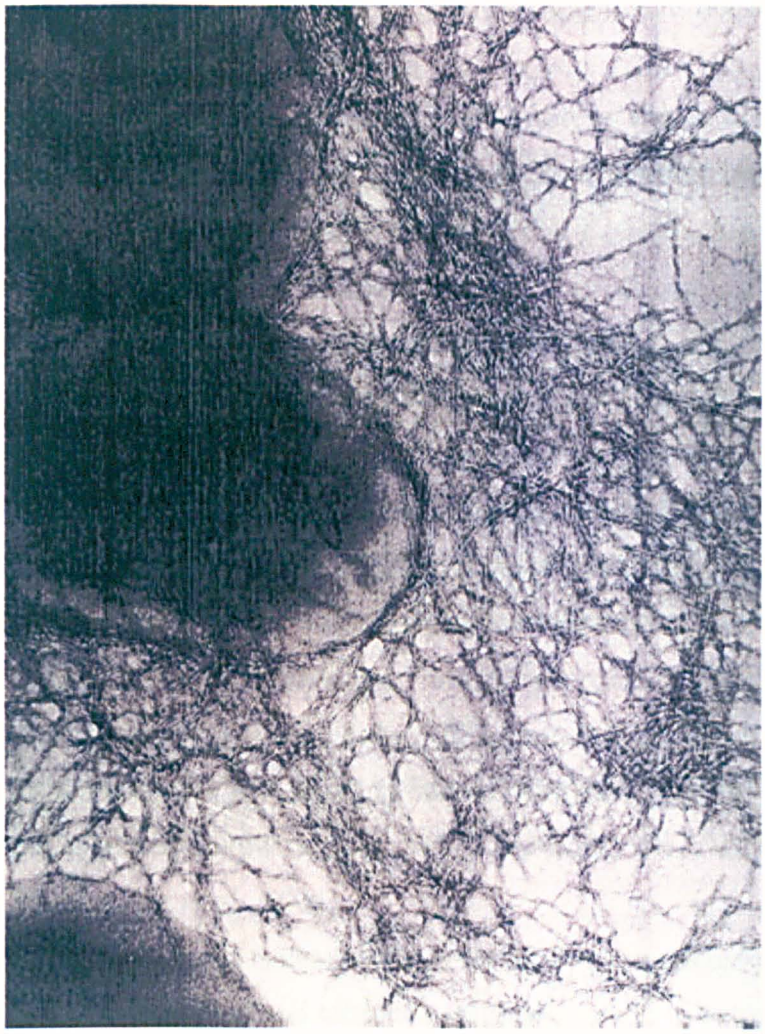

Figure 1.5: Transmission electron micrograph showing the cable-pilus produced by the *B. cenocepacia* ET-12 lineage. Reproduced from Goldstein *et al.*, 1995.

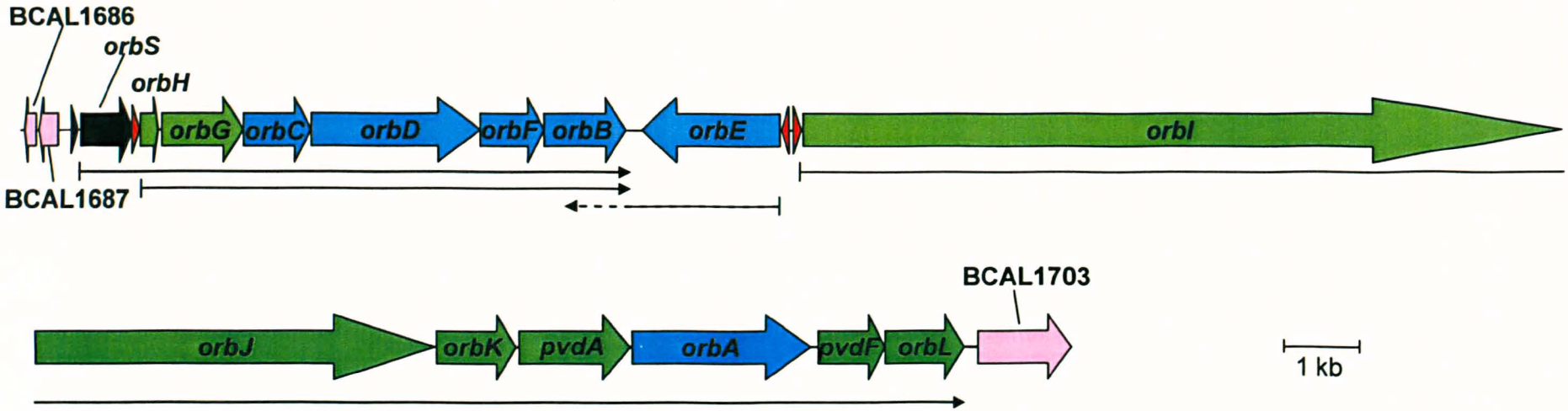

Figure 5.4: Transcriptional organisation of the *B. cenocepacia* ornibactin gene cluster. Genes are shown as block arrows, with putative ornibactin biosynthetic genes depicted in green, transport and utilisation genes in blue and the putative σ-factor gene responsible for transcription of the ornibactin operon shown in black. Genes flanking the ornibactin gene cluster and not thought to be involved in ornibactin production and utilisation have been shown in pink. Predicted promoters within the ornibactin gene cluster are represented as triangles: red fill for the putative OrbS-dependent promoters and black fill for the putative σ^{70}-type *orbS* promoter region. Transcripts predicted from RT-PCR, RPA and primer extension analysis have been indicated using black arrows. A broken arrow indicates that the extent of transcription has not been determined. The ornibactin gene cluster is located on chromosome 1. In the preliminary *B. cenocepacia* J2315 sequence annotation, genes *orbS-orbL* have been designated BCAL1688-BCAL1702 (www.sanger.ac.uk/projects/B_cenocepacia/).

size. No transcripts of the correct size were detectable by RT-PCR when RNA from iron replete cells was used, demonstrating that transcription of the ornibactin gene cluster is down-regulated in the presence of iron. No products were obtained when reverse transcriptase was omitted from the reactions, showing that the purified RNA was not contaminated with DNA.

The absence of evidence for co-transcription of *orbE* and *orbI* is consistent with the divergent arrangement of these genes. However, the apparent lack of co-transcription of *orbJ* and *orbK* was unexpected, since there are only 22 base pairs between the stop codon of *orbJ* and the start codon for *orbK*. This region contains the putative Shine-Dalgarno sequence for *orbK*, but is too small to accommodate a transcriptional terminator for *orbJ* and a promoter for *orbK*. However, a promoter for *orbK* could be located within the *orbJ* coding sequence. While a positive RT-PCR result can confirm that a transcript spans a particular region, a negative result only demonstrates that the RT-PCR was unsuccessful, and does not prove that two genes are not co-transcribed. To corroborate these negative results, it was decided to use another technique, the RNAse protection assay (RPA).

5.2.2: Analysis of ornibactin gene transcription by RNAse protection assay

The RNAse protection assay (RPA) was used to analyse the *orbJ* to *orbK* intergenic region. Radiolabelled RNA probes were constructed by *in vitro* transcription of part of the intergenic region in question, using the primers listed in Table 5.2. Probes were designed to be complementary to the corresponding predicted transcript. These labelled probes were purified and incubated with RNA isolated from cultures grown under conditions of iron starvation. The incubation conditions used favoured hybridisation of complementary RNA sequences. The reaction mixture was then treated with a ribonuclease to degrade unhybridised probe. Analysis of products was carried out using polyacrylamide gel electrophoresis (PAGE) under denaturing conditions, and the results visualised using autoradiography. RPA was carried out using Ambion's RPA III kit, as described in Section 2.3.2. RPA is analogous to the S1 nuclease protection assay, but ribonuclease is considered less prone to degrading double-stranded nucleic acid than S1 nuclease (Friedberg, 1990). It should be noted

Table 5.2: Primers used to construct probes for RPA, and resultant probe sizes.

Intergenic region	Primer[a]		Size (bases)	
	Forward	Reverse	Probe[b]	Protected band[c]
orbJ-orbK	IVTorbJorbKF	IVTorbJorbKR	288	230
orbI-orbJ	IVTorbIorbJF	IVTorbIorbJR	365	293
orbE-orbI	IVTorbEorbIF	IVTorbEorbIR	403	322

[a] Primers extended across the indicated intergenic regions.
[b]RNA probes were produced by *in vitro* transcription using PCR-amplified DNA as a template and the primers shown.
[c]Expected size of protected band, should the genes flanking the intergenic region be co-transcribed.

that the primers used to amplify the template DNA for *in vitro* transcription to generate the RNA probes were designed so as to contain a tail that is not homologous to *B. cenocepacia* genomic DNA. The total non-homologous region when two such primers were used to amplify the *in vitro* transcription template constituted ~10 % of the total size of the probe. Thus, if such a probe were hybridised to mRNA present in the RPA, the resultant protected band would be 10 % smaller than the probe control band, showing that the ribonuclease was functioning correctly.

A positive control for the *orbJ-orbK* RPA was included, consisting of the *orbI* to *orbJ* intergenic region, as these genes had been shown by RT-PCR to be co-transcribed. A negative control was also carried out, consisting of the *orbE* to *orbI* intergenic region, which did not give rise to a product during RT-PCR and contains an intrinsic transcription terminator (discussed in Section 5.6). Figure 5.5 shows the results of the RPA.

Protected RNA fragments of the expected sizes were present for the primers spanning the *orbJ* to *orbK* and the *orbI* to *orbJ* intergenic regions. This demonstrated that *orbJ* and *orbK* are co-transcribed, despite the negative result obtained through RT-PCR. RPA also confirmed the absence of co-transcription of the divergent *orbE* and *orbI* genes.

As *orbE* is transcribed in the opposite direction to the other ornibactin genes, the results gained from RT-PCR and RPA suggest that the ornibactin operon comprises three transcriptional units, one extending from *orbS* to *orbB,* one containing *orbE*, and one extending from *orbI* to *orbL.* Figure 5.4 illustrates this organisation, which is discussed further at the end of the chapter. The lack of co-transcription of the divergently transcribed *orbE* and *orbI* genes, and of *orbS* with the upstream gene BCAL1687, suggest that the regions between these genes contain the promoter elements for the transcriptional units identified. These regions contain three of the promoters predicted by *in silico* analysis, the fourth being situated between *orbS* and *orbH.*

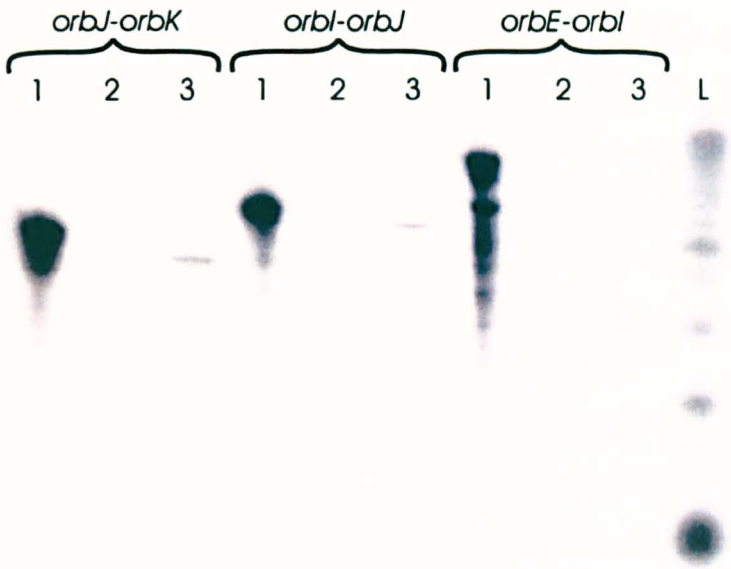

Figure 5.5: RPA analysis of the organisation of the ornibactin gene cluster. RPA analysis was carried out as detailed within Section 2.3.2. The intergenic regions analysed are indicated above the gel. Lane numbers represent the following: 1. Control, RNA probe incubated with control yeast RNA, no ribonuclease added (probe not degraded); 2. Negative control, RNA probe incubated with control yeast RNA, ribonuclease added (probe degraded); 3. Experimental sample, RNA probe incubated with *B. cenocepacia* 715j RNA, ribonuclease added (note that where the probe is protected it is ~90% of the original probe size). L indicates radiolabelled single-stranded 50 bp DNA ladder (Amersham), used as an approximate size marker.

5.3: Localisation and regulation of the ornibactin gene cluster promoters.

DNA fragments bearing the putative *orbS* promoter and OrbS-dependent promoters were PCR amplified using the primers listed in Figure 5.6. Each amplified fragment bore at least the first 8 codons of the gene downstream of the putative promoter, and at least 140 bp of sequence upstream of the predicted -35 sequence. The amplified fragments were digested with *Eco*RI and *Hin*dIII and cloned into pBluescript II KS digested with the same enzymes (see Figure 5.6). Transformants were selected on LB agar containing ampicillin, IPTG and X-gal.

pBluescript II KS is a blue-white screening vector, meaning that its MCS is within the coding sequence for the LacZ α peptide. This is capable of complementing the *lacZΔM15* mutation present in many purpose-built *E. coli* transformation strains, resulting in blue colonies on agar containing IPTG and X-gal. When the *lacZ* fragment is disrupted, the LacZ α peptide is no longer produced, and white colonies result.

White colonies were restreaked, and purified plasmid DNA was analysed for inserts of the appropriate size by restriction digestion using *Eco*RI and *Hin*dIII. The DNA fragments were sequenced to ensure that no errors had occurred during PCR. The resultant plasmids, pBS-porbSfl, pBS-porbHfl, pBS-porbIfl and pBS-porbEfl, were then used as a source of the promoter fragments introduced into the reporter vector pKAGd4 and for other experiments. The four pBluescript II KS derivatives were digested with *Bam*HI and *Hin*dIII, and the promoter fragments were extracted from an agarose gel for ligation with pKAGd4, which was cut with *Bgl*II (this enzyme generates cohesive ends that are compatible with those produced by cleavage with *Bam*HI) and *Hin*dIII (see Figure 5.7). Transformants were selected on LB agar containing chloramphenicol and X-gal. Successful insertion of the promoter fragments was confirmed by digestion with *Eco*RI and *Hin*dIII, and *Not*I and *Hin*dIII. The resultant plasmids (pKAGd4-porbSfl, pKAGd4-porbHfl, pKAGd4-porbEfl and pKAGd4-porbIfl) were transferred into *B. cenocepacia* 715j and 715j-orbS::Tp for β-galactosidase assay. β-galactosidase assays were carried out under conditions of iron sufficiency and iron limitation in M9 salts medium containing casamino acids and chloramphenicol. Figure 5.8 shows the results of the assays.

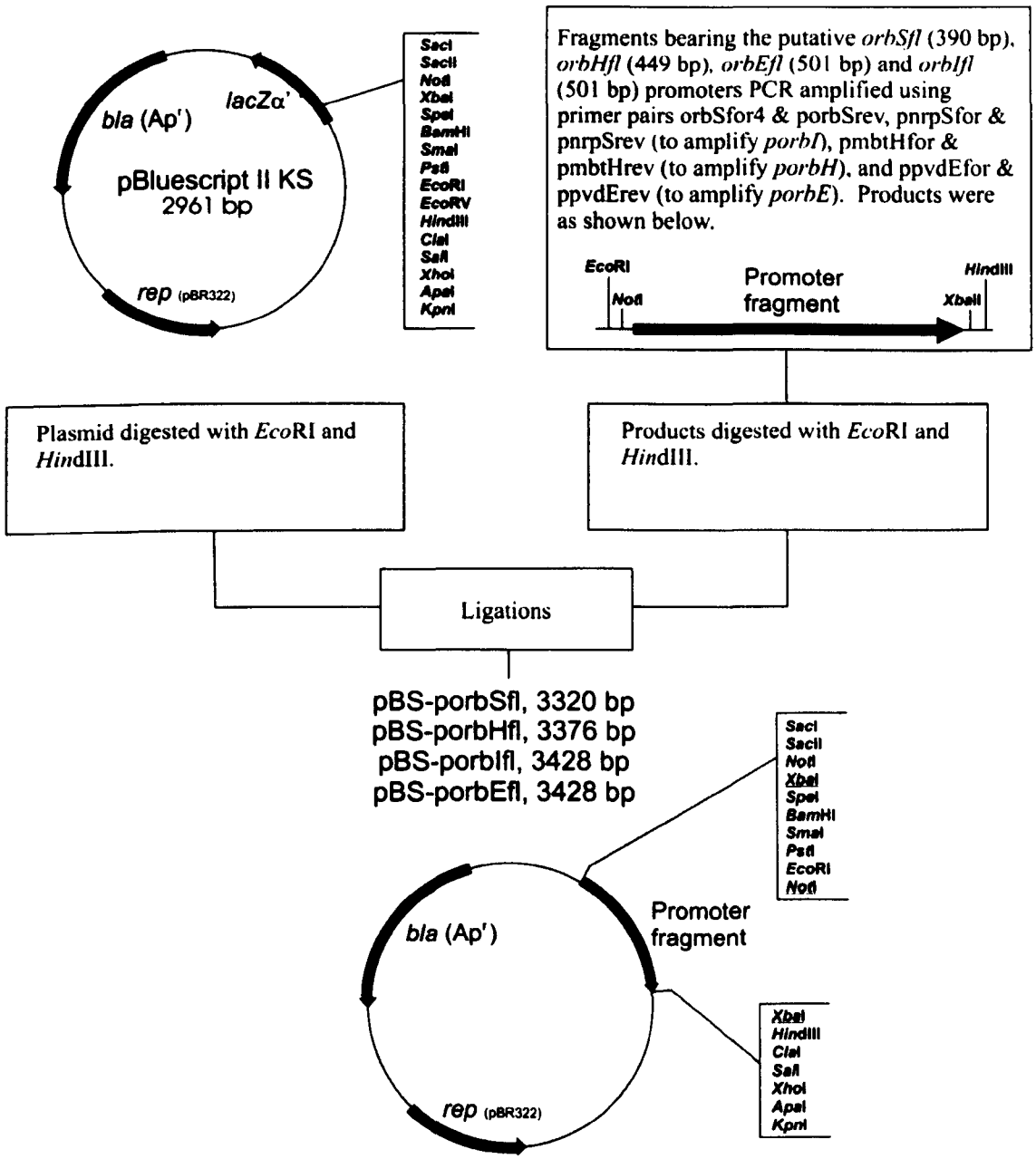

Figure 5.6: Scheme for cloning DNA fragments bearing ornibactin gene promoters into pBluescript II KS. Non-unique sites are underlined.

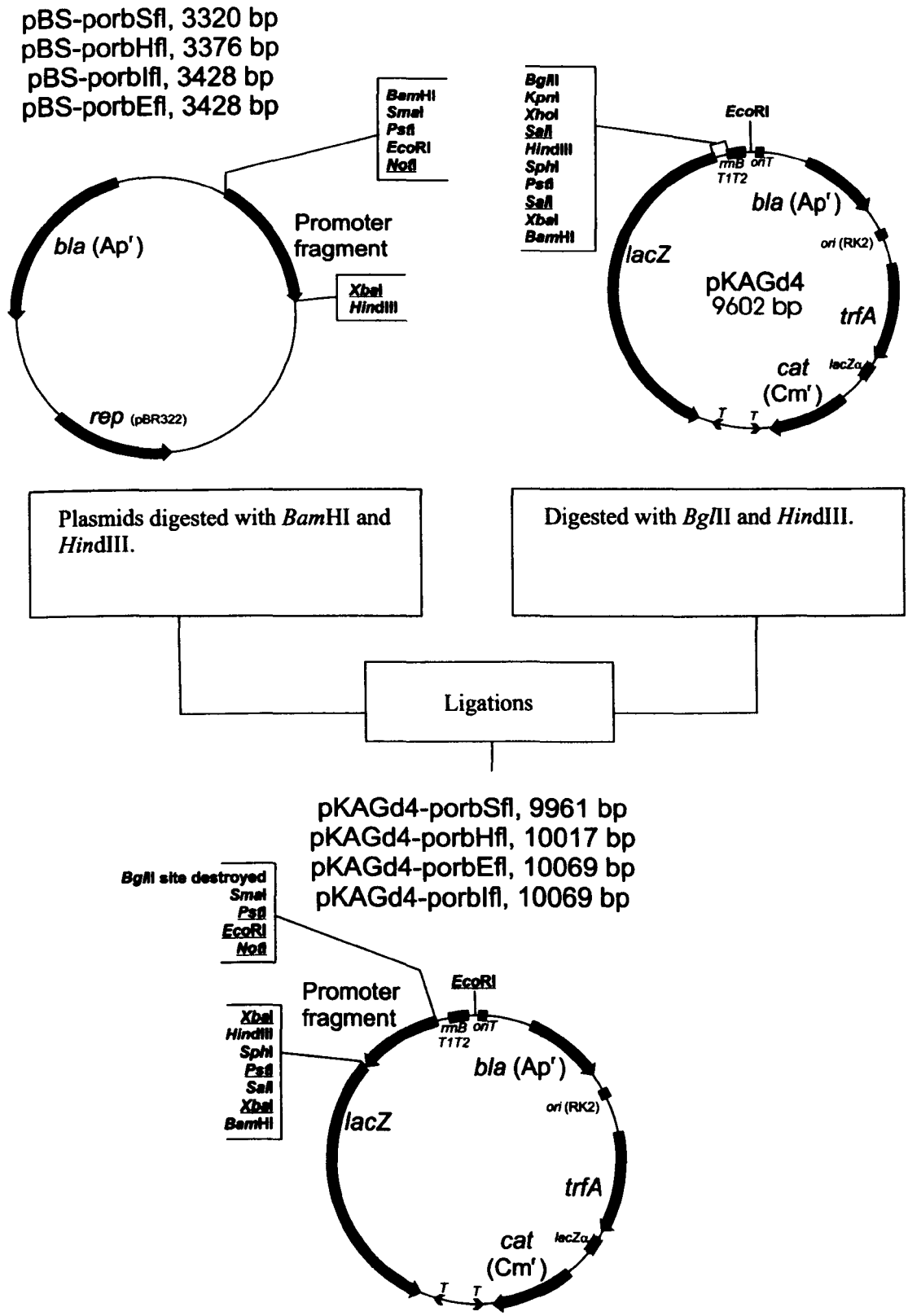

Figure 5.7: Scheme for cloning the ornibactin gene cluster promoter fragments into pKAGd4. Only pertinent restriction sites are shown. Non-unique sites are underlined.

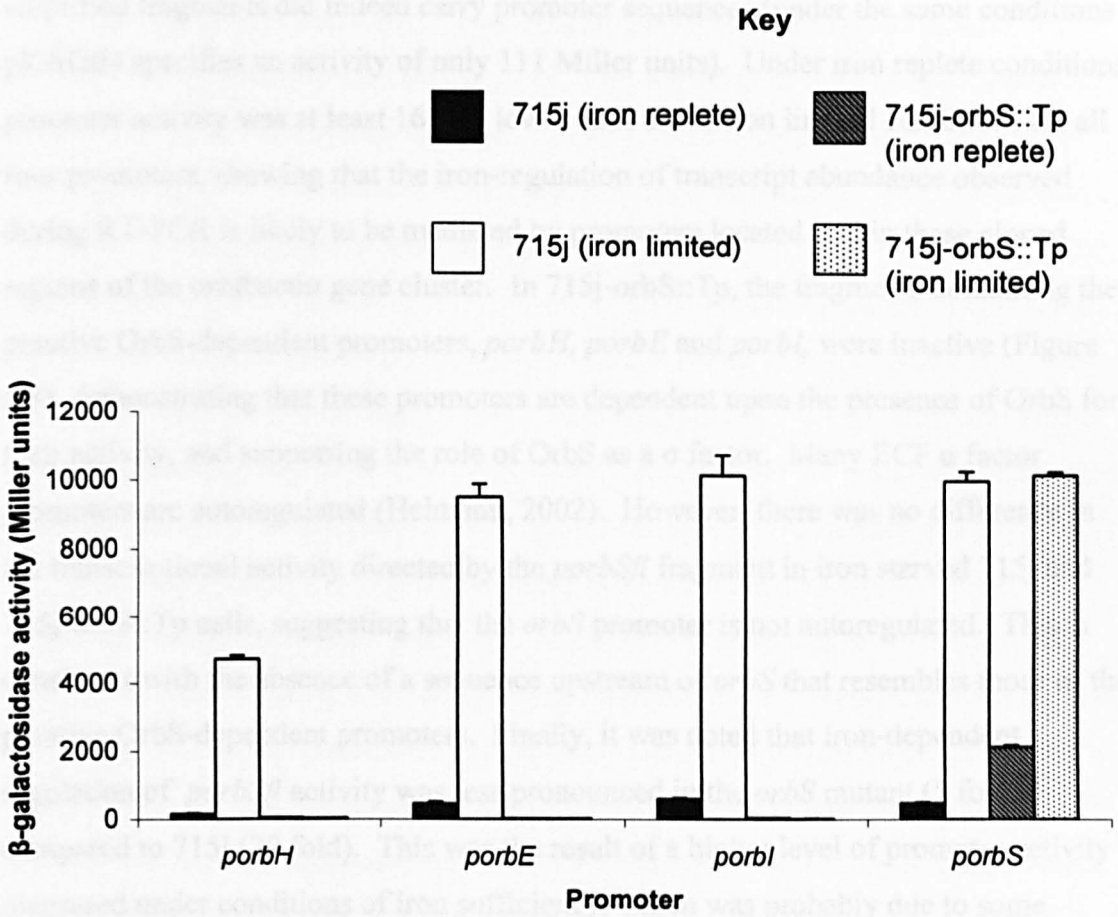

Figure 5.8: Ornibactin gene promoter activity in response to iron availability and the presence or absence of functional *orbS*. pKAGd4 derivatives bearing *porbSfl, porbHfl, porbEfl* and *porbIfl* were introduced into *B. cenocepacia* 715j and 715j-orbS::Tp. β-galactosidase activities were measured in cells grown in M9 salts medium containing casamino acids (0.1 %) and chloramphenicol, under iron replete and iron limited conditions. Assays were performed on triplicate cultures, and error bars represent the standard deviations of the activities from the mean. Values were corrected by subtracting the background activity specified by pKAGd4 in the strain and under the conditions used.

In 715j, all four DNA fragments resulted in a high level of β-galactosidase activity under iron-limiting conditions (>4,000 Miller units), showing that the amplified fragments did indeed carry promoter sequences (under the same conditions pKAGd4 specifies an activity of only 111 Miller units). Under iron replete conditions, promoter activity was at least 16 fold lower than under iron limited conditions for all four promoters, showing that the iron-regulation of transcript abundance observed during RT-PCR is likely to be mediated by promoters located within these cloned regions of the ornibactin gene cluster. In 715j-orbS::Tp, the fragments containing the putative OrbS-dependent promoters, *porbH, porbE* and *porbI,* were inactive (Figure 5.8), demonstrating that these promoters are dependent upon the presence of OrbS for their activity, and supporting the role of OrbS as a σ factor. Many ECF σ factor promoters are autoregulated (Helmann, 2002). However, there was no difference in the transcriptional activity directed by the *porbSfl* fragment in iron starved 715j and 715j-orbS::Tp cells, suggesting that the *orbS* promoter is not autoregulated. This is consistent with the absence of a sequence upstream of *orbS* that resembles those of the putative OrbS-dependent promoters. Finally, it was noted that iron-dependent regulation of *porbSfl* activity was less pronounced in the *orbS* mutant (5 fold) compared to 715j (20 fold). This was the result of a higher level of promoter activity measured under conditions of iron sufficiency, which was probably due to some degree of iron starvation of the ornibactin-deficient *orbS* mutant, even when iron was abundant.

5.4: Deletion analysis of the *orbS* promoter

As mentioned previously, located upstream of *orbS* are two sequences that resemble σ^{70}-type promoters (Section 5.1). Two approaches were used to determine which of these two sequences, if either, constituted the *orbS* promoter. The first of these approaches was to attempt to complement the *orbS* mutant, OM3, for ornibactin production, using the cloned *orbS* gene with various lengths of upstream DNA. The second approach was to make a series of deletions of the *orbS* promoter region and fuse them to *lacZ* carried on pKAGd4 for β-galactosidase assay. Figure 5.9 illustrates the DNA fragments produced for both of these approaches. The endpoints of these deletion constructs will be referred to by their distance from the putative transcription start site (TSS) of the most downstream promoter, which is illustrated in Figure 5.1.

B. cenocepacia OM3 had previously been successfully complemented for ornibactin production using a derivative of pBBR1MCS bearing a DNA fragment containing the *orbS* gene, with an upstream endpoint at -178 (Agnoli, 2003; Agnoli *et al.*, 2006). This complementation can be easily visualised on CAS agar plates (see below). Attempts to complement OM3 for ornibactin production using pBBR1MCS bearing *orbS* with an upstream endpoint of +5 relative to the TSS were unsuccessful (Agnoli, 2003), suggesting that the tandem *cat* and *lac* promoters present on pBBR1MCS were unable to direct efficient transcription of *orbS*. Two additional DNA fragments were amplified, bearing the *orbS* gene with upstream endpoints at -40 and -69 relative to the putative TSS (Figure 5.9). These fragments were cloned into the *Hin*dIII and *Bam*HI sites of pBBR1MCS, in the same orientation as the *cat* gene (see Figure 5.10). Transformants were selected on LB agar containing chloramphenicol, IPTG and X-gal, and plasmids of the appropriate size were identified. The resultant plasmids, pBBR-orbS-69 and pBBR-orbS-40 were introduced into *B. cenocepacia* OM3 by conjugation, and streaked on CAS agar containing 10 μM $FeCl_3$ (low iron) and 60 μM $FeCl_3$ (iron replete).

CAS is an iron-sequestering dye with a blue-green colour when bound to iron. Siderophores can scavenge iron from CAS, resulting in a yellow halo surrounding the bacteria. As Figure 5.11 A shows, strain OM3 (Pch^-, Orb^-) produces no CAS-detectable siderophores. The introduction of pBBR-orbS into OM3 restores ornibactin

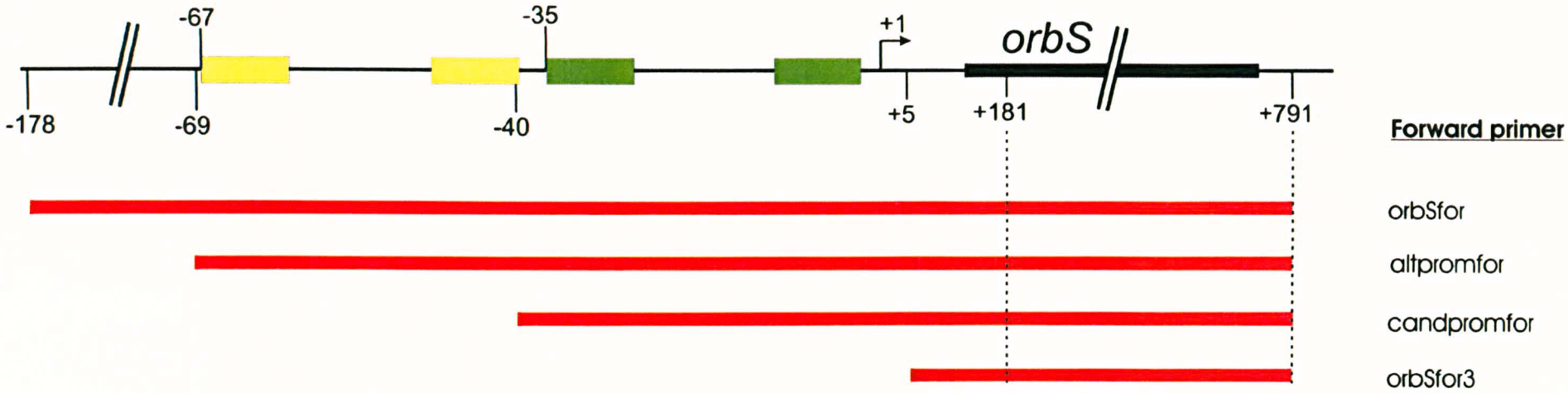

Figure 5.9: Deletion analysis of the *orbS* promoter region. Yellow and green blocks represent the -35 and -10 elements of the two candidate *orbS* promoters. In each case the position of the most upstream base of the candidate -35 element has been shown. -178, -69, -40 and +5 represent the upstream ends of the DNA fragments amplified for OM3 complementation and reporter analysis of the *orbS* promoter, and +181 and +791 represent the downstream end of the fragments used in the reporter assays and the complementation analysis, respectively, which are shown in red. Positions are numbered with respect to the predicted transcription start site (+1) of the downstream candidate promoter. The forward primer used to amplify each fragment is shown. The reverse primer used to amplify fragments for the complementation analysis was orbSrev2. The reverse primer used to amplify fragments for reporter analysis was porbSrev. The thickest black line represents the *orbS* ORF. The DNA sequence of this region is shown in Figure 5.1. Diagram not to scale.

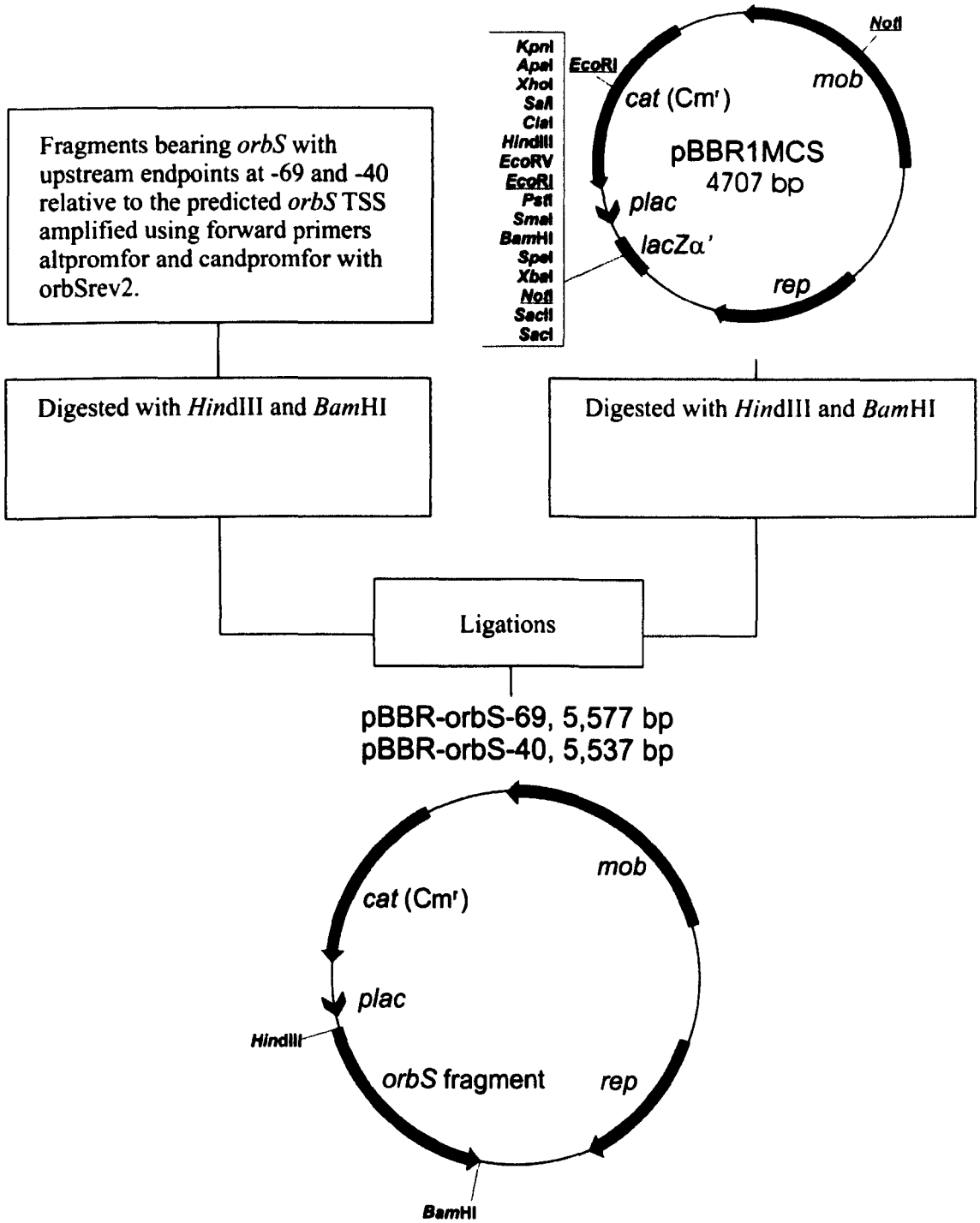

Figure 5.10: Scheme for the construction of pBBR-orbS-69 and pBBR-orbS-40. Only pertinent restriction sites within pBBR-orbS-69 and pBBR-orbS-40 have been shown. Non-unique sites in pBBR1MCS have been underlined.

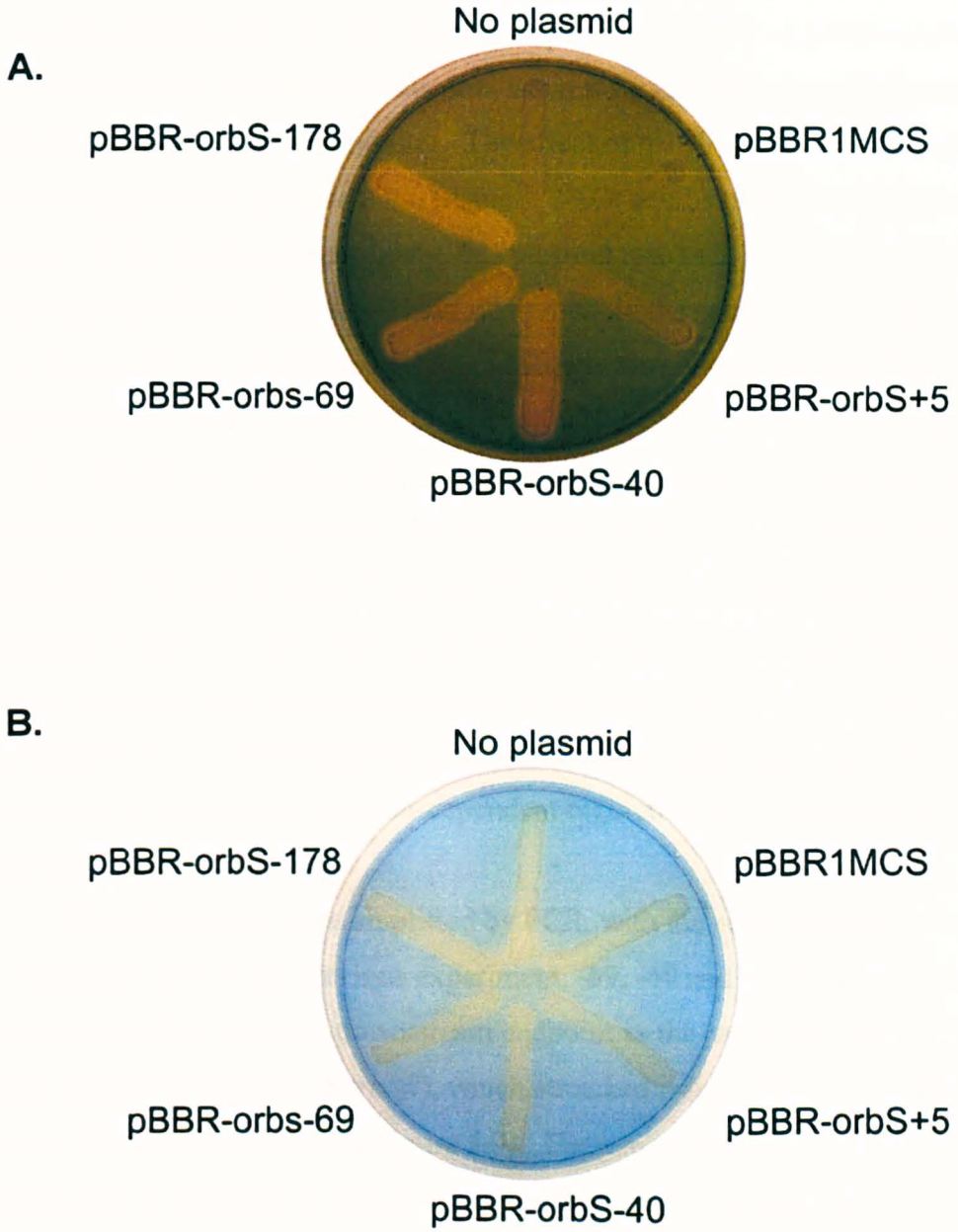

Figure 5.11: CAS plate analysis of *B. cenocepacia* OM3 containing pBBR1MCS derivatives bearing *orbS* with different upstream endpoints. Cultures of OM3 containing the indicated plasmids were grown overnight in BHI broth at 37 °C, and streaked on iron-depleted and iron replete CAS agar plates as explained in Section 2.1.3. These plates were incubated for ~16 hours at 37 °C. pBBR-orbS-178 refers to pBBR-orbS (Agnoli, 2003; Agnoli *et al.*, 2006) **A:** CAS plate containing 10 μM $FeCl_3$. **B:** CAS plate containing 60 μM $FeCl_3$.

production as shown previously (Agnoli *et al.*, 2006), resulting in a yellow halo around the bacterial growth. Introduction of pBBR-orbS-69 and pBBR-orbS-40 into OM3 also restored ornibactin production, suggesting that the downstream putative promoter is the actual *orbS* promoter. The effect of pBBR-orbS+5 (pBBR-orbSΔP) on ornibactin production is also shown (Agnoli, 2003; details of this plasmid are given in Section 7.3.1). As shown previously, this plasmid results in a very small halo when introduced into OM3. This small halo was probably the result of leaky transcription from the *cat* and *lac* promoters. pBBR1MCS was also introduced into OM3 as a negative control, and the resultant phenotype is identical to plasmid-less OM3 (Figure 5.11 A). On the iron replete plate, none of the strains tested produced detectable ornibactin, demonstrating that ornibactin production by OM3 complemented with pBBR-orbS-178, pBBR-orbS-69 and pBBR-orbS-40 had retained iron-dependent regulation (Figure 5.11 B). Having gained a qualitative result suggesting that the putative promoter with upstream endpoint at -40 was responsible for *orbS* transcription, a *lacZ*-fusion approach was used to gain quantitative data to allow comparison of the activity and iron-dependent regulation of the promoter region fragments.

Three fragments were amplified by PCR, with the same upstream endpoints as the fragments used in the previous experiment, -69, -40 and +5 relative to the TSS. The fragments had the same downstream endpoint as the previously assayed 'full-length' promoter fragment (*porbSfl*), which stretched from -178 to +181 relative to the putative TSS (Section 5.3) (see Figure 5.9). These were inserted into the *Xba*I and *Hin*dIII sites of pKAGd4 (Figure 5.12). *E. coli* MC1061 transformants were selected using LB agar containing chloramphenicol and X-gal. After confirming the integrity of the cloned DNA fragments by PCR and DNA sequencing, the plasmids were introduced into *B. cenocepacia* 715j by conjugation. The promoter activity of the fragments was determined by β-galactosidase assay, using cells grown in M9 salts medium containing casamino acids (0.1 %) and chloramphenicol, under iron replete and iron limited conditions. The results are shown in Figure 5.13, including the activity of the *porbSfl* promoter (also shown in Figure 5.8). Deletion of the DNA upstream of *orbS* to position -40 had little effect on β-galactosidase activity in comparison to the -178 promoter derivative when cells were grown under iron limited conditions. Furthermore, iron regulation was retained when upstream DNA was

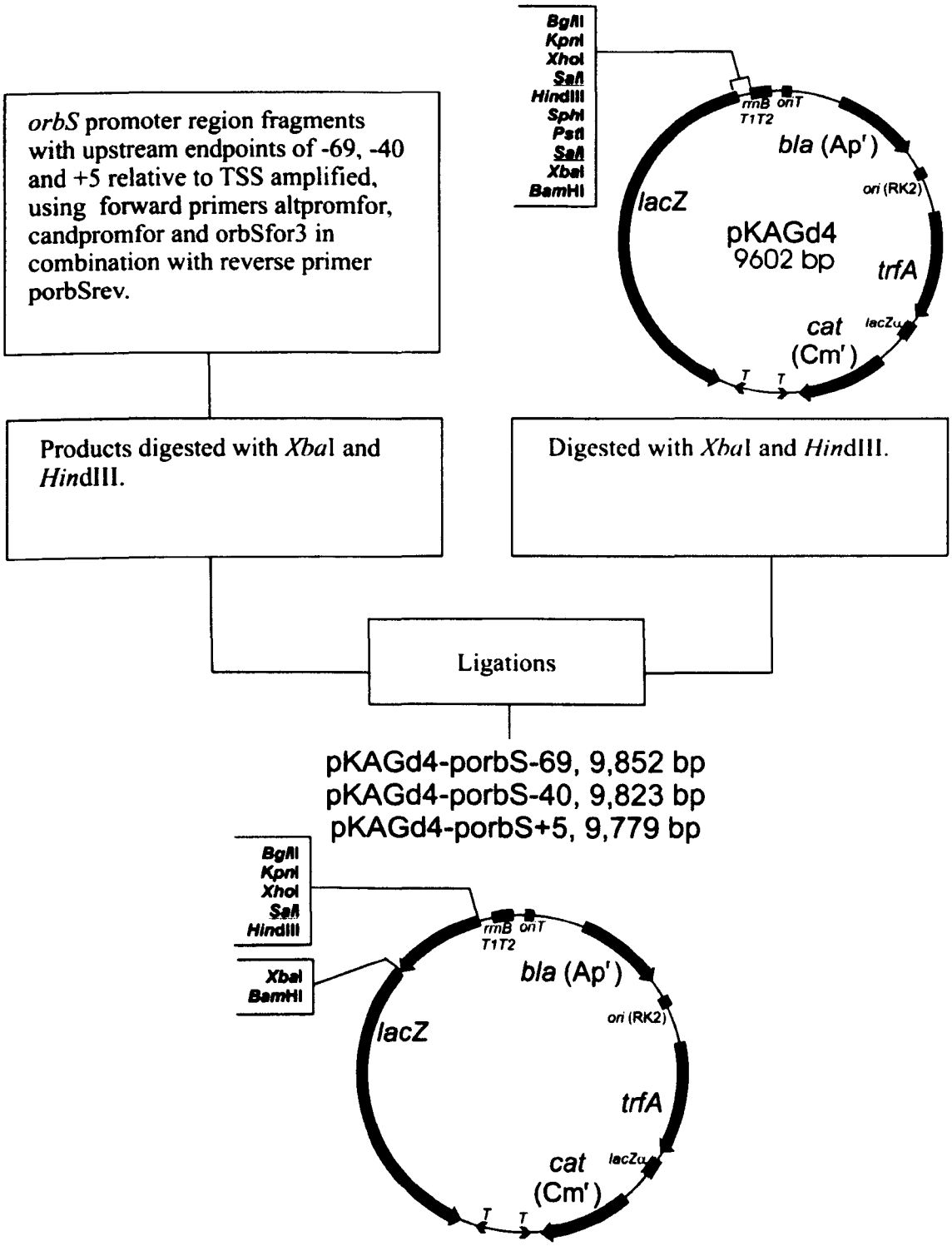

Figure 5.12: Scheme for the construction of *porbS-lacZ* fusion plasmids.

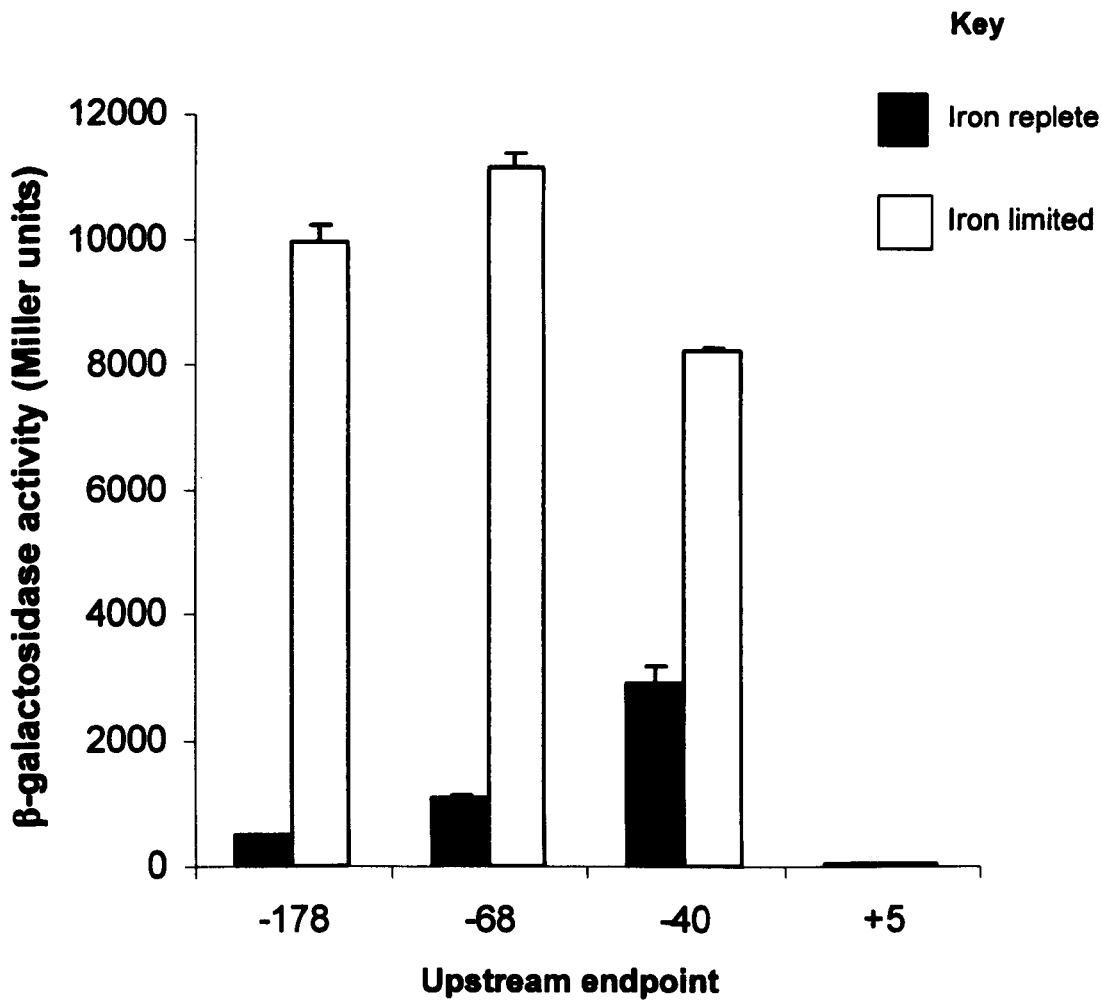

Figure 5.13: Localisation of the *orbS* promoter. Promoter activities of DNA fragments extending from the indicated endpoints upstream of *orbS* (numbered relative to the putative TSS of the downstream promoter-like sequence), to +181. *B. cenocepacia* cells were grown in M9 salts medium supplemented with casamino acids and chloramphenicol under iron replete and iron limited conditions (as indicated). Each assay was performed on triplicate cultures, and corrected by subtracting the background activity specified by pKAGd4. Error bars represent standard deviation from the mean of each set of triplicate cultures assayed.

deleted to -40. However, the extent of regulation decreased from 21 fold for the -178 promoter fragment to 3 fold for the -40 endpoint. When both promoter-like regions were deleted (i.e. the promoter fragment with endpoint at +5), promoter activity was abolished. These results and those of the complementation analysis suggest that the promoter-like sequence located downstream of -40 is the *orbS* promoter, and that iron-regulation also requires sequences downstream of or overlapping position -40.

5.5: Location of the transcription start sites of the ornibactin gene promoters.

Promoters are generally made up of two conserved regions, with which the RNAP holoenzyme interacts (via the σ factor), one around position -10 and the other around position -35 relative to the TSS. Determination of the TSS can therefore be used to pinpoint the location of the promoter directing synthesis of the transcript concerned. Two methods for TSS determination were initially attempted, both without success. The first of these was a variant of the conventional primer extension procedure, in which a fluorescent primer is used to extend mRNA to the TSS, and the resultant product electrophoresed in a single polyacrylamide capillary gel with size standards, which are labelled with a different fluorescent marker. The peak gained for the primer extension can be overlaid with the marker reaction peaks, and the probable TSS calculated. Although this was attempted several times, it was without success, and this method was abandoned as the accuracy of the calculated TSS was in doubt. The second method attempted was 'rapid amplification of cDNA ends' (5' RACE), in which a reverse transcription is carried out to generate a cDNA product with the 3' end corresponding to the TSS. Terminal deoxynucleotidyl transferase is then used to add a homopolymeric tail to the 3' end of the transcript. The resultant cDNA can be PCR-amplified using a primer that will anneal to the homopolymeric tail, and one that anneals to the known sequence at the 5' end of the cDNA. The product can then be cloned and sequenced to reveal the TSS (which will immediately follow the known homopolymeric tail sequence). This method will generally only allow determination of the most common TSS if more than one is present (for example, if there are overlapping or closely spaced tandem promoters), and furthermore was expensive, and unsuccessful when attempted. Conventional primer extension was therefore used instead.

In primer extension, an antisense primer is designed to anneal to transcript RNA, radiolabelled, and used in a reverse transcription from mRNA. The primer is also used to produce a sequencing ladder from the corresponding DNA template. These are then separated by PAGE under denaturing conditions. The size of the primer extended product can be compared with the primer-generated DNA sequencing ladder to determine precisely where the TSS is located. Total *B. cenocepacia* mRNA

was isolated from cells grown in M9 salts medium under iron limited and iron replete conditions using the RNaqueous Midi Kit (Ambion). The sequencing ladder was made using the Sequenase Version 2.0 kit (USB). Primer SKorbSRev was used to determine the *orbS* TSS, using pBS-porbSfl (Figure 5.6) as a template to generate a sequencing ladder. Primer pvdEpvdIrev was used to determine the *orbI* TSS, using pBS-porbIfl (Figure 5.6) as a template to generate a sequencing ladder. Primer orbSmbtHrev was used to generate a primer extension product for determination of the *orbH* TSS.

Three cDNA products were generated with the *orbS*-specific primer, which corresponded to mRNA 5' endpoints located 25, 24 and 18 bp upstream of the most upstream of the putative translation initiation codons for *orbS* (Figures 5.14 A and 5.15 A). The largest (and also the most abundant) cDNA product probably indicated the true TSS for *orbS,* as smaller products are likely to have occurred as a result of premature termination of reverse transcription due to secondary structure features in the mRNA, or due to degradation of the mRNA itself. This places the TSS 25 bp upstream of the first initiation codon for *orbS.* The fact that the second largest cDNA product is only one nucleotide shorter than the largest cDNA product suggests that transcription may also initiate 24 bp upstream of the first translation initiation codon, but with less efficiency. This information was used to identify the promoter for *orbS* transcription.

In general, -10 regions for σ^{70}-dependent promoters (consensus sequence TATAAT) are located between 12 and 7 bp upstream of the TSS (position +1). The -35 motif (consensus sequence TTGACA) is most frequently located a further 17 bp upstream (i.e. between positions -35 and -30 relative to the TSS). Taking the T located 25 bp upstream of the first ATG codon as the TSS, this would identify the sequence TTGAGA $(N)_{17}$ TAAATT as the *orbS* promoter (Figure 5.15 A). This corresponds precisely to the downstream candidate promoter sequence, which was proposed to be the *orbS* promoter based on deletion analysis (Section 5.4).

The *orbI*-specific primer gave rise to a single cDNA product with a 3' end located 62 bp upstream of the putative translation initiation codon for *orbI* (Figures 5.14 B and 5.15 B). This corresponds to the *orbI* TSS (+1). Located 33-29 and 12-9 bp upstream of this position are the -35 and -10 motifs of the predicted *orbI* promoter

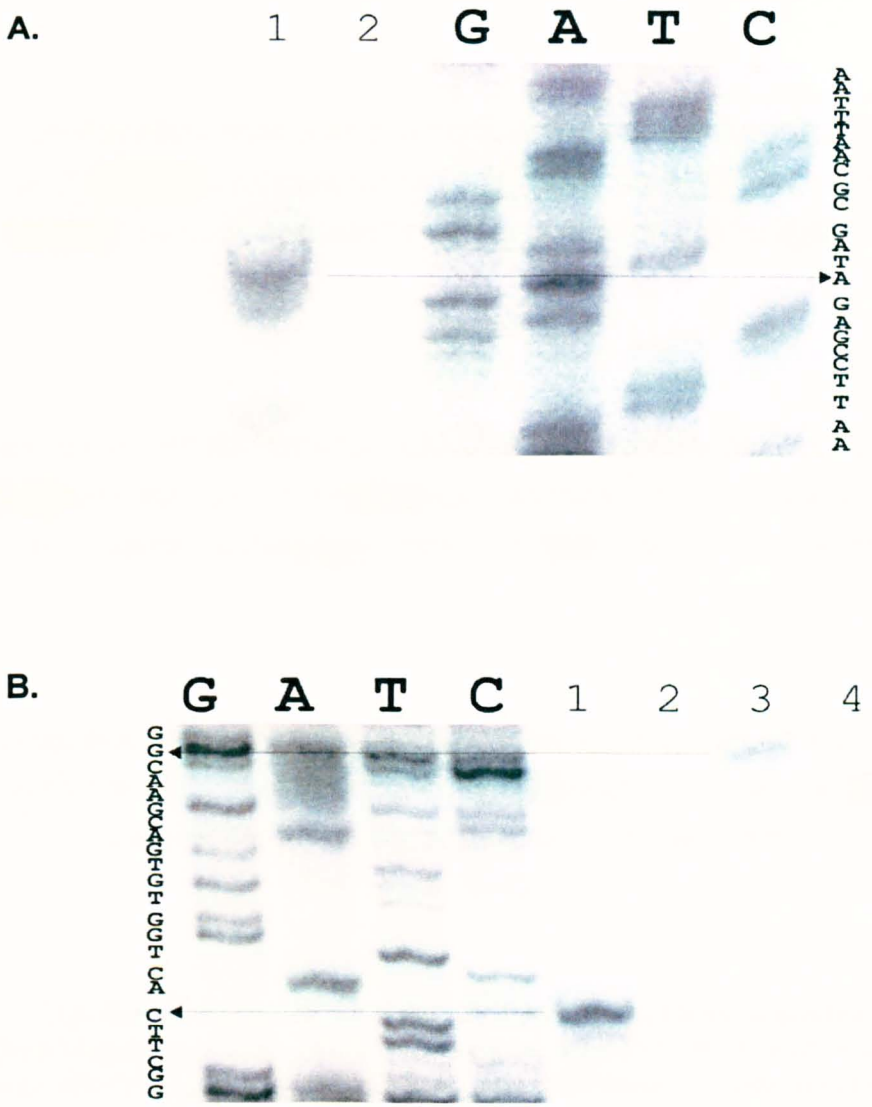

Figure 5.14: Determination of the transcription start sites for of *orbS, orbI* and *orbH* by primer extension. Primer extension was carried out using *B. cenocepacia* RNA, with pBluescript II KS bearing the appropriate sequence employed as a template for the sequencing ladder. **A**: Determination of the *orbS* TSS. 1, primer extension products obtained from primer SKorbSrev, using RNA isolated from iron limited cells (the arrow indicates the cDNA most likely to represent the TSS; 2, cDNA products were not present when primer extension was carried out (from primer SKorbSrev) on RNA isolated from iron replete cells. Sequencing ladder was generated using primer SKorbSrev. **B.** Determination of the *orbI* and *orbH* TSSs. 1, Primer extension product obtained from primer pvdEpvdIrev, using RNA isolated from iron limited cells (the arrow indicates the cDNA most likely to represent the TSS); 2, cDNA products were not present when primer extension was carried out (from primer pvdEpvdIrev) on RNA isolated from iron replete cells. 3, Primer extension product obtained from primer orbSmbtHrev, using RNA isolated from iron limited cells (the arrow indicates the cDNA most likely to represent the TSS); 2, cDNA products were not present when primer extension was carried out (from primer orbSmbtHrev) on RNA isolated from iron replete cells. The sequencing ladder was generated using primer pvdEpvdIrev.

A.

ACCGTCCGCGCGGCGCAGACGCACCCATGTCCGCTCCGGCAACGATTCGGATCATTGTTC
AGACAAATCCTGACAACCGAAAGGGTCATCCTGTAATCGGATTGAGAATGATTTGCGTTT
ACGTTAAATTGCGCTATCTCGGAATTTGACGGAGCAGATCGATGGCCATGGCGGAAGTGC

B.

GCCGCGCAAATATTTAGCCCCATCGTCAAAAAAAGCCGCCGTACGCACTTTGCACGCAAAAC
GGTAAAAAATCGGCCGCGCCGTTCGTCACACCAGTGAAGCCGCCCCAAGCGGCCCCGAGACTT
GGCCGAAGCGGCCGGACCGAAGGACTTCACGCACATGACGAGTTTCCCGACTGCGCTGCAT

C.

CGCGACGCGGAGCGCCACTGCGCGGAATGCCTCGACGCGTGCCATCGCGGCGTCGCCTGTCCG
GTGTTCCTGGGCGGTCGCGCGCGGCGGCGGTAAAAAAACGCGCCGGCCAACCGTCTATCAGAC
AGGAGCGGCCGAATCCGCCGCTTCGCCTCCTTCAACCGCCCAGCGATTTCCGATCATGAC

Figure 5.15: Transcription start sites of the *orbS* and the OrbS-dependent promoters. A. The DNA sequence upstream of *orbS*, showing the *orbS* TSS. **B.** The DNA sequence upstream of *orbI*, showing the *orbI* TSS. **C.** The DNA sequence upstream of *orbH,* showing the approximate *orbH* TSS.
The TSS (+1) determined for each promoter has been indicated by a bent arrow. The putative -35 and -10 promoter regions for each promoter have been enclosed in green boxes. The putative ribosome binding site for each gene has been emboldened and underlined, and the putative start codon(s) for translation of the each gene have been highlighted in grey. The inactive promoter-like sequence upstream of the *orbS* promoter have been enclosed in yellow boxes.

(TAAAA $(N)_{16}$ CGTC) (Figure 5.15B), thus confirming this sequence as the true *orbI* promoter.

At the time these experiments were carried out, no template was available containing cloned *orbH*. Thus, for the primer extension experiment with the *orbH*-specific primer, an *orbH* PCR product was used in an attempt to generate the corresponding DNA sequencing ladder. As this was unsuccessful, it was decided to electrophorese the labelled cDNA products generated with the *orbH*-specific primer adjacent to the DNA sequencing ladder generated with the *orbI*-specific primer. This would give a fairly accurate indication of the *orbH* TSS, but may not be precise due to possible differences in electrophoretic mobility of DNA fragments of different sequences. The *orbH*-specific primer gave rise to a single cDNA product that migrated with the same mobility as the *orbI* DNA ladder fragment terminating at position -16 with respect to the *orbI* TSS (Figure 5.14 B). This fragment has a length of 119 nucleotides (including the *orbI*-specific primer). A cDNA fragment of such a length generated with the *orbH*-specific primer would have a 3' endpoint corresponding to a position located 56 bp upstream of the putative translation initiation codon for *orbH* (Figure 5.15 C). This corresponds approximately (± ~2 bases) to the *orbH* TSS (+1). The locations of the -35 and -10 motifs of the predicted *orbH* promoter are respectively 32-28 and 11-8 bp upstream of the approximate TSS determined by primer extension, consistent with the prediction that the *orbH* promoter sequence is TAAAA $(N)_{16}$ CGTC.

The correspondence between the OrbS-dependent promoter sequences determined experimentally and those identified *in silico* indicate that the *orbE* promoter was correctly predicted.

5.6: Discussion

As discussed in Section 5.1, two candidate σ^{70}-type promoters were identified upstream of *orbS*, and putative OrbS-dependent promoters were identified upstream of *orbH*, *orbE* and *orbI*. RT-PCR analysis of the organisation of the ornibactin genes suggested that *orbS* is not co-transcribed with its upstream gene (BCAL1687), and therefore it was considered likely that a promoter was located in the intergenic region. This approach also demonstrated that *orbS* and *orbH* were co-transcribed, providing no evidence for the requirement of a promoter in the *orbS-orbH* intergenic region. This suggests that a promoter within the intergenic region between *orbS* and the upstream gene specifies transcription of not only *orbS*, but also of the downstream genes from *orbH* to *orbB*. However, reporter gene analysis of a DNA fragment containing the *orbS-orbH* intergenic region demonstrated that a promoter was present within this region. This implies that genes *orbH* to *orbB* are transcribed from both the *orbS* and *orbH* promoters.

The transcripts initiated from the *orbS* and *orbH* promoters are probably terminated at a predicted intrinsic terminator located between *orbB* and *orbE*. Intrinsic terminators consist of two sequence motifs, one encoding a G+C-rich RNA-stem loop that causes RNA to leave the binding site of core RNAP, and another encoding a uridine-rich stretch of >3 nt immediately downstream of the stem-loop. Uridine forms comparatively weak bonds with the adenosine residues of the DNA sequence in the template strand, resulting in the dissociation of core RNAP from the template DNA (Santangelo and Roberts, 2004). The predicted intrinsic terminator located between *orbB and orbE* has the sequence ATCGCCGGCACACTGCCACTGCAGCGTGCCGGCGATTTTTT (on the sense strand), with complementary bases predicted to form an RNA stem-loop underlined.

As expected, the divergent genes *orbE* and *orbI* were shown by RT-PCR and RPA analysis not to be co-transcribed, suggesting that two divergent promoters must be present within this intergenic region. This was confirmed by reporter analysis using a DNA fragment spanning this region, which was cloned upstream of *lacZ* in either orientation.

RT-PCR gave rise to a product spanning the region between the two convergent genes, *orbB* and *orbE*. This is most likely the result of transcription

proceeding from the *orbE* promoter across the intergenic region, resulting in antisense *orbB* RNA, since both forward and reverse primers were present during the reverse transcription, as previously mentioned. Intrinsic terminators require a downstream stretch of T residues on the sense strand to function, and therefore the predicted terminator downstream of *orbB* would not disrupt the production of antisense mRNA originating from the *orbE* promoter (Wilson and Hippel, 1995).

No transcripts were detectable by RT-PCR when the template consisted of RNA from iron replete cells, demonstrating that transcription of the ornibactin gene cluster is down-regulated in the presence of iron. This was expected as these promoters specify the biosynthesis and utilisation of ornibactin, which is only produced when iron availability is limited (Meyer *et al.*, 1995). Furthermore, the β-galactosidase activity specified by the DNA fragments bearing the *orbH*, *orbE* and *orbI* promoters was found to be down-regulated in response to iron availability. The activity specified by these fragments was dependent upon the presence of functional *orbS*, supporting the role of OrbS as a σ factor.

The furthest upstream from *orbS* of the two promoter-like sequences has the sequence CTGACA $(N)_{16}$ TGTAAT, which represents a 5/6 base match to the consensus σ^{70} promoter sequence (TTGACA $(N)_{17}$ TATAAT (Wösten, 1998)) at each of the hexameric promoter elements, but has a sub-optimal spacer of only 16 bases. The closer of the two promoter-like sequences to *orbS* has the sequence TTGAGA $(N)_{17}$ TAAATT, which as before represents a 5/6 base match to the consensus σ^{70} promoter sequence at each of the hexameric promoter elements, and also has a spacer region of optimal length. A study examining the effects on promoter activity of single-base substitutions within the -35 and -10 elements of a σ^{70}-dependent promoter found that substituting a different base for the consensus at positions 1-5 of the -35 element, and positions 1, 2 and 6 of the -10 element, had the greatest detrimental effect on σ^{70}-dependent promoter activity (Moyle *et al.*, 1991). Both candidate *orbS* promoters differ from the -35 element consensus at a position that should have a large detrimental effect according to the results of this study. However, the -10 element of the nearer of the two candidate promoters to *orbS* differs from the consensus at an apparently less important position to that of the other candidate promoter. Therefore the nearer of the candidate promoters to *orbS* would appear to constitute a better match for the σ^{70}-dependent consensus, both on the grounds of its sequence and its spacer length.

Deletion analysis was used to determine which of the two putative promoters upstream of *orbS* fulfils this function, and showed that a DNA fragment bearing only the closest promoter-like sequence to *orbS* specified a high level of β-galactosidase activity.

The primer extension results were consistent with the deletion analysis. The promoters for *orbI* and *orbH* were also found to be located in the regions predicted by *in silico* analysis. This suggests that the putative *orbE* promoter, identified by *in silico* analysis, is responsible for the β-galactosidase activity specified by the DNA fragment containing the region upstream of *orbE*.

The mechanism for the observed iron-dependent regulation of the four promoters is unclear. Such regulation is most often mediated by the ferric uptake regulator, Fur, as detailed in Section 1.9. However, no Fur binding site was apparent upstream of the *orbS* or OrbS-dependent promoters. Hence, the mechanism of iron-dependent regulation of the activity of the *orbS* and OrbS-dependent promoters was investigated (Chapter 7).

Chapter 6

Determination of the DNA sequence requirements for promoter utilisation by OrbS

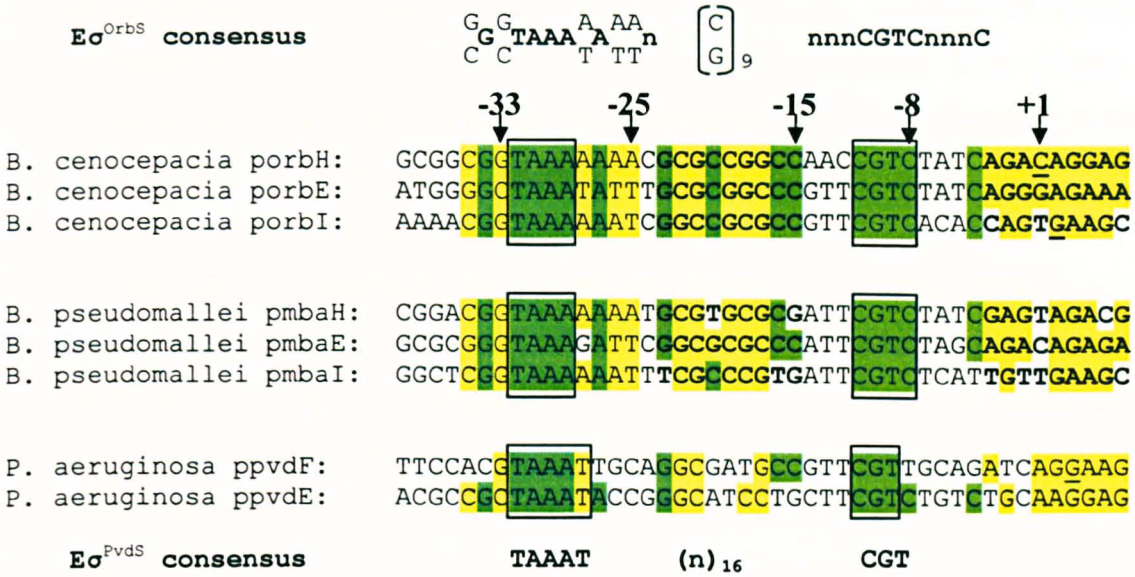

Figure 6.1: Alignment of the OrbS, MbaS and PvdS-dependent promoters. Bases within the OrbS-dependent promoters that are identical in all three sequences have been highlighted in green. The two absolutely conserved regions predicted to constitute at least part of the -10 and -35 regions of the promoters have been boxed. The approximate TSSs for *porbH,* and the TSSs for *porbI* and *ppvdF* have been underlined. Arrows indicate base position relative to the *porbH* TSS (+1), and for consistency have been used to refer to the corresponding positions in the other promoters. G+C, A+G and A+T bases within the G+C-rich block, A+G-rich block and extended A+T tract, respectively, have been highlighted in yellow. Four such areas are present in OrbS- and MbaS-dependent promoters: a 3 bp G+C-rich block at positions -35 to -33, relative to the TSS, a 4 bp A+T region within the spacer, located immediately downstream of the -35 element (positions -28 to -25) (the extended A+T tract), a 9 bp G+C-rich region from positions -23 to -15 (the G+C-rich spacer block, also emboldened in the OrbS- and MbaS-dependent promoters), and a 9 bp A+G rich block from positions -3 to +6 (also emboldened). The consensus sequence for OrbS-dependent promoters has been indicated at the top of the figure (n = any base). However, this does not incorporate elements of the A+G-rich block, as this is less well conserved than the other regions. Beneath the 3 OrbS-dependent promoter sequences are the three putative MbaS-dependent promoters, and beneath these two PvdS-dependent promoters are shown. Bases in these two sequences that are identical to the absolutely conserved bases of the OrbS-dependent promoters have been highlighted green, whereas bases that are consistent with those present within the 4 conserved regions of the OrbS-dependent promoters have been highlighted yellow. The consensus promoter sequence for PvdS recognition has been shown at the bottom of the figure (Ochsner *et al.,* 2002; Wilson *et al.*, 2001).

6.1: Introduction

The putative σ factor OrbS is highly homologous to the ECF σ factor PvdS and putative σ factor MbaS, as previously discussed (see Section 1.11). MbaS directs the transcription of the *mba* operon of *B. pseudomallei,* which is responsible for the biosynthesis and transport of the siderophore malleobactin, as discussed in Section 1.11 (Alice *et al.*, 2006). Malleobactin is recognised by the *B. cenocepacia* receptor for ferric ornibactin uptake, OrbA, and restores growth to ornibactin biosynthetic mutants under iron-limiting conditions. Ornibactin can similarly complement malleobactin biosynthetic mutants. The high degree of similarity between the ornibactin and malleobactin operons suggests that these systems are orthologous (Alice *et al.*, 2006).

The status of PvdS as a σ factor has been confirmed by *in vitro* assembly of functional RNA polymerase holoenzyme from core RNA polymerase and purified PvdS (Leoni *et al.*, 2000). The similarities between OrbS and other ECF σ factors (especially PvdS), and the dependency of the *orbH, orbE* and *orbI* promoters upon the availability of OrbS for their activity provide strong evidence that OrbS is a σ factor, but do not prove that this is the case. Hence, the potential functional interchangeability of OrbS and PvdS was investigated.

The homology between OrbS and PvdS prompted the inspection of the regions upstream of the putative OrbS-dependent genes for sequences resembling PvdS-dependent promoters. This led to the identification of the candidate *orbH, orbE* and *orbI* promoters, as discussed in Section 1.7.2. The ability of these sequences to act as OrbS-dependent promoters was strongly supported by reporter gene analysis and determination of transcription start sites (TSS) (Sections 5.3 and 5.5). Figure 6.1 illustrates the homology between the three OrbS-dependent promoters, two PvdS-dependent promoters, and the three predicted MbaS-dependent promoters.

From the alignment of the three OrbS-dependent promoter sequences, the consensus appeared to be $(G/C)_3$ TAAA(A/T)A$(A/T)_2$n$(G/C)_9$n$_3$CGTCn$_3$C, on the non-template strand (Figure 6.1). The -35 and -10 elements were each predicted to consist of 4 absolutely conserved bases (see Figure 6.1), and four additional conserved regions were identified. These regions consist of (i) 3 consecutive G+C base pairs located immediately upstream of the putative -35 element (i.e. positions -35 to -33

relative to the approximate TSS of *porbH*); (ii) four consecutive A+T base pairs located immediately downstream of the putative -35 element (i.e. positions -28 to -25) (the 'extended A+T tract'); (iii) A 9 bp G+C-rich block from positions -23 to -15 (the 'G+C-rich spacer block'); and (iv) a 9 bp A+G-rich region spanning positions -3 to +6 (the 'A+G-rich block') (Figure 6.1). These regions are also largely conserved throughout the putative MbaS-dependent promoters.

The PvdS-dependent promoter consensus is similar to that of the OrbS-dependent promoters, and consists of TAAAT $(N)_{16}$ CGT (Figure 6.2) (Ochsner *et al.*, 2002; Wilson *et al.*, 2001). Regions (i)-(iv) of the OrbS promoters are present in some of the PvdS-dependent promoters, but are less well conserved. The OrbS-dependent consensus appears to be more stringent than that of the PvdS-dependent promoters, and therefore OrbS-dependent promoters seem to represent a sub-group of those recognised by PvdS. The main difference between the promoters utilised by these σ factors appears to be the presence of a conserved C residue at the fourth position of the putative -10 element of the OrbS-dependent promoters (position -8 relative to the TSS), which is present in only three PvdS-dependent promoters within the pyoverdine (*pvd*) gene clusters (*ppvdE, ppvdH* and *ppvdM*, see Figure 6.2). It was therefore decided to investigate the sequence requirements for promoter recognition by OrbS, and compare these requirements to those of PvdS. It should be noted that although the TSSs for two PvdS-dependent promoters have been determined, leading to the establishment of the PvdS-dependent consensus sequence (Ochsner *et al.*, 2002; Wilson *et al.*, 2001), the precise sequence requirements for promoter recognition by PvdS have yet to be established. Also, the predicted MbaS-dependent promoters have been inferred from their similarity to PvdS-dependent promoters, and have not been confirmed (Alice *et al.*, 2006).

Two PvdS-dependent promoters were chosen for investigation of promoter recognition by OrbS. These were the *pvdE* and *pvdF* promoters. The *pvdE* promoter contains the additional C residue found within the OrbS-dependent promoter consensus sequence at position -8 relative to the *porbH* TSS (position 4 of the putative -10 element) whereas the *pvdF* promoter contains a T, which is the most frequent base at this position among PvdS-dependent promoters. Both promoters have an A+G-rich region overlapping the TSS, and two G+C base pairs immediately upstream of the -35 motif (see Figure 6.1).

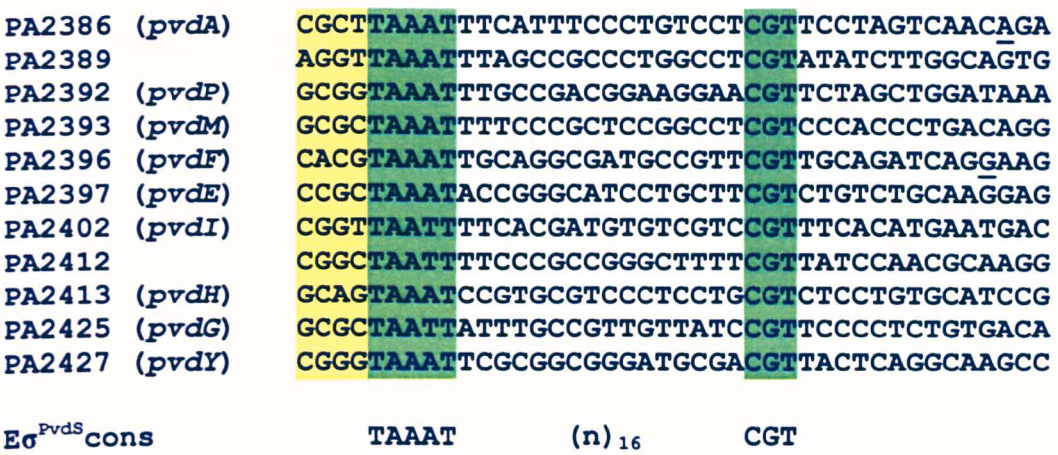

Figure 6.2: Alignment of the PvdS-dependent promoters of the *pvd* gene clusters. The designation and name (where available) of the gene downstream of each promoter is indicated. The consensus sequence has been shown below (n = any base). The conserved regions predicted to constitute the –35 and –10 elements are highlighted in green. G+C-rich sequences flanking the –35 region are highlighted in yellow. The TSSs for *pvdA* and *pvdF* have been underlined (Leoni *et al.*, 1996; Wilson *et al.*, 2001). Modified from Thomas, 2007.

6.1.1: Objectives

- To test for functional interchangeability between OrbS and PvdS.
- To compare promoter sequence requirements for recognition by OrbS and PvdS.

6.2: Investigation of the utilisation of OrbS- and PvdS-dependent promoters by PvdS and OrbS, respectively

6.2.1: Construction of pKAGd4-ppvdEfl and pKAGd4-ppvdFfl

To compare the ability of OrbS and PvdS to utilise OrbS- and PvdS-dependent promoters, PvdS-dependent promoter-*lacZ* fusions were constructed. A PCR was carried out using the primers detailed in Figure 6.3 to amplify a 564 bp fragment bearing both *ppvdE* and *ppvdF*, which are divergently arranged, from *P. aeruginosa* PAO1 genomic DNA. The fragment bearing the two promoters was digested with *Bam*HI and *Hin*dIII and cloned into pKAGd4 digested with either *Bam*HI and *Hin*dIII or *Bgl*II and *Hin*dIII. Since digestion with *Bam*HI and *Bgl*II gives compatible ends, and the restriction sites for these enzymes are on either side of the *Hin*dIII site in the pKAGd4 MCS, this enabled the same PCR fragment to be cloned in either orientation (Figure 6.3). Transformants harbouring recombinant pKAGd4 derivatives were selected using LB agar containing chloramphenicol and X-gal. Two plasmid clones (one bearing the appropriate PCR fragment with *ppvdE* driving *lacZ* transcription, and one bearing the fragment with *ppvdF* driving *lacZ* transcription) were selected following analysis by restriction digestion and DNA sequencing, and were named pKAGd4-ppvdEfl and pKAGd4-ppvdFfl, respectively.

6.2.2: Analysis of *pvdE* and *pvdF* promoter activity in *P. aeruginosa*

Plasmids pKAGd4-ppvdEfl and pKAGd4-ppvdFfl were introduced into *P. aeruginosa* PAO1 and PAO1-pvdS::Gm by conjugation, to confirm the iron- and PvdS-dependent regulation of these promoters. β-galactosidase assays were carried out on cells grown under conditions of iron sufficiency and iron starvation. To obtain iron starvation conditions, 100 μM 2'2-dipyridyl was added to M9 salts medium, as this concentration was previously shown to be iron limiting for *B. cenocepacia* growth (see Section 3.3.1). The results show that, as expected, these promoters were iron-dependently regulated in the wild type parent strain, PAO1 (Figure 6.4 A). The PvdS-dependent *pvdE* and *pvdF* promoters were, respectively, 3 and 8 fold repressed in

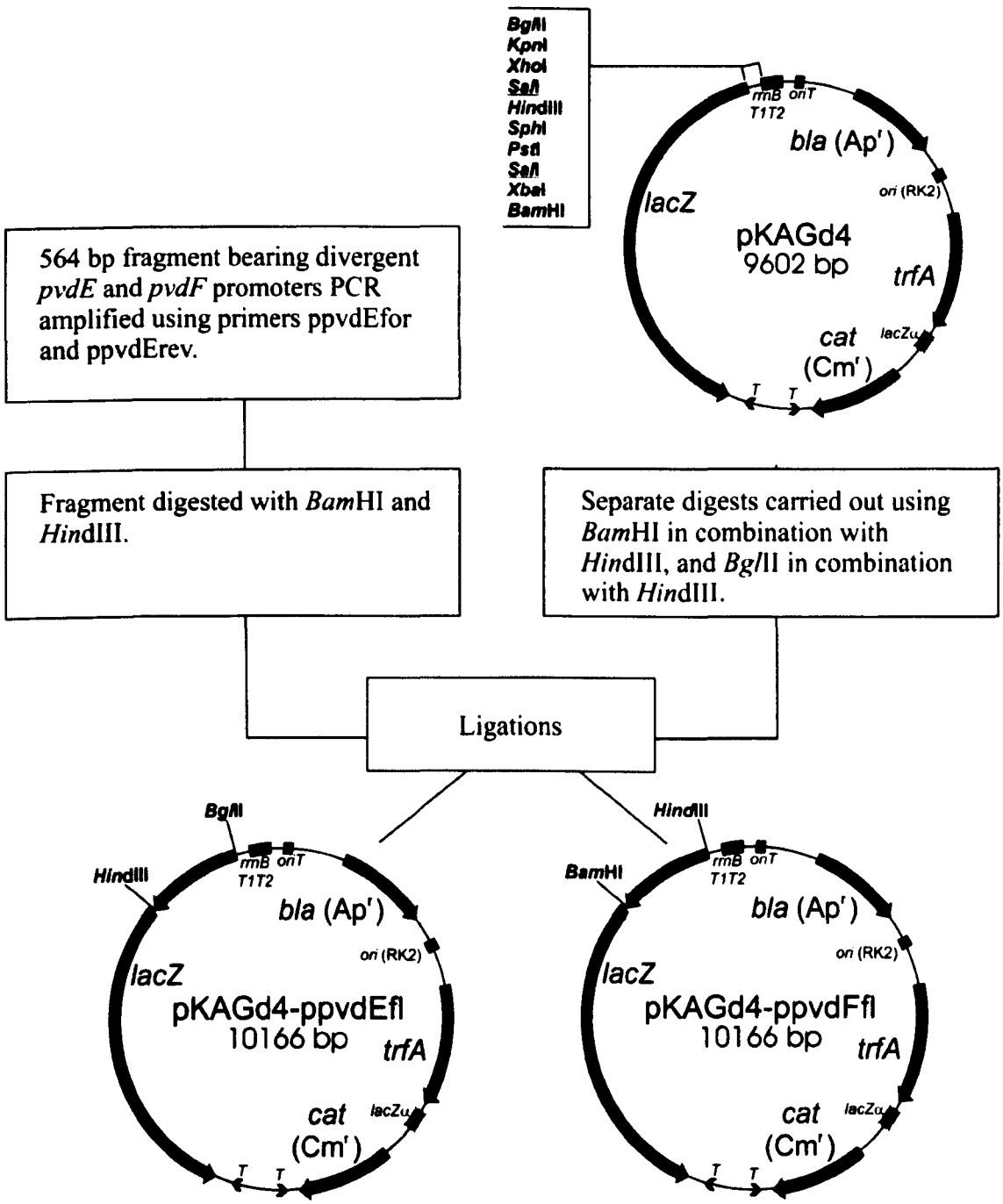

Figure 6.3: General scheme for construction of pKAGd4-ppvdEfl and pKAGd4-ppvdFfl. Only pertinent restriction sites are shown.

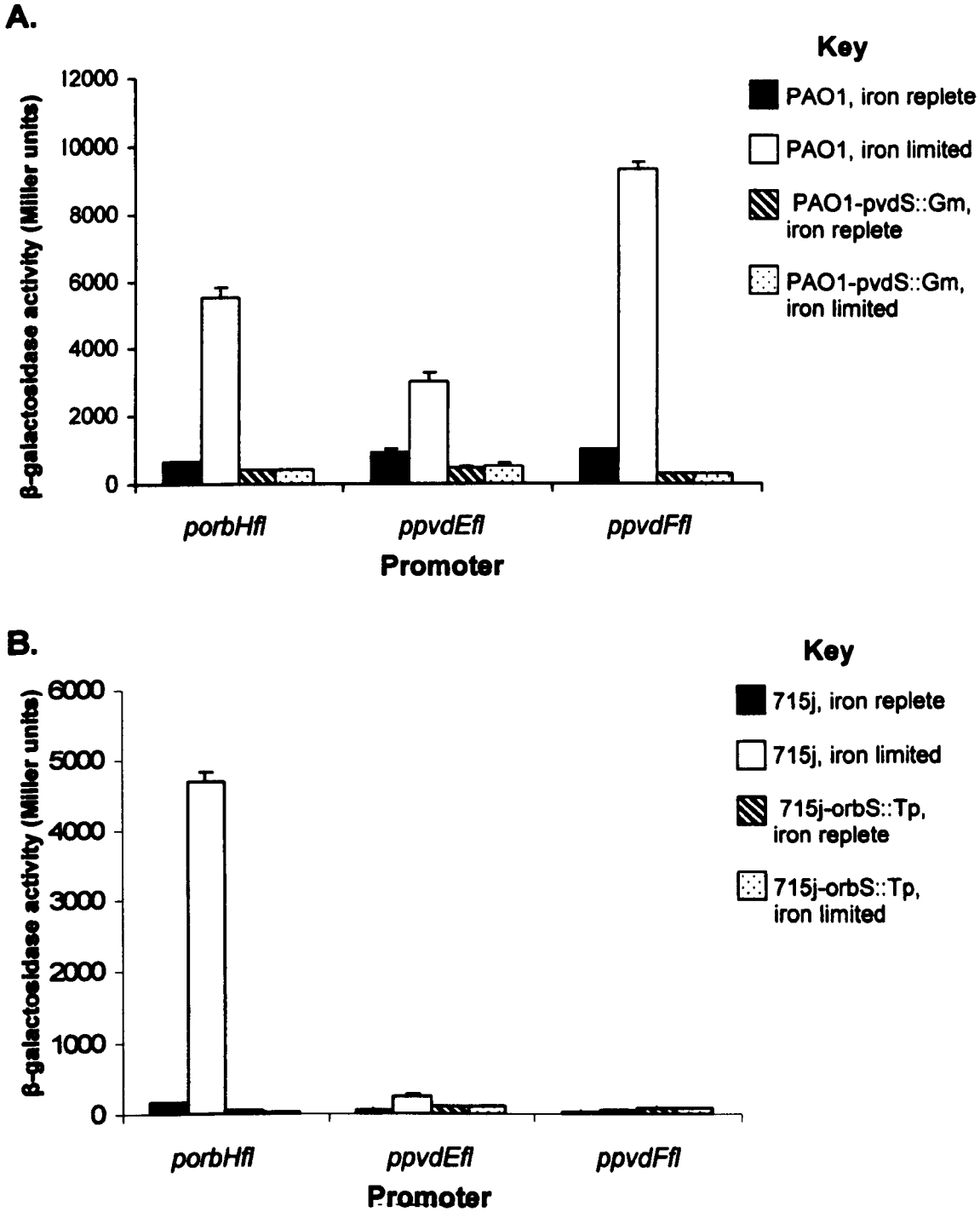

Figure 6.4: Promoter activity in response to OrbS and PvdS. A: PvdS-dependent activities of *porbHfl*, *ppvdEfl* and *ppvdFfl*, which were cloned into pKAGd4 for *lacZ*-fusion analysis in *P. aeruginosa* strains PAO1 and PAO1-pvdS::Gm grown under iron replete and iron limited conditions. B. OrbS-dependent activities of *porbHfl*, *ppvdEfl* and *ppvdFfl*, which were cloned into pKAGd4 for *lacZ*-fusion analysis in *B. cenocepacia* strains 715j and 715j-orbS::Tp grown under iron limited and iron replete conditions.
Assays were carried out on cultures grown in M9 salts medium supplemented with chloramphenicol. The promoter fused to *lacZ* is indicated below each set of bars. Activities were corrected by subtraction of the background pKAGd4 activity in the appropriate strain. Assays were performed in triplicate and the mean value is shown. Error bars represent the standard deviation of the activities of the three cultures assayed.

response to iron sufficiency in PAO1. This is because the synthesis and activity of PvdS is regulated in response to iron availability (Cunliffe *et* al., 1995; Ochsner *et al.*, 2002). Also as expected, in the *pvdS* mutant these promoters were much less active, and they were not subject to iron-dependent regulation.

6.2.3: Activity of the *orbH* promoter in *P. aeruginosa*

The activity of *porbH* in the *P. aeruginosa* strain PAO1, growing under iron-starvation conditions, was investigated and was found to be comparable to the activities of the two PvdS-dependent promoters, *ppvdE* and *ppvdF*, growing under the same conditions (Figure 6.4 A). Under conditions of iron sufficiency, the *orbH* promoter showed a decrease in activity of 8 fold, similar to that of *ppvdF*, indicating that the *orbH* promoter is also regulated in response to environmental iron levels in *P. aeruginosa*. In the *pvdS* mutant strain of *P. aeruginosa*, *orbH* promoter activity was very low under both iron limited and iron sufficient conditions, demonstrating that the iron-regulated activity of this promoter in *P. aeruginosa* is dependent upon the PvdS σ factor.

6.2.4: Activities of the *pvdE* and *pvdF* promoters in *B. cenocepacia*

As previously discussed (Section 5.3), the activity of the *orbH* promoter was regulated 30 fold in response to iron, and its activity was negligible in the *orbS* mutant. The activity of *ppvdEfl* in wild type (WT) *B. cenocepacia* growing under iron-starvation conditions was found to be almost 20 fold lower than the activity of *porbHfl* under the same conditions, indicating that *ppvdE* is utilised less efficiently than *porbH* by OrbS (Figure 6.4 B). Under conditions of iron-sufficiency the activity of *ppvdEfl* is decreased further, showing a degree of iron-dependent regulation that is probably the result of the regulation of OrbS production, rather than direct repression of *ppvdE*, as this promoter is not directly regulated in response to iron availability (Vasil and Ochsner, 1999; Ochsner *et al.*, 2002) The activity of the *pvdE* promoter fragment is also extremely low in the *B. cenocepacia orbS* mutant under both sets of conditions, suggesting that the low level of *ppvdE* activity observed in the wild type strain under iron-starvation conditions is OrbS-dependent. In contrast, *ppvdFfl* did not exhibit any OrbS-dependent activity. These results suggest that OrbS recognises the

pvdE promoter sequence very inefficiently, but completely fails to recognise the *pvdF* promoter sequence.

The results of these two experiments demonstrate that while the OrbS- and PvdS-dependent consensus promoter sequences appear highly similar, sequence recognition by OrbS is more specific than that of PvdS, which can recognise both classes of promoter.

6.3: Investigation of the ability of OrbS and PvdS to functionally substitute for one another in *P. aeruginosa* and *B. cenocepacia*, respectively

6.3.1: Construction of *orbS* and *pvdS* expression plasmids

In order to investigate the ability of OrbS to substitute for PvdS in *P. aeruginosa,* and for PvdS to substitute for OrbS in *B. cenocepacia, pvdS* and *orbS* null mutants of *P. aeruginosa* and *B. cenocepacia,* repectively, were required as host strains for a plasmid harbouring a *porbH-lacZ* or *ppvdE-lacZ* fusion and a compatible plasmid expressing either *pvdS* or *orbS*. Since the previously constructed *orbS* mutant strain, 715j-orbS::Tp (Agnoli *et al.*, 2006), is sensitive only to chloramphenicol, it was not possible to select for two different plasmids in this strain. Therefore, the *orbS*::Tp null allele was introduced into the aminoglycoside-sensitive *B. cenocepacia* strain, H111, by allelic replacement, resulting in strain H111-orbS::Tp (Agnoli *et al.*, 2006).

To construct *orbS* and *pvdS* expression plasmids specifying resistance to an aminoglycoside, pBBR-orbS DNA was digested with *Bam*HI and *Hin*dIII, and pUCP22-pvdS DNA was digested with *Hin*dIII and *Kpn*I. The fragments bearing *orbS* and *pvdS* were excised from an agarose gel, and ligated with pBBR1MCS-2 DNA digested with the corresponding enzymes. pBBR1MCS-2 is a broad host-range plasmid that was derived from pBBR1MCS. It bears a kanamycin resistance cassette (*aph*) (Kovach *et al.*, 1994). Both H111 and PAO1 are sufficiently sensitive to kanamycin to allow its use in plasmid selection. As pUCP22-pvdS does not contain the *pvdS* promoter, the *pvdS* gene was cloned so as to be transcribed from the *aph* and *lac* promoters of pBBR1MCS-2. Transformants of *E. coli* JM83 harbouring pBBR1MCS-2 derivatives were selected on LB agar containing kanamycin, IPTG and X-gal. The resultant plasmids were named pBBR-2-orbS and pBBR-2-pvdS (Figures 6.5 and 6.6).

The *orbHfl* and *pvdEfl* promoter-*lacZ* fusion plasmids were introduced into H111-orbS::Tp and PAO1-pvdS::Gm by conjugation. Plasmids pBBR-2-orbS, pBBR-2-pvdS, and pBBR1MCS-2 (as a control) were separately introduced by the same process. β-galactosidase activity was then measured under conditions of iron starvation and iron sufficiency (see Figure 6.7).

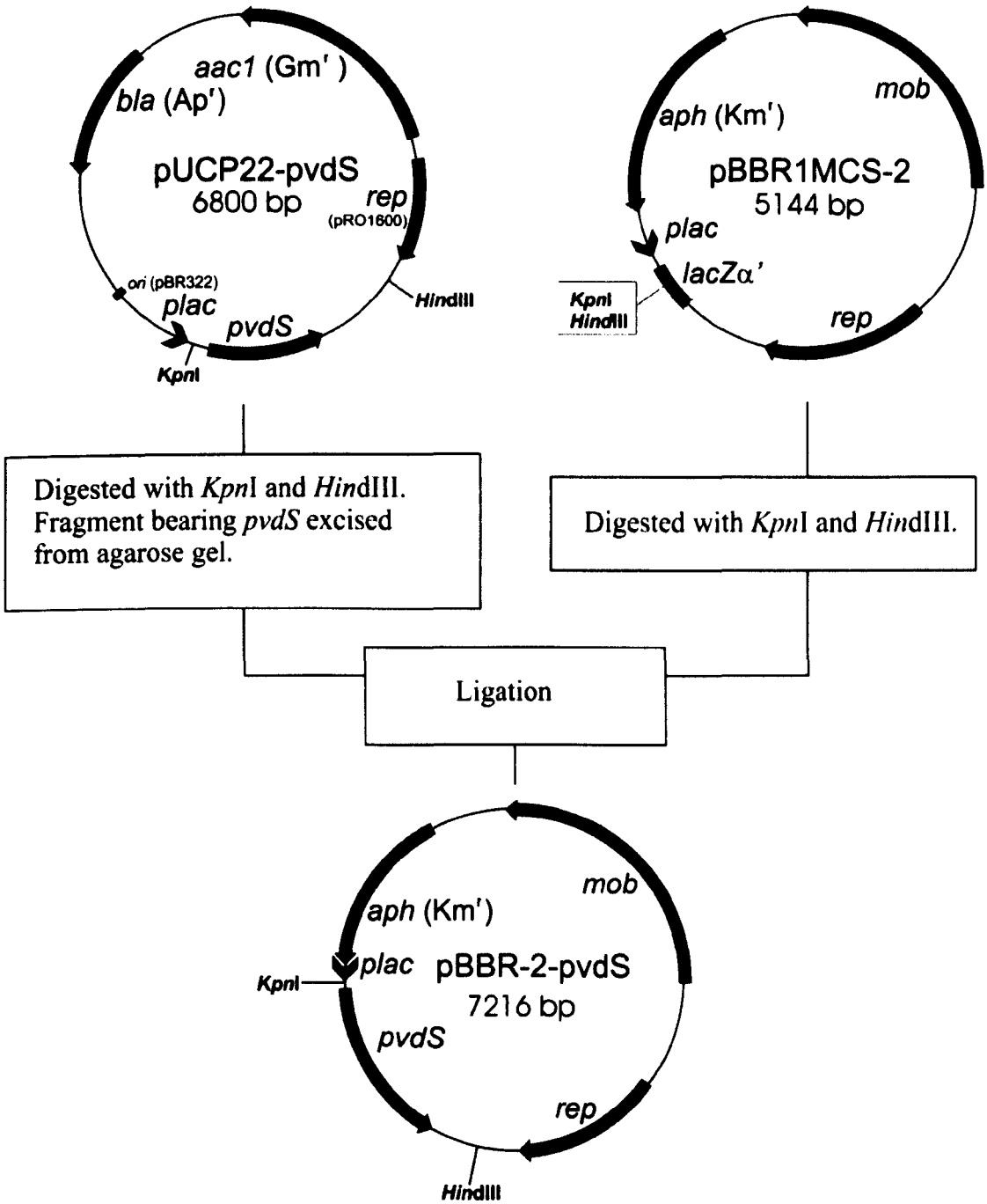

Figure 6.5: Scheme for the construction of pBBR-2-pvdS. Only pertinent restriction sites are shown. The *pvdS* gene cloned into pUCP22-pvdS (and pBBR-2-pvdS) is devoid of its cognate Fur-regulated promoter.

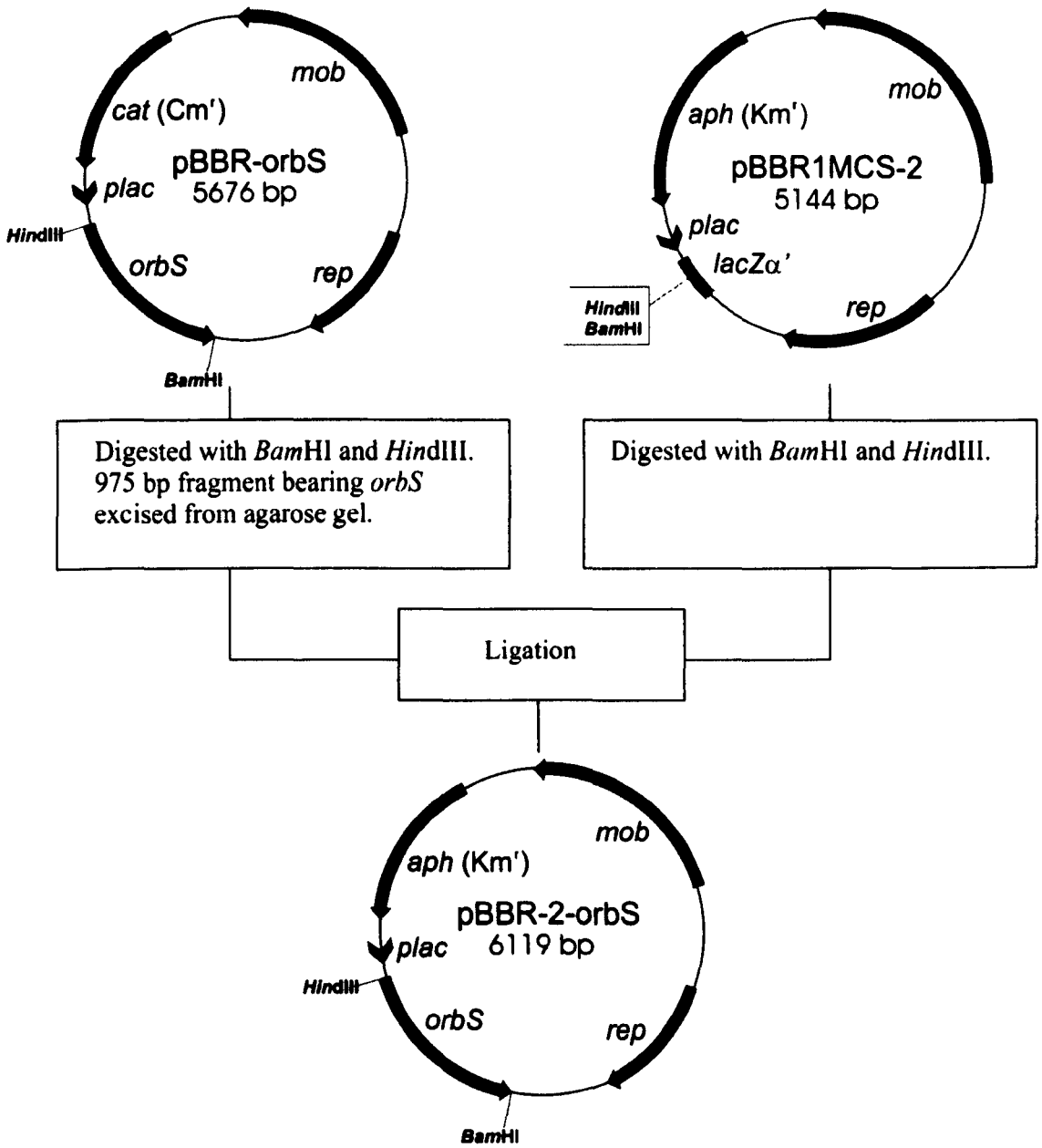

Figure 6.6: Scheme for the construction of pBBR-2-orbS. Only pertinent restriction sites are shown.

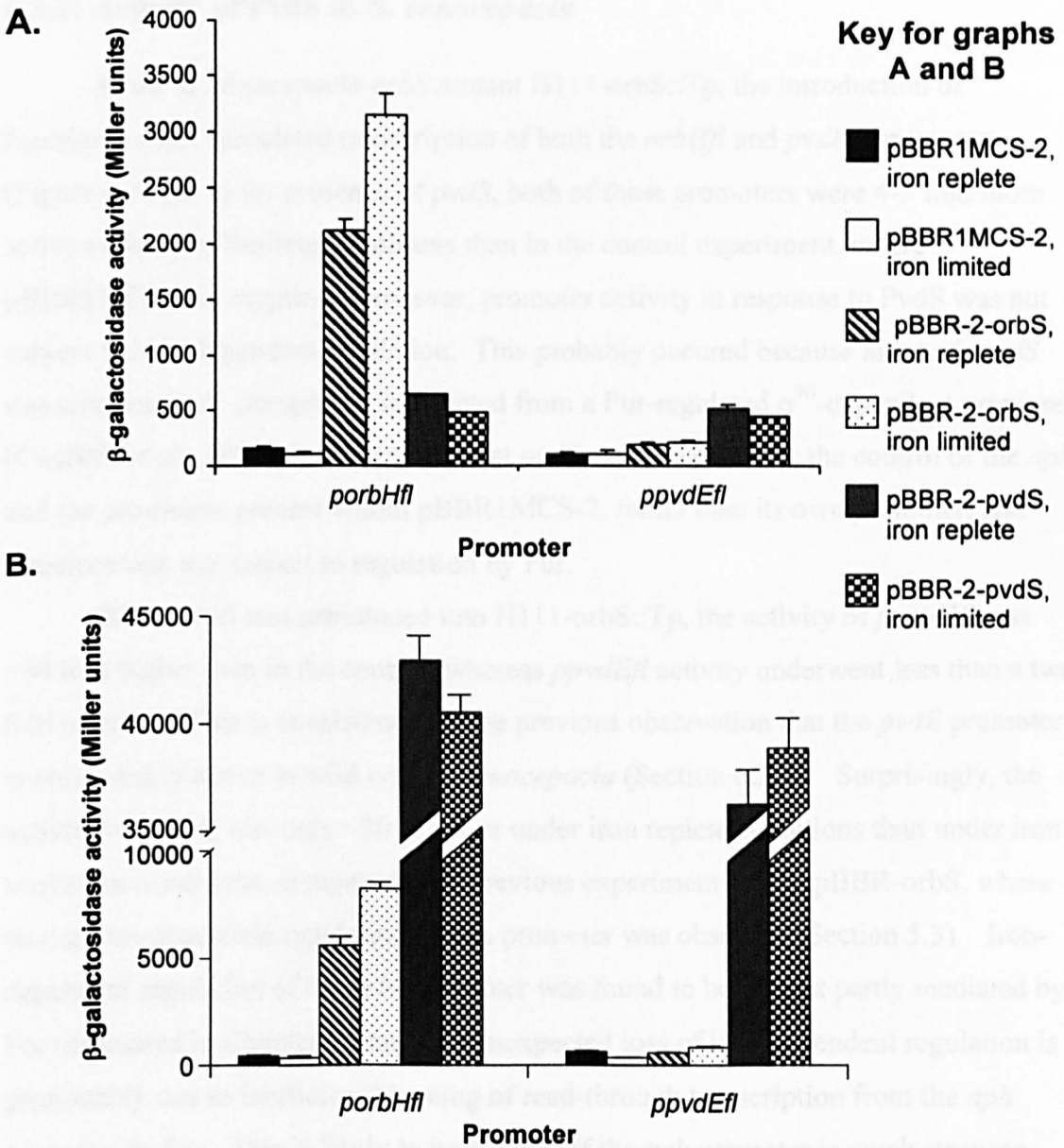

Figure 6.7: OrbS and PvdS activity in *B. cenocepacia* and *P. aeruginosa*. **A:** *porbHfl* and *ppvdEfl* activities in *B. cenocepacia* in response to OrbS and PvdS. *B. cenocepacia* H111-orbS::Tp harbouring pBBR1MCS-2, pBBR-2-orbS or pBBR-2-pvdS in combination with pKAGd4 bearing either *porbHfl* or *ppvdEfl* was assayed for β-galactosidase activity under iron limited and iron replete conditions.. **B:** *porbHfl* and *ppvdEfl* activities in *P. aeruginosa* in response to OrbS and PvdS. *P. aeruginosa* PAO1-pvdS::Gm harbouring pBBR1MCS-2, pBBR-2-orbS or pBBR-2-pvdS in combination with pKAGd4 bearing either *porbHfl* or *ppvdEfl* was assayed for β-galactosidase activity.
Assays were performed in triplicate, using cultures grown in M9 salts medium supplemented with chloramphenicol and kanamycin. The key shows which pBBR1MCS-2 derivative was present, and also whether conditions were iron limited or iron replete (see Table 2.3). The promoter fused to *lacZ* is indicated below each set of bars. Activities were corrected by subtraction of the background pKAGd4 activity in the appropriate strain growing under the same conditions. Error bars represent the standard deviation of the each set of three results.

6.3.2: Activity of PvdS in *B. cenocepacia*

In the *B. cenocepacia orbS* mutant H111-orbS::Tp, the introduction of functional *pvdS* stimulated transcription of both the *orbHfl* and *pvdEfl* promoters (Figure 6.7 A). In the presence of *pvdS*, both of these promoters were 4-5 fold more active under iron-limiting conditions than in the control experiment, where pBBR1MCS was supplied. However, promoter activity in response to PvdS was not subject to iron-dependent regulation. This probably occured because although *pvdS* transcription in *P. aeruginosa* is directed from a Fur-regulated σ^{70}-dependent promoter (Cunliffe *et al.*, 1995), in this experiment *pvdS* was placed under the control of the *aph* and *lac* promoters present within pBBR1MCS-2, rather than its own promoter, and therefore was not subject to regulation by Fur.

When *orbS* was introduced into H111-orbS::Tp, the activity of *porbHfl* was >30 fold higher than in the control, whereas *ppvdEfl* activity underwent less than a two fold increase. This is consistent with the previous observation that the *pvdE* promoter is only weakly active in wild type *B. cenocepacia* (Section 6.2.4). Surprisingly, the activity of *porbH* was only ~30 % lower under iron replete conditions than under iron starvation conditions, compared with previous experiments using pBBR-orbS, where strong iron-dependent regulation of this promoter was observed (Section 5.3). Iron-dependent regulation of the *orbS* promoter was found to be at least partly mediated by Fur (discussed in Chapter 7), and this unexpected loss of iron-dependent regulation is presumably due to inefficient blocking of read-through transcription from the *aph* promoter by Fur. This is likely to be the case if the *aph* promoter is much stronger than the *cat* promoter.

Although this experiment showed that *porbHfl* is less active in the presence of PvdS than in the presence of OrbS in *B. cenocepacia*, the fact that the introduction of *pvdS* into H111-orbS::Tp significantly increased the activity of *porbH* confirms that PvdS can recognise OrbS-dependent promoters, as shown in the previous experiment (Section 6.2.3). Moreover, this result demonstrates that PvdS can form a functional complex with *B. cenocepacia* core RNA polymerase. This is consistent with the proposed role of OrbS as an ECF σ factor.

6.3.3: Activity of OrbS in *P. aeruginosa*

In *P. aeruginosa* PAO1-pvdS::Gm, the introduction of *pvdS* on pBBR-2-pvdS increased the activity of *ppvdEfl* and *porbHfl* relative to a control culture containing pBBR1MCS-2 (Figure 6.7 B). This is consistent with previous results demonstrating that PvdS can utilise OrbS-dependent promoters (Sections 6.2.3 and 6.3.2). Promoter activities were very highly stimulated by the expression of *pvdS* from pBBR1MCS-2 (~40,000 Miller units compared to <10,000 Miller units when PvdS is provided from the single, Fur-regulated chromosomal copy of *pvdS* in wild type *P. aeruginosa* PAO1, see Section 6.2.3). Again, there was no significant effect of iron on the level of PvdS-dependent transcription from either promoter. The lower level of PvdS-dependent *porbH* activity relative to OrbS-dependent activity in *B. cenocepacia* may be due to less efficient assembly of PvdS with *B. cenocepacia* core RNA polymerase.

The introduction of *orbS* into PAO1-pvdS::Gm stimulated a high level of activity of the *orbH* promoter under both iron limited and iron replete conditions, as was also observed when *orbS* was introduced into *B. cenocepacia* H111-orbS::Tp (Section 6.3.2). Again, under iron replete conditions only a small decrease in *ppvdE* and *porbH* promoter activity was observed. Consistent with previous results in *B. cenocepacia*, the introduction of *orbS* only weakly activated the *pvdE* promoter.

These results indicate that OrbS can form a functional complex with *P. aeruginosa* core RNA polymerase, and confirm that OrbS cannot recognise PvdS-dependent promoters.

6.4: Analysis of DNA sequence requirements for promoter recognition by OrbS and PvdS.

The previous experiments showed that despite the similarity between OrbS- and PvdS-dependent promoters, and between OrbS and PvdS, OrbS recognises PvdS-dependent promoters extremely inefficiently while PvdS efficiently recognises an OrbS-dependent promoter. Although *ppvdEfl* was utilised more efficiently by OrbS than *ppvdFfl*, suggesting that the C at position 4 of the proposed -10 element contributes positively to promoter utilisation by OrbS, other positions must also play an important role. Therefore, experiments were designed to determine the key positions for promoter utilisation by OrbS and PvdS. This involved the introduction of *lacZ* fusions to *orbH* promoter derivatives containing defined sequence modifications into a bacterial host and determination of the resultant β-galactosidase activity in the presence of functional *orbS* and *pvdS*.

It was desirable to establish a more convenient model system in which to investigate the features important for promoter recognition by OrbS and PvdS, rather than using *B. cenocepacia* H111-orbS::Tp and *P. aeruginosa* PAO1-pvdS::Gm as hosts, as this involves time-consuming conjugation experiments. For this purpose the *E. coli* strain MC1061 was chosen. *E. coli* strain MC1061 is faster-growing than *B. cenocepacia*, and has been assigned to Hazard Group 1, while *B. cenocepacia* and *P. aeruginosa* are Hazard Group 2 organisms. MC1061 is deleted for the *lac* operon, facilitating the use of the *lacZ* reporter system. MC1061 is also sensitive to all antibiotics commonly used for plasmid selection within the laboratory, and therefore the previously constructed pBBR1MCS-2 derivatives bearing *orbS* and *pvdS* (Section 6.3.1) can be maintained within this strain in addition to a pKAGd4 derivative.

6.4.1: Construction of *porbH-lacZ* fusion plasmids

For each of the promoter constructs analysed, pairs of complementary single-stranded oligonucleotides were synthesised so as to give staggered ends on annealing. The staggered end upstream of the promoter was designed to be complementary to *Hin*dIII-digested ends, and the staggered end downstream of the promoter was designed to be complementary to *Bam*HI-digested ends. Annealing of each

oligonucleotide pair was carried out as described in Section 2.2.2. Double-stranded oligonucleotides were ligated with *Bam*HI- and *Hin*dIII-double-digested pKAGd4 DNA (Figure 6.8). Following transformation of MC1061 cells, chloramphenicol resistant colonies were selected using agar that also contained X-gal. The presence of the correct promoter sequence within each construct was confirmed by PCR screening using primers AP10 and AP11, that anneal to sequences flanking the pKAGd4 MCS (see Appendix 1), and by DNA sequencing using the reverse primer AP10 that anneals to *lacZ* sequences.

6.4.2: Determination of a 'minimal' *orbH* promoter for utilisation by OrbS and PvdS

To reduce the size of the oligonucleotides to be used for constructing the various *orbH* promoter derivatives, it was neccessary to determine the minimum promoter length required for recognition by OrbS and PvdS. Therefore, a series of *orbH* promoter derivatives possessing different lengths of DNA upstream of the putative -35 region and downstream of the putative -10 region were fused to *lacZ* in pKAGd4 as described in Section 6.4.1. The activity of the 'full-length' *orbH* promoter fragment (*porbHfl*) had been previously determined under iron limited and iron replete conditions in *B. cenocepacia* 715j and *P. aeruginosa* PAO1, and its activity had been shown to be dependent on the presence of the OrbS or PvdS σ factor (Sections 6.2.3 and 6.2.4). The first two promoter deletion derivatives to be tested were *porbHds1* and *porbHds2* (see Figure 6.9). The *orbHds1* promoter fragment had its upstream endpoint at -36 and downstream endpoint at -4 relative to the approximate TSS determined by primer extension (see Figure 6.1). *porbHds2* had its upstream endpoint at -39 and its downstream endpoint at +35 relative to the TSS. pKAGd4 containing the *orbHds1*, *orbHds2* and *orbHfl* promoters were introduced into strain MC1061, and functional copies of *pvdS* and *orbS* were introduced using plasmids pBBR-2-orbS and pBBR-2-pvdS (described in Section 6.3.1). As a control, pBBR1MCS-2 was also introduced. β-galactosidase assays were carried out using cultures grown in LB broth under iron-limiting conditions.

The *orbHds2* promoter was highly active in the presence of either *orbS* or *pvdS*, giving rise to ~6,500 and ~24,000 Miller units of β-galactosidase activity,

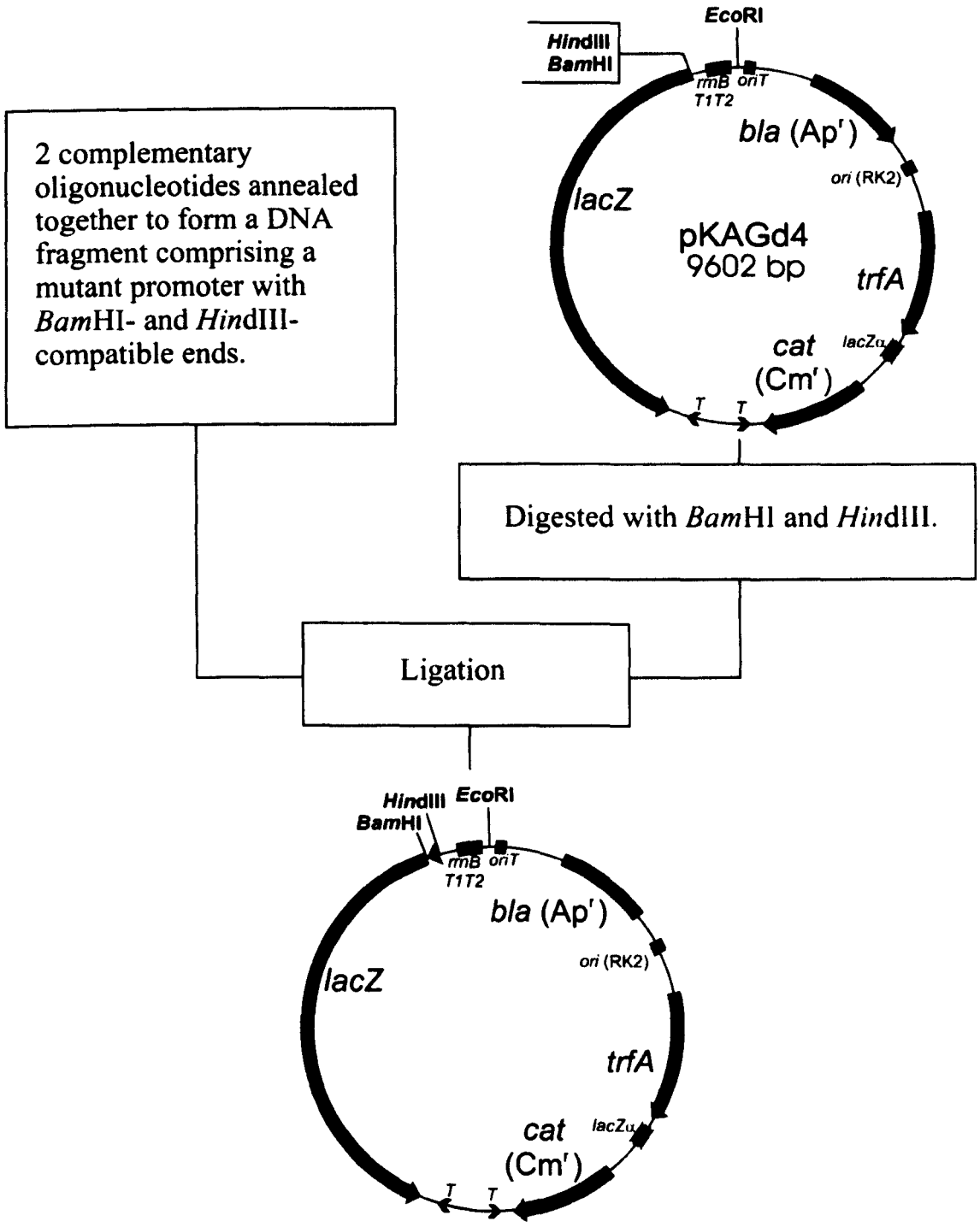

Figure 6.8: General scheme for insertion of double-stranded oligonucleotides containing *porbH* and *ppvdE* promoter derivatives into pKAGd4. Only pertinent restriction sites have been shown. Promoter derivatives are represented by a black triangle.

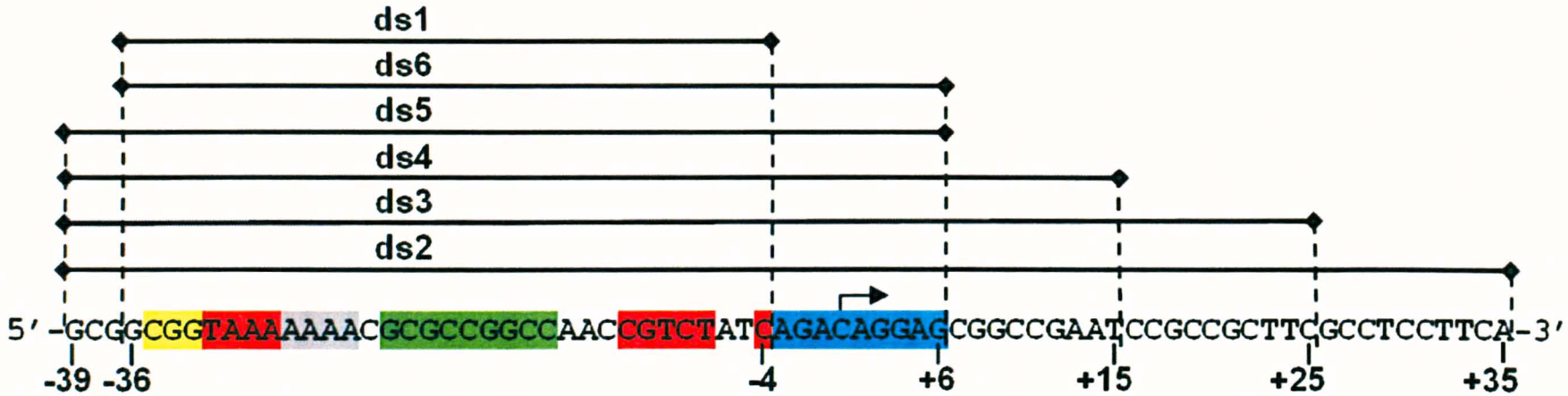

Figure 6.9: Promoter deletion derivatives for the determination of a minimal *orbH* promoter. The endpoints of the *porbH* fragments relative to the sense-strand are shown. Bases highlighted in red are conserved in all 3 OrbS-dependent promoters. The 3 bp upstream G+C-rich block, the extended A+T tract, the G+C-rich spacer block and A+G-rich block conserved in all 3 OrbS-dependent promoters have been highlighted in yellow, grey, green and blue, respectively. The approximate location of the TSS, determined by primer extension, has been indicated by a bent arrow. The positions of the end-points of the *orbH* promoter fragments relative to the TSS have been indicated. *porbHfl* has not been shown. This promoter fragment has endpoints at -347 and +68 relative to the TSS.

respectively (see Figure 6.10), and inactive in the presence of pBBR1MCS-2 (~20 Miller units). *porbHds1* activity was lower than that of *porbHds2* in the presence of either σ factor, exhibiting a decrease of 3.5 fold with PvdS and of 7 fold with OrbS, relative to *porbHds2*. Curiously, *porbHfl* activity was also very low (<10 % of the activity of *porbHds2*) in the presence of *orbS* or *pvdS*. These results suggested that the minimal *orbH* promoter was contained within *porbHds2*, and that important residues were absent from the shorter *porbHds1* promoter (Figure 6.9). Three further promoter derivatives were therefore constructed: *porbHds3*, *porbHds4* and *porbHds5* which have the same upstream endpoint as the *porbHds2* promoter (i.e. at position -39), and downstream endpoints at +25, +15 and +6, respectively. These promoter derivatives were inserted into pKAGd4 and their activities in response to OrbS and PvdS determined in *E. coli* MC1061, as previously. Figure 6.10 illustrates the results of these assays. As expected, the β-galactosidase activity specified by these plasmids was negligible when the pBBR1MCS-2 control plasmid was present (results not shown). The activities of all three promoters were consistently high in the presence of *orbS* or *pvdS*. These results suggest that the minimal promoter length for recognition by both OrbS and PvdS has a downstream endpoint between that of *porbHds1* (position -4) and *porbHds5* (position +6). *porbHds5* contains the additional, 9 bp A+G-rich region downstream of the conserved CGTC -10 motif, that is not present in *porbHds1*, and at least part of which is evidently crucial for utilisation by OrbS and PvdS.

Finally, a promoter derivative was constructed (*porbHds6*) which combined the upstream endpoint of *porbHds1* and the downstream endpoint of *porbHds5*. This promoter derivative specified a similar level of β-galactosidase activity to *porbHds5*, demonstrating that the three bases at the upstream end of *porbHds5* are unnecessary for promoter recognition by OrbS or PvdS. Thus, it was decided to use *porbHds6* as the template for an analysis of promoter sequence requirements for OrbS and PvdS recognition. It should be noted that an RNAse III processing site is present on pKAGd4 between the MCS and *lacZ* gene of pKAGd4. The *lacZ* transcript produced from each promoter would be cleaved at this site, standardising the 5' end of the mRNA produced by each construct, which should minimise any differences in apparent promoter activity owing to differences in mRNA stability or translational efficiency.

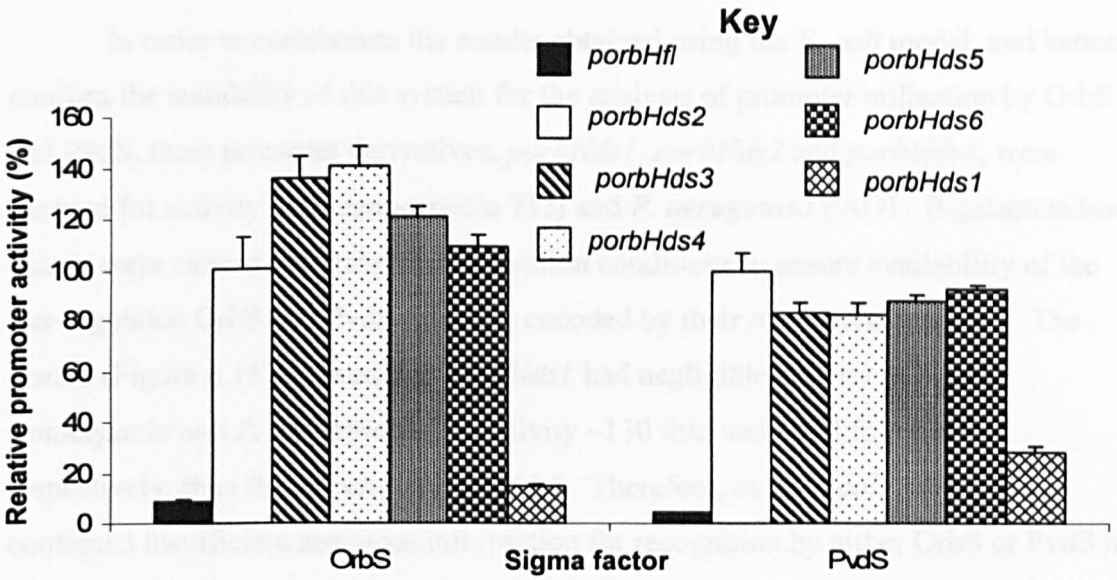

Figure 6.10: Activities of *orbH* promoter deletion derivatives in *E. coli*. *E. coli* MC1061 bearing either pBBR-2-orbS or pBBR-2-pvdS (indicated beneath graph) together with pKAGd4 bearing one of the following *porbH* derivatives: *porbHfl*, *porbHds2*, *porbHds3*, *porbHds4*, *porbHds5*, *porbHds6* or *porbHds1* was assayed for β-galactosidase activity. Assays were carried out in triplicate on cells grown in LB medium supplemented with kanamycin and chloramphenicol, under iron-limiting conditions. Activities were corrected by subtraction of the background pKAGd4 activity in the appropriate background (MC1061 bearing pKAGd4 and pBBR-2-orbS or pBBR-2-pvdS) and are expressed relative to that of *porbHds2* (100 %=2,940 Miller units in response to OrbS, 23,901 Miller units in response to PvdS). Error bars represent standard deviation of the activities of the triplicate cultures assayed.

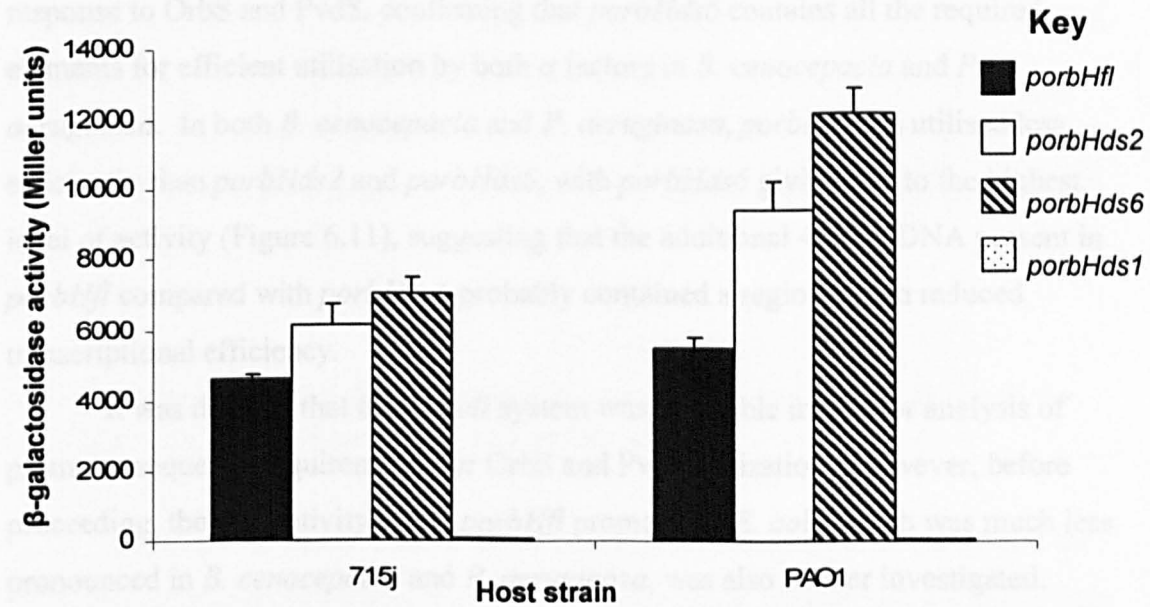

Figure 6.11: Activity of *orbH* promoter deletion derivatives in *B. cenocepacia* and *P. aeruginosa*. pKAGd4 containing the *orbHds1*, *orbHds2*, *orbHds6* and *orbHfl* promoters were introduced into *B. cenocepacia* strain 715j and *P. aeruginosa* strain PAO1. β-galactosidase assays were performed in triplicate on cultures grown in minimal salts medium containing chloramphenicol and 2'2-dipyridyl. Values have been corrected for by subtraction of the background pKAGd4 activity. Error bars represent standard deviation between the triplicate assays.

In order to corroborate the results obtained using the *E. coli* model, and hence confirm the suitability of this system for the analysis of promoter utilisation by OrbS and PvdS, three promoter derivatives, *porbHds1*, *porbHds2* and *porbHds6*, were assayed for activity in *B. cenocepacia* 715j and *P. aeruginosa* PAO1. β-galactosidase assays were carried out under iron starvation conditions to ensure availability of the Fur-regulated OrbS and PvdS σ factors encoded by their respective genomes. The results (Figure 6.11) showed that *porbHds1* had negligible activity in both *B. cenocepacia* and *P. aeruginosa,* i.e. activity ~130 fold and ~400 fold lower, respectively, than the activity of *porbHds6*. Therefore, as in *E. coli*, *porbHds1* contained insufficient sequence information for recognition by either OrbS or PvdS in these bacteria. In *E. coli,* the activity of *porbHds1* was much higher than in *B. cenocepacia* and *P. aeruginosa*, being only ~3.3 fold lower than that of *porbHds6* in response to OrbS and 7.4 fold lower in response to PvdS. This suggests that the increased abundance of OrbS and PvdS resulting from the expression of these σ factors from multi-copy pBBR1MCS-2 in *E. coli*, as opposed to the single chromosomal copy present in *B. cenocepacia* and *P. aeruginosa,* may be responsible for the increased activity of *porbHds1*. In contrast, *porbHds2* and *porbHds6* were utilised efficiently in both *B. cenocepacia* and *P. aeruginosa*, as they were in *E. coli* in response to OrbS and PvdS, confirming that *porbHds6* contains all the required elements for efficient utilisation by both σ factors in *B. cenocepacia* and *P. aeruginosa*. In both *B. cenocepacia* and *P. aeruginosa*, *porbHfl* was utilised less efficiently than *porbHds2* and *porbHds6*, with *porbHds6* giving rise to the highest level of activity (Figure 6.11), suggesting that the additional 449 bp DNA present in *porbHfl* compared with *porbHds6* probably contained a region which reduced transcriptional efficiency.

It was decided that the *E. coli* system was a suitable model for analysis of promoter sequence requirements for OrbS and PvdS utilisation. However, before proceeding, the low activity of the *porbHfl* promoter in *E. coli*, which was much less pronounced in *B. cenocepacia* and *P. aeruginosa*, was also further investigated.

6.4.3: Investigation of low *porbHfl* activity in *E. coli*

Introduction of pKAGd4-porbHfl (which bears the *orbHfl* promoter spanning from – 347 to +68 relative to the TSS) into *E.coli* containing pBBR-2-orbS or pBBR-2-pvdS gave rise to <10 % of the activity observed for pKAGd4-porbHds6 (which spans from position -36 to +35) under the same conditions. In *B. cenocepacia* 715j and *P. aeruginosa* PAO1, the activity of the *orbHfl* promoter was also decreased compared to that of *porbHds6*, but to a lesser extent (<50 %). To investigate the low activity of *porbHfl* in *E. coli*, a *porbH* promoter derivative extending from position -39 to + 68 was inserted into pKAGd4. Hence, this promoter had the same upstream end as the *porbHds2-porbHds5* derivatives, but the same downstream endpoint as *porbHfl*. This promoter, *porbHds18*, was constructed from four oligonucleotides (porbHds18-F1, F2, R1 and R2), which were annealed in the same manner as the double-stranded oligonucleotides (Section 6.4.1). The activity of this promoter in MC1061 was similar in response to both pBBR-2-orbS and pBBR-2-pvdS (see Figure 6.12). However, while the activity of the *orbHfl* promoter was <10 % of that of *porbHds6* (i.e. 9 % and 4 % in response to *orbS* and *pvdS*, respectively), the *porbHds18* promoter was 36% and 45% as active as *porbHds6* in response to *orbS* and *pvdS*, respectively. The activity of *porbHds2* was similar to that of *porbHds6*, as mentioned previously. This suggests that elements present on the *orbHfl* promoter fragment located between positions +35 and +68 downstream of the TSS, and between -347 and -39 upstream of the TSS both lead to a decrease in *porbH* activity that is more pronounced in *E. coli* than in *B. cenocepacia* and *P. aeruginosa*.

6.4.4: Investigation of the promoter sequence requirements of OrbS by construction of *orbH-pvdE* hybrid promoters

Examination of the OrbS-dependent promoters from *B.cenocepacia* and the (probably orthologous) MbaS-dependent promoters of *B. pseudomallei* showed four conserved DNA sequence blocks, not including the putative -35 and -10 elements (as previously mentioned in Section 6.1). These regions are the 3 bp G+C-rich block, at positions -35 to -33 relative to the TSS, directly upstream of the -35 element, the 4 bp extended A+T-tract, at positions -28 to -25 relative to the TSS, the 9 bp G+C-rich

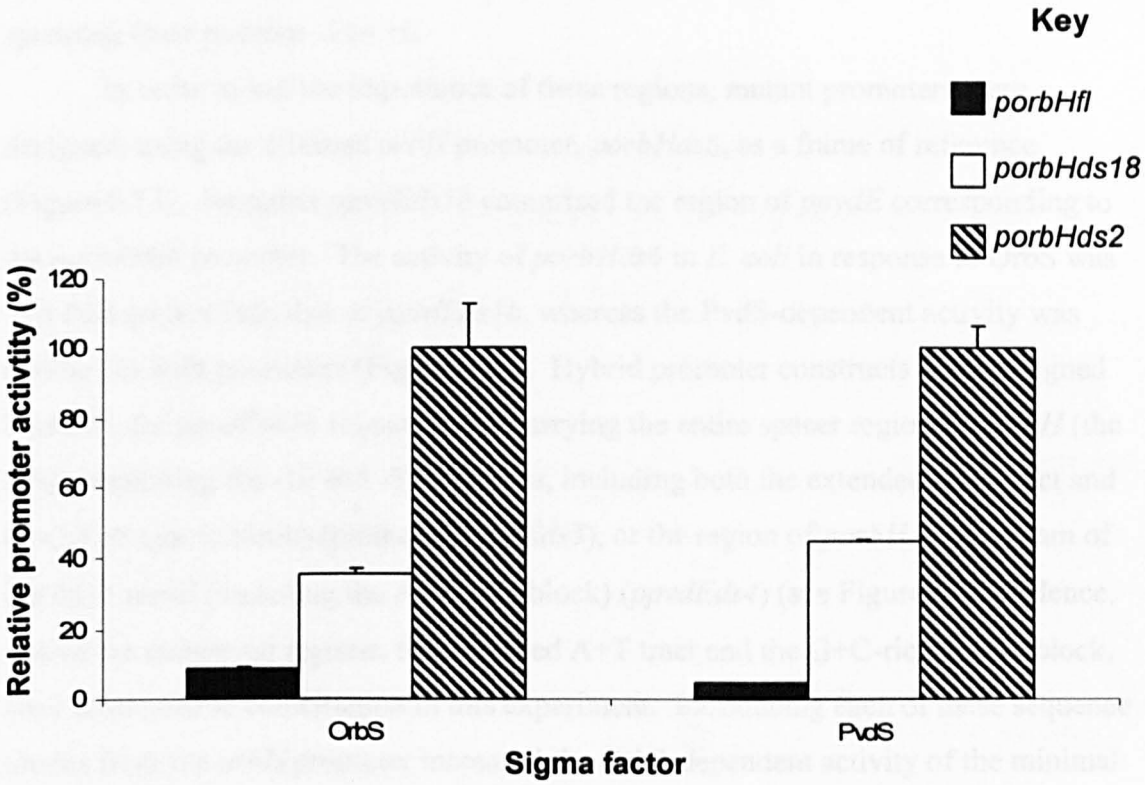

Figure 6.12: Role of downstream sequences in inhibition of *porbHfl* activity in *E. coli*. *E. coli* MC1061 bearing either pBBR-2-orbS or pBBR-2-pvdS (as indicated beneath graph) together with pKAGd4 bearing one of the following *porbH* derivatives: *porbHfl*, *porbHds18*, *porbHds2* was assayed for β-galactosidase activity. Assays were carried out in triplicate on cells grown in LB medium supplemented with kanamycin and chloramphenicol, under iron-limiting conditions. Activities were background corrected by subtracting the pKAGd4 activity in the appropriate background (MC1061 bearing pKAGd4 and pBBR-2-orbS or pBBR-2-pvdS) and are expressed relative to that of *porbHds6* (100 % = 3,122 Miller units in response to OrbS, 22,200 Miller units in response to PvdS). Error bars represent standard deviation of the activities of each set of three cultures.

spacer block, which spans from positions -23 to -15, and the 9 bp A+G-rich block, spanning from position -3 to +6.

In order to test the importance of these regions, mutant promoters were designed, using the minimal *orbH* promoter, *porbHds6*, as a frame of reference (Figure 6.13). Promoter *ppvdEds1b* comprised the region of *ppvdE* corresponding to the *porbHds6* promoter. The activity of *porbHds6* in *E. coli* in response to OrbS was ~70 fold greater than that of *ppvdEds1b*, whereas the PvdS-dependent activity was similar for both promoters (Figure 6.14). Hybrid promoter constructs were designed based on the *ppvdEds1b* sequence, but carrying the entire spacer region of *porbH* (the DNA separating the -10 and -35 elements, including both the extended A+T tract and G+C-rich spacer block) (promoter *ppvdEds3*), or the region of *porbH* downstream of the CGT motif (including the A+G-rich block) (*ppvdEds4*) (see Figure 6.14). Hence, two of the conserved regions, the extended A+T tract and the G+C-rich spacer block, were examined in combination in this experiment. Introducing each of these sequence blocks from the *orbH* promoter increased the OrbS-dependent activity of the minimal *ppvdE* promoter. In the case of the transfer of the *porbH* spacer region, the activity of *ppvdE* was increased 7 fold, while the activity was increased 11 fold when the downstream A+G-rich block of *porbH* was present. An additional hybrid promoter, *ppvdEds5*, was designed to test the combined effect of exchanging the spacer region and the A+G-rich block. These changes resulted in an ~15 fold increase in *ppvdE* activity (Figure 6.14). Since these changes did not account for the complete 70 fold difference in activity between the minimal *porbH* and *ppvdE* promoters in response to OrbS, a further hybrid promoter, *ppvdEds6*, was tested. In this promoter, the region upstream of the *porbH* spacer had been substituted for the corresponding region of *ppvdE*, i.e. the putative -35 region and four additional G or C bases immediately upstream. *ppvdEds6* showed an ~6 fold increase in OrbS-dependent activity compared to wild-type *ppvdE*. This promoter also had the lowest PvdS-dependent activity of this series of promoters (~28 % decrease relative to wild-type *ppvdE*), suggesting that exchanging this fragment is most detrimental to PvdS-dependent activity. These results showed that all four regions analysed contributed to OrbS-specificity, although in no case did substitution of one or more of these regions of *porbH* for the corresponding region of *ppvdE* confer efficient OrbS-dependence on the promoter. In order to determine which bases within these regions are important for OrbS-specificity, and also to define the limits of the -10 and -35 regions, a scanning

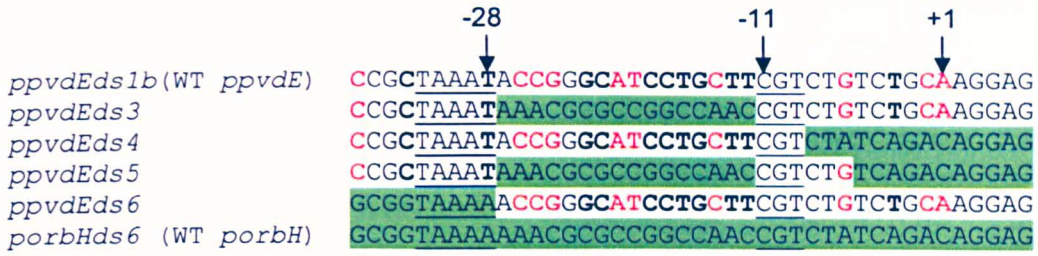

Figure 6.13: *ppvdE-porbH* hybrid promoters constructed to determine the contribution of four conserved regions of *porbH* to OrbS promoter specificity. Only the sense strand is shown for simplicity. Sequences derived from *porbH* are highlighted in green. Bases in wild type *ppvdE* that differ from all OrbS- and (its orthologue) MbaS-dependent promoters at the corresponding position have been emboldened and shown in red font. Bases differing from *porbH* at the corresponding position, but not in all of the other OrbS- and the MbaS-dependent promoters have been emboldened and shown in black font. The -35 and -10 sequences of *ppvdE* and corresponding sequences in *porbH* are underlined. The approximate *porbH* TSS has been indicated (+1), as have positions -11 and -28 relative to this TSS.

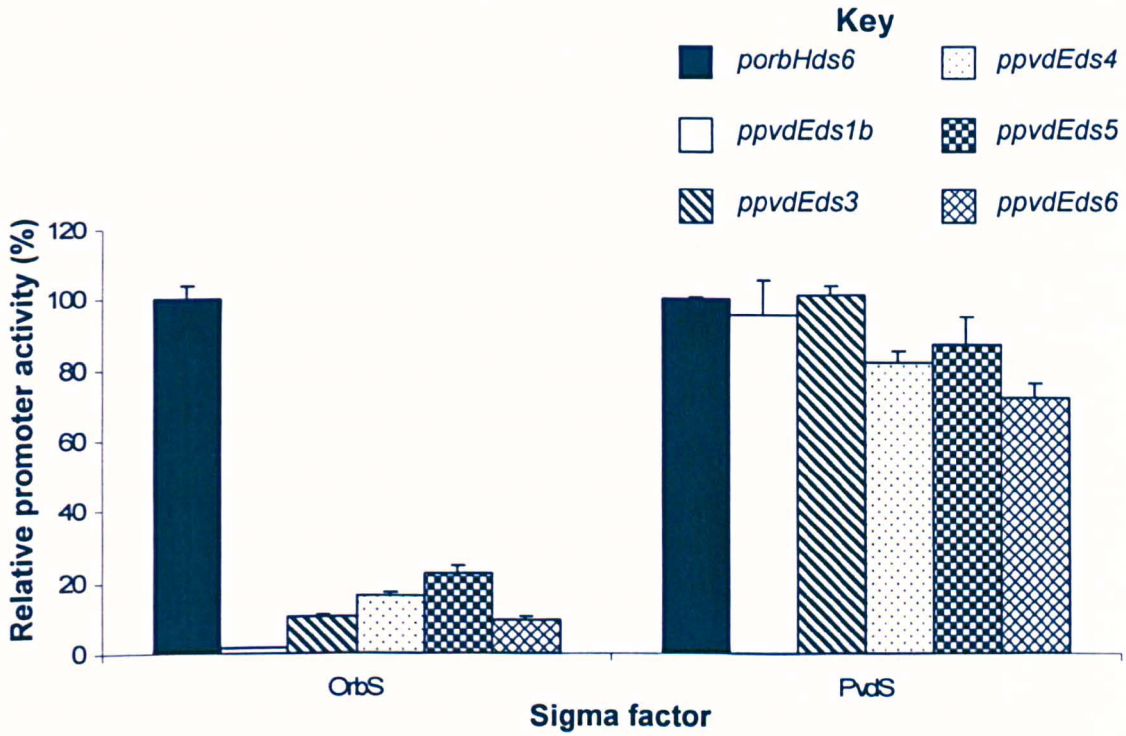

Figure 6.14: Activities of *ppvdE-porbH* hybrid promoters. *E. coli* MC1061 bearing either pBBR-2-pvdS or pBBR-2-orbS (as indicated below the graph) and pKAGd4 bearing the promoters shown in Figure 6.13 as indicated in the key was assayed for β-galactosidase activity. Assays were carried out in triplicate on cells grown in LB medium supplemented with kanamycin and chloramphenicol, under iron-limiting conditions. Activities were corrected by subtracting the background pKAGd4 activity measured in the appropriate background (i.e. MC1061 containing pKAGd4 and either pBBR-2-orbS or pBBR-2-pvdS). The activities shown are relative to the activity of *porbHds6* in response to each of the σ factors introduced (100% = 3,122 Miller units in response to OrbS, and 22,200 Miller units in response to PvdS). Error bars represent standard deviation of each set of activities determined.

approach was taken in which the *porbH* sequence was systematically changed base by base (Section 6.4.5).

6.4.5: Investigation of OrbS and PvdS promoter recognition by single base substitution analysis of the *orbH* promoter

To determine the contribution of individual base pairs to OrbS and PvdS promoter recognition, single nucleotide substitutions were introduced into the *porbHds6* sequence from positions -36 to -24 and from -14 to +6 (relative to the *orbH* TSS). The substitutions made were 'extreme' base changes, where purines were replaced with non-complementary pyrimidines, and *vice versa*. Promoter fragments were synthesised as double-stranded oligonucleotides and cloned into pKAGd4 for β-galactosidase assay in *E. coli* MC1061 as described previously (Section 6.4.1). Figure 6.15 shows the locations of the point mutations introduced, and displays the resultant activities in the presence of functional *orbS* and *pvdS*.

The results show that there are two regions where single base changes severely impair *porbH* utilisation by OrbS and PvdS (i.e. activity <20 % of the wild type promoter). For OrbS, these regions are located at -32 to -29 and -11 to -8 with respect to the *porbH* TSS, and therefore constitute the -35 and -10 elements. Interestingly, the most downstream position of each of the two motifs are not important for utilisation by PvdS. Therefore, if these results were taken in isolation, the -35 and -10 recognition sequences for OrbS would be TAAA and CGTC, respectively, and for PvdS they would be TAA and CGT, respectively. Mutations in the -35 element exerted a less profound effect than mutation at all but the most upstream position (-11) in the -10 region for both σ factors. This is due to the fact that mutation at the most upstream position of the -10 motif (position -11) was less detrimental for promoter utilisation by either σ factor than mutation of the other positions within the -10 element (i.e. substitution here resulted in ~12 % of wild type activity, while substitution of the other nucleotides in the -10 element resulted in <2 % of the wild type activity in response to either σ factor).

The PvdS-dependent promoter consensus sequence is TAAAT $(N)_{16}$ CGT (Wilson *et al.*, 2001; Ochsner *et al.*, 2002). As well as the TAA component of the -35 region, the T at the fifth position is absolutely conserved within the PvdS-dependent

Figure 6.15: Effects of single base substitutions on the activity of the *orbH* promoter. Promoter fragments based on *porbHds6* were cloned into the *lacZ*-reporter vector pKAGd4 and were then introduced into *E. coli* MC1061 containing pBBR1MCS bearing either the *orbS* or *pvdS* σ factor gene. The wild-type *orbH* promoter sequence is shown beneath each graph, and base positions are shown relative to the approximate *orbH* TSS, determined in Section 5.5 (+1 position). Single base substitutions were introduced at each position shown in bold face type, while bases not mutated singly are shown in blue (the G+C-rich spacer block). Base substitutions were as follows: purine bases were substituted for non-complementary pyrimidines and *vice versa,* that is T, C, G and A were substituted for G, A, T and C, respectively. At position -28, the complementary T base was also substituted (bar shown in yellow). The bars representing the positions where substitutions have the strongest negative effect on promoter utilisation by OrbS (and are presumed to represent the -10 and -35 regions of *porbH*) are shown in pink in both graphs. Activities have been shown as a percentage of the activity of the *orbHds6* promoter (shown in green), and were corrected by subtracting the background activity (activity of MC1061 bearing pBBR-2-orbS or pBBR-2-pvdS and pKAGd4 measured under iron limited conditions as appropriate). 100 % = 3,122 Miller units in response to OrbS, and 22,200 Miller units in response to PvdS. β-galactosidase assays were carried out on triplicate cultures grown in LB medium supplemented with chloramphenicol and kanamycin under iron limiting conditions. Error bars represent the standard deviation of the activities of these triplicate cultures.

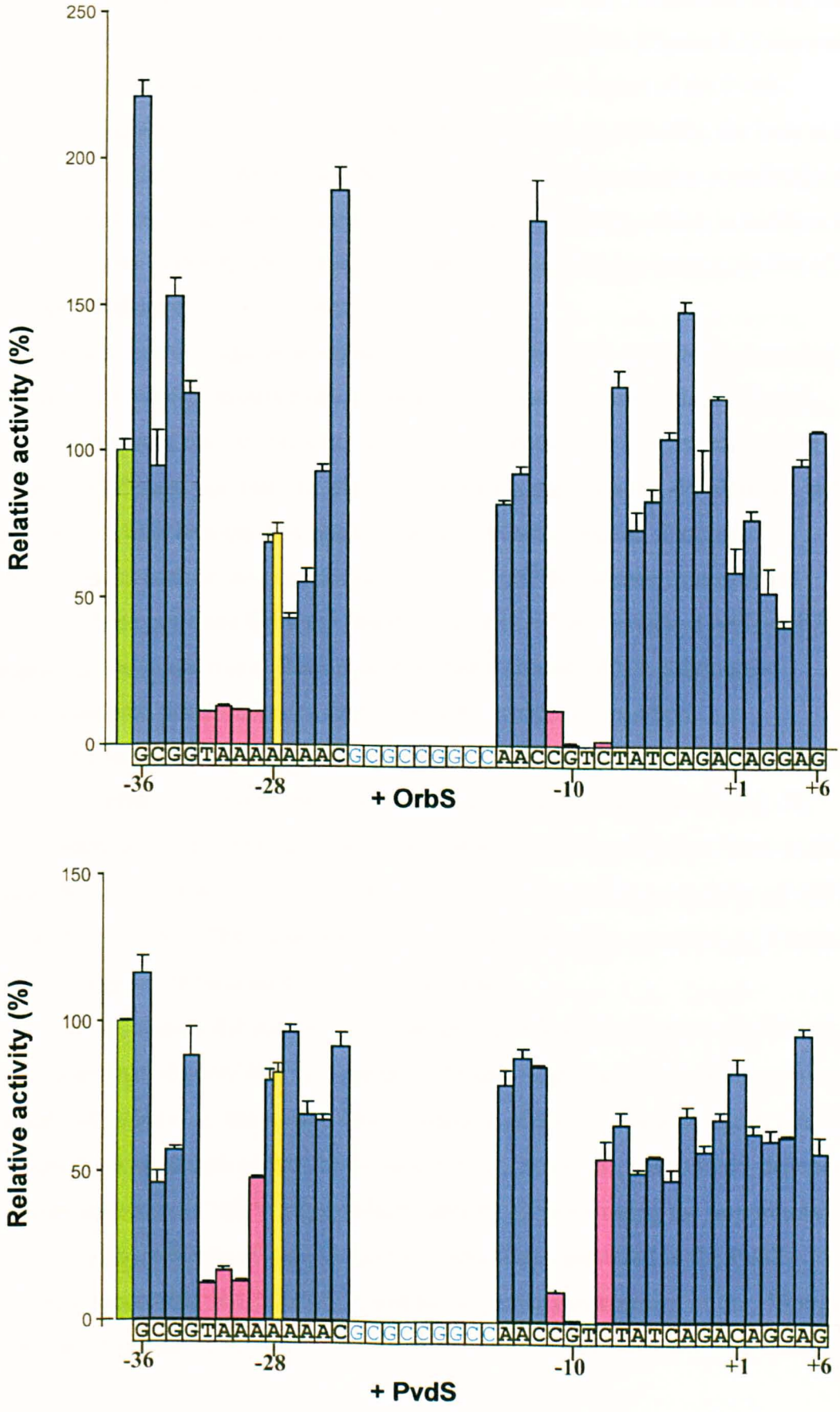

Figure 6.15. Effects of single-base substitutions on the activity of the *orbH* promoter. For legend see facing page.

promoters of the *pvd* clusters (Thomas, 2007, and Figure 6.2). Alignment of the OrbS-dependent promoters and putative MbaS-dependent promoters (Figure 6.1) showed that the base corresponding to the fifth position in the -35 region of the PvdS-dependent promoters is A, T or G. In the *orbH* promoter, specifically, the base at this position (-28 relative to the *porbH* TSS) is A. To explore the relative contributions of these bases at this position, a T residue was introduced at this position in addition to a G (the 'extreme' substitution). Both substitutions were found to exert a similar effect, and depressed *orbH* promoter activity by 25 %.

A number of single base substitutions led to an increase in OrbS-dependent activity, most notably substitutions at positions -36 and -34 within the G+C-rich region upstream of the -35 element, position -24 immediately downstream of the extended A+T tract, position -12 which immediately precedes the -10 element, and position -3, which is at the first position of the A+G-rich region. Extreme substitutions at each of these positions led to a 50-150 % increase in *porbHds6* activity. These positions flank the essential -10 and -35 elements and A+G-rich block, suggesting that mutations at these positions might enhance RNA polymerase interactions with these regions, or facilitate open complex formation.

The single substitutions outside of the -10 and -35 elements that had the most detrimental effect on OrbS-dependent activity occurred at positions -29 and -30, downstream of the -35 element (within the extended A+T tract), and at three positions within the A+G-rich block (+1, +3, +4), all of which resulted in an activity of <60 % of that of *porbHds6*. This demonstrates the importance of the extended A+T tract and A+G-rich region for promoter utilisation by OrbS.

At no position did substitution of single bases lead to activities significantly greater than that of *porbHds6* in response to PvdS. Single substitutions at positions -35 and -34 (relative to the *porbH* TSS), upstream of the -35 element, and at a number of positions downstream of the -10 element (-4, -5, -6 and -8), led to PvdS-dependent promoter activities of <60 % of *porbHds6* activity, demonstrating the importance of the G+C bases upstream of the -35 element (which are conserved in the PvdS-dependent promoters, see Figure 6.2) and the sequence downstream of the -10 region for promoter utilisation by PvdS.

6.4.6: Investigation of the role of the G+C-rich spacer block and the A+G-rich block in promoter utilisation by OrbS and PvdS

The conserved 9 bp G+C-rich spacer block (positions -23 to -15) and the 9 bp A+G-rich block (positions -3 to +6) were also analysed by introducing multiple base substitutions. The G+C-rich spacer block was examined as a whole, rather than base by base, as it seemed likely from examination of the promoter alignment that the specific conformation induced by the G+C richness of this block, rather than its specific sequence, might be important for utilisation by OrbS. Two promoter variants were tested, one in which extreme substitutions of all 9 G+C bp of *porbH* were made, and one in which extreme substitutions were introduced at every alternate base. The latter construct was made in case the extensive A+T-rich sequence resulting from substitution of the entire block exerted a detrimental effect on promoter activity through a change in DNA conformation (Table 6.1). The importance of the 9 bp A+G-rich block was examined as a whole owing to the low activity of *porbHds1*, which lacks this region, compared to the activities of *porbHds6* derivatives containing single base substitutions in this region. The least active of these promoters possessed 40 % of *porbHds6* activity. Therefore, the effect of making extreme substitutions of this entire block was examined to determine if the cumulative effect of these substitutions gave rise to a similar level of activity to that of *porbHds1*.

Nucleotide substitution of the entire 9 bp G+C-rich spacer block in the *orbH* promoter (*porbHds40*) gave rise to a 27 % and a 39 % drop in activity relative to *porbHds6* in response to OrbS and PvdS, respectively (Table 6.1). Substitution of every alternate base (i.e. 4 of the 9 bases) (*porbHds41*), had no effect on activity in response to OrbS, but led to a 35 % drop in activity in response to PvdS, relative to *porbHds6* (Table 6.1). This showed that this region is of some limited importance, but did not shed light on the reasons for OrbS being unable to recognise PvdS-dependent promoters.

Nucleotide substitution of the entire A+G-rich block located downstream of the -10 element (*porbHds17*) resulted in a large decrease in promoter activity in *E. coli* in the presence of either σ factor (i.e. activities for either σ factor were equivalent to 1.3% and 0.7% of *porbHds6* activity when *orbS* and *pvdS* were introduced, respectively) (Figures 6.16 and 6.17). However, results from the single base

Table 6.1: Activity of *porbH* promoter derivatives bearing substitutions in the G+C-rich spacer block.

Promoter derivative	Promoter sequence[a]	Activity (%)[b]	
		+ OrbS	+ PvdS
porbHds6	gcggtaaaaaaacGCGCCGGCCaaccgtctatcagacagga	100	100
porbHds40	gcggtaaaaaaacTATAATTAAaaccgtctatcagacagga	73	61
porbHds41	gcggtaaaaaaacGAGACTGACaaccgtctatcagacagga	102	65

[a]G+C-rich spacer block sequences have been emboldened and shown in upper case, with *porbHds6* sequence as a reference. Base substitutions have been highlighted in green. The -10 and -35 motifs determined in Section 6.4.5 are underlined.
[b]Activities are shown relative to that specified by *porbHds6* (100 % = 3,122 Miller units in response to OrbS, and 22,200 Miller units in response to PvdS). Assays were performed on triplicate cultures of MC1061, containing the indicated pKAGd4 derivatives in combination with pBBR-2-orbS or pBBR-2-pvdS grown in LB broth supplemented with chloramphenicol and kanamycin. Standard deviation for each set of three cultures was ≤ 5 % of mean value. Activities were corrected by subtraction of the background activity of MC1061 bearing pBBR-2-orbS or pBBR-2-pvdS and pKAGd4 measured under iron limited conditions.

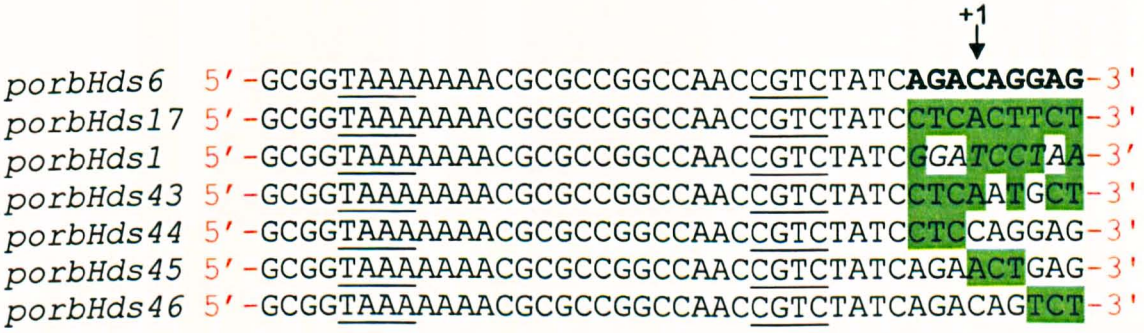

Figure 6.16: Sequences of *orbH* promoter derivatives altered in the A+G-rich block. The non-template strand of *porbHds6* and mutant derivatives altered in the downstream A+G-rich block are shown. The A+G-rich block in the *porbHds6* sequence is emboldened. The *porbHds1* sequence shown has been extended into pKAGd4 at the 3' end (the extended sequence has been italicized). The -35 and -10 regions determined in Section 6.4.5 are underlined, and the approximate location of the TSS (+1) is indicated. Base pair changes in the A+G-rich block are highlighted in green.

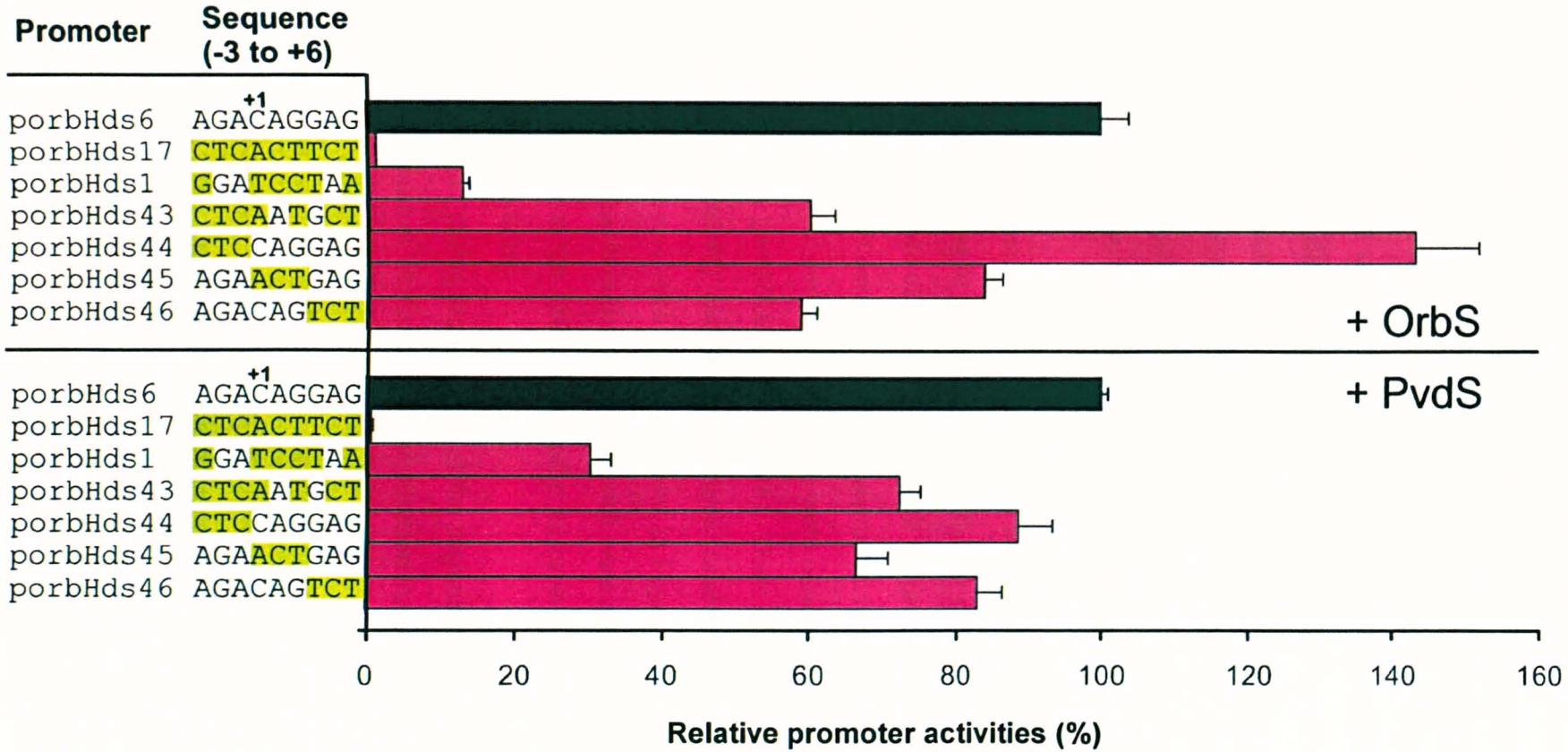

Figure 6.17: Activities of *orbH* promoter derivatives with substitutions within the A+G-rich block. Promoter derivatives of *porbHds6* were cloned into the *lacZ*-reporter vector pKAGd4 and introduced into *E. coli* MC1061 containing pBBR1MCS bearing either the *orbS* or *pvdS* σ factor gene. The sequence of the A+G-rich block is shown to the left of the appropriate bar. *porbHds6* has been included as a reference. Bases blocked in green differ from the *porbHds6* sequence. β-galactosidase assays were carried out on triplicate cultures grown in LB medium supplemented with chloramphenicol and kanamycin under iron limiting conditions. Activities are shown as a percentage of *porbHds6* (100 % = 3,122 Miller units in response to OrbS, and 22,200 Miller units in response to PvdS), and were corrected by subtracting the background activity (activity of MC1061 bearing pBBR-2-orbS or pBBR-2-pvdS and pKAGd4 measured under iron limited conditions). Error bars represent the standard deviation from the mean activity of each set of three cultures.

substitutions in this region (Section 6.4.5) suggest that while this block is essential for the binding of both σ factors, no single position is crucial for promoter activity. The deleted promoter variant *porbHds1* exhibited ~10 fold greater OrbS-dependent activity than *porbHds17*. Both of these promoter derivatives are lacking the A+G-rich block. However, the sequence of pKAGd4 that is adjacent to the downstream endpoint of *porbHds1* contains identical bases to the native *porbHds6* sequence at some positions (Figure 6.16). These identical bases are probably responsible for the large difference in activity between *porbHds1* and *porbHds17*. However, it must be noted that in both *B. cenocepacia* and *P. aeruginosa*, *porbHds1* activity was much lower than in *E. coli*, and therefore the activity of *porbHds1* and *porbHds17* might have been comparable in these backgrounds (see Figures 6.10 and 6.11).

The downstream A+G-rich region is 9 nucleotides in length in *porbH*, but is only 6 nucleotides long in *ppvdE* (see Figure 6.1 for comparison). In order to further examine the importance of the A+G-rich block for promoter utilisation by OrbS and PvdS, four new *porbH* derivatives were constructed in which the A+G-rich sequence was altered at multiple positions, and these were introduced into pKAGd4 for β-galactosidase assay (*porbHds43-porbHds46*). Three of the promoter derivatives (*porbHds44-porbHds46*), each contained three consecutive 'extreme' base pair substitutions in the A+G-rich block, as shown in Figure 6.16. In the fourth derivative (*porbHds43*), two bases in the A+G-rich block were retained as in wild type *porbH* (+2 and +4 relative to the TSS), but all other bases in the block were substituted as in *porbHds17* (Figure 6.16).

Figure 6.17 shows the activities of the promoters containing A+G-rich block substitutions. None of the three triple substitution mutants (*porbHds44-porbH46*) exerted a strong negative effect on promoter activity, with decreases of 15-40 % for OrbS-dependent activity and 10-35 % for PvdS-dependent activity.

As discussed above, the alteration of single bases of the A+G-rich region had little effect on OrbS and PvdS-dependent promoter activity (Figure 6.15), whereas the alteration of the entire block led to activities of 0.7 % and 1.3 % of *porbHds6* activity in response to PvdS and OrbS, respectively. However, the promoter derivative with only positions 5 and 7 of the A+G-rich block (positions +2 and +4 relative to the TSS)

identical to wild type (i.e. *porbHds43*) had an activity of 60 % of that of *porbHds6* in response to OrbS and 72 % in response to PvdS (Figure 6.17).

To conclude, it would appear that promoter utilisation by both OrbS and PvdS is equally affected by changes in the A+G-rich block. While this region is clearly important for utilisation by these σ factors, any negative effects on activity only occur with substantial changes in this region.

6.4.7: Investigation of the role of the extended A+T tract in promoter utilisation by OrbS and PvdS

The results described above did not identify any DNA sequence feature unique to *porbH* that would explain the failure of OrbS to recognise the *pvdE* promoter. Apart from the C at the fourth position within the -10 region, and to some degree the A at position 4 of the -35 region, no single bases appeared to discriminate between the ability of OrbS to utilise OrbS- and PvdS-dependent promoters (see Figure 6.15). As these bases are retained at both positions in *ppvdE*, some other aspect of the promoter architecture was clearly important for OrbS-dependent activity. However the bases outside of the -10 and -35 elements of *porbH* that appeared to be most important in the single-base substitution screen (leading to activities of ~50% when mutated), were found to be either the same in *porbH* and *ppvdE*, or to differ in other OrbS-dependent promoters, such as the A at position -27, which gave rise to <50 % activity in response to OrbS when substituted, but is present not only in all three OrbS-dependent promoters, but also *ppvdE*.

These observations seemed to suggest that subtle conformational changes between *ppvdE* and *porbH*, rather than the actual nucleotide sequence, might be influencing promoter binding or utilisation by OrbS. A recent study by Lane and Darst (2006) investigated ECF σ factor-dependent -35 regions, and identified a highly conserved 'AA' dinucleotide followed by a number of A/T bases within these regions (the corresponding AA motif occurs at positions -31 and -30 of *porbH*). This 'AA' motif does not directly interact with RNAP, but rather induces a specific localised DNA conformation necessary for ECF σ-factor binding.

In this light, a series of promoter derivatives were constructed to test whether the shorter A+T tract of *ppvdE* was responsible for preventing OrbS recognition.

Three of the new promoters (*porbHds49-porbHds51*) were based upon *porbH*. Derivative *porbHds49*, which contained a dinucleotide substitution at positions -29 and -28 relative to the TSS, was designed to test for conformation-specific activity of PvdS (mutation at either position alone does not cause strong down effects on promoter activity in response to PvdS, despite the conservation of these bases amongst PvdS-dependent promoters). Since one of the bases substituted in this promoter mutant (position -29) has been shown to be essential for OrbS-dependent activity, this promoter was expected to have low activity in response to OrbS. Promoter mutants *porbHds50* and *porbHds51* were designed to test whether bases in the extended A+T tract that had been found to be unimportant for OrbS recognition when mutated singly would abolish activity when mutated in pairs. A further promoter derivative (*ppvdEds7*) was designed in which the A+T tract of *ppvdE* was replaced with the 7 base poly A tract of *porbH*, to determine whether this would lead to increased OrbS-dependent activity. This promoter derivative would also be comparable to *ppvdEds3*, in which the residues at positions -27 to -12 (numbering with respect to *porbH*) were exchanged for their *porbH* counterparts, resulting in an AAATAAA tract at -31 to -25 (in which the T should not change the conformation, according to Mack and colleagues (Mack *et al.*, 2001)) (see Figure 6.18).

The activity of each of the *porbH* promoter fragments is shown in Figure 6.19. As expected, *porbHds49* (which had substitutions at positions -29 and -28) had only low activity in response to OrbS (approximately the same level as when the -29 base alone was mutated). The activity of this promoter in response to PvdS was also greatly reduced, corresponding to ~28 % of the wild type (*porbHds6*) level. Note that, although the -35 region of PvdS-dependent promoters is considered to have the consensus sequence TAAAT (Wilson *et al.*, 2001; Ochsner *et al.*, 2002), mutation of the T residue at position 5 of the -35 alone (i.e. position -28 relative to the *orbH* TSS) has no effect on promoter utilisation, and mutation of the A residue at position 4 alone (i.e. position -29 relative to the *orbH* TSS) results in a 50 % decrease in promoter activity in response to PvdS (Figure 6.15). This A residue is the only base in the TAAAT motif that is not absolutely conserved in the PvdS-dependent promoters present in the *pvd* clusters, being replaced by a T residue in three cases (Thomas, 2007). The fact that mutation at both positions in combination has a more profound effect than single base substitutions demonstrates the selective pressure maintaining

```
ppvdEds1b 5′-CCGCTAAATACCGGGCATCCTGCTTCGTCTGTCTGCAAGGAG-3′
ppvdEds7  5′-CCGCTAAAAAAAGGGCATCCTGCTTCGTCTGTCTGCAAGGAG-3′
ppvdEds3  5′-CCGCTAAATAAACGCGCCGGCCAACCGTCTGTCTGCAAGGAG-3′
                    -31                          +1
porbHds6  5′-GCGGTAAAAAAAACGCGCCGGCCAACCGTCTATCAGACAGGAG-3′
porbHds49 5′-GCGGTAACCAAACGCGCCGGCCAACCGTCTATCAGACAGGAG-3′
porbHds50 5′-GCGGTAAAAACCCGCGCCGGCCAACCGTCTATCAGACAGGAG-3′
porbHds51 5′-GCGGTAAACCAACGCGCCGGCCAACCGTCTATCAGACAGGAG-3′
```

Figure 6.18: Promoter derivatives constructed to test the importance of the length of the -35 region extended A+T tract. *ppvdEds1* (WT *ppvdE*), *porbHds6* (WT *porbH*), and *ppvdEds3* sequences have been shown for reference purposes. Bases differing from those of the WT promoter (*ppvdE* for *ppvdEds7* and *ppvdEds3*, *porbH* for *porbHds49-porbHds51*) have been highlighted in green. The entire A+T tracts (-35 element + extended A+T tract) of *ppvdE* and *porbH* have been underlined and emboldened in *ppvdEds1b* and *porbHds6*, respectively. The -35 and -10 elements for utilisation by OrbS as determined by mutagenesis are shown in red. The approximate TSS (+1) of *porbH*, determined by primer extension, is indicated, as is position -31 relative to this TSS.

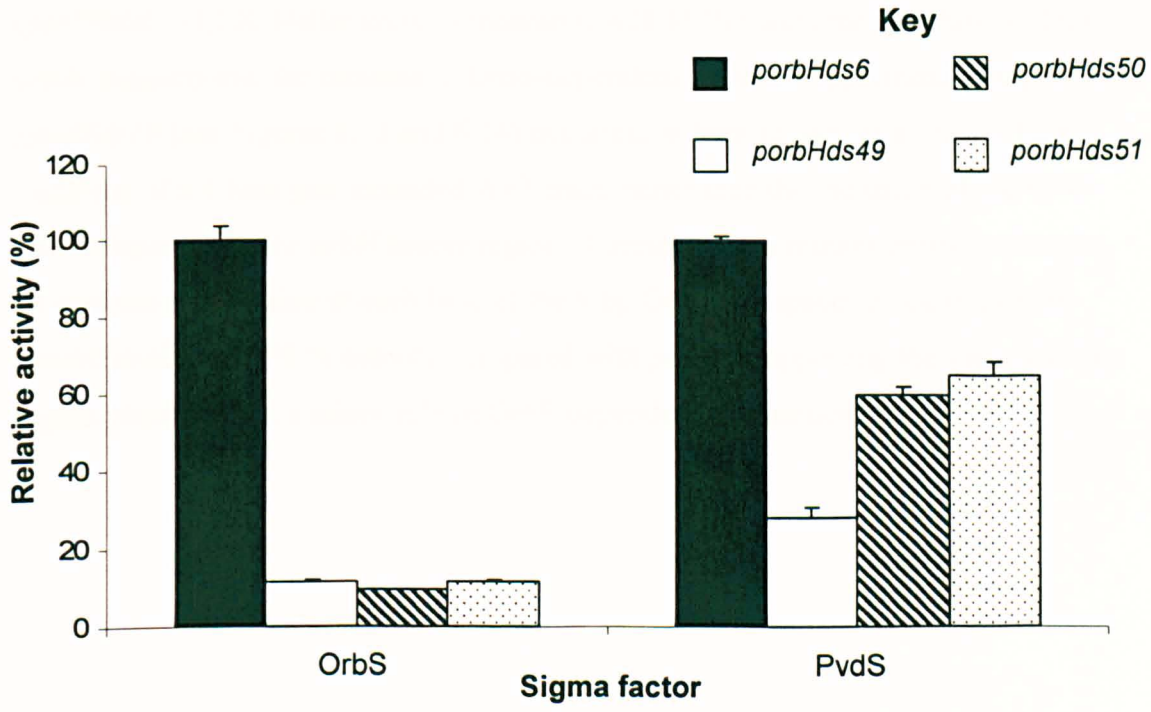

Figure 6.19: Activities of *orbH* promoter derivatives with substitutions within the extended A+T-tract. Promoter derivatives of *porbHds6* were cloned into the *lacZ*-reporter vector pKAGd4 and introduced into *E. coli* MC1061 containing pBBR1MCS bearing either the *orbS* or *pvdS* σ factor gene (indicated below graph). β-galactosidase assays were carried out on triplicate cultures grown in LB medium supplemented with chloramphenicol and kanamycin under iron limiting conditions. Activities are shown as a percentage of *porbHds6* (100 % = 3,122 Miller units in response to OrbS, and 22,200 Miller units in response to PvdS). Values were corrected by subtracting background activity (activity of MC1061 bearing either pBBR-2-orbS or pBBR-2-pvdS and pKAGd4 measured under iron limited conditions). Error bars represent the standard deviation from the mean activity of each set of three cultures.

this conservation. This is also consistent with the hypothesis that the 6 consecutive A+T bases in *ppvdE* induce a specific DNA conformation at this region.

Promoters *porbHds50* (which is analogous to *ppvdEds1b* with respect to the length of its A+T tract) and *porbHds51* had similar low activity levels in response to OrbS, even though substitutions were not in the tetranucleotide -35 element. This clearly demonstrates the importance of the extended A+T tract for OrbS recognition. In contrast, the activity of these promoters in response to PvdS was ~60 % of the wild type level, demonstrating that while the extended A+T tract might enhance the ability of PvdS to recognise *porbH*, it is not essential.

Finally, the substitution of the extended A+T tract of *porbH* for the corresponding region of *ppvdE*, to give *ppvdEds7*, led to an ~9 fold increase in OrbS-dependent activity of *ppvdE* (compare *ppvdEds7* with *ppvdEds1b*) (Table 6.2). However, the activity was still much lower than that of the wild type *orbH* promoter (*porbHds6*, ~3,100 Miller units, compared to 428 Miller units for *ppvdEds7*). This result suggests that the increase in OrbS-dependent activity of *ppvdEds3* compared to *ppvdEds1b* (see Figures 6.13 and 6.14) occurred, at least in part, as a result of the inclusion of a 4 base pair extended A+T tract, rather than the inclusion of the G+C-rich component of the *orbH* spacer region. Furthermore, a mutant promoter bearing an extreme substitution at each base of the 9 bp G+C-rich spacer block of *porbH* (*porbHds40*) had >70 % activity compared with *porbH*, supporting the view that this region plays at most a minor role in OrbS-dependent recognition.

Table 6.2: Activity of *pvdE* promoter derivatives bearing substitutions in the extended A+T tract region.

Promoter derivative[a]	Activity (%)[b]	
	+ OrbS	+ PvdS
ppvdEds1b	1.5	95.7
ppvdEds7	13.7	64.7
ppvdEds3	10.5	101.2

[a]Promoter derivatives of *ppvdEds1b* were cloned into the *lacZ*-reporter vector pKAGd4 and introduced into *E. coli* MC1061 containing pBBR1MCS bearing either the *orbS* or *pvdS* σ factor gene (indicated). β-galactosidase assays were carried out on triplicate cultures grown in LB medium supplemented with chloramphenicol and kanamycin under iron-limiting conditions.

[b]Activities are shown as a percentage of that specified by *porbHds6* (100 % = 3,122 Miller units in response to OrbS, and 22,200 Miller units in response to PvdS). Values were corrected by subtraction of the background activity (activity of MC1061 bearing either pBBR-2-orbS or pBBR-2-pvdS and pKAGd4 measured under iron limited conditions). Standard deviation for each set of three cultures was ≤ 5 % of mean value.

6.5: Bioinformatic analysis of the OrbS regulon

The PvdS σ factor of *P. aeruginosa* is responsible for the transcription of a large number of genes in response to iron limitation, which constitutes a signal that the bacterium has entered a host organism. These genes comprise not only those specifying pyoverdine utilisation and biosynthesis (the *pvd* genes), but also a number of virulence factors, such as an endoprotease, PrpL, and (indirectly) exotoxin A.

Just as PvdS controls transcription of a range of *P. aeruginosa* virulence factors, OrbS could fulfil this function in *B. cenocepacia*. Therefore, an *in silico* analysis was carried out using the Fuzznuc program (http://anabench.bcm.umontreal.ca/anabench/AnabenchJsp/Applications/fuzznuc.jsp?APPLICATIONID=81&APPLICATIONNAME=fuzznuc), in which the *B. cenocepacia* J2315 genome was searched for the experimentally determined functional OrbS-dependent promoter sequence.

The J2315 genome, which has a total size of 8.056 Mb and consists of three chromosomes (3.870 Mb, 3.217 Mb and 0.876 Mb in size) and a plasmid (pBCA, 92.7 kb), was searched for the sequence TAAA $(A/T)_4 (N)_{13}$ CGTC, with 1 mismatch allowed. This search resulted in 76 hits, 51 on chromosome 1, 23 on chromosome 2 and 2 on chromosome 3. No matching sequences were found within the *B. cenocepacia* J2315 megaplasmid. All hits in which the mismatch allowed in the search occurred within the essential four base pairs of the -10 and -35 elements were discounted, leaving just 10 hits. Three of these were the *orbH*, *orbE* and *orbI* promoters, as expected. Figure 6.20 shows an alignment of the remaining seven candidate OrbS-dependent promoters (CODPs). From this alignment, the CODPs that appeared to be most likely to act as such were CODP 1, 3 and 7. These three promoters all had A+G-rich sequences at the region corresponding to the A+G-rich block. CODPs 3 and 7 have identical sequences, and lack the most downstream A or T of the extended A+T-tract of the known OrbS-dependent promoters. All 7 CODPs could potentially be utilised by OrbS, as they contain the necessary sequence elements.

The possible function of the putative coding sequences located around each candidate promoter was identified where possible. For each CODP, the nucleotide sequence of each downstream gene in the correct orientation was analysed using BLASTN. The gene immediately upstream of the promoter was also analysed in this

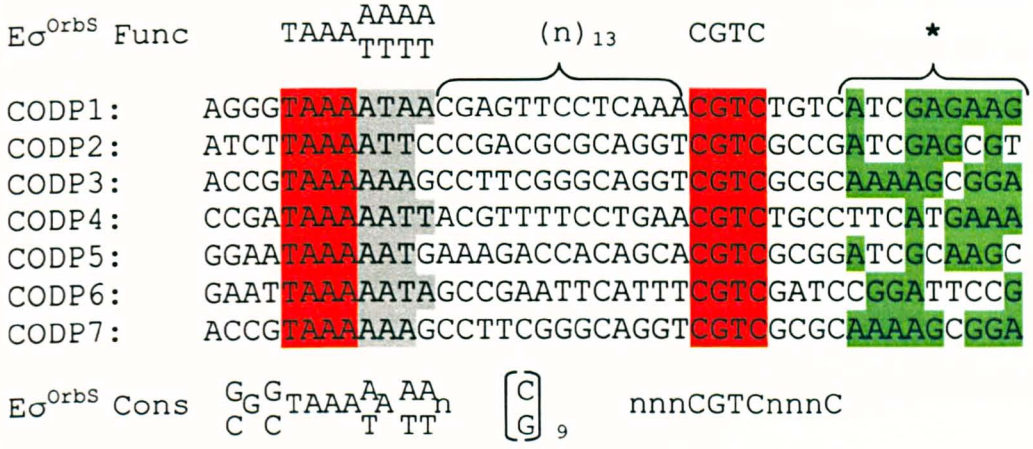

Figure 6.20: Alignment of the candidate promoters of the OrbS regulon. The candidate promoters have been numbered and are located on the following chromosomes: CODP1-4, chromosome 1; CODP5, chromosome 2; CODP6 and CODP7, chromosome 3. The consensus OrbS-dependent promoter sequence has been shown below the alignment ($E\sigma^{OrbS}$ Cons). The experimentally determined functional requirements for promoter utilisation have been shown above the alignment ($E\sigma^{OrbS}$ Func). One mismatch within the extended A+T tract was found to be permissible. A+T bases within the extended A+T tract have been highlighted in grey. The asterisk indicates the A+G rich region. A+G bases within this region have been highlighted in green. The absolutely conserved bases constituting the -35 and -10 elements have been highlighted in red. The OrbS-dependent promoters of the ornibactin cluster have been omitted.

way, as was the first downstream gene in the opposite orientation to the promoter. Figures 6.21 and 6.22 represent the genetic loci examined. Four of the CODPs (CODP1, CODP4, CODP5, and CODP6) are located in intergenic regions, while the remaining three are located within genes (although CODP3 and CODP7 are at the 3' end of the gene). In each case, the gene downstream of the CODP was in the same orientation as that candidate promoter, and so could potentially be transcribed from it.

CODP1, which from the alignment (Figure 6.20) appeared to be the best match for an OrbS-dependent promoter amongst the candidates (having a full 4 bp extended A+T tract, and 7 A+G bases within the 9 bp A+G-rich block), is located upstream of a putative ferredoxin NADP reductase (FNR) gene (BCAL0536). Ferredoxin NADP reductases are iron-sulphur cluster proteins involved in electron transfer (Carrillo and Ceccarelli, 2003). There is a 416 bp intergenic region between BCAL0536 and BCAL0535, which could contain a promoter for the downstream genes BCAL0535-BCAL0532.

CODP 2 is located 276 bp upstream of the putative BCAL2506 stop codon. No putative functions could be assigned to the downstream genes. It should be noted that homologues of these genes are absent from the sequenced *B. cenocepacia* strains AU1054 and HI2424. CODP2 is less likely to be a promoter than the other CODPs, owing to its intragenic location.

CODP3 and CODP7 are identical, and are located between integrase and transposase genes within identical insertion sequence (IS) elements. These insertion elements are absent from the corresponding loci in *B. cenocepacia* strains AU1054 and HI2424, in which the homologues of the genes flanking the IS elements (i.e. BCAL2754 and BCAL2757, and BCAM1928 and BCAM1931) are adjacent. If CODPs 3 and 7 prove to function as promoters, they would only specify transcription of the downstream integrase gene, and not of any potential virulence factors, as in each case the following downstream gene is in the opposite orientation to the CODP.

CODP4 is positioned upstream of a number of genes specifying the production of a urease. Ureases are involved in the hydrolysis of urea to yield ammonia and carbamic acid (which undergoes spontaneous hydrolysis to form carbonic acid and a second ammonia molecule). They are associated with virulence in some bacteria, contributing to the formation of kidney stones and stomach ulcers, and are also common amongst soil bacteria (such as the Bcc), as they enable the acquisition of nitrogen (Mobley and Hausinger, 1989). The urease is made up of α, β and γ subunits,

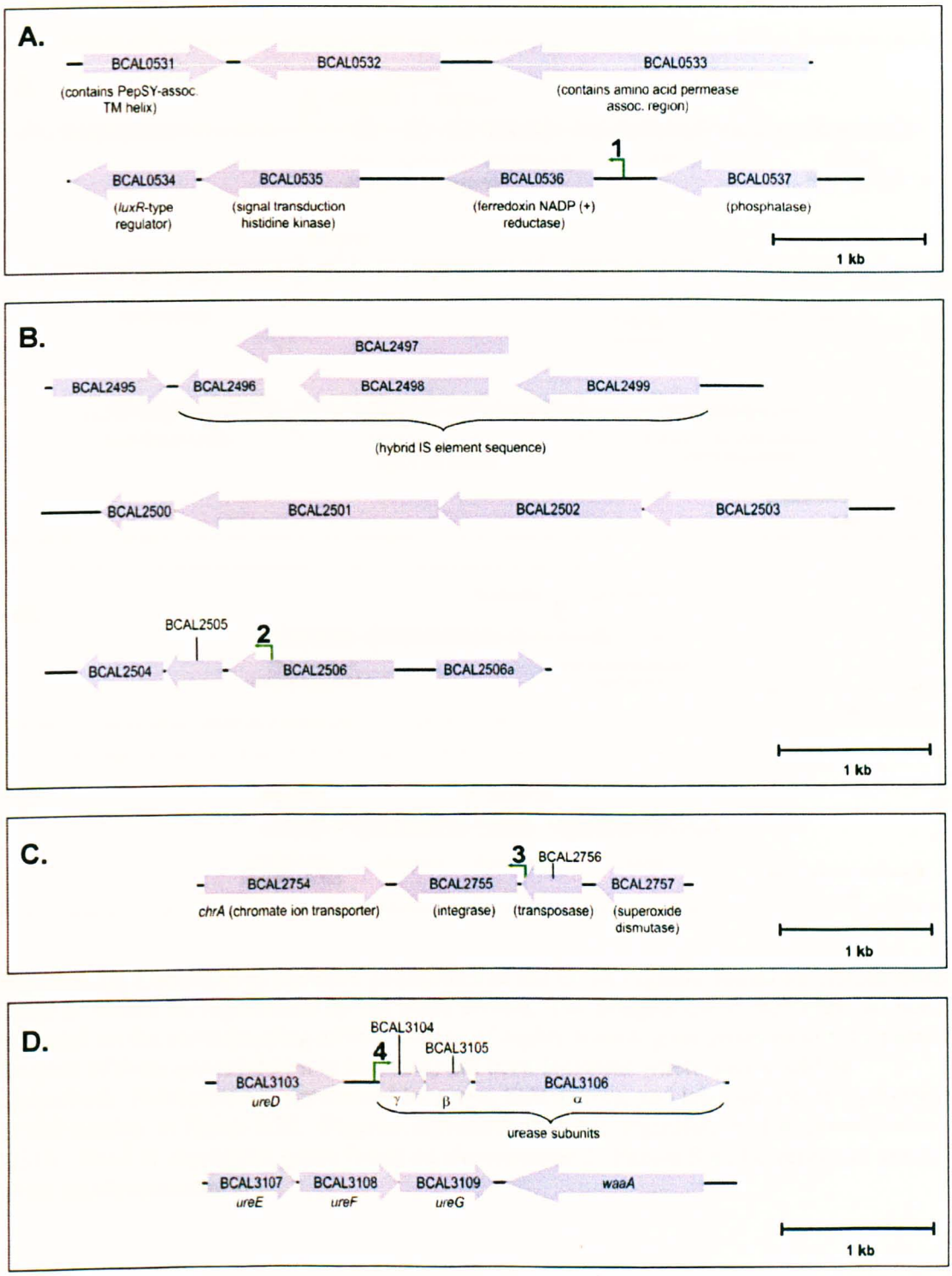

Figure 6.21: Localities of putative promoters of the OrbS regulon found on chromosome 1. Genes are represented by red block arrows. The designation of each gene has been indicated on the corresponding arrow. Names of highly homologous genes and/or the putative function of these genes (shown in brackets) have been indicated where such could be determined. Promoters are represented by green, bent arrows, labelled according to their CODP number in Figure 6.20. Diagram represents the gene organisation of *B. cenocepacia* J2315.

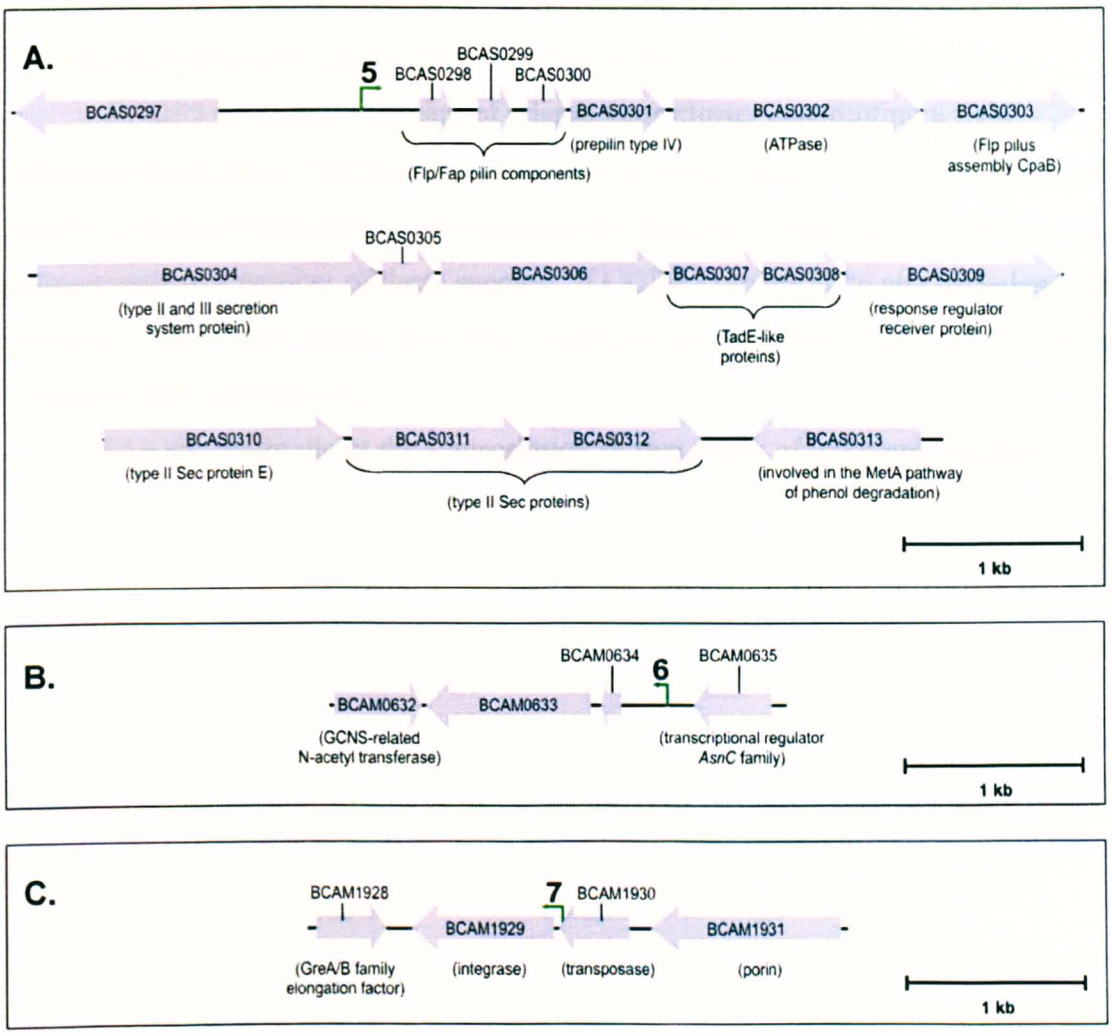

Figure 6.22: Localities of putative promoters of the OrbS regulon found on chromosomes 2 and 3. Genes are represented by red block arrows. The designation of each gene has been indicated on the corresponding arrow. Names of highly homologous genes and/or the putative function of these genes (shown in brackets) has been indicated where such could be determined. Promoters are represented by green, bent arrows, and labelled according to their CODP number in Figure 6.20. Diagram represents the gene organisation of *B. cenocepacia* J2315. Panel A. represents genes found on chromosome 2. Panels B and C represent genes found on chromosome 3.

and a nickel metallocentre is inserted by three to four accessory proteins (in this case it would appear four, *ureD, ureE, ureF, ureG*) (Koper *et al.*, 2004). If CODP4 is indeed a promoter, it does not specify the production of the UreD accessory protein.

CODP5 is located upstream of a large gene cluster constituting a tight adherence (*tad*) locus. Similar loci are present in a multitude of pathogenic bacterial species, and have been shown to be essential for biofilm formation, colonisation and pathogenesis in a number of these species. If CODP5 proves to be an OrbS-dependent promoter, this would indicate that OrbS could play an additional important role in the virulence of *B. cenocepacia.*

CODP6 might direct the transcription of two genes of unknown function.

6.6: Discussion

Determination of the activity of two *P. aeruginosa* PvdS-dependent promoters, *ppvdE* and *ppvdF*, in *B. cenocepacia* using a *lacZ*-fusion vector, showed that OrbS cannot efficiently utilise these sequences. The *pvdE* promoter, which has identical -35 and -10 motifs to the OrbS-dependent promoter consensus (see Figure 6.1), gave rise to a very low level of β-galactosidase activity, whereas the *pvdF* promoter, which differed at the fourth position of the -10 element from this consensus, was effectively inactive. However, the activity of *porbH* in *P. aeruginosa* PAO1 was similar to that of the native *pvdE* and *pvdF* promoters, and was subject to iron-dependent regulation.

Introduction of the *orbH* promoter into an *orbS* null mutant strain of *B. cenocepacia* supplemented with plasmid-borne *pvdS* confirmed that PvdS can recognise this promoter, and also demonstrated that PvdS can assemble with *B. cenocepacia* core RNA polymerase. This was in apparent contrast to the results of a previous experiment, in which a PvdS expression vector, pBBR-pvdS, was found to be incapable of restoring ornibactin production to the *B. cenocepacia orbS* null mutant OM3, despite this vector being capable of restoring pyoverdine production to a *P. aeruginosa pvdS* null mutant (Agnoli, 2003). The reason for this lack of complementation is not apparent, given that PvdS was shown above to be capable of forming a complex with core RNA polymerase and of utilising the *orbH* promoter. However, it is possible that PvdS cannot utilise the *orbE* and/or *orbI* promoters efficiently, although the sequences of these promoters appear to conform to the requirements for utilisation by PvdS. Another possibility is that the observed lack of complementation was due to less efficient transcription of *pvdS* from pBBR-pvdS in comparison to pBBR-2-pvdS, which was used in the promoter dissection experiments within this chapter.

The *orbH* promoter was inactive in a *pvdS* null mutant of *P. aeruginosa,* but was activated when plasmid-borne *orbS* was introduced into this strain, suggesting that OrbS can assemble with *P. aeruginosa* core RNA polymerase. However, consistent with the previous experiment, OrbS did not recognise the *pvdE* promoter in *P. aeruginosa*. Nevertheless, the fact that functional *pvdS* restores the activity of *porbH* to OrbS-negative *B. cenocepacia* supports the classification of OrbS as a σ factor.

The shortest downstream deletion derivative of the *orbH* promoter tested and found to be efficiently utilised by OrbS (and also PvdS) in an *E. coli* model was *porbHds6*, which has a downstream endpoint of +6 relative to the approximate *orbH* TSS determined by primer extension. This promoter contained the entire downstream A+G-rich block, and was fully active in *B. cenocepacia* and *P. aeruginosa*.

The promoters recognised by different ECF σ-factors have well conserved -35 regions, and spacing (but not sequence) between the -35 and -10 regions (Enz *et al.*, 2003, Lonetto *et al.*, 1994). The -35 regions of these promoters tend to contain an AAC motif (not present in the putative -35 elements of the OrbS- and PvdS-dependent promoters), with an optimal spacer length of 17 bp between the -10 and -35 elements (Helmann, 2002). However, the -10 regions of ECF σ-factor promoters are less well conserved, being specific for a particular σ factor. This is reflected in the greater amino acid sequence conservation of region 4.2 (the region responsible for -35 recognition) than of region 2.4 (the region responsible for -10 recognition) in these σ factors (Helmann, 2002). This suggests that the -10 region of ECF σ factor promoters act as discriminators for the binding of specific σ factors. Since the *pvdE* promoter appears to have the OrbS-dependent promoter consensus sequence, and yet is not recognised by OrbS, it was clear that further elements within the promoter must be crucial for utilisation by OrbS.

The -35 and -10 regions required for promoter utilisation by OrbS were each found to consist of 4 nucleotides (TAAA and CGTC respectively), while the -35 and -10 elements for promoter utilisation by PvdS were each shown to consist of only the first 3 positions necessary for OrbS-dependent utilisation. Mutation of single bases within the -35 region dramatically reduced, but did not completely abolish, promoter activity (to ~10 % of the wild type level), as has previously been observed with promoters recognised by other ECF σ factors (Leoni *et al.*, 2000; Enz *et al.*, 2003). The higher conservation of -35 regions amongst different ECF σ factor-dependent promoters than -10 regions, suggests that region 4.2 of the σ factor is more loosely bound to the -35 region, and that -10 regions are more important for σ specificity. It is likely that substitutions in the -35 regions did not abolish promoter activity owing to this looser binding. Substitution of the base at position 1 of the -10 region reduced promoter activity to ~10 % in response to either σ factor, whereas substitution of any of the other bases within the -10 region abolished activity. Thus it is unsurprising that the *P. aeruginosa pvdF* promoter was inactive in *B. cenocepacia*, given that this

promoter carries a different base to the OrbS-dependent promoters at position 4 of its -10 element.

The extended A+T tract of *porbH* was shown to be essential for fully efficient OrbS-dependent recognition. Poly A tract DNA has a rigid, straight geometry, with a narrow minor groove, and a high degree of propeller twist (where the two bases of a pair are twisted relative to one-another). Single T bases within an A tract also lead to straight DNA, because roll compression (where neighbouring base pairs are folded one on top of the other) is blocked by physical clashes between the methyl group of the thymine and the sugar/phosphate backbone. This induces a high degree of propeller twist (Mack *et al.*, 2001). The *B. cenocepacia* OrbS-dependent promoters have an 8 base pair A+T tract (-32 to -25), as do the *B. pseudomallei* MbaS-dependent promoters (apart from *pmbaE*, where this tract is interrupted by a single G). The PvdS-dependent *pvdE* and *pvdF* promoters have shorter A+T tracts of 6 A+T bases (*ppvdH* has a 5 bp A+T tract, while the A+T tracts of the *pvdA, pvdM, pvdP, pvdI* and *pvdY* promoters are 6-8 bp in length). It would be interesting to test the OrbS-dependence of the *pvdM* promoter, which has an 8 bp A+T tract and a C residue at position 4 of the -10 region.

It was previously observed that mutation of single bases within the -35 region of the *rpoEp3* promoter of *Salmonella enterica* serovar Typhimurium, which is utilised by *E. coli* σ^E, did not abolish promoter activity, except at the two conserved A bases at positions 2 and 3 of the -35 element (Miticka *et al.*, 2004). Darst and Lane speculate that the mutation might be compensated for by interactions between RNA polymerase and the remainder of the -35 element (Darst and Lane, 2006). This could explain why single substitutions within the extended A+T tract of *porbH* do not greatly affect OrbS-dependent activity.

The substitution of the full length A+T tract of *porbH* for the corresponding *pvdE* promoter sequence resulted in a 9 fold increase in OrbS-dependent activity compared to *ppvdE*. Furthermore, the upstream G+C-rich block of *porbHds6* (-36 to -33) and the region downstream of the -10 element, which includes the A+G-rich block (-5 to +6), were both found to contribute to promoter utilisation by OrbS, as substitution of these blocks from *porbH* for *ppvdE* sequence increased the OrbS-dependent activity of *ppvdE*. These results show that other factors in addition to the presence of the extended A+T tract influence promoter utilisation by OrbS. Since these two regions (-5 to +6 and -36 to -33) are important for promoter utilisation by OrbS, but the individual bases in these regions were found not to be important when

singly mutated, it is possible that the conformation of these regions, rather than their DNA sequence, is important for OrbS recognition, as is the case for the A+T tract. The presence of at least one of the two A bases downstream of the PvdS-dependent promoter -35 element (at positions -27 and -28 relative to the *porbH* TSS) was found to be important for promoter recognition by PvdS.

Finally, it should be noted that *ppvdEds5*, the sequence of which differs from *porbHds6* at only 4 positions (-36, -33, -28 and -5 relative to the *porbH* TSS) (Figure 6.13), had only ~25 % of the activity of *porbHds6*. Of these 4 bases, the most important appeared from the single base mutation screen to be that at position -36 (wild type base G), which when replaced with a T gave rise to >200 % activity compared to *porbHds6*. In *ppvdEds5* the base at this position is a C, which could have adversely affected OrbS-dependent activity. Of the other differing bases, the one at position -33 did not appear to be important from the single base mutation screen, and the others (positions -28 and -5) had only minor importance (giving rise to promoters with activities of ~75 % of *porbHds6* activity when mutated). The combined effect of two or more of these bases must be responsible for the observed low activity of *ppvdEds5*.

To conclude, for efficient utilisation by OrbS, a promoter requires several features. The presence of the 4 bp G+C-rich region upstream of the -35 element was shown to increase the OrbS-dependent activity of the *pvdE* promoter. The -35 element was shown to consist of TAAA. Immediately downstream of the -35 element, the 4 bp extended A+T tract was essential for OrbS-dependent activity of the *orbH* promoter, although a single substitution within this tract was permissible. The -10 region consists of CGTC, with a 17 bp spacer between the -35 and -10 elements. No promoters with spacers of altered length were tested. However, the importance of the length of the spacer region for promoter activity has been well documented for other promoters, this spacing being necessary to place the centres of the -10 and -35 elements on the same face of the DNA double-helix, ~2 turns apart (Auble *et al.*, 1986; Shultzaberger *et al.*, 2006). Downstream of the -10 region, the presence of at least part of the A+G-rich region of *porbH* was shown to be necessary for OrbS function. However, certain synthetic promoter derivatives conforming to the above specification were found to be poorly active in response to OrbS, demonstrating that OrbS has further requirements of its promoters.

The requirements for promoter utilisation by PvdS were also elucidated in this study. PvdS has fewer sequence requirements than OrbS for promoter utilisation. Bases within the highly conserved G+C-rich region upstream of the -35 element of the PvdS-dependent promoters (Figure 6.2) appeared to be of some importance for efficient promoter utilisation. The -35 element for recognition by PvdS was found to consist of TAA, and the presence of at least one of the two A bases directly downstream of this motif was necessary for efficient promoter utilisation by PvdS. The PvdS-dependent -10 region consists of CGT, and the presence of at least part of the downstream A+G region (which is present in most PvdS-dependent promoters, but is 6 bp long, rather than the 9 bp of the OrbS-dependent promoters), was also found to be essential for efficient promoter utilisation by PvdS.

As previously discussed, PvdS is involved in the regulation of a range of virulence factors in response to iron starvation. Ochsner and colleagues (2002) used a GeneChip approach to identify PvdS-dependent promoters, and Figure 6.23 shows an alignment of the PvdS-dependent promoters thus identified. The majority of the promoters shown specify the transcription of the *pvd* (pyoverdine biosynthesis and utilisation) genes. The *pvd* promoters fit well within the requirements determined for utilisation by PvdS. Each of these promoters contains the upstream C+G-rich block and the 2 bp extended A+T-tract. Most of these promoters also contain the downstream A+G-rich block. In a 6 bp random DNA sequence, one would expect to find on average 3 A+G bases. The *pvdI, pvdH* and *pvdY* promoters all contain only 2-3 A+G bases. However, as evidenced by the PvdS-dependent activity of *porbHds43*, PvdS is capable of utilising certain promoter sequences in which this 6 bp region is not A+G-rich. The remaining PvdS-dependent promoters shown in Figure 6.23 are less well conserved than the *pvd* promoters at the upstream G+C-rich block and the extended A+T tract. The presence of the upstream G+C-rich block appeared to enhance PvdS-dependent promoter activity, but was not essential for it, as discussed above. The single-base substitution screen showed that replacement of the A with a C residue at position -28 (relative to the approximate TSS of *porbH*) (as is present in the extended A+T tracts of the *PA2531* and *PA1134* promoters) has little effect on PvdS-dependent promoter activity (see Figure 6.15). Therefore these promoters might still be highly active.

Seven candidate promoters of the OrbS regulon (CODPs) were identified using Fuzznuc. These sequences fulfilled the experimentally-identified requirements for

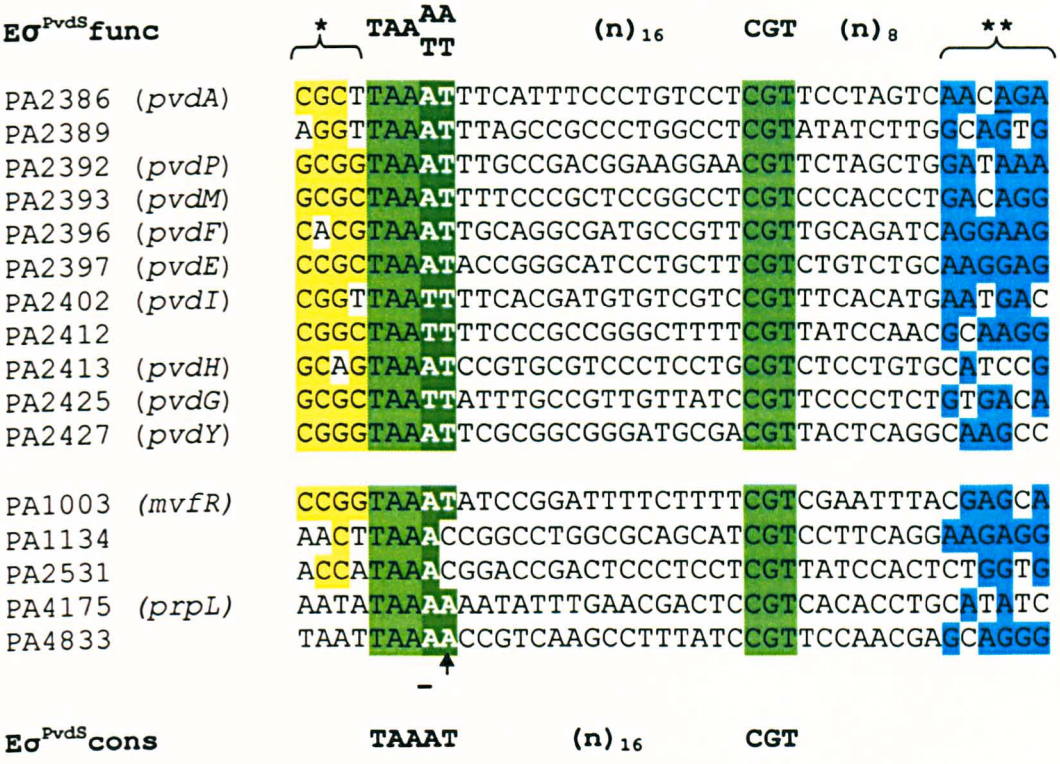

Figure 6.23: Alignment of PvdS-dependent promoters. This alignment contains all 11 proven PvdS-dependent promoters of the Pvd clusters (above the space), and 5 other PvdS-dependent promoters detailed by Ochsner and colleagues (2002) (below the space). The products encoded by the genes directed by these promoters are as follows: PA1003 - MvfR transcriptional regulator, necessary in *P. aeruginosa* for full virulence; PA1134 – 2 hypothetical proteins; PA2531 – an aminotransferase; PA4175 – PrpL proteinase; PA4833 – a hypothetical protein. Only promoters that shared the essential bases of the -35 and -10 elements (TAA and CGT respectively) have been included, as Ochsner and colleagues gave no indication of promoter strength. The TSS of *pvdA* has been underlined. Position -28 with respect to the *porbH* TSS, which is referred to in the text, has been indicated.
The experimentally determined functional sequence of a PvdS-dependent promoter ($E\sigma^{PvdS}$func)has been shown at the top of the alignment. N represents any base. * represents the 4 bp upstream G+C-rich block. ** represents the 6 bp downstream A+G rich block. The consensus PvdS-dependent promoter sequence ($E\sigma^{PvdS}$cons) has been shown at the bottom of the alignment.
All G+C bases within the 4 bp G+C upstream block have been highlighted yellow. The bases of the -35 and -10 elements that were found to be essential during the single-base screen (TAA and CGT respectively) have been highlighted green. A+T bases within the extended A+T tract (the 2 bp immediately downstream of the -10 element) have been highlighted dark green, with white lettering. A+G bases within the 6 bp A+G block have been highlighted blue.

utilisation by OrbS, although further sequence requirements have yet to be elucidated, and therefore these sequences might not be utilised by OrbS. Some of these CODPs might specify the transcription of genes important for *B. cenocepacia* virulence. CODP4 might partially specify the production of a urease, and CODP 5 might direct transcription of genes involved in biofilm formation and colonisation (the *tad* locus genes). In order to test whether these candidate promoters are indeed utilised by OrbS, these sequences could be synthesised as double-stranded oligonucleotides and inserted into pKAGd4, for β-galactosidase assay using *E. coli* MC1061, as used throughout this chapter. Primer extension could then be used to confirm that any CODPs found to have OrbS-dependent activity are indeed promoters.

Chapter 7

Investigation of the mechanisms of iron-dependent regulation of the ornibactin gene cluster

7.1: Introduction

Although iron is essential for bacterial cell growth, excess iron can catalyse the formation of toxic superoxides. Therefore iron uptake is regulated to maintain intracellular concentrations within acceptable limits. This regulation is achieved in a multitude of bacterial species by the ferric uptake regulator, Fur, discussed earlier (Section 1.9) (Escolar *et al.*, 1999). Fur binds to specific motifs known as Fur boxes that are located within the promoter regions of iron-regulated genes. These motifs have the consensus sequence GATAATGATAATCATTATC (Baichoo and Helmann, 2002). The promoter regions of *orbS* and the OrbS-dependent genes were examined for sequences resembling the Fur box consensus, but no strong matches were apparent.

The production of ECF σ factors responsible for the biosynthesis and utilisation of siderophores, such as the FecI σ factor of *E. coli*, is generally regulated at the level of transcription, mediated by the ferric uptake regulator, Fur. Furthermore, the activity of such σ factors is frequently modulated by specific cytoplasmic-membrane associated anti-σ factors. In the absence of a certain extracytoplasmic stimulus, such anti-σ factors bind their cognate σ factor, rendering it inactive (see Section 1.8.1). The anti-σ factors involved in regulating siderophore biosynthesis and utilisation can functionally interact with a ferric siderophore receptor. In such cases, the σ factor is activated or released by the anti-σ factor in response to a conformational change in the signalling domain present in the N-terminal periplasmic extension of the ferric siderophore receptor, following binding of the ferric siderophore complex (as described in Section 1.8.1) (Koebnik, 2005). A TBLASTN search of the *B. cenocepacia* J2315 genome using the amino acid sequence of the anti-PvdS factor, FpvR, found one good match (43 % identity) (M. Thomas, personal communication). The gene encoding this homologous protein (BCAL1370) is part of a cluster of 4 genes that appears to be organised into an operon. One of these genes encodes a putative TonB-dependent siderophore receptor with a high degree of similarity to the receptor for the siderophore ferrichrome in *E. coli*. As anti-σ factors involved in the modulation of ECF σ factor activity tend to be co-transcribed with their cognate σ factor it is unlikely that the anti-σ factor encoded by BCAL1370 modulates OrbS activity. Furthermore, the N-terminal periplasmic extension of the ferric ornibactin receptor, OrbA, which contains the TonB box, lacks the signalling domain present in

the TonB-dependent transducer class of siderophore receptors (Section 1.8.1). The absence of this signalling region in OrbA suggests that the activity of OrbS is not modulated by an anti-σ factor.

7.1.1: Objectives

- To determine the mechanism of iron-dependent regulation of *orbS* transcription.
- To investigate possible mechanisms for the regulation of OrbS activity.

7.2: Investigation of the transcriptional regulation of *orbS*

7.2.1: Iron-dependent regulation of *porbS* in *E. coli*

The activity of the *orbS* promoter was previously shown to be iron-regulated in *B. cenocepacia* (Figure 5.8). The activity of the *orbS* promoter and the OrbS-dependent promoters were then assayed in *E. coli* strain MC1061 using pKAGd4 harbouring the *porbSfl*, *porbHfl*, *porbEfl* and *porbIfl* promoter derivatives (Figure 5.7). *porbSfl* was found to be active in *E. coli*, whereas the OrbS-dependent promoters were inactive (Figure 7.1). The *E. coli* genome does not encode the OrbS σ factor, and hence no activity of the OrbS-dependent promoters was anticipated in this experiment. As Figure 7.1 shows, the activity of *porbS* in *E. coli* was regulated in response to iron. The observed iron-dependent regulation of *porbSfl* when introduced into both *B. cenocepacia* and *E. coli* shows that the factor responsible for this regulation must be present in both species.

Fur is the most common and best studied iron-responsive regulator (IRR) of bacterial promoters. *B. cenocepacia* Fur has been used to complement an *E. coli* Fur mutant (Lowe *et al.*, 2001), demonstrating the high functional conservation among these proteins. Therefore, despite the lack of a strong candidate Fur box at the *orbS* promoter, *porbS* was investigated for Fur-dependent regulation.

7.2.2: Investigation of the role of Fur in the regulation of *porbS*

To test whether the observed iron-responsive regulation of the *orbS* promoter was dependent upon Fur, the activity of the *porbS* promoter was measured in the presence and absence of a functional *fur* gene. Previous attempts at the construction of a *B. cenocepacia fur* mutant had failed, suggesting that the presence of a functional *fur* gene is essential for *B. cenocepacia* viability, as is the case for other strict aerobes such as *P. aeruginosa* (Barton *et al.*, 1996; Lowe *et al.*, 2001). Therefore an *E. coli fur* mutant strain, QC1732, was used for this assay. *orbS* promoter activity was measured in this strain using a *porbSfl-lacZ* fusion.

A derivative of the expression vector pTrc99A called pAHA21 was also

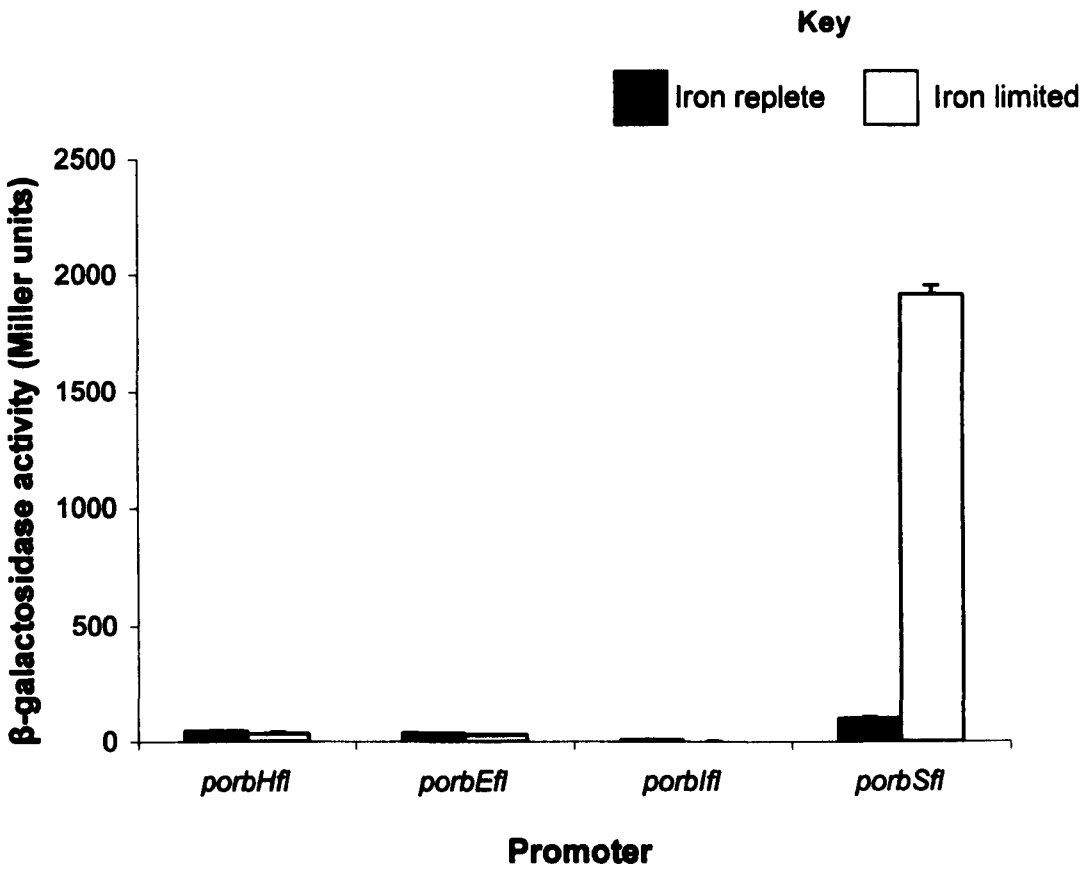

Figure 7.1: Activity of *porbS* and the OrbS-dependent promoters in *E. coli*. pKAGd4 derivatives bearing *porbSfl*, *porbHfl*, *porbEfl* and *porblfl* were introduced into *E. coli* MC1061. β-galactosidase assays were performed on triplicate cultures grown in LB broth containing chloramphenicol, under iron replete and iron limited conditions, as indicated. Activities were background corrected by subtracting the activity specified by pKAGd4 in MC1061 under the conditions used. Error bars represent the standard deviation from the mean of the triplicate cultures assayed.

employed. This plasmid contains a functional copy of *B. cenocepacia fur* under the control of the *trc* promoter (Lowe *et al.*, 2001). pTrc99A bears the *bla* (ampicillin resistance) gene, which is also present in pKAGd4, and therefore in order to allow selection of both of these plasmids the *bla* gene of pKAGd4 was disrupted by the insertion of the *nptII* (kanamycin resistance) gene from p34E-Km. Thus, *nptII* was excised from p34E-Km by digestion with *Sma*I, and inserted into the *Sca*I site within the pKAGd4 *bla* gene (Figure 7.2), resulting in pKAGd4ΔAp. The *porbSfl* promoter was then excised from pBS-porbSfl by digestion with *Pst*I and *Xba*I, and inserted into pKAGd4ΔAp digested with the same restriction enzymes. The resultant plasmid was named pKAGd4ΔAp-porbSfl (Figure 7.3).

The activity of *porbS* in QC1732 host cells bearing either pTrc99A or pAHA21 was determined by β-galactosidase assay. Assays were carried out on cells grown in LB broth under both iron limited and iron replete conditions. The background activity of pKAGd4ΔAp was also assayed in QC1732 bearing either the pTrc99A expression vector or pAHA21. Figure 7.4 illustrates the results of these assays. In the absence of *fur*, *porbS* was not regulated in response to iron availability, whereas in the presence of functional *fur*, 120 fold regulation was observed between the iron limited and iron replete conditions used. This demonstrates that Fur is involved in the regulation of the *orbS* promoter. The activity of the *orbS* promoter was ~4 fold higher under iron limiting conditions in the absence of *fur* than in its presence, suggesting that the conditions used were not sufficiently iron limiting to allow for complete derepression of *porbS*.

The results of this experiment demonstrate that the activity of the *orbS* promoter is Fur regulated, but they do not show that this regulation is the result of a Fur binding site at this promoter. The *orbS* promoter could have been regulated by a factor whose transcription was regulated by Fur (although this factor would have to be common to *B. cenocepacia* and *E. coli*). In order to investigate whether Fur directly binds the *orbS* promoter region, the Fur titration assay was employed.

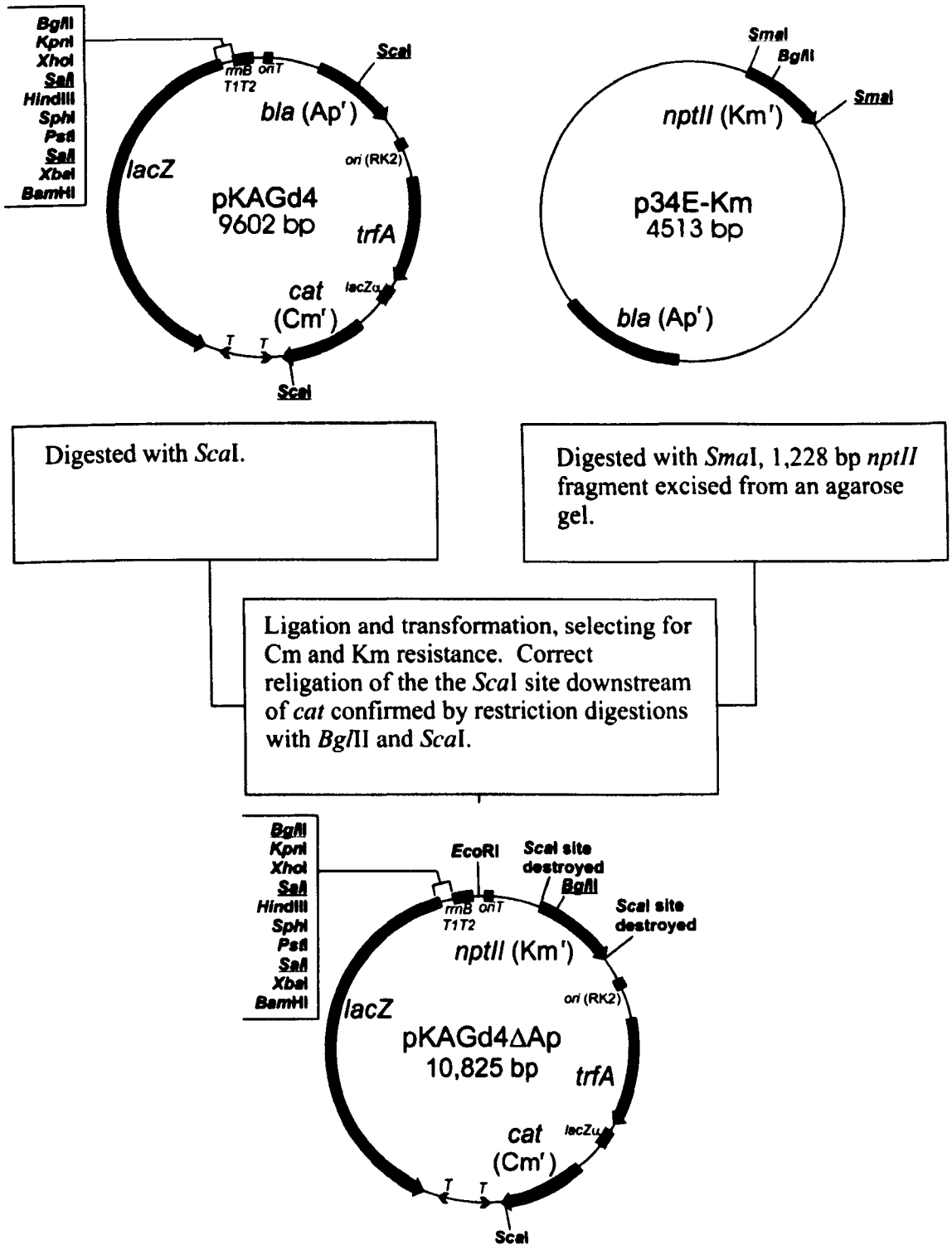

Figure 7.2: Scheme for the construction of pKAGd4ΔAp. Only pertinent restriction sites are shown. Non-unique restriction sites are underlined.

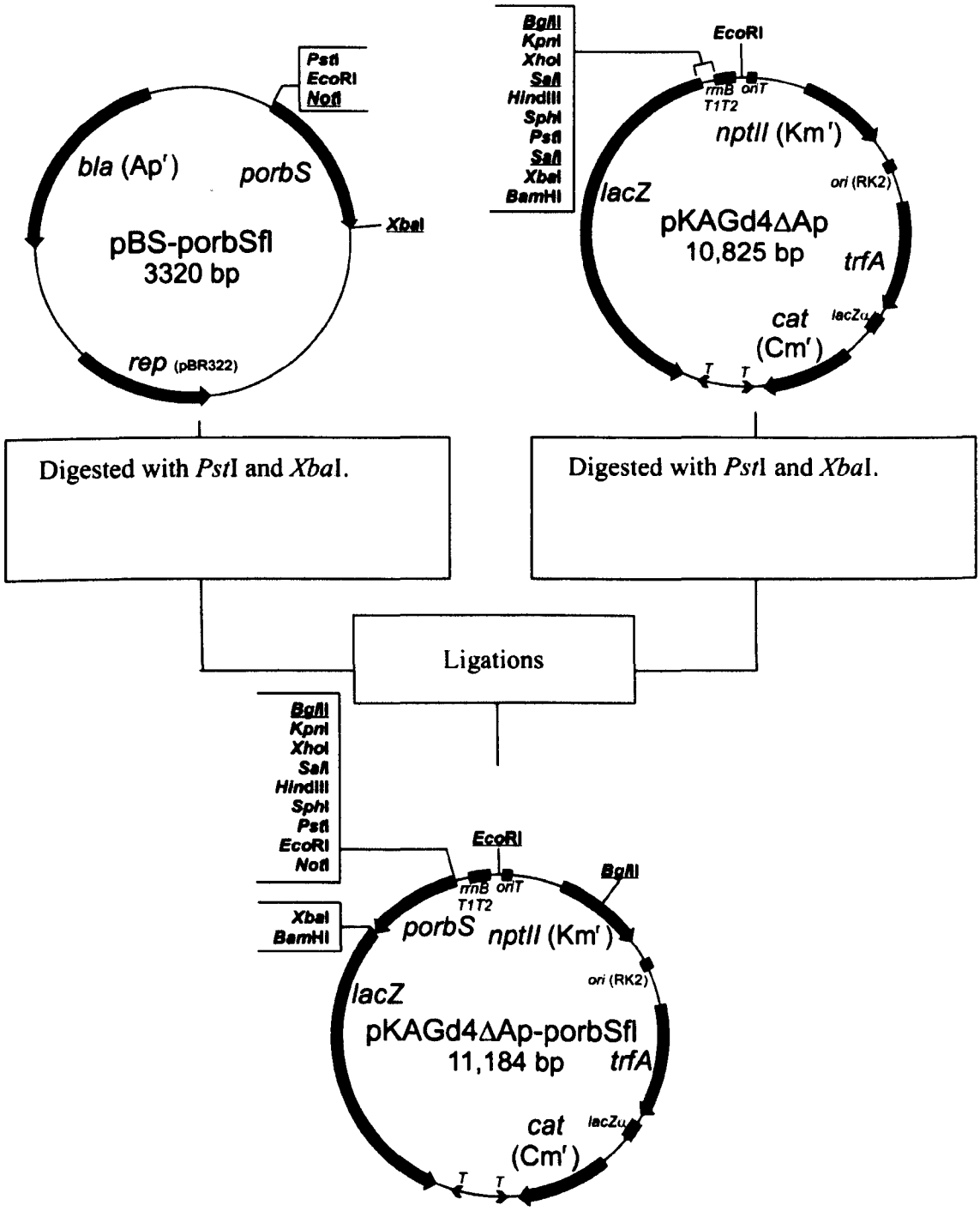

Figure 7.3: Scheme for the construction of pKAGd4ΔAp-porbSfl. Only pertinent restriction sites are shown. Non-unique restriction sites are underlined.

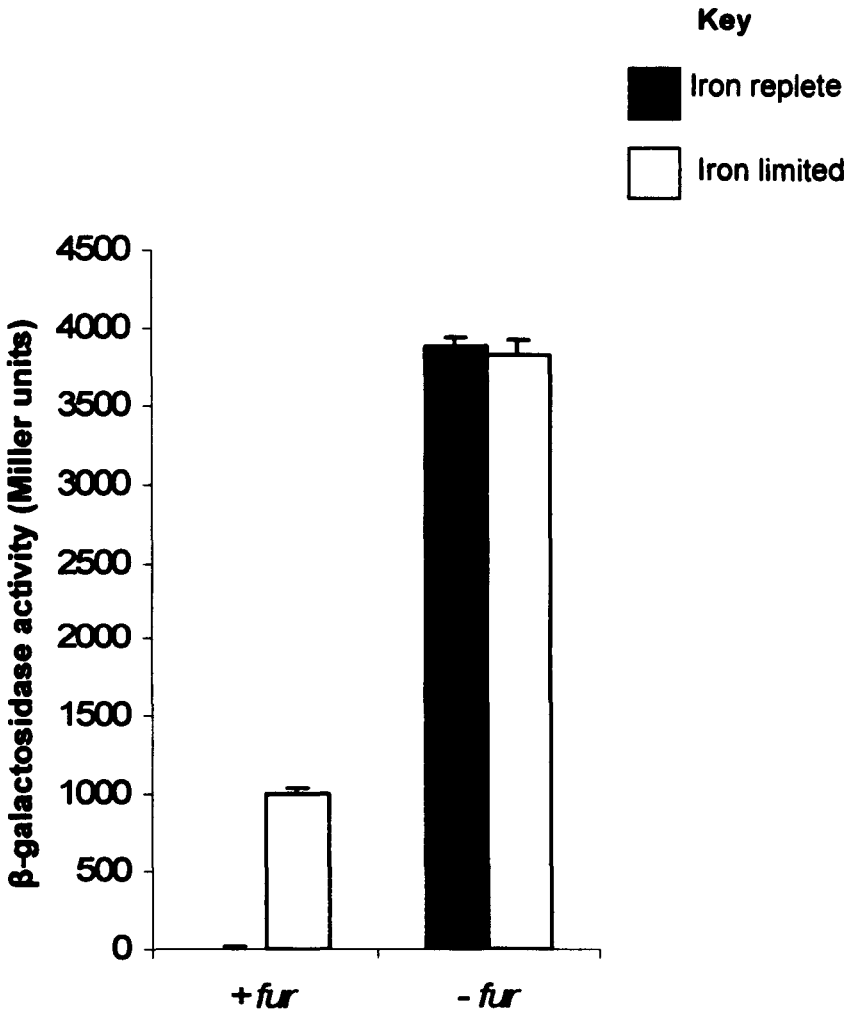

Figure 7.4: Regulation of the *orbS* promoter is dependent on Fur. β-galactosidase assays were carried out on triplicate cultures of *E. coli* QC1732 cells containing pKAGd4ΔAp-porbSfl grown in LB broth containing chloramphenicol and ampicillin, under iron replete and iron limited conditions. Functional *fur* was introduced on plasmid pAHA21 (+*fur*), a derivative of expression vector pTrc99A (-*fur*). Activities were corrected by subtracting the activity of QC1732 containing pKAGd4ΔAp in each of the *fur* backgrounds. Error bars represent standard deviation from the mean of the triplicate cultures.

7.2.3: Determination of the location of the Fur binding site at *porbS* by FURTA

The Fur titration assay (FURTA) was used to examine *porbS* and the OrbS-dependent promoter regions for the presence of a Fur box. FURTA utilises an *E. coli* strain, H1717, which carries a chromosomal *fhuF-lacZ* fusion. The *fhuF* promoter contains a Fur box. Thus, under iron replete conditions, Fur represses transcription of *lacZ*, giving rise to a Lac^- phenotype. If a plasmid with a copy number of > 20 copies per cell bearing a Fur box is introduced into this system, it will titrate Fur away from the single chromosomal Fur box, relieving Fur repression and allowing increased utilisation of lactose even in iron-rich environments (Stojiljkovic *et al.*, 1994).

This phenomenon can be visualised using MacConkey lactose agar- a medium that can be used to screen bacteria for the ability to utilise lactose. This medium contains the pH indicator neutral red. Bacterial fermentation of lactose results in the production of lactic acid, which lowers the pH of the surrounding medium, resulting in the production of red colonies. Bacteria unable to ferment lactose give rise to white colonies. Thus, under iron replete conditions, H1717 gives rise to white colonies on MacConkey lactose agar. When a high copy number plasmid bearing a Fur box, however, is introduced into H1717, Fur repression is relieved giving rise to red colonies under iron replete conditions (Stojiljkovic *et al.*, 1994). This is illustrated in Figure 7.5.

To optimise the conditions for FURTA, a plasmid containing the consensus *E. coli* Fur box (p3ZFBS) was introduced into H1717, and pBluescript II KS was introduced as a negative control for the relief of Fur-mediated repression. The two strains were then streaked onto MacConkey lactose agar containing 20, 30 or 40 μM $Fe(NH_4)_2(SO_4)_2$ to investigate their Lac phenotype under iron replete conditions. 40 μM $Fe(NH_4)_2(SO_4)_2$ gave good colour definition between colonies harbouring p3ZFBS (Lac^+) and those harbouring pBluescript II KS (Lac^-), and was therefore subsequently used for iron replete media for further FURTAs. The previously constructed pBluescript II KS derivatives bearing the full length *porbS*, *porbH* and *porbE/I* fragments (see Figure 5.6) were introduced into H1717.

Figure 7.6 A. shows the results of FURTA analysis of the fragments bearing

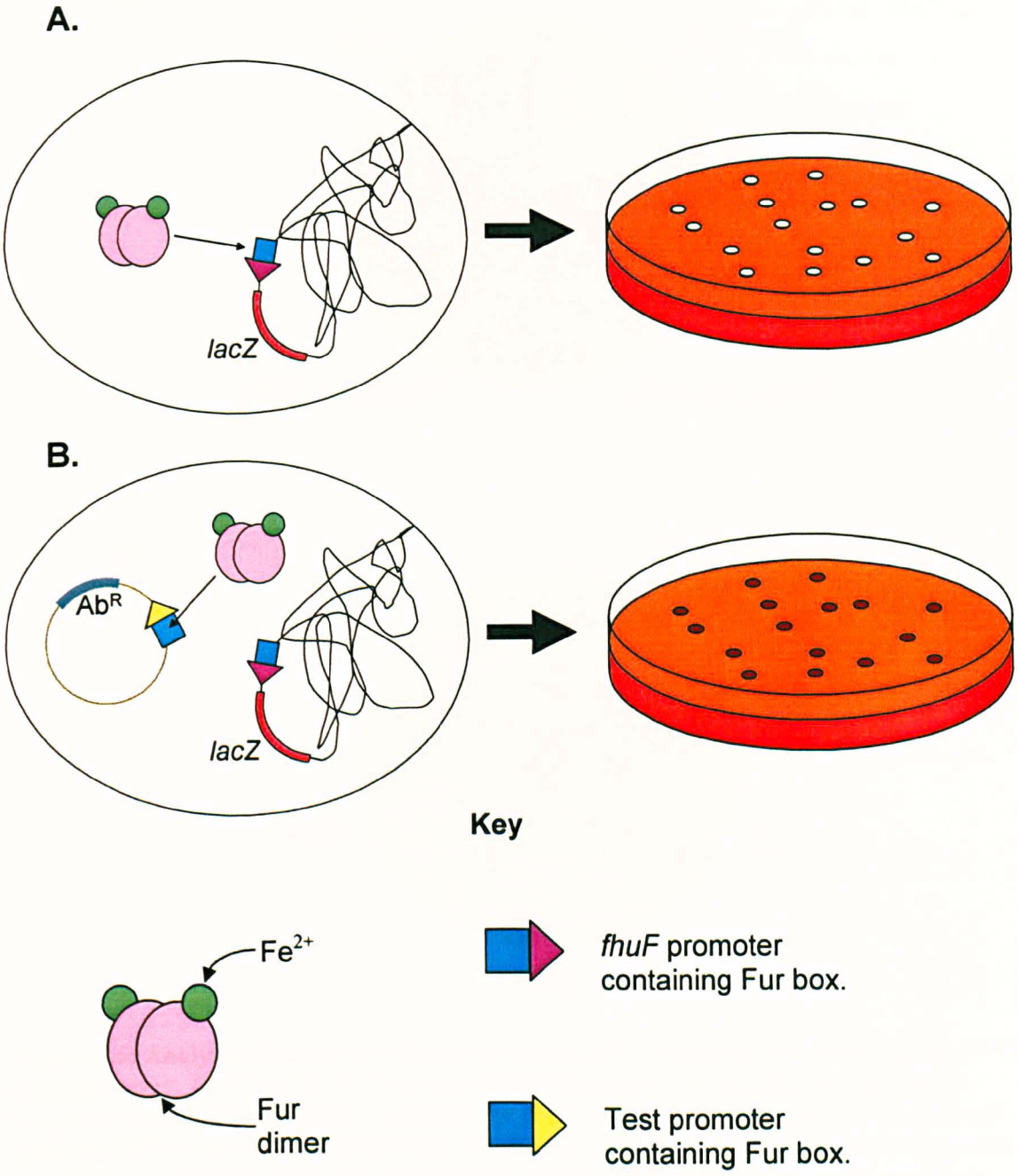

Figure 7.5: The Fur titration assay (FURTA). A. H1717 gives rise to white colonies on iron replete (40 μM $Fe(NH_4)_2(SO_4)_2$) MacConkey lactose agar, as Fur binds the *fhuF* promoter located upstream of *lacZ*, decreasing *lacZ* transcription. **B.** The introduction of a high copy number plasmid (only one copy shown) bearing a Fur box titrates Fur away from the chromosomal Fur box, relieving repression of *lacZ* transcription, resulting in red colonies on iron replete MacConkey lactose agar.

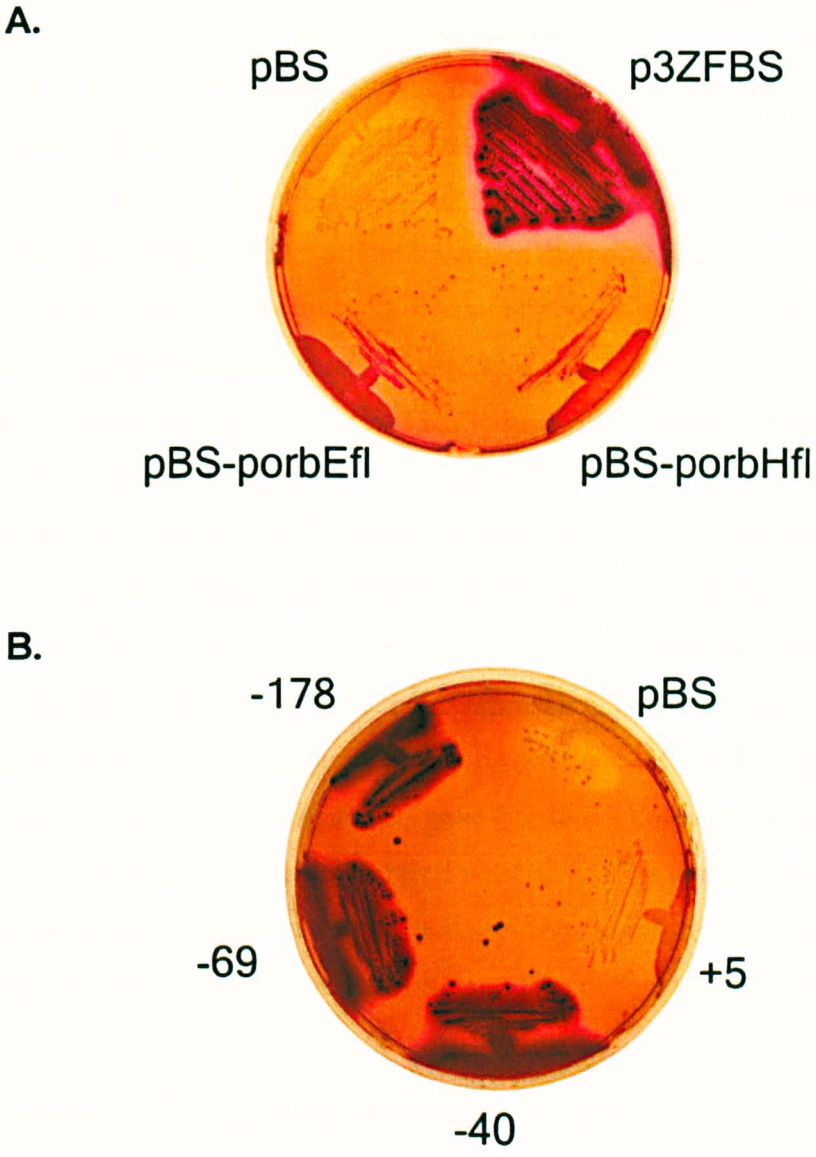

Figure 7.6: Analysis of promoters for the presence of Fur binding sites using the Fur titration assay. A. *E. coli* H1717 bearing p3ZFBS (positive control), pBluescript II KS (negative control, labelled pBS), or pBluescript II KS derivatives bearing *porbEfl* and *porbIfl* (pBS-porbEfl) or *porbHfl* (pBS-porbHfl). **B.** *E. coli* H1717 bearing *orbS* promoter fragments with differing upstream endpoints as indicated. Downstream endpoint was +181, relative to the *orbS* TSS (determined by primer extension, see Section 5.5), in each case. The *porbS* fragment with an upstream endpoint of -178 was *porbSfl*. Strains were streaked onto MacConkey lactose agar supplemented with ampicillin and 40 μM $Fe(NH_4)_2(SO_4)_2$, and incubated overnight at 37 °C.

the OrbS-dependent promoters. The Lac$^-$ phenotype observed under iron replete conditions suggested that these promoters do not contain Fur binding sites, although the resultant colonies were redder than the negative pBluescript II KS control. In contrast H1717 bearing *porbSfl* gave rise to deep red colonies on iron replete MacConkey lactose agar, demonstrating the likely presence of a Fur box within this promoter fragment (Figure 7.6 B). The upstream endpoint of *porbSfl* is -178 relative to the *orbS* TSS. To more precisely locate the Fur box within the *orbS* promoter region, *orbS* promoter fragments with upstream endpoints at -69, -40 and +5 were amplified and cloned into pBluescript II KS to give pBS-porbS-69, pBS-porbS-40 and pBS-porbS+5, respectively (Figure 7.7). Figure 7.6 B shows the FURTA results for H1717 bearing these plasmids. Introduction into H1717 of pBluescript II KS containing *porbS* fragments with upstream endpoints at -69 and -40 relative to the TSS gave rise to Lac$^+$ colonies on iron replete medium, whereas the fragment with upstream endpoint at +5 did not relieve Fur repression, resulting in a Lac$^-$ phenotype. This suggests that Fur binds to a site located downstream of -40, but upstream of or overlapping +5. As expected, all strains gave rise to red colonies when streaked onto MacConkey lactose agar not supplemented with iron. This confirmed their ability to utilise lactose as a carbohydrate source, and that lactose utilisation by H1717 containing pBluescript II KS is dependent upon iron concentration in the medium.

7.2.4: Analysis of Fur binding to *porbS* by EMSA

The results obtained by the FURTA were confirmed by Dr. S. I. Husnain, using the electromobility shift assay (EMSA). EMSA is used to analyse the ability of a specific protein, in this case Fur, to bind DNA sequences *in vitro*. The *porbHfl*, *porbEfl*, *porbS-69*, *porbS-40* and *porbS*+5 fragments previously assayed using the FURTA were end-labelled with ^{32}P and incubated with *E. coli* Fur under conditions known to promote DNA binding by Fur. The products of this incubation were separated by polyacrylamide gel electrophoresis under non-denaturing conditions. Where Fur bound a DNA fragment, the migration of the fragment through the gel was retarded. Clear shifts occurred when *orbS* promoter fragments with upstream endpoints at -69 and -40 relative to the TSS were incubated with Fur, whereas the promoter fragment with an upstream endpoint at +5 was not shifted (Figure 7.8).

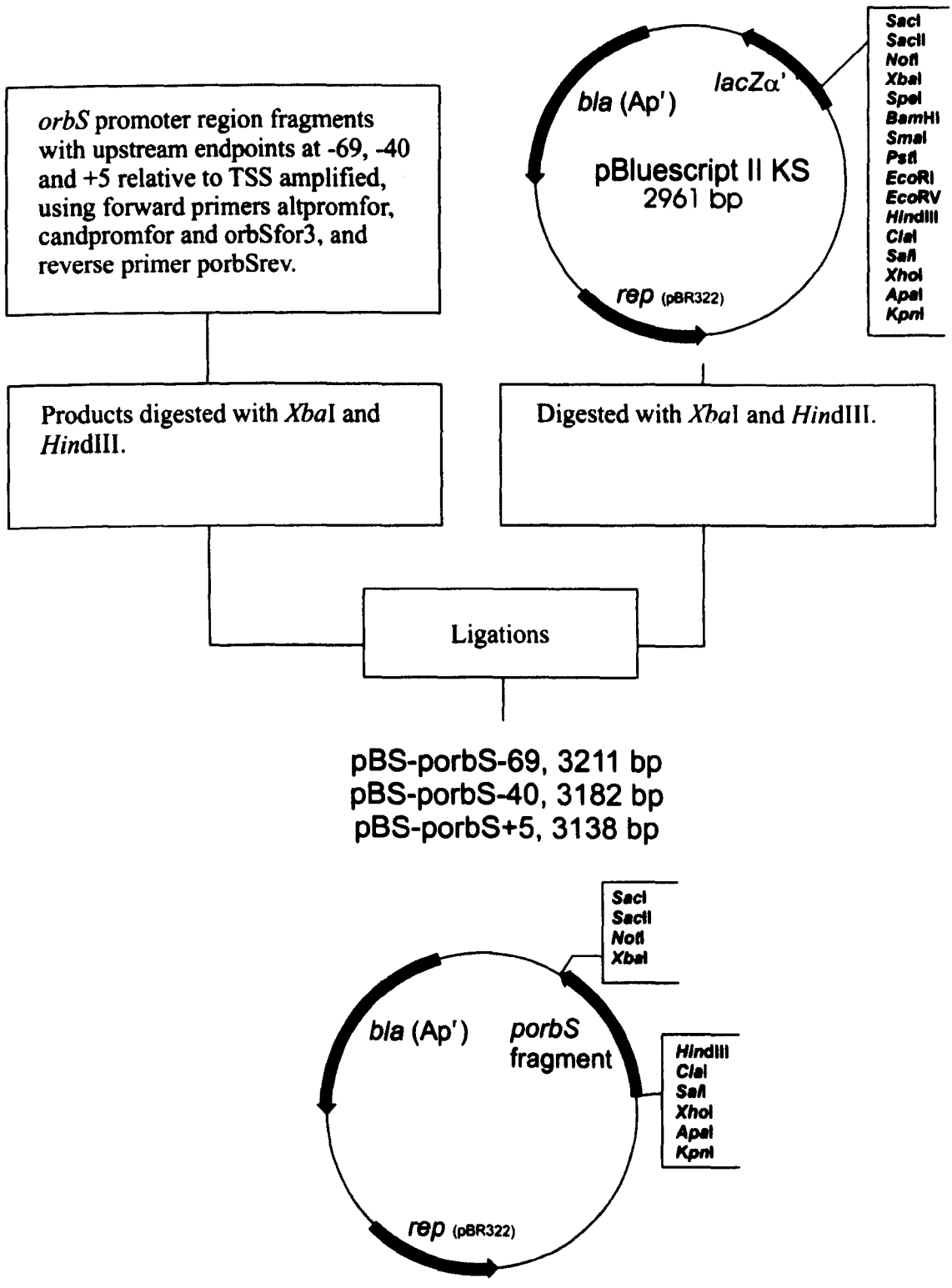

Figure 7.7: Scheme for the construction of pBluescript II KS derivatives containing *porbS* fragments with different upstream endpoints. Only pertinent restriction sites have been shown.

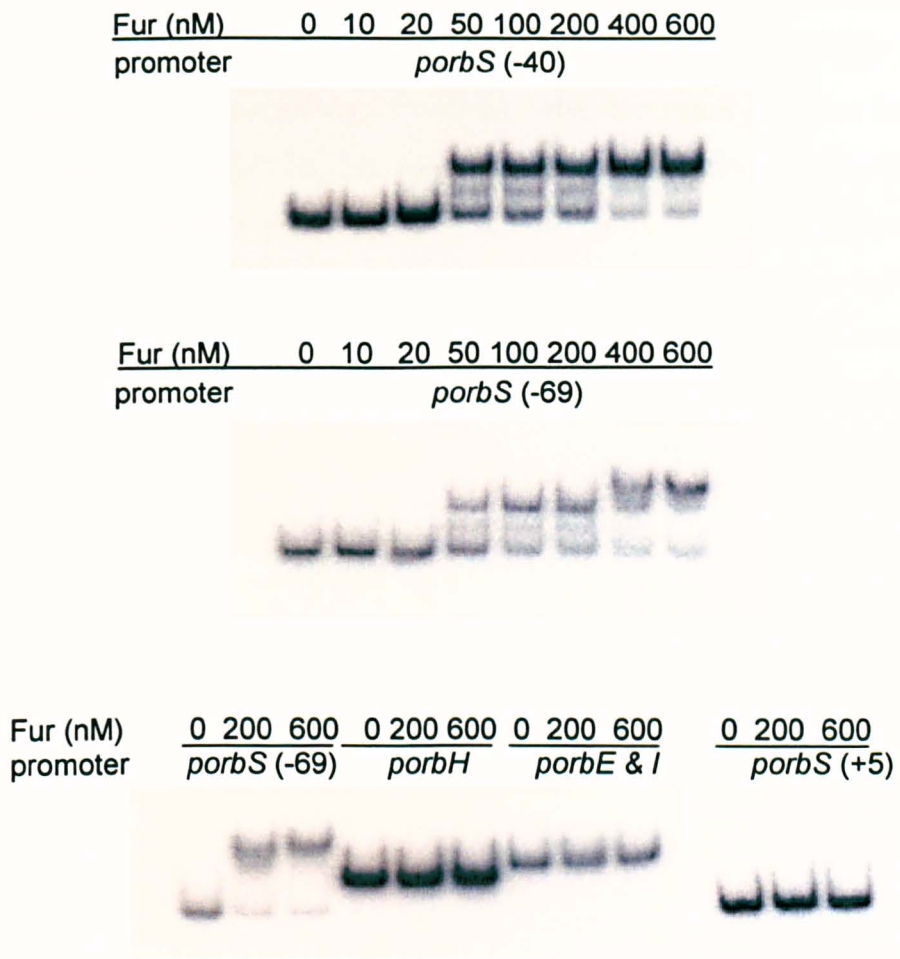

Figure 7.8: EMSA analysis of Fur binding to *porbS* and OrbS-dependent promoters. Fur concentrations and promoters present on each fragment were as indicated. Numbers in brackets represent upstream endpoints of *porbS* deletion fragments. EMSA was carried out by Dr. S. I. Husnain as follows: DNA fragments were amplified employing the primers used in the construction of derivatives of pBluescript II KS containing ornibactin operon promoters (Figures 5.6 and 7.7). The amplified products were digested with *Hin*dIII, separated in a 6 % polyacrylamide gel, and purified using the crush-soak method (Ross *et al.*, 2001). The fragments were then end-labelled with 20 μCi [α-^{32}P] dATP (3,000 Ci mMol^{-1}), using DNA polymerase Klenow fragment. 0.4 nM DNA was incubated for 30 min at 37 °C with purified *E. coli* Fur (kindly provided by S. Andrews, Reading) in a mixture of 1 X binding buffer (10 mM bis Tris-borate (pH 7.5), 40 mM KCl, 1 mM $MgCl_2$, 0.1 mM $MnCl_2$), 20 μg ml^{-1} sonicated calf thymus DNA (to prevent band shifting resulting from non-specific binding of Fur), and glycerol (10 %). Electrophoresis was carried out in a 6 % polyacrylamide gel at 4 °C, loaded under tension, with 40 mM bis Tris-borate (pH 7.5) and 0.1 mM $MnCl_2$ present in both the gel and the running buffer. The resultant gel was analysed using a phosphorimager. For full details of this experiment see Agnoli *et al.*, 2006.

porbS-40 gave rise to two shifted species at Fur concentrations of 50-200 nM, and *porbS-69* gave rise to an additional shift at Fur concentrations of ≥ 400 nM. No shift was observed when Fur was incubated with the OrbS-dependent promoter fragments, *porbHfl* and *porbEfl*, confirming that these fragments, which gave rise to reddish colonies in the Fur titration assay, are not bound by Fur.

7.3: Investigation of possible mechanisms for the modulation of OrbS activity

As previously discussed, some ECF σ factors involved in iron uptake are controlled both at the level of transcription by Fur, and in their activity by an anti-σ factor. The activity of OrbS, however, does not appear to be modulated by an anti-σ factor, unlike the σ factors FecI and PvdS. Inspection of the amino acid sequence of OrbS suggested a novel mechanism for intrinsic modulation of OrbS activity. Four cysteine residues are present at the C-terminus of OrbS (Figure 7.9). Cysteine residues are capable of co-ordinating with certain transition metal atoms via the sulphur atom within their thiol group (Figure 7.10). Fe-S proteins, in which iron is co-ordinated by cysteine thiols, play a key role in electron transfer and metabolic reactions within almost all organisms (Kiley and Beinart, 2003). Hence, the four cysteines at the C-terminus of OrbS might co-ordinate intracellular Fe^{2+}. Figure 7.11 illustrates a model for the direct control of OrbS activity via its potential iron-binding properties. In this model, free iron within the cell is co-ordinated by OrbS, either preventing incorporation of OrbS into the RNAP holoenzyme or disrupting promoter recognition by $E\sigma^{OrbS}$. When intracellular iron is limited (as a result of iron starvation), Fe^{2+} bound by OrbS dissociates, allowing OrbS to function as a σ factor. Pertinently, three of the C-terminal cysteine residues in OrbS are not present at the corresponding position in PvdS.

7.3.1: Construction of a constitutive *orbS* expression vector

According to the model proposed in Section 7.3, a constitutively expressed *orbS* gene would still give rise to some degree of iron-regulated expression from OrbS-dependent promoters, as the activity of OrbS would be modulated by iron concentration. To test this, it was desirable to construct an expression vector from which *orbS* would be constitutively produced, and therefore OrbS levels would not be subject to regulation by Fur.

Previously, a pBBR1MCS derivative had been constructed bearing *orbS* without its native promoter, such that *orbS* was placed under the tandem control of the *cat* (chloramphenicol acetyl transferase) and *lacZ* (β-galactosidase) promoters (Agnoli,

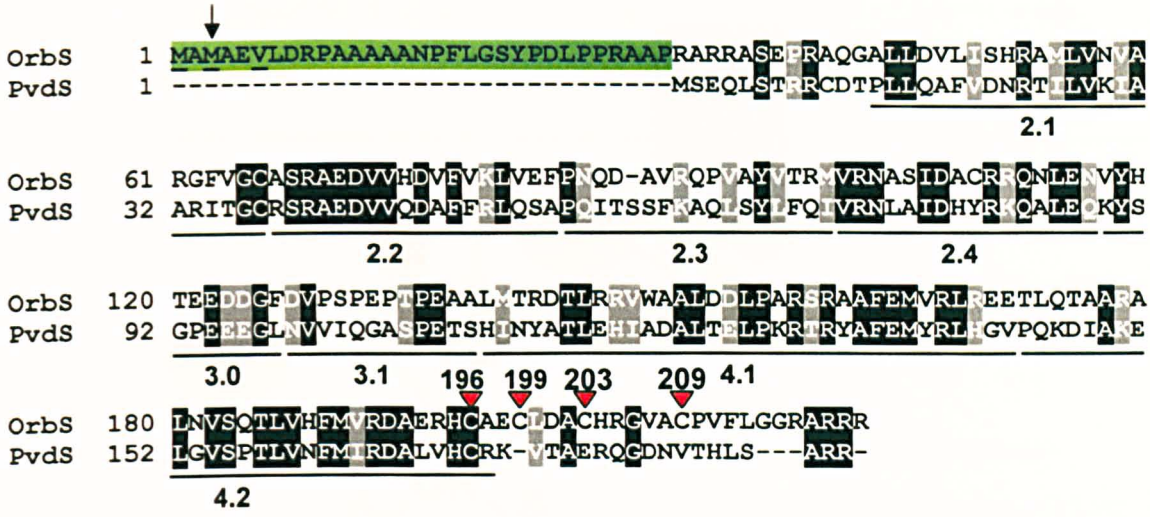

Figure 7.9: Amino acid sequence alignment of PvdS and OrbS. Important regions for σ factor function are indicated by underlining and are labelled accordingly. Identical residues are shown in white font and shaded black, and similar residues are shown in white font and shaded grey. The red triangles indicate the four C-terminal cysteine residues proposed to be involved in regulation of ornibactin synthesis through binding Fe^{2+}. These have been numbered with respect to the second putative initiation codon (indicated by a black arrow). The N-terminal extension of OrbS relative to PvdS is highlighted in green, and the three potential N-terminal amino acids of the protein have been underlined. Alignment was carried out using ClustalW.

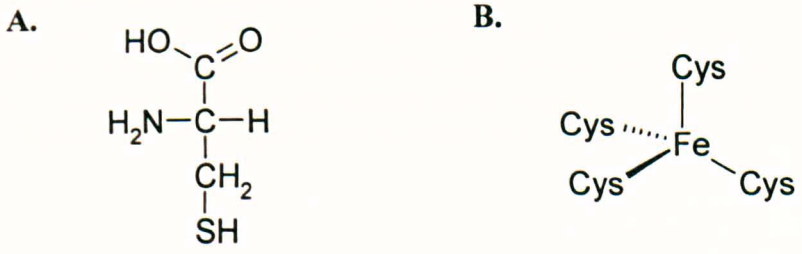

Figure 7.10: The structure of cysteine and the geometry of iron co-ordination by cysteine thiols. A: The structure of cysteine. **B:** Iron co-ordination by cysteine residues in rubredoxin. The lone electron pair of the sulphur atom within the thiol group forms a ligand to the central Fe^{2+} atom.

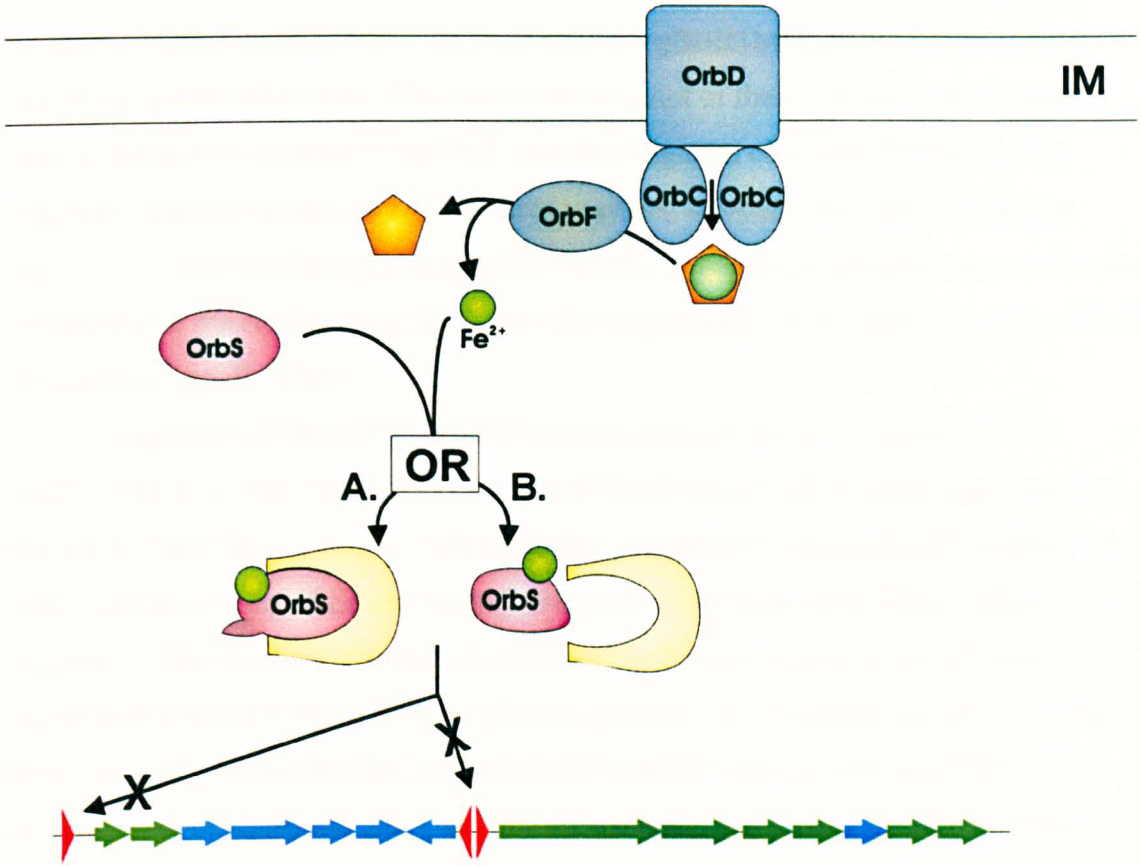

Figure 7.11: Proposed model for iron-dependent regulation of ornibactin synthesis. Ferric ornibactin enters the cell through the two membranes (only the inner membrane (IM) is shown). Fe^{3+} is reduced to Fe^{2+} by the OrbF reductase, thereby releasing it from ornibactin. Fe^{2+} complexes with OrbS, leading to either **A.** a change in the conformation within region 4.2, responsible for promoter recognition; or **B.** a change in conformation that prevents formation of the RNAP holoenzyme. When intracellular Fe^{2+} is low, iron dissociates from OrbS, allowing OrbS to adopt its active conformation, and thereby facilitating promoter recognition. The ornibactin operon is shown at the bottom of the diagram, with the OrbS-dependent promoters depicted as red triangles (colour coding is as shown in Figure 1.11).

2003). To construct this plasmid, *orbS* was amplified without its promoter, using primers orbSfor3 and orbSrev2, and inserted into pBBR1MCS between the *Bam*HI and *Hin*dIII restriction sites. The upstream endpoint of the amplified *orbS* fragment was at position +5 relative to the TSS, and this fragment contained 21 bp of *orbS* sequence upstream of the first of the three potential translational start codons (see Figure 5.1). The resultant plasmid, pBBR-orbSΔP, was found not to restore ornibactin production to the *orbS* mutant, OM3, despite the presence of the upstream *cat* and *lacZ* promoters (Agnoli, 2003).

Inspection of the pBBR-orbSΔP sequence revealed that the translational reading frame of *orbS* was different to that of the β-galactosidase α peptide-encoding sequence. Therefore, it was hypothesised that translation of the *lacZ* mRNA reads into *orbS*, and thereby could be blocking ribosome binding to the *orbS* Shine-Dalgarno sequence. Therefore a derivative of pBBR-orbSΔP was constructed in which a translational termination codon was placed upstream of *orbS* and in the same reading frame as *lacZ*. To do this, the MCS of pBBR-orbSΔP was cut with *Asp*718I (an isoschizomer of *Kpn*I) and *Xho*I, and the cohesive ends produced by both enzymes were filled in using Klenow large fragment DNA polymerase. Re-ligation of the plasmid resulted in an 11bp deletion within the MCS, which changed the reading frame and thereby placed a TGA stop codon in frame with *lacZ*. The resultant plasmid was named pBBR-orbSΔP2 (Figure 7.12). However, this plasmid, when introduced into *B. cenocepacia* OM3 by conjugation, also failed to restore ornibactin production to *B. cenocepacia* mutant OM3 (Figure 7.13). The *orbS* gene present on this plasmid contained both the putative Shine-Dalgarno site and all three candidate translational start codons for *orbS*, and therefore the lack of complementation of ornibactin production was unexpected. It was considered possible that the *cat* and *lac* promoters were only weakly active in *B. cenocepacia* (particularly the *lac* promoter, as this requires the cAMP receptor protein (CRP), which is not encoded within the *B. cenocepacia* genome, for full activity in *E. coli*). Therefore the *tac* promoter, which had been found to be highly active in *B. cenocepacia* 715j (specifying a β-galactosidase activity of ~9,000 Miller units in pKAGd4, see Figure 4.7) was cloned upstream of the *orbS* fragment. To do this, pBS-ptac was digested with *Kpn*I and *Xho*I, and the *ptac* fragment excised from an agarose gel. The *Kpn*I (*Asp*718I) site present in pBBR-orbSΔP was destroyed in the construction of pBBR-orbSΔP2, and

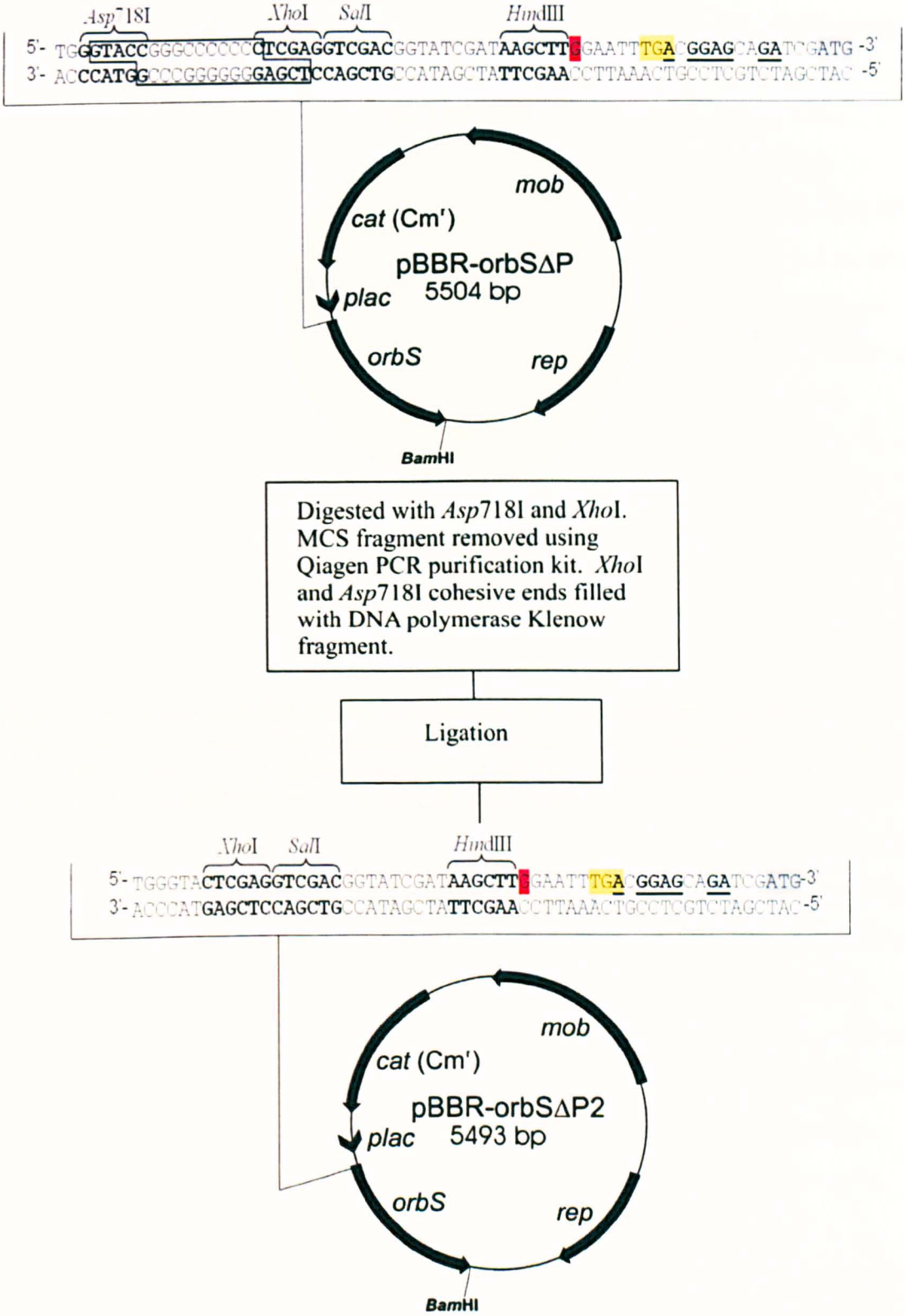

Figure 7.12: Scheme for the construction of pBBR-orbSΔP2. Only pertinent restriction sites are shown. The DNA fragment lost following digestion of pBBR-orbSΔP with *Asp*718I and *Xho*I is enclosed in a box. The most upstream base of the *orbS* translation initiation region (at position +5 relative to the TSS) is highlighted in red. The most upstream of the three candidate translational start codons is highlighted in grey, and the preceding TGA stop codon, which is in the same reading frame as *orbS* in pBBR-orbSΔP2, is highlighted yellow. The putative ribosome binding site has been emboldened and underlined

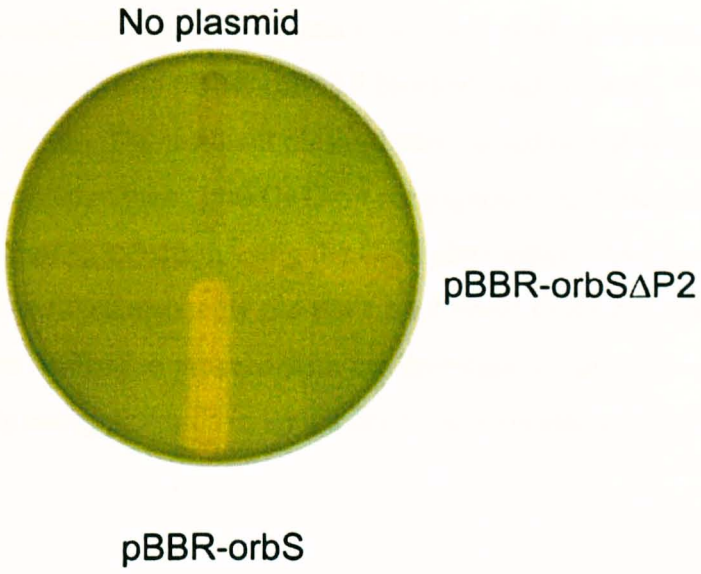

Figure 7.13: pBBR-orbSΔP2 fails to complement OM3 for ornibactin production. Cultures of *B. cenocepacia* OM3 containing the plasmids indicated were grown overnight at 37 °C, and streaked on a CAS plate containing 10 μM $FeCl_3$, which was incubated at 37 °C for ~16 hours. The unlabelled streak was not part of this experiment.

therefore *ptac* could not be easily cloned into this plasmid. Therefore, pBBR-orbSΔP was digested with *Kpn*I and *Xho*I, and ligated with the *ptac* promoter fragment (Figure 7.14). The *ptac* fragment contained nonsense codons in all three reading frames, and therefore insertion of this fragment into pBBR-orbSΔP blocked read-through translation of the LacZ α-peptide. The resultant plasmid was named pBBR-orbSΔP-ptac. pBBR-orbSΔP-ptac was introduced into OM3 by conjugation, and the resultant strain was tested for siderophore production using the CAS plate assay. As Figure 7.15 shows, pBBR-orbSΔP-ptac unexpectedly did not complement OM3 for ornibactin production. It was therefore decided to proceed with the investigation into the modulation of OrbS activity using plasmids in which *orbS* was expressed from its own promoter.

7.3.2: Investigation of the role of the C-terminal cysteines of OrbS in iron-dependent regulation of OrbS activity

In order to investigate whether the proposed model for the regulation of OrbS illustrated in Figure 7.11 could be operating, OM3 was complemented for ornibactin production with *orbS* in which the C-terminal cysteine codons were modified to specify alanines. The 4 C-terminal cysteines are at positions 196, 199, 203 and 209 in OrbS, with respect to the second methionine codon (see Figure 7.9). If the model were correct, substitution of alanine for cysteine residues should disrupt iron co-ordination, which could lead to a derepression of siderophore production under iron replete conditions (as the activity of the σ factor can no longer be inactivated by the binding of iron). Ideally, these cysteine codon substitutions would have been introduced into *orbS* transcribed from a constitutive promoter, avoiding regulation of ornibactin production mediated by Fur. However, the expression vectors harbouring *orbS* without its promoter, constructed as described above, were incapable of complementing OM3 for ornibactin production. It was therefore decided to construct codon substitution mutants of *orbS* complete with its native promoter. The plasmid pBBR-orbS (Figure 6.6) served as a control for this experiment. The introduction of pBBR-orbS into OM3 complemented this strain for ornibactin production, giving rise to a halo on standard CAS agar (Figure 7.16 A). Iron-dependent regulation of OrbS abundance mediated by Fur, and also, potentially, decreased OrbS activity mediated

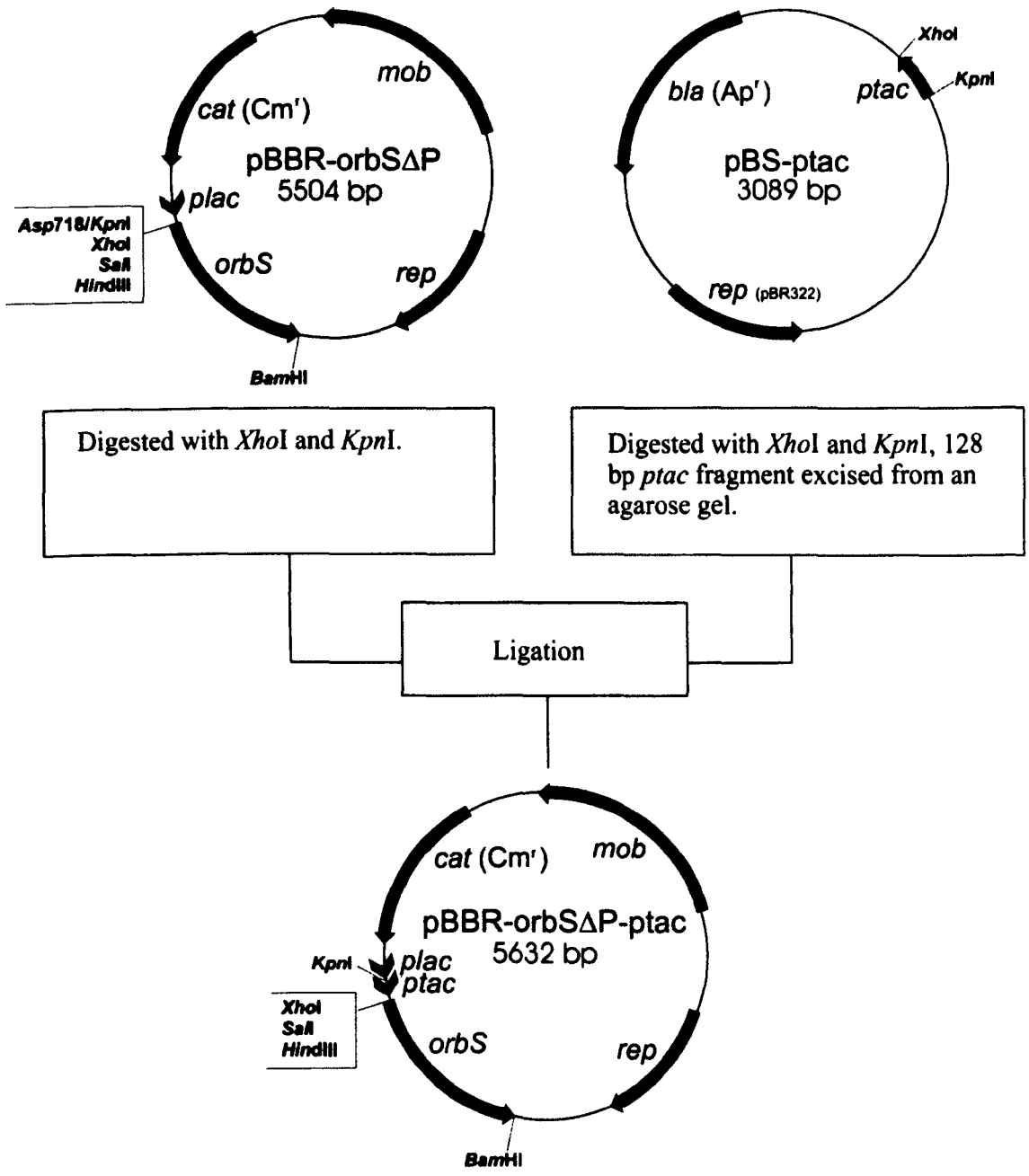

Figure 7.14: Scheme for the construction of pBBR-orbSΔP-ptac. Only pertinent restriction sites have been shown.

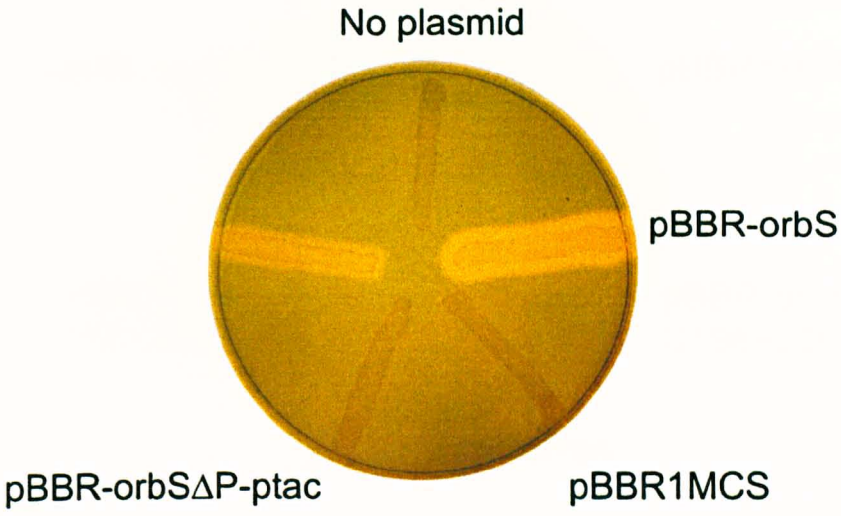

Figure 7.15: pBBR-orbSΔP-ptac fails to complement OM3 for ornibactin production. Cultures of *B. cenocepacia* OM3 containing the plasmids indicated were grown overnight at 37 °C, and streaked on a CAS plate containing 10 μM $FeCl_3$, which was incubated at 37 °C for ~16 hours. The unlabelled streak was not part of this experiment.

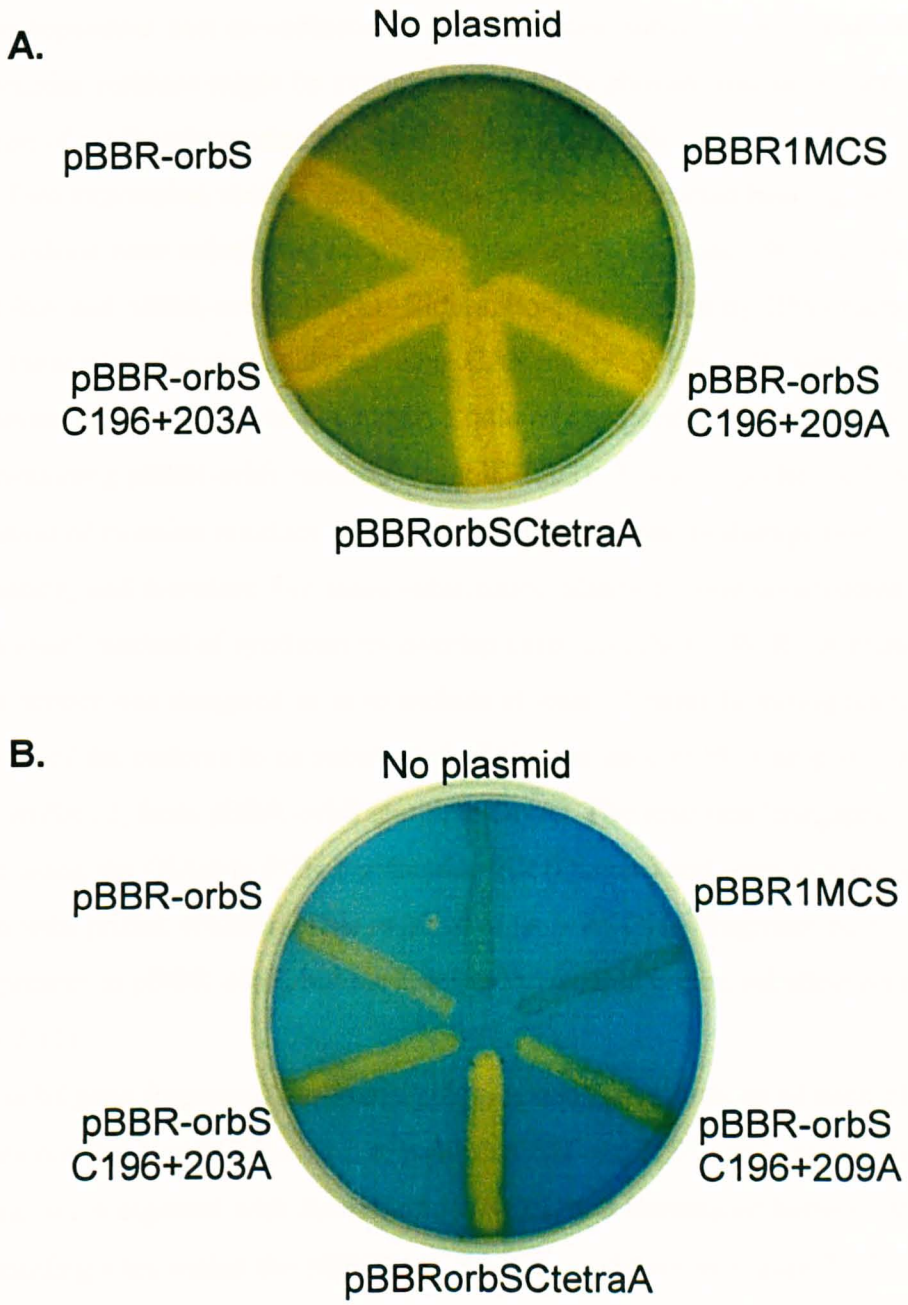

Figure 7.16: Analysis of ornibactin production by OM3 following introduction of plasmids containing cysteine-alanine codon substitutions. Cultures of *B. cenocepacia* OM3 containing the plasmids indicated were grown overnight at 37 °C, and streaked on CAS plates, which were incubated at 37 °C for ~16 hours. **A**: Standard CAS plate containing 10 μM $FeCl_3$. **B**: Iron replete CAS plate containing 60 μM $FeCl_3$.

by the proposed cysteine-dependent iron co-ordination model, resulted in a much smaller halo on iron replete CAS agar (compare Figures 7.16 A and B). Thus, if the cysteine-dependent iron co-ordination model operates, substitution of alanines for these cysteine residues might be expected to partially abolish iron-dependent regulation of ornibactin production, leading to a larger halo on iron replete CAS agar.

Two expression vectors had previously been constructed bearing *orbS* in which alanine codons were substituted for cysteine codons at positions 196 and 199 (pBBR-orbSC196A and pBBR-orbSC199A). Siderophore production by OM3 harbouring each of these plasmids was analysed using CAS plates. When cells were streaked onto both standard and iron replete CAS agar, a halo of comparable size to that produced by OM3 containing pBBR-orbS resulted (Agnoli, 2003). It was hypothesised that single substitution of cysteine residues 196 and 199 might not totally disrupt iron coordination, and therefore five more substitution plasmids were constructed using the 'megaprimer' method of synthesis by overlap extension (SOE) PCR. A mutagenic forward primer was designed so as to include at least 10 bases homologous to *orbS* on either side of the codon/s to be substituted. This was used to PCR amplify *orbS,* with primer orbSrev2, from pBBR-orbS template DNA. The resultant 'megaprimer' was purified using the QIAspin PCR Purification Kit (Qiagen) and used in a second PCR reaction with primer orbSfor. This resulted in an *orbS* DNA fragment corresponding to that present in pBBR-orbS, but harbouring the desired codon substitution mutations (Figure 7.17).

orbS gene fragments harbouring single codon substitutions of each of the two cysteines not previously mutated (i.e. positions 203 and 209) were constructed. These fragments were digested with *Bam*HI and *Hin*dIII, and introduced between the corresponding sites within the pBBR1MCS MCS, as shown in Figure 7.17. *orbS* gene fragments were also constructed harbouring combinations of substituted codons and inserted into pBBR1MCS in the same way as the single substitution fragments. These combinations consisted of two double substitutions, of the cysteine codons at positions 196 and 203, and at positions 196 and 209, and also a quadruple substitution. The plasmids containing these fragments were named pBBR-orbSC196+203A, pBBR-orbSC196+209A and pBBR- orbSCtetraA respectively. Alanine was chosen for substitution because it is of a similar size to cysteine, and is non-charged and non-polar, to cause minimal disruption of the conformation of OrbS.

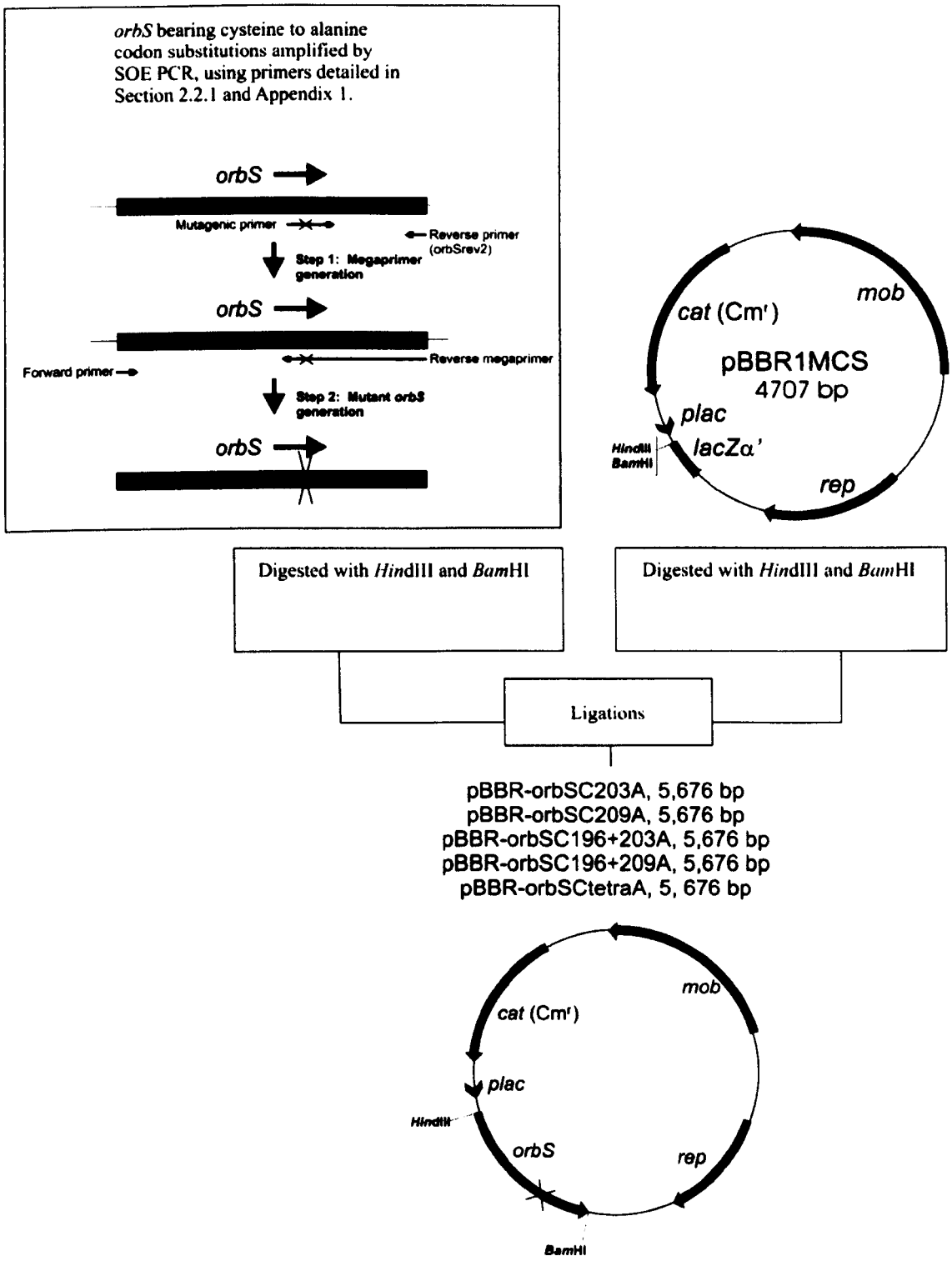

Figure 7.17: Scheme for the construction of alanine for cysteine substitution plasmids by SOE. Only key restriction sites have been shown. One or more alanine for cysteine codon substitutions are represented as a large cross.

The 5 new "alanine-for-cysteine" substitution plasmids were introduced into *B. cenocepacia* strain OM3 by conjugation. Figure 7.16 shows the results of the CAS plate assay used to screen for the complementation of OM3 by the plasmids bearing *orbS* harbouring double cysteine codon substitutions and the quadruple cysteine codon substitution. CAS plate analysis of siderophore production by OM3 complemented with *orbS* harbouring single cysteine codon substitutions gave identical results to those of the double substitutions, and have therefore not been shown.

Ornibactin production was restored to OM3 on standard low iron CAS plates by introduction of each of the *orbS* cysteine codon substitution plasmids (Figure 7.16 A). This indicates that none of the cysteine residues near the C-terminus of OrbS are required for association with core RNA polymerase and transcriptional activity. As shown in Figure 7.16 B, at 60μM $FeCl_3$ a much smaller halo formed around the strains harbouring the cysteine substitution plasmids. However, the yellow halo surrounding OM3 containing pBBR-orbSCtetraA grown on this medium was more intense than that surrounding OM3 bearing pBBR-orbS (see Figure 7.16 B). To ensure that this difference was not an inoculum effect, further liquid cultures were grown and the CAS plate analysis was repeated. A more intensely coloured halo was also present around OM3 cells containing the quadruple cysteine substitution plasmid in this second analysis (not shown). Although the results of the cysteine substitution analysis did not provide convincing evidence in support of the postulated cysteine-mediated iron co-ordination model for modulation of OrbS activity, they did not rule this hypothesis out, as Fur regulation of OrbS abundance might have masked this phenomenon. Furthermore, ornibactin production by OM3 containing pBBR-orbSCtetraA did appear to be less subject to iron-dependent regulation than ornibactin production by OM3 containing pBBR-orbS, as evidenced by the more intensely coloured halo surrounding this strain on iron replete CAS agar. A further attempt was therefore made to assay possible iron regulation of OrbS activity in the absence of Fur repression.

7.3.3: Investigation of iron-dependent regulation by OrbS in the absence of Fur

As attempts at the expression of *orbS* from a constitutively active promoter were unsuccessful, and the construction of a *B. cenocepacia fur* mutant was apparently

not possible, it was decided to investigate OrbS-dependent gene regulation in an *E. coli fur* mutant strain. Thus, the activity of a *porbH-lacZ* fusion was assayed under conditions of iron limitation and iron sufficiency, in *E. coli* strain QC1732, in the presence of functional *orbS,* to test whether *porbH* activity remained iron-regulated in the absence of Fur.

As QC1732 contains a kanamycin resistance gene inserted into the *fur* gene, and pKAGd4 contains a chloramphenicol resistance gene, it was not possible to use derivatives of plasmids pBBR-orbS or pBBR-2-orbS to supply functional *orbS.* Therefore, derivatives of pBBR1MCS-5, which carries a selectable marker for gentamycin resistance, were constructed that expressed wild type *orbS* and mutant *orbS* in which alanine codons had been substituted for the 4 C-terminal cysteine codons. To do this, pBBR1MCS-5 was digested with *Bam*HI and *Hin*dIII, and ligated with *orbS* excised from pBBR-orbS and pBBR-orbSCtetraA using the same enzymes, as illustrated in Figure 7.18. The resultant plasmids were named pBBR-5-orbS and pBBR-5-orbSCtetraA, and in both cases transcription of *orbS* was directed by the native *orbS* promoter. A further plasmid was constructed as a negative control for iron-dependent regulation in the absence of Fur, using PvdS, which lacks the C-terminal cysteine-rich motif of OrbS. Promoterless *pvdS* was available within pBBR1MCS-2, from which it was excised using *Kpn*I and *Hin*dIII and transferred into these same sites in pBBR1MCS-5 (Figure 7.19). Thus, in pBBR-5-pvdS, the *pvdS* gene is expressed from the vector *lac* promoter in *E. coli.*

The *orbH* promoter was delivered using pKAGd4-porbHds6, which contains *porbH* on a 42 bp DNA fragment (see Section 6.4.2). The activity of the *orbH* promoter within QC1732 cells bearing pBBR-5-orbS, pBBR-5-orbSCtetraA, pBBR1MCS-5, or pBBR-5-pvdS, was determined by β-galactosidase assay following growth under both iron limited and iron replete conditions. Cells containing pBBR1MCS-5 had low β-galactosidase activity (251 Miller units for cells grown under iron limited and 175 Miller units for cells grown under iron replete conditions). This activity was used for background correction of the strains harbouring the other three pBBR1MCS-5 derivatives. The results showed that pBBR1MCS-5 derivatives containing *orbS*, *orbSCtetraA* and *pvdS* were able to strongly activate transcription from *porbH* in *E. coli* (Figure 7.20). Furthermore, in the absence of Fur, *porbH* activity was not significantly repressed in response to iron in the presence of

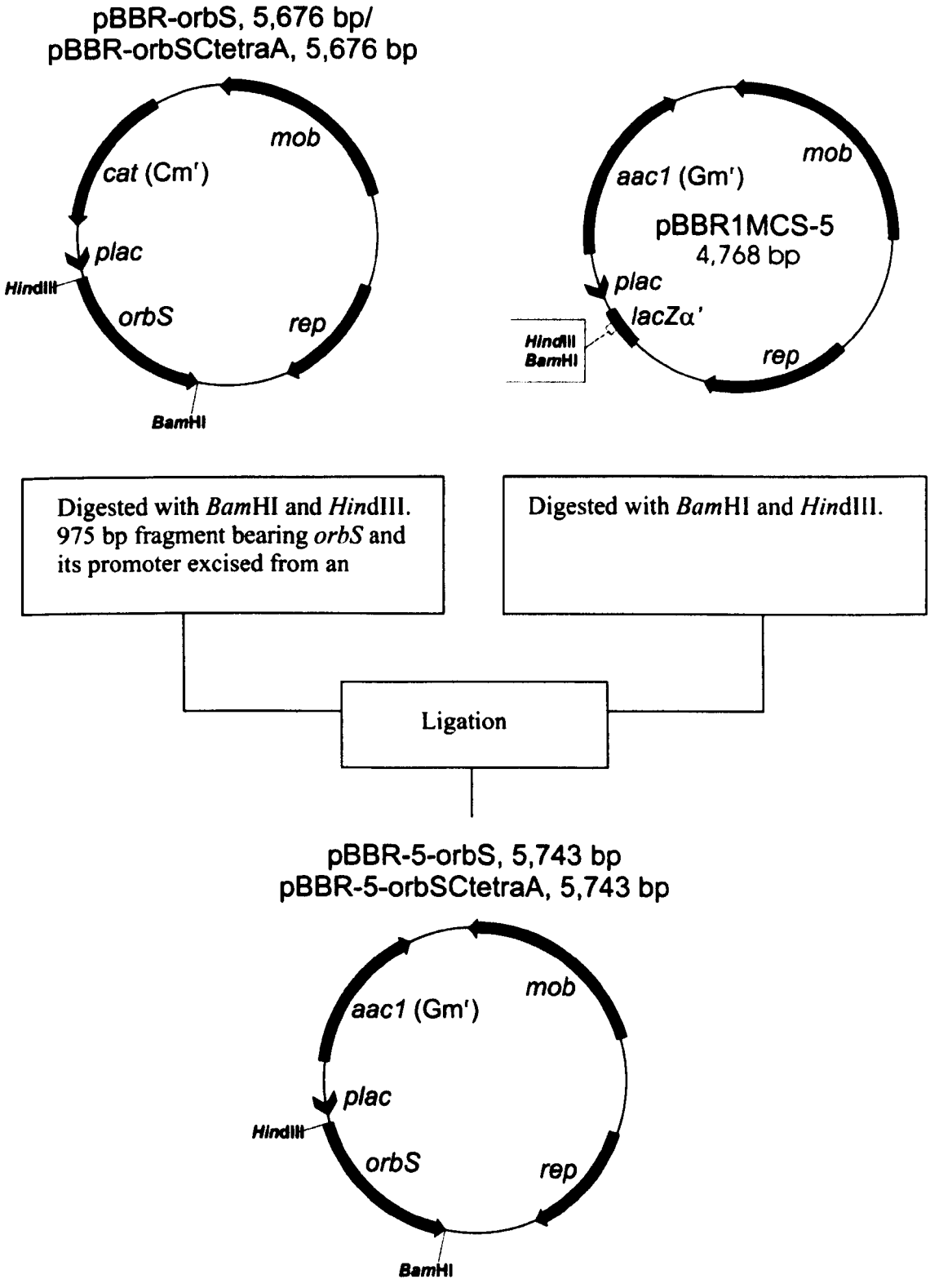

Figure 7.18: Scheme for the construction of pBBR-5-orbS and pBBR-5-orbSCtetraA. Only pertinent restriction sites shown.

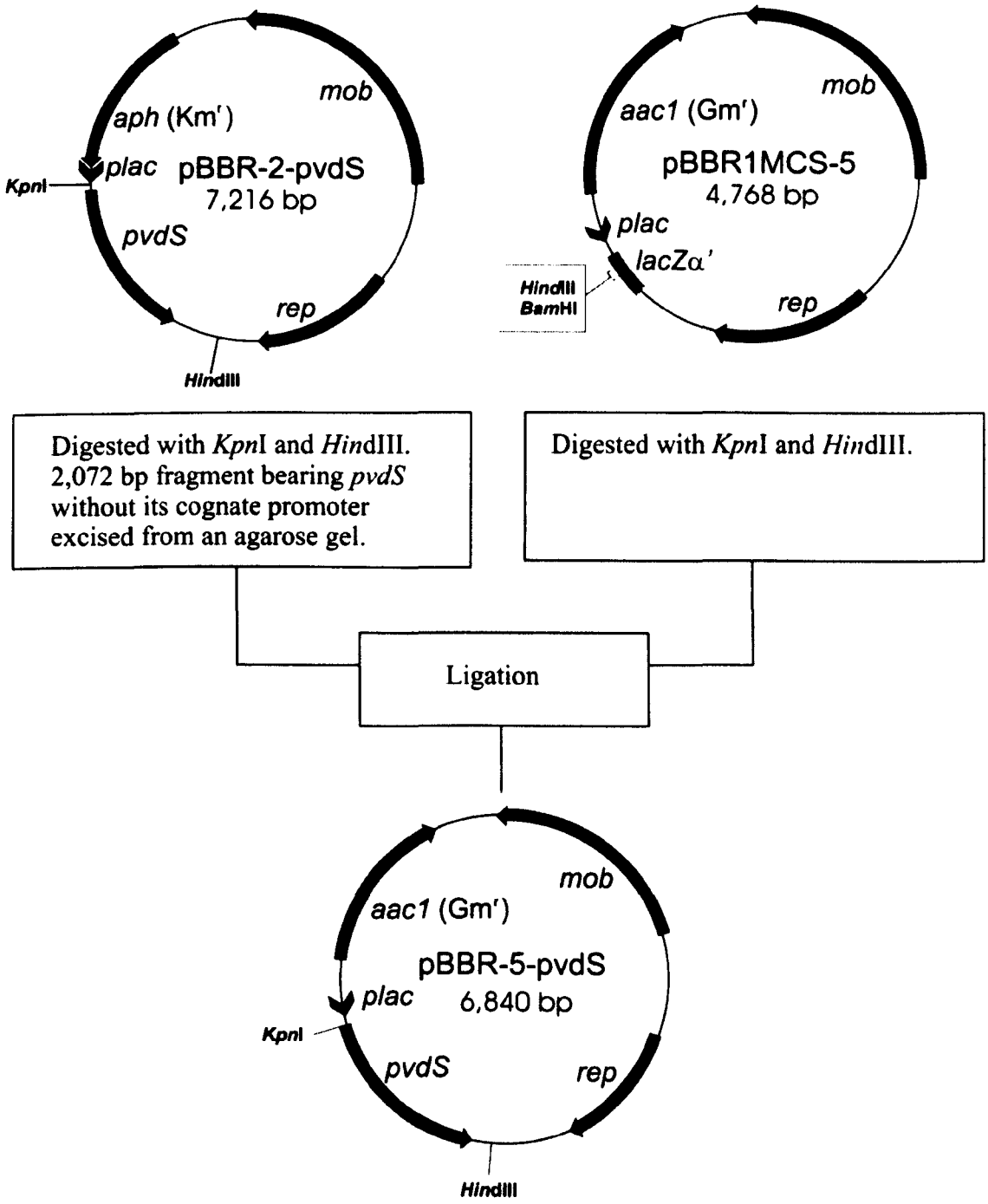

Figure 7.19: Scheme for the construction of pBBR-5-pvdS. Only pertinent restriction sites are shown.

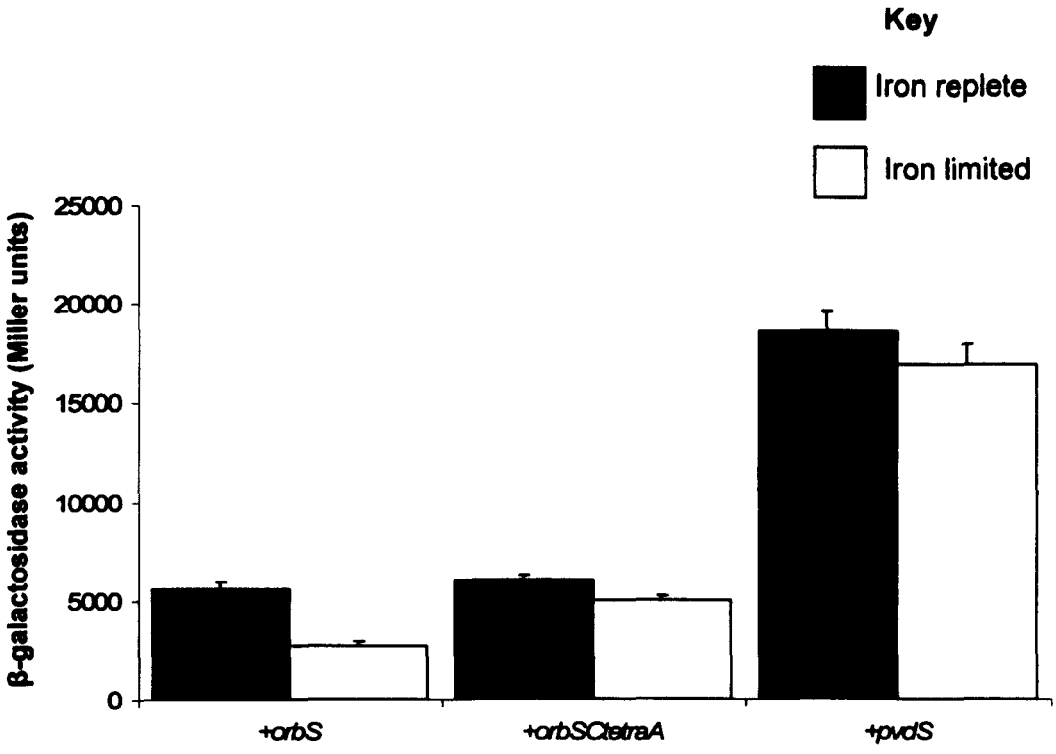

Figure 7.20: Iron-dependent regulation of *porbH* by OrbS in the absence of Fur. β-galactosidase assays were carried out on triplicate cultures of *E. coli* QC1732 cells containing pKAGd4-porbHds6 and pBBR1MCS-5 bearing the σ factor genes indicated along the x axis. These cells were grown in LB broth containing chloramphenicol and gentamycin, under iron replete and iron limited conditions. Activities were corrected by subtracting the activity of QC1732 containing pKAGd4-porbSds6 and pBBR1MCS-5. Error bars represent the standard deviation from the mean of the activities of each set of three cultures.

OrbSCtetraA or PvdS (Figure 7.20). In the presence of OrbS, however, *porbH* was ~2 fold less active under iron replete conditions than under iron starvation conditions. This suggests that some aspect of the OrbS protein, such as the C-terminal cysteines, may play a role in iron-dependent regulation of the ornibactin genes. In order to further investigate this possibility, attempts were made to purify OrbS, to allow spectroscopic analysis of any iron-binding properties of this protein.

7.3.4: Development of a system for purification of OrbS

To determine whether OrbS binds Fe^{2+}, as postulated in the cysteine-mediated iron co-ordination model shown in Figure 7.11, attempts were made to purify this protein for analysis by atomic absorption spectroscopy. This technique can be used to measure the concentration of different elements, such as iron, within samples. Two expression plasmids were constructed bearing *orbS*, using the parent plasmids pET-14b and pGEX-KG to 'tag' the OrbS product for ease of purification. pET-14b attaches an N-terminal hexahistidine (His6) tag to the protein product of a gene cloned within its MCS, allowing purification by a nickel or cobalt chelate column. pGEX-KG attaches an N-terminal glutathione S-transferase (GST) tag to the protein product of a gene cloned into its MCS, allowing purification using a glutathione resin column. *orbS* fragments were amplified by PCR, and inserted into these two expression vectors so that the reading frame of the amino acid tag was the same as that of *orbS*. The upstream endpoint of the *orbS* fragments cloned into the vectors was +26 relative to the TSS. The base at position +26 is the first base of the most upstream of the three candidate translational initiation codons for *orbS*. The construction of these vectors is detailed in Figures 7.21 and 7.22.

Overexpression of *orbS* in *E. coli* BL21λDE3 was carried out as described in Section 2.4.2. However, overproduction of OrbS from pET-orbS was inconsistent, despite attempts to ascertain optimal conditions for overexpression (BL21λDE3 cells containing pET-orbS were grown at 37 °C, and harvested 3 hours after induction of the *tac* promoter with 2 mM IPTG). When expression was successful, OrbS appeared to form inclusion bodies. It was therefore decided to proceed only with pGEX-orbS. SDS-PAGE analysis of *E. coli* BL21λDE3 cells containing pGEX-orbS grown at 37 °C demonstrated that a large quantity of protein of approximately the size expected for

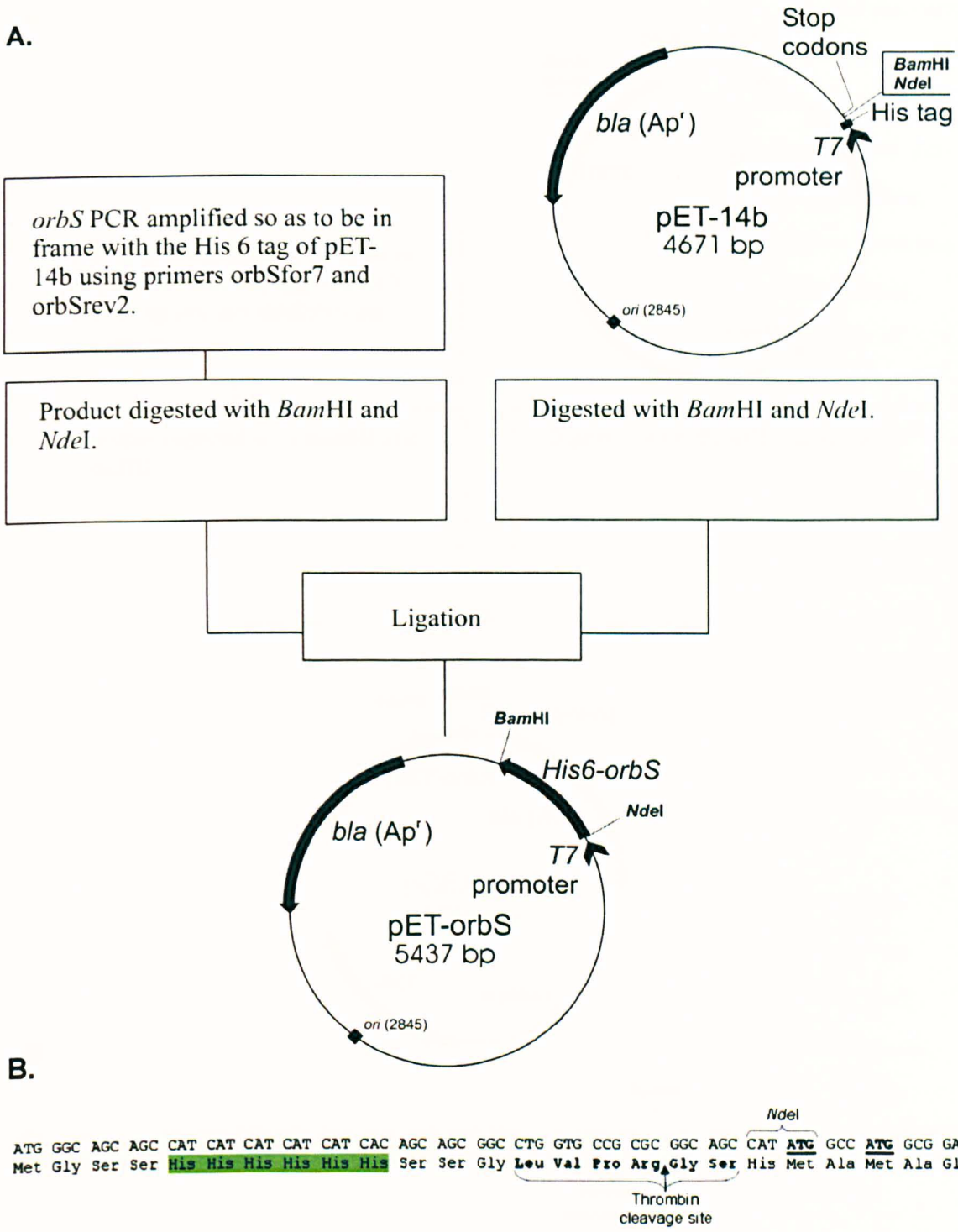

Figure 7.21: The construction of pET-orbS. **A.** Scheme for pET-orbS construction. Only pertinent restriction sites are shown. **B.** DNA and amino acid sequence showing the 6 His tag fused to *orbS* at the most upstream candidate start codon. The *Nde*I site used for the cloning of *orbS* is indicated. The three candidate *orbS* start codons are underlined and emboldened. The 6 His tag is highlighted in green, and the thrombin cleavage site is emboldened and labelled accordingly.

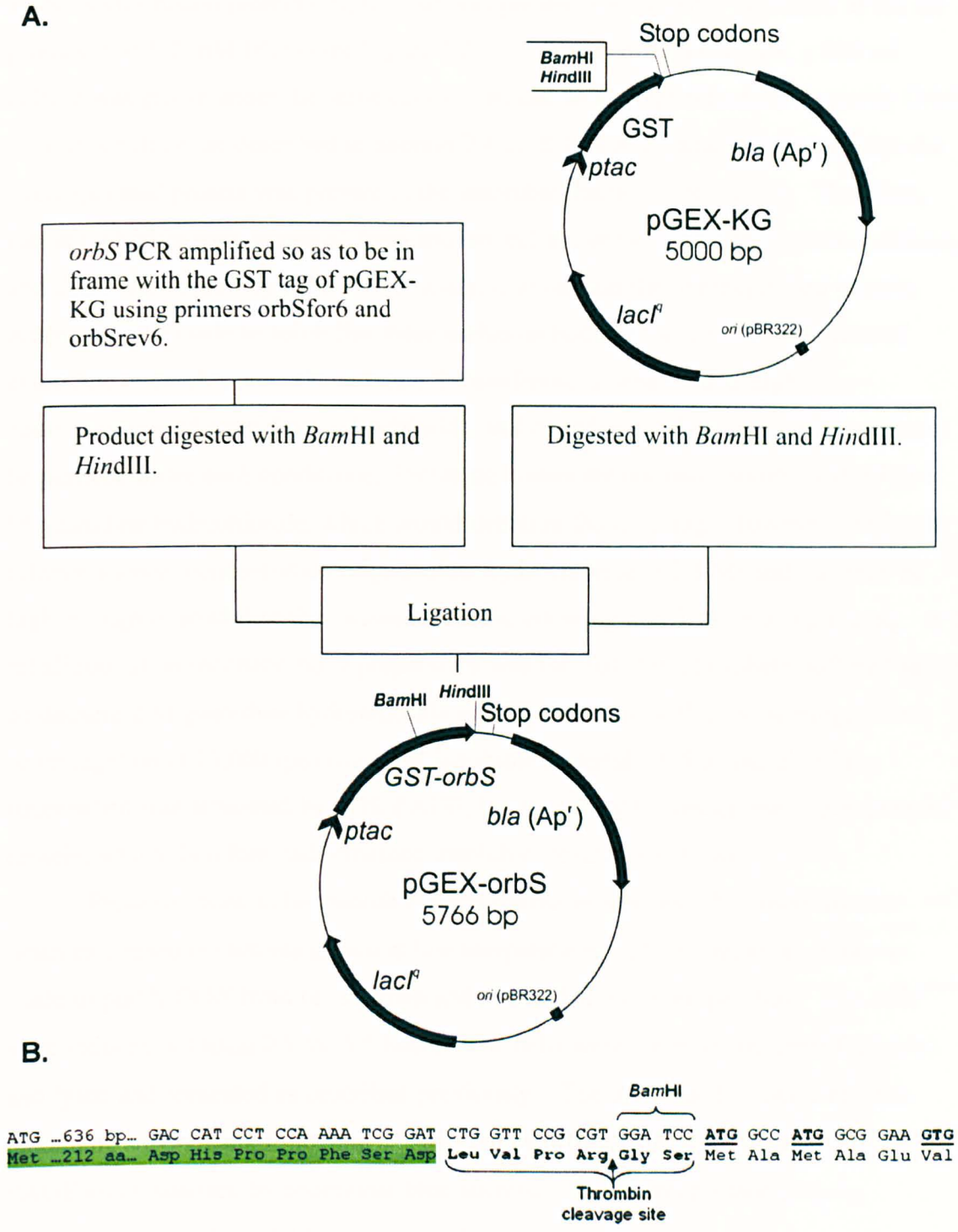

Figure 7.22: The construction of pGEX-orbS. **A.** Scheme for pGEX-orbS construction. Only pertinent restriction sites are shown. **B.** DNA and amino acid sequence showing the part of the GST tag fused to *orbS* at the most upstream candidate start codon. The *Bam*HI site used for the cloning of *orbS* is indicated. The three candidate *orbS* start codons are underlined and emboldened. The GST tag is highlighted in green, and the thrombin cleavage site is emboldened and labelled accordingly.

a GST-OrbS fusion protein (50,917 Da) was present 3 hours after induction of the *tac* promoter with 2 mM IPTG (see Figure 7.23). In a scaled-up procedure, a 500 ml culture was grown under the same conditions, and an attempt was made to purify OrbS from this culture, as described in Section 2.4.2. SDS-PAGE analysis showed that the overexpressed protein was present in the insoluble fraction (not shown). Therefore, inclusion bodies were prepared from another culture grown under the same conditions, and these were found by SDS-PAGE analysis to contain the overexpressed protein. Attempts were made to solubilise these inclusion bodies in a low concentration of guanidine hydrochloride. Glutathione S-transferase is denatured at high concentrations of guanidine hydrochloride, and therefore GST-tagged proteins cannot be purified under such conditions. Inclusion bodies are normally solubilised using 6 M guanidine hydrochloride, which would denature the GST-tag. However, GST can tolerate a lower concentration of guanidine hydrochloride (<2.5 M) and this may be high enough to solubilise the inclusion bodies, allowing purification using the tag. A 1 ml aliquot of an inclusion body preparation was incubated in phosphate buffered saline containing 2 M guanidine hydrochloride at 4 °C overnight with slow stirring, before centrifugation at 13,000 rpm to collect insoluble material. A 5 µl sample of the supernatant was separated by SDS-PAGE, but found not to contain the overexpressed protein, which therefore had remained insoluble (results not shown).

Proteins found to be insoluble when overexpressed are often more soluble when expressed in cultures grown at low temperatures. Therefore, an attempt was made to purify OrbS from cells grown and induced at room temperature. The cells were induced at OD_{600} 0.5 for 5.5 hours. The cells were collected by centrifugation, and lysed and sonicated as described previously. The total lysed sonicate and the remaining supernatant, following a clarifying centrifugation, were separated by SDS-PAGE and visualised by coomassie blue staining. The overexpressed protein, however, remained insoluble (result not shown).

If the purification of OrbS had been successful, it would not only have been analysed by atomic absorption spectroscopy, but would also have been used to raise antibodies for Western blot analysis. As pBBR-orbSΔP, pBBR-orbSΔP2, pBBR-orbSΔP-ptac and pBBR-orbSΔX (see Section 7.4.2) did not complement OM3 for ornibactin production, a Western blotting analysis would allow determination of whether OrbS was actually being produced from these plasmids. Functional

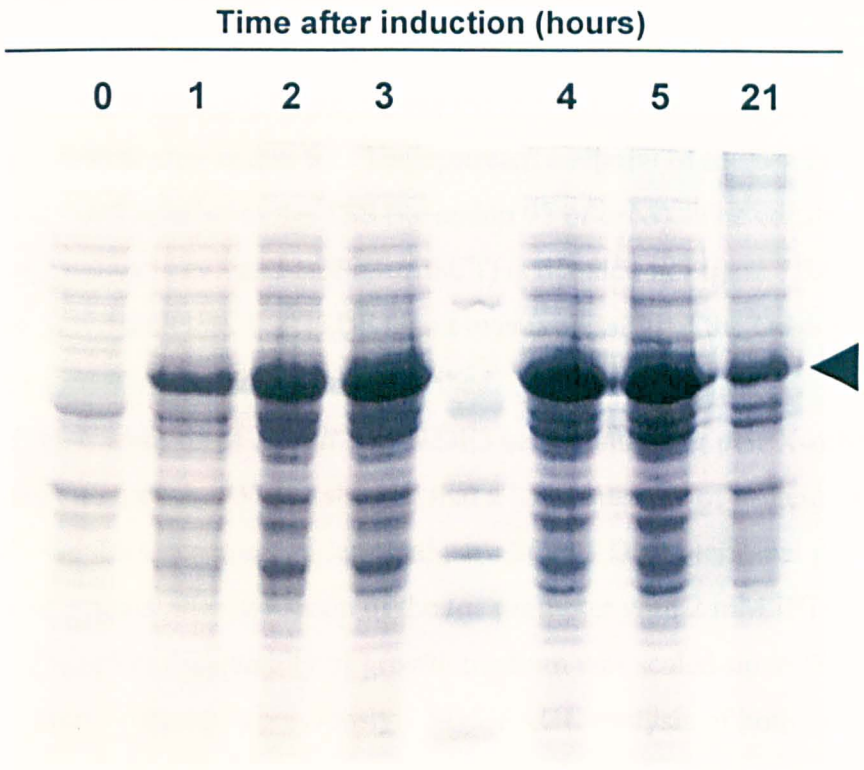

Figure 7.23: Polyacrylamide gel electrophoretic analysis of OrbS overproduction. *E. coli* BL21λDE3 cells containing pGEX-KG-orbS were grown at 37 °C in LB broth supplemented with ampicillin to OD600 0.5. 2 mM IPTG was added to induce expression of the *tac* promoter located upstream of *orbS*. Samples were taken at the timepoints (in hours) indicated above the gel photograph, and analysed by SDS-PAGE using a 12 % gel as described in Section 2.4.2. Ladder shown is Sigma Molecular Weight Marker (M.W. 14,000-66,000 Da). The black arrowhead indicates the band likely to constitute the overexpressed OrbS-GST protein (50,917 Da).

antibodies can be produced using only a part of a protein, and it was conjectured that one half of OrbS, when overproduced, might not form inclusion bodies. Therefore, DNA fragments encoding N-terminal and C-terminal segments of OrbS were cloned into pGEX-KG, to investigate whether either part was soluble when overproduced.

orbS fragments were amplified by PCR, and inserted into pGEX-KG so that the reading frame encoding the GST tag was the same as that of *orbS*. The upstream endpoint of the *orbS* N-terminal fragment was the same as for *orbS* cloned into pGEX-orbS, and it terminated after codon 92. The upstream endpoint of the *orbS* C terminal fragment was at +308 relative to the TSS (i.e codon 93 of *orbS*). The construction of these vectors (pGEX-orbSNT and pGEX-orbSCT) is detailed in Figure 7.24. The plasmids were introduced into BL21λDE3, and overexpression of the OrbS protein fragments was carried out as previously described.

SDS-PAGE analysis of *E. coli* BL21λDE3 cells containing pGEX-orbSNT and pGEX-orbSCT, grown at 37 °C, showed that a large quantity of protein of approximately the sizes expected (N-terminal part: 36,395 Da, C-terminal part: 40,832 Da) was present 3 hours after induction of the *tac* promoter with 2 mM IPTG (see Figure 7.25). Therefore the quantity of growth medium was scaled-up to 500 ml and the experiment was repeated as previously. SDS-PAGE analysis of both the total and soluble protein fractions was carried out, and both the C-terminal and N-terminal overexpressed OrbS sections were found to be insoluble (Figure 7.25). Owing to time constraints, attempts to purify OrbS were ceased at this point.

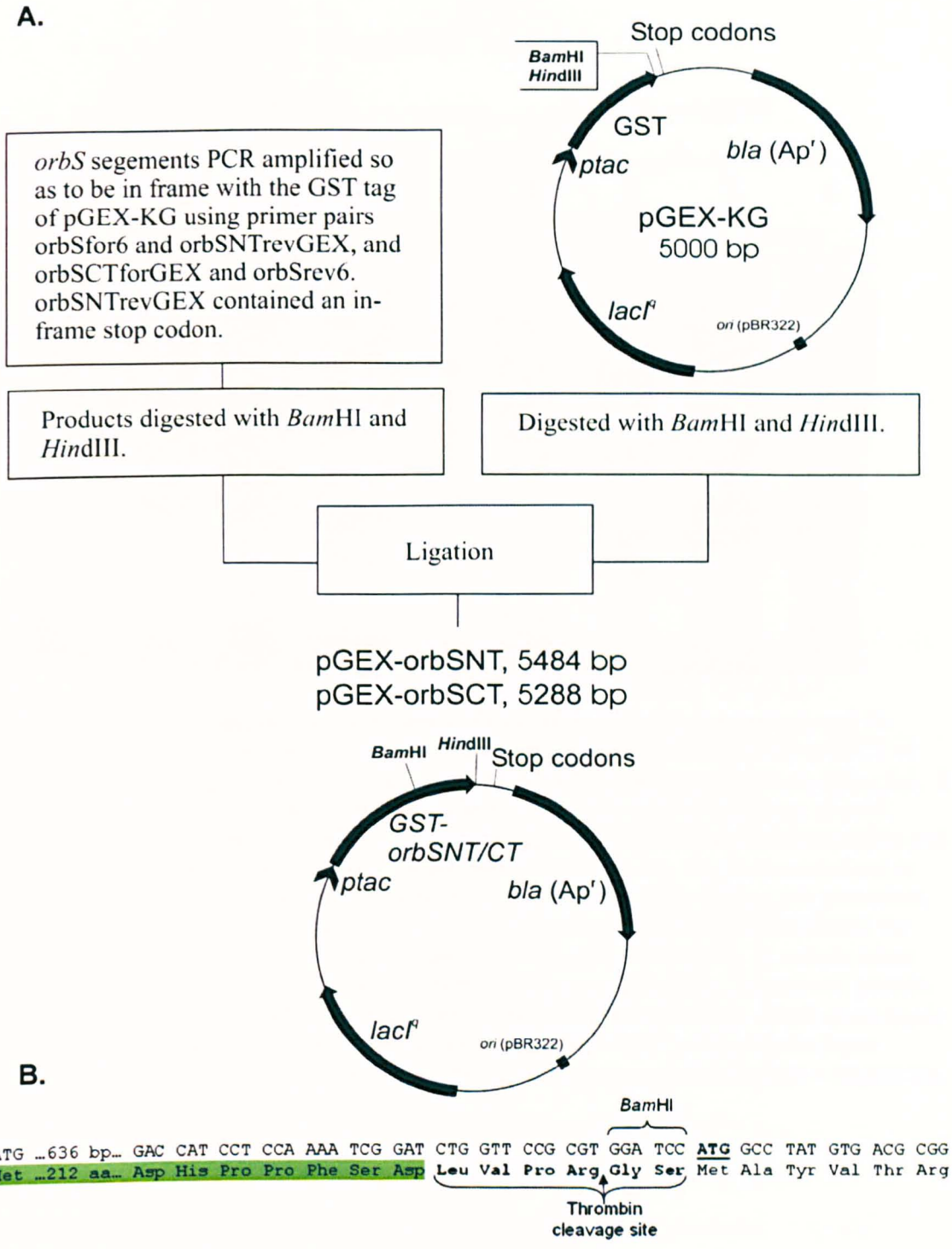

Figure 7.24: The construction of pGEX-orbSNT and pGEX-orbSCT. **A.** Scheme for pGEX-orbSNT and pGEX-orbSCT construction. Only pertinent restriction sites are shown. **B.** DNA and amino acid sequence showing the part of the GST tag fused to *orbS* in pGEX-orbSCT. The *Bam*HI site used for the cloning of *orbS* is indicated. The GST tag is highlighted in green, and the thrombin cleavage site is emboldened and labelled accordingly. The corresponding sequence of pGEX-orbSNT was as shown in Figure 7.21 B.

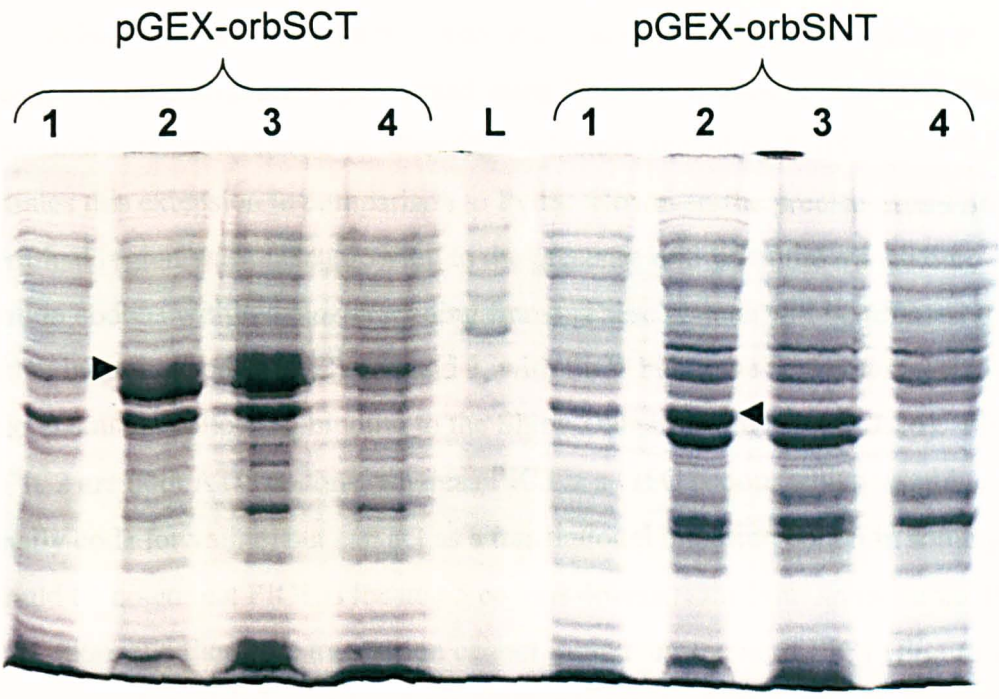

Figure 7.25: Polyacrylamide gel electrophoretic analysis of OrbS C-terminal and N-terminal fragment overexpression. *E. coli* BL21λDE3 cells containing pGEX-orbSCT or pGEX-orbSNT were grown at 37 °C in LB broth supplemented with ampicillin to OD_{600} 0.5. 2 mM IPTG was added to induce expression of the *tac* promoter located upstream of *orbS*. Cells were harvested three hours after induction, resuspended in phosphate buffered saline and sonicated, as described in Section 2.4.2. A clarifying centrifugation was then carried out to remove insoluble material. Samples were taken at various time points during this procedure, and analysed by SDS-PAGE using a 12 % gel. The plasmid present within BL21λDE3 for each sample analysed has been indicated. Lane numbering was as follows: 1, sample taken immediately prior to induction. 2, sample taken 3 hours post-induction. 3, total cell protein. 4, total soluble protein. Protein ladder (L) was Proteoladder 100 (Norgen). Black arrowheads indicate the bands likely to represent the overexpressed OrbS-GST proteins in the lanes numbered 2. Predicted sizes corresponded to the protein markers, OrbSCT-GST = 40,832 Da, OrbSNT-GST = 36,395 Da.

7.4: Investigation of the N-terminal region of OrbS

A BLASTP search using the OrbS amino acid sequence, followed by a multiple sequence alignment (performed using ClustalW), showed that OrbS bears an N- terminal extension relative to other ECF σ factors, including PvdS. Figure 7.9 illustrates this extension in comparison to PvdS. However, the precise extent of this N-terminal region was unclear, owing to the presence of 3 potential translation initiation codons within the *orbS* reading frame. These codons will be referred to as putative initiation codon (PIC) 1, 2 and 3, with PIC1 being the first codon a ribosome would encounter following binding to the Shine-Dalgarno site (Figure 7.26). PIC1 and PIC2 are both ATG codons, whereas PIC3 is a GTG codon, which would normally code for valine, but can act as a translational initiation codon in some genes. It should be noted that PIC1 is located 5 codons downstream from an in-frame TGA (stop) codon, and therefore translation cannot initiate upstream of PIC1 (Figure 7.26). The next possible initiation codon from PIC3 is located a further 42 codons downstream. This GTG codon was considered unlikely to serve as the initiation codon for *orbS*, as it is not preceded by a Shine-Dalgarno sequence. In order to determine the length of the N-terminal extension of OrbS, identification of the true translational initiation codon was necessary.

7.4.1: Identification of the *orbS* translation initiation codon

To determine which, if any, of the putative initiation codons (PICs) is responsible for transcriptional initiation, derivatives of pBBR1MCS were constructed bearing *orbS* containing codon substitution mutations at these PICs, resulting in a termination codon or a codon for an amino acid other than methionine. The ability of these plasmids to rescue ornibactin production by OM3 was then assayed.

SOE PCR, described in Section 2.2.1, was used to introduce mutations at the PICs. A mutagenic reverse primer overlapping the codon to be altered, covering at least 10 bases on either side of this mutation, was used in a PCR with primer orbSfor to produce a 'megaprimer', using pBBR-orbS DNA as a template. This megaprimer was purified using the Qiagen PCR purification kit, and used in a second amplification

Figure 7.26: The *orbS* coding sequence. The three potential translational initiation codons (PIC1-PIC3) have been emboldened and labelled accordingly. The *Nco*I site used in the construction of pBBR-orbSΔX (Section 7.4.2) has been underlined. Stop codons in-frame with the *orbS* reading frame (including one located 13 bp upstream of PIC1) have been shown in upper case and emboldened. An asterisk indicates the *orbS* termination codon. The -10 and -35 elements of the *orbS* promoter (as determined by primer extension analysis) have been enclosed in boxes and highlighted green. The putative Shine-Dalgarno sequence for *orbS* is shown in red.

with primer orbSrev2 to generate the full-length *orbS* gene, once again using pBBR-orbS as the template. The resultant fragments were digested with *Bam*HI and *Hin*dIII, and inserted into the corresponding sites of pBBR1MCS (Figure 7.27). The *orbS* fragments thus produced had identical endpoints to the *orbS* fragment present in pBBR-orbS, which was used successfully to complement OM3 for ornibactin production (Figure 7.16).

Codon substitution plasmids constructed were as follows: pBBR-orbSi1-TAA (which contained *orbS* with a nonsense codon substituted for PIC1), pBBR-orbSi2-TAA (which contained *orbS* with a nonsense codon substituted for PIC2), pBBR-orbSi3-TAA (which contained *orbS* with a nonsense codon substituted for PIC3), pBBR-orbSi2-GCC (which contained *orbS* with an alanine codon substituted for PIC2), pBBR-orbSi3-GTC (which contained *orbS* with a non-initiating valine codon substituted for PIC3). These plasmids were introduced into *B. cenocepacia* OM3 by conjugation. The resultant strains were then analysed for their ability to produce ornibactin using the CAS plate assay.

Introduction of *orbS* containing a nonsense codon in place of the PIC3 GTG did not complement OM3 for ornibactin production, whereas introduction of *orbS* bearing an alternative valine codon at that position led to the production of a similar amount of ornibactin to OM3 complemented with pBBR-orbS (Figure 7.28). This suggests that translation initiates upstream of this codon. Substitution of a nonsense codon for PIC1 did not abolish the ability of *orbS* to complement OM3 for ornibactin production, although it did reduce production somewhat, as evidenced by the smaller halo produced by OM3 containing this construct compared to OM3 containing pBBR-orbS. The plasmid bearing *orbS* in which PIC2 was altered to a nonsense codon failed to complement OM3 for ornibactin production, while substitution of an alanine for PIC2 resulted in a large reduction in ornibactin production. The small amount of ornibactin produced by OM3 harbouring *orbS* with an alanine codon in place of PIC2 probably results from inefficient initiation at PIC1. These results indicate that PIC2 is probably the initiation codon for *orbS* translation, and that the N-terminal extension of OrbS relative to PvdS is 29 amino acids in length.

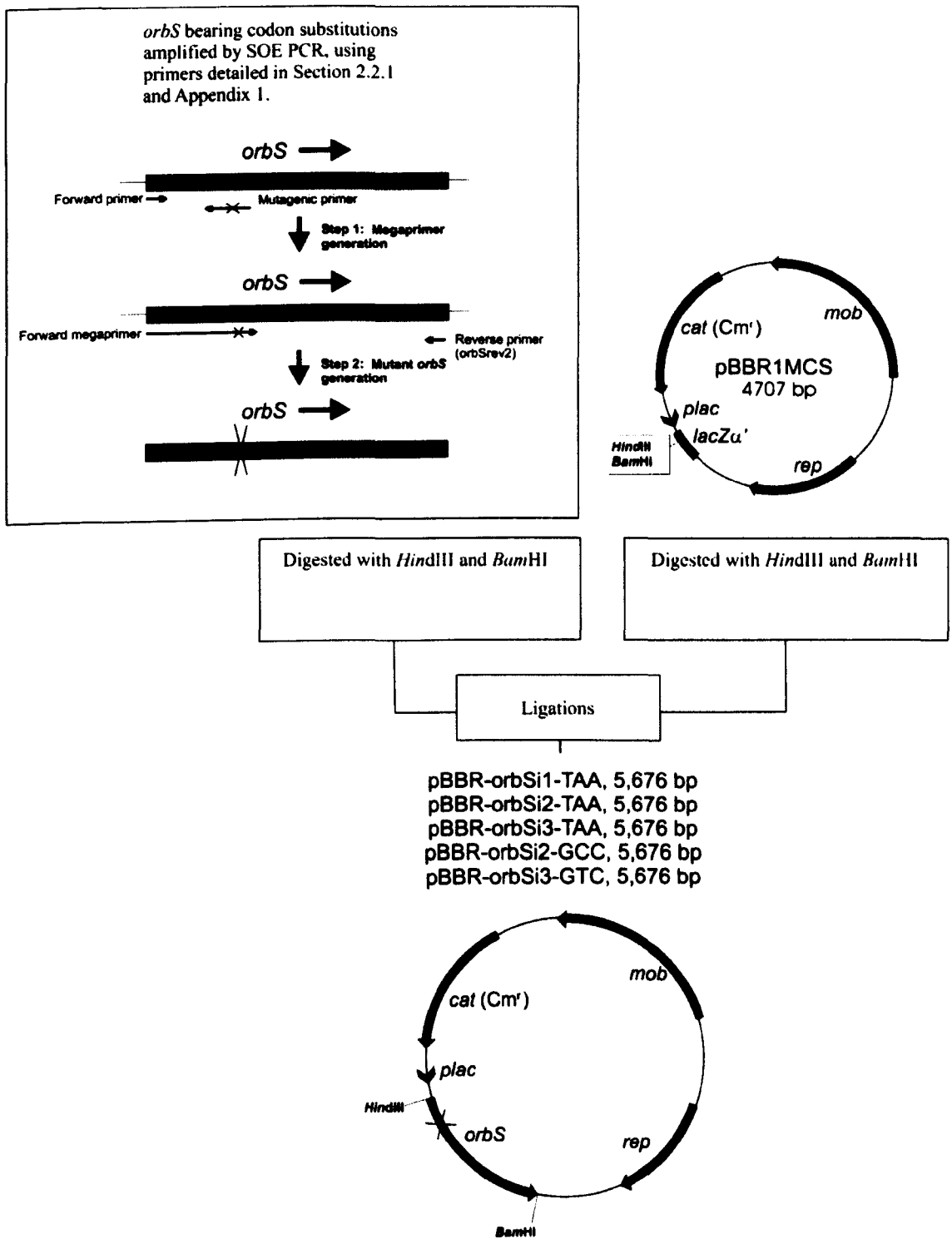

Figure 7.27: Scheme for the construction of pBBR-orbS bearing mutations within the possible *orbS* translation initiation codons. All pBBR-orbS derivatives contain the *orbS* promoter. Only pertinent restriction sites have been shown. Translation initiation codon substitutions are represented as a large cross.

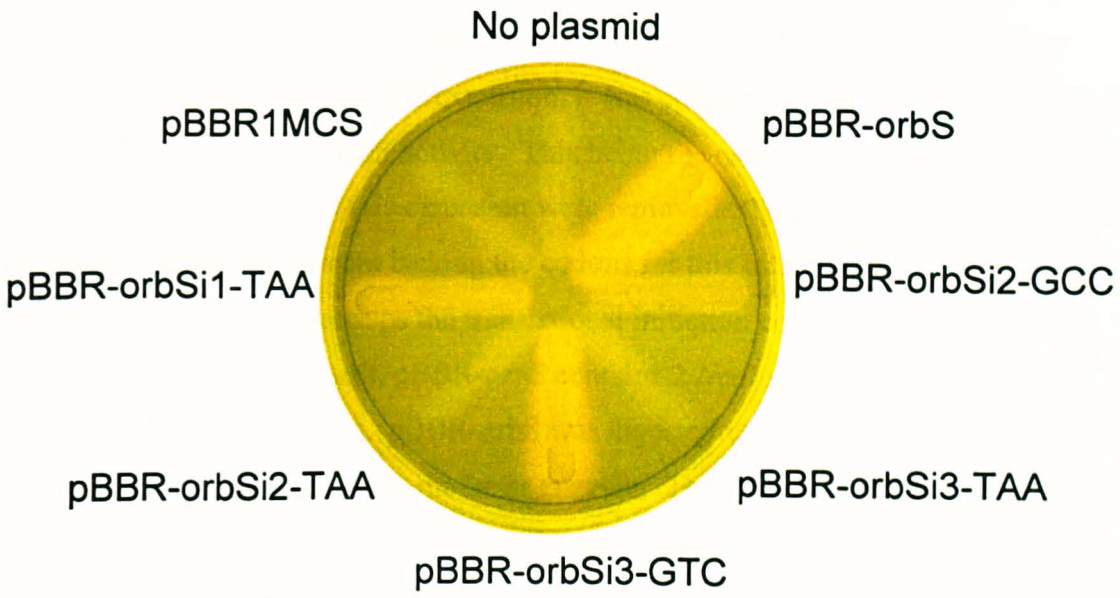

Figure 7.28: identification of the *orbS* translational initiation codon. Cultures of *B. cenocepacia* OM3 containing the plasmids indicated were grown overnight at 37 °C, and streaked on a CAS plate containing 10 μM $FeCl_3$, which was incubated at 37 °C for ~16 hours.

7.4.2: Investigation of the importance of the N-terminal extension of OrbS

Since OrbS and MbaS appear to be the only ECF σ factors harbouring the previously discussed N-terminal extension, it was considered that this extension might play a role in regulating OrbS activity. This being the case, it was possible that OrbS would retain its activity if this extension were removed. To investigate this possibility, an *orbS* fragment lacking the codons for this extension was constructed as follows. An *Nco*I site overlaps the translational initiation codon for *orbS* (i.e. PIC2, see Figure 7.26). As a result, pBBR-orbS contains 2 *Nco*I sites (the other site being located within the *cat* gene). pBBR-orbS was digested with *Bam*HI and *Nco*I, so as to gain only partial digestion with the latter enzyme. The large vector DNA fragment (~5 kb), corresponding to pBBR-*orbS* cut at the *Bam*HI site and the *Nco*I site within *orbS*, was extracted from an agarose gel. This fragment contained the *orbS* promoter and translational initiation codon.

Part of the *orbS* gene was amplified by PCR, utilising pBBR-orbS DNA as a template, using a forward primer (orbSΔX) complementary to the codons immediately downstream of the N-terminal extension coding sequence, and containing an *Nco*I site at its 5' end. The resultant DNA fragment lacked the codons for the N-terminal extension, except for the translation initiation codon (i.e. codons 2-29 were deleted). This amplified *orbS* fragment was digested with *Bam*HI and *Nco*I, and inserted into the previously digested pBBR-orbS vector fragment DNA, to produce pBBR-orbSΔX (Figure 7.29). Figure 7.30 shows the predicted amino acid sequence of OrbS without its N-terminal extension, as encoded by pBBR-orbSΔX.

pBBR-orbSΔX was introduced into the *B. cenocepacia* ornibactin mutant OM3 by conjugation. OM3 containing pBBR-orbSΔX was streaked onto CAS agar, alongside OM3 bearing pBBR1MCS and OM3 bearing pBBR-orbS (Figure 7.31). OM3 harbouring pBBR-orbSΔX did not give rise to a halo when streaked on this medium, whereas pBBR-orbS restored the ability of OM3 to produce siderophores. It was unclear whether or not *orbS* was being translated (even though the OrbS Shine-Dalgarno site was present) or if the mutant OrbS protein was non-functional or highly unstable. To determine whether any OrbS activity was present, a more sensitive assay for OrbSΔX activity was designed.

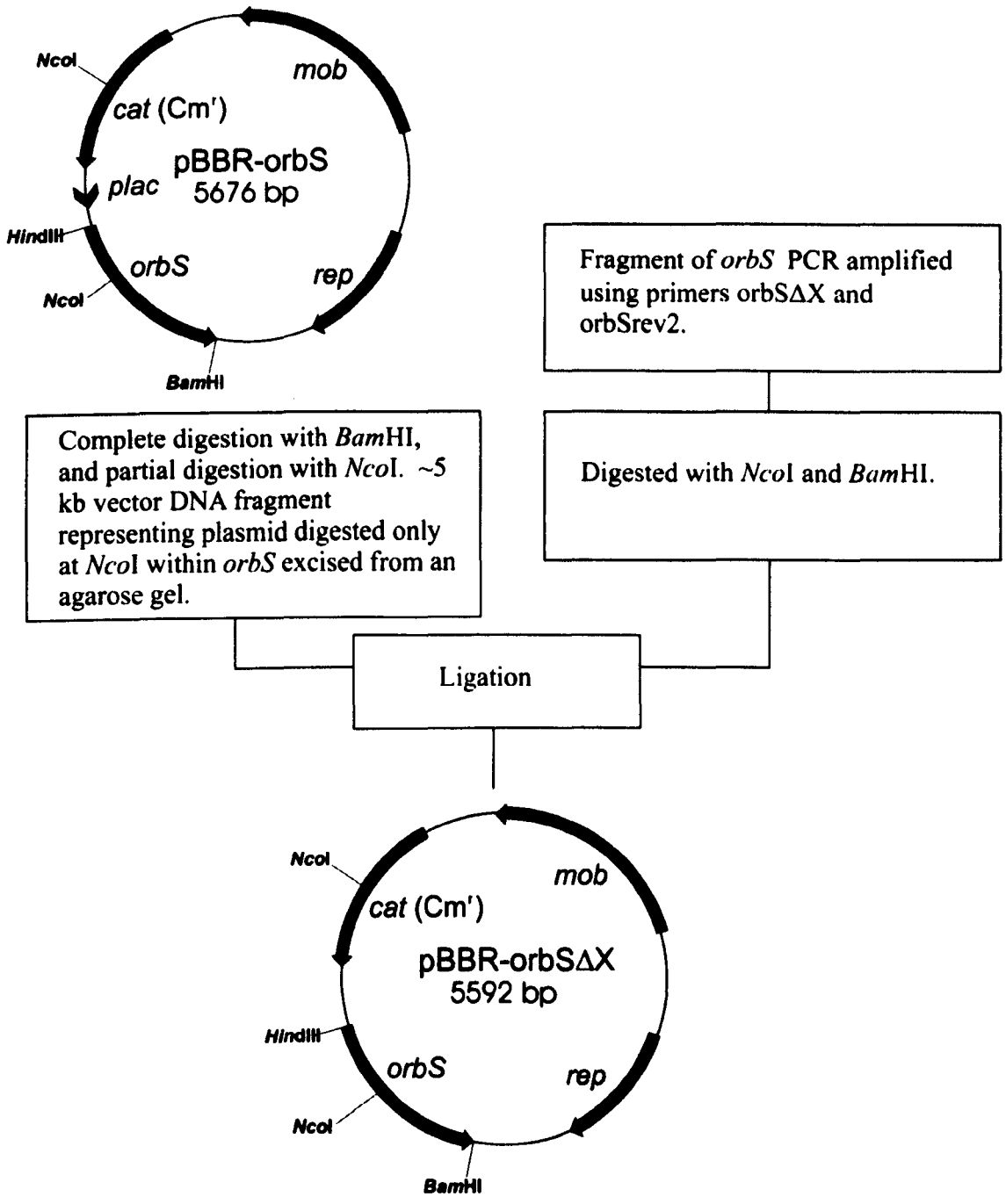

Figure 7.29: Scheme for the construction of pBBR-orbSΔX. The orbSrev2 primer overlaps the 5'end of the downstream *orbH* gene. Only pertinent restriction sites are shown.

```
OrbS      1   MAEVLDRPAAAAANPFLGSYPDLPPRAAPRARRASEPRAQGALLDVLISHRAMLVNVA
OrbSΔX    1   ----------------------------MAARRASEPRAQGALLDVLISHRAMLVNVA
PvdS      1   ----------------------------MSEQLSTRRCDTPLLQAFVDNRTLLVKIA
```

Figure 7.30: The N-terminal amino acid sequence of OrbSΔX. An alignment of the N-termini of OrbSΔX, OrbS and PvdS is shown.

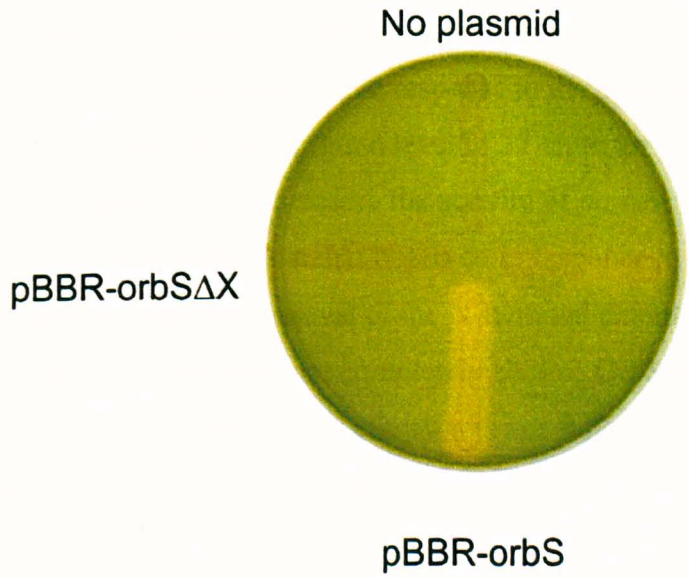

Figure 7.31: pBBR-orbSΔX fails to complement OM3 for ornibactin production. Cultures of *B. cenocepacia* OM3 containing the plasmids indicated were grown overnight at 37 °C, and streaked on a CAS plate containing 10 μM $FeCl_3$, which was incubated at 37 °C for ~16 hours. The unlabelled streak was not part of this experiment.

7.4.3: Detection of OrbSΔX activity using an *orbH-lacZ* fusion.

As a more sensitive test for OrbSΔX activity, it was decided to assay transcription from an OrbS-dependent promoter. The *E. coli* model system used successfully to assay *porbH* activity (see Chapter 6) was employed for this purpose. The *orbH* promoter was provided using pKAGd4-porbHds6 (see Section 6.4.2), which contains a *porbH-lacZ* fusion. As the selectable marker present within both pBBR-orbSΔX and pKAGd4-porbHds6 is the chloramphenicol resistance gene, *cat*, a pBBR1MCS-2 derivative was constructed bearing the truncated *orbS* fragment. Thus, pBBR-orbSΔX was digested with *Bam*HI and *Hin*dIII, and the ~900 bp *orbS* fragment excised from an agarose gel for insertion between the corresponding sites in pBBR1MCS-2, giving rise to pBBR-2-orbSΔX. This plasmid was introduced into *E. coli* MC1061 cells containing pKAGd4-porbHds6 by transformation. Cells were grown for β-galactosidase assay in LB broth containing chloramphenicol and kanamycin under iron limiting conditions, to maximise *orbSΔX* expression. A low level of *porbH* activity was observed in response to the presence of pBBR-2-orbSΔX (233 Miller units above the background level of 37 units for pBBR1MCS-2 and pKAGd4) (see Figure 7.32). Therefore the activity of *porbHds6* in response to pBBR-2-orbSΔX was 13 fold lower than that observed in response to pBBR-2-orbS. These results demonstrated that the removal of the N-terminal extension of OrbS significantly decreases but does not completely abolish OrbS-dependent promoter activity. Presumably the remaining activity was not sufficient in OM3 to give a positive result with the CAS plate assay.

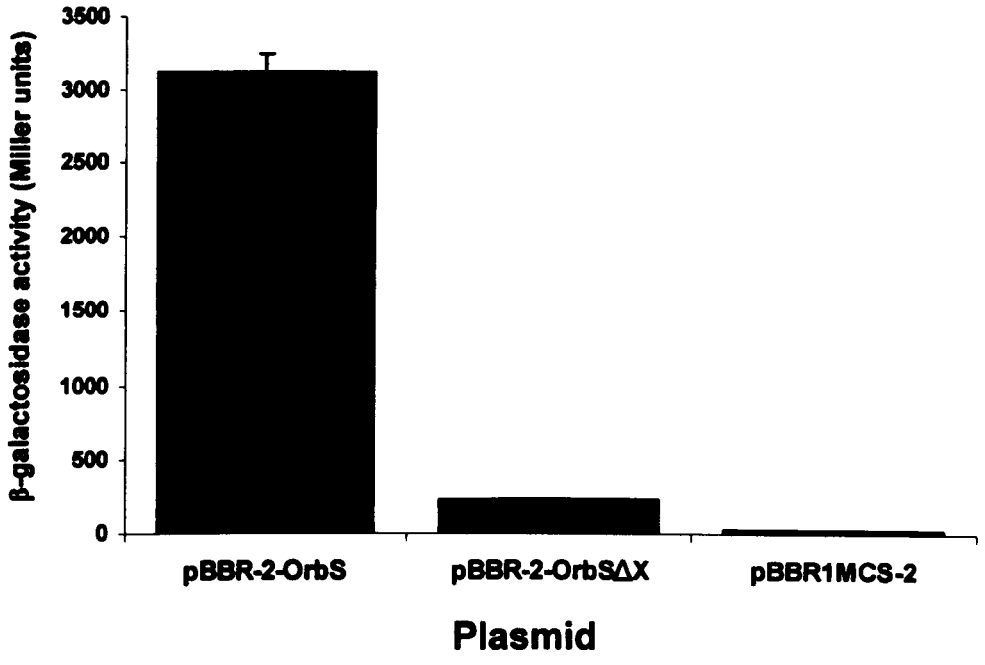

Figure 7.32: Detection of OrbSΔX-dependent transcriptional activity in *E. coli*. β-galactosidase assays were carried out on triplicate cultures of *E. coli* MC1061 containing pKAGd4-porbHds6 and the plasmid indicated below the x-axis. These cells were grown in LB broth containing chloramphenicol and kanamycin, under iron limited conditions. Values were corrected by subtracting the activity of MC1061 containing pKAGd4 and the plasmid indicated below the x-axis. Error bars represent standard deviation from the mean of the activities of the triplicate cultures.

7.5: Discussion

The *orbS* promoter is directly regulated by Fur, as demonstrated by the FURTA and EMSA. The OrbS-dependent promoters are not directly regulated by Fur, but they are indirectly regulated by Fur through its involvement in the regulation of OrbS production. FURTA and EMSA analysis of *porbS* bearing upstream deletions indicated that Fur binds between -40 and +5 relative to the TSS for *orbS*. A 13 out of 19 bp match to the (*E. coli*) consensus Fur box overlaps the *orbS* promoter, and is located between these positions on the template strand (GTAAACGCAAATCATTCTC, bases that match the consensus Fur box are underlined) (Figure 7.33). This is very likely to act as the Fur box for the *orbS* promoter. This potential Fur binding site was initially overlooked, being a fairly poor match to the consensus.

Clear mobility shifts occurred when the *porbS* fragments with upstream endpoints of -69 and -40 were incubated with Fur. Indeed, there appear to be two shifted species occurring between concentrations of 50 and 200 nM Fur. Based on the structure of Fur, it appears that two Fur dimers bind to the 19 bp Fur box, one dimer on each side of the DNA molecule (Pohl *et al.*, 2003). It is possible, therefore, that the faster migrating shifted species occurs as a result of only one Fur dimer binding to the fairly poor Fur box overlapping *porbS* at lower Fur concentrations. An additional (third) shifted species of even lower mobility was observed for the *orbS* fragment with an upstream endpoint of -69 at Fur concentrations $\geq$ 400 nM. This was probably the result of low-affinity binding of an additional Fur dimer to DNA upstream of the Fur box, as has been observed at the *pvdS* promoter (Ochsner *et al.*, 1995).

The four cysteine residues located at the C-terminus of OrbS may be involved in direct regulation of OrbS activity in response to iron availability. This was evident by loss of an iron-dependent, two-fold repression of OrbS-directed transcription from an OrbS-dependent promoter in a *fur*$^-$ background. However, this was only observed when all four C-terminal cysteines were substituted. A number of regulatory mechanisms involve the co-ordination of metal ions by the thiol group of cysteine residues, in a similar manner to that proposed for the direct modulation of OrbS activity. The proteins involved in this form of regulation are known as 'thiol based

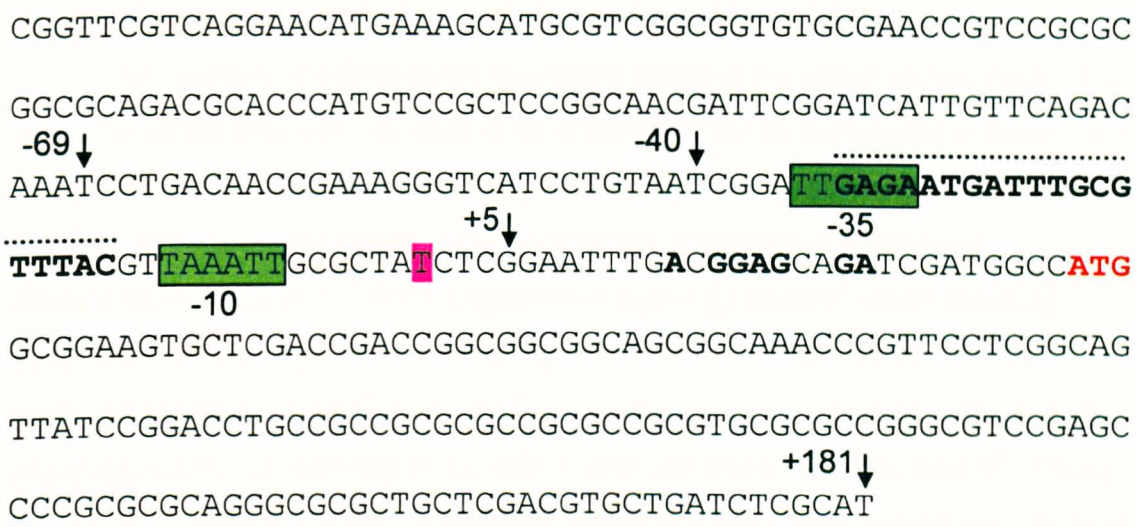

Figure 7.33: Location of the Fur box at the *orbS* promoter region of *B. cenocepacia* 715j. The -35 and -10 regions of the promoter are highlighted in green and enclosed in boxes. The *orbS* translational initiation codon has been emboldened and shown in red. The putative Shine-Dalgarno region has been indicated by emboldening bases complementary to the 3' end of *B. cenocepacia* 16S RNA. A dotted line indicates the probable Fur binding site overlapping the *porbS* -35 region. Arrows show the endpoints of *orbS* promoter fragments constructed during this study, with locations indicated relative to the TSS, which is highlighted in purple. +181 indicates the downstream endpoint of each of these fragments, while the remaining arrows represent upstream endpoints

regulatory switches'. The cysteine thiols in these proteins co-ordinate a metal ion (generally Zn^{2+}) under reducing conditions, but release the metal to form cystines under oxidizing conditions, changing the activity of the protein (Paget and Buttner, 2003). Cystine, where 2 cysteines are linked by a disulphide bond, is an important feature of the structure of many proteins (Paget and Buttner, 2003).

An example of a thiol-based regulatory switch is the anti-σ factor, RsrA. Anti-σ factors inhibit promoter recognition by σ factors either by binding the σ factor when free or in complex with the RNA polymerase holoenzyme. RsrA is the anti-σ of σ^R, which is responsible for transcription of oxidative stress response genes of *Streptomyces coelicolor*. RsrA (regulator of sigma R) binds σ^R under reducing conditions, preventing it from associating with core RNA polymerase. This is mediated by the co-ordination of a Zn^{2+} ion by three cysteine residues in RsrA under reducing conditions, resulting in a conformation that allows RsrA to bind σ^R. Under oxidizing conditions, the Zn^{2+} is released, preventing RsrA from competing effectively with core RNA polymerase for σ^R (Paget *et al.*, 2001).

The simple co-ordination of one Fe^{2+} by four cysteines, as takes place in rubredoxin, is not the only type of iron-sulphur cluster. A number of other types of cluster exist, which involve three to six cysteines, and also free sulphur. In addition to the rubredoxin-type cluster, two other forms of iron-sulphur cluster are known that involve four cysteines. These are the [2Fe-2S] and [4Fe-4S] clusters, present in the xanthine oxidase and iron hydrogenase protein families respectively (see Figure 7.34) (Kiley and Beinert, 2003; Brzóska *et al.*, 2006). If the C-terminal cysteines of OrbS do indeed form an iron-sulphur cluster, this could take the form of rubredoxin, or of one of these more elaborate clusters.

Mutational analysis of the putative initiation codons of *orbS* indicated that translation initiates from an ATG codon located 32 bp downstream from the *orbS* TSS (Figure 7.34). The reduction in *orbS* expression observed when the preceding ATG codon was substituted with a stop codon may be the result of less efficient binding of the 30S ribosomal subunit to mRNA, as a result of altering the sequence flanking the initiation codon. This might also occur as a result of translation being initiated partially from PIC1, supported by the production of a small amount of ornibactin by OM3 containing pBBR-orbSi2-GCC.

The N-terminal extension is clearly very important for OrbS function, as

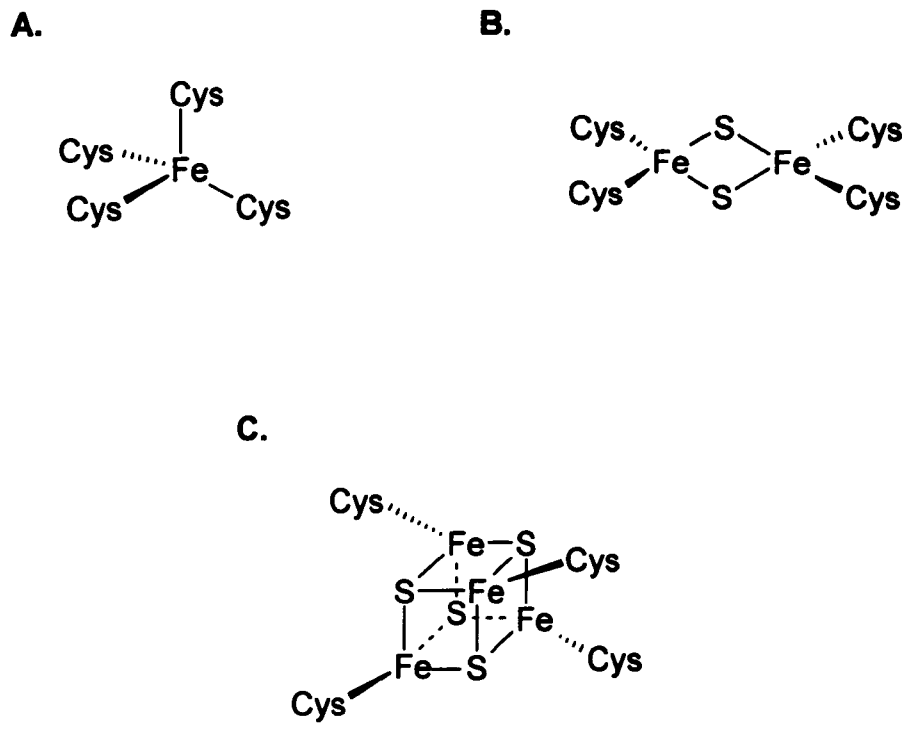

Figure 7.34: Iron-sulphur clusters involving four cysteines. A. Rubredoxin-type cluster. B. [2Fe-2S] cluster. C. [4Fe-4S] cluster. Adapted from Kiley and Beinert, 2003 and Brzóska *et al.*, 2006.

removal of this extension resulted in the inability of OrbS to complement a *B. cenocepacia orbS* null mutant. However, it is not possible at this stage to conclude whether this is owed to decreased translation of *orbS* mRNA, decreased stability of the OrbS protein or the impairment of OrbS activity. Western blot analysis could be used to compare the abundance of the OrbS and OrbSΔX proteins produced by OM3 containing the appropriate pBBR1MCS derivative, and hence determine if the removal of the N-terminal extension has resulted in a decrease in the translation of *orbS*.

Chapter 8

Final discussion and future directions

8.1: Final discussion

This study aimed to investigate the regulation of the ornibactin production and utilisation genes of *B. cenocepacia*. Ornibactin production and utilisation were found to be specified by an operon, which is dependent upon the alternative σ factor OrbS for its transcription. This operon appears to be transcribed from 3 OrbS-dependent promoters and, in addition, from read-through transcription originating from the σ^{70}-dependent *orbS* promoter. Iron-dependent regulation of the ornibactin operon is mediated by Fur, which controls *orbS* transcription. In addition, a more novel mechanism might operate, whereby the activity of OrbS is directly modulated by intracellular iron concentrations. Figure 8.1 illustrates aspects of the *orbS* regulatory region investigated during this study, and the results obtained.

The translational initiation codon for OrbS was determined (Figure 8.1). This showed that OrbS has a 29 amino acid N-terminal extension relative to PvdS, which does not align with any other ECF σ factors, apart from its putative orthologue in *B. pseudomallei*, MbaS. This extension is essential to OrbS function, although its purpose is as yet unknown.

A number of features necessary for promoter recognition by OrbS have been determined. These are a -35 element consisting of TAAA, followed downstream by 4 bases that continue the relatively straight, rigid conformation of this region (generally A residues). The -10 element consists of CGTC, and is followed downstream by four bases, which are upstream of an A+G rich block of ~9 nt.

An alternative σ factor of *P. aeruginosa*, PvdS, which shares 33 % identity with OrbS, recognises OrbS-dependent promoter sequences, although its own promoter consensus does not fulfil the requirements for recognition by OrbS. The most important components of the functional PvdS-dependent promoter sequence appear to be TAA (A/T)(A/T) (N_{16})CGT(N_8). Six nucleotides are present immediately downstream of this which have high AG content. PvdS is responsible for the transcription of a large number of genes in response to iron limitation, which constitutes a signal that the bacterium has entered a host organism. These genes comprise not only those specifying pyoverdine utilisation and biosynthesis, but also a number of virulence factors, such as an endoprotease, PrpL, and (indirectly) exotoxin A.

Figure 8.1: The *orbS* promoter region of *B. cenocepacia* 715j. The -35 and -10 regions of the promoter, as determined by primer extension and reporter analysis, are highlighted in green and boxed. Upstream sequences resembling a σ^{70}-type promoter have been highlighted in yellow and boxed. Possible codons for translation initiation have been emboldened and shown in red. The actual translation initiation codon, as determined by mutational analysis, has been italicised. The putative Shine-Dalgarno region has been indicated by emboldening bases complementary to the 3' end of *B. cenocepacia* 16S rRNA. A dotted line indicates the probable Fur binding site overlapping the *porbS* -35 region. The upstream end of the sequence shown is at -178 with respect to the TSS, and the downstream end is at +181.

Just as PvdS controls transcription of a range of *P. aeruginosa* virulence factors, OrbS could fulfil this function in *B. cenocepacia*. An *in silico* analysis carried out using Fuzznuc (Section 6.5) found seven further potential OrbS-dependent promoter sequences within the *B. cenocepacia* J2315 genome, some of which might be involved in virulence.

8.2: Future directions

Several unsuccessful attempts were made during this study to construct an *orbS* expression vector that would constitutively express *orbS*, to allow examination of *orbS* expression in the absence of regulation by Fur. Each of the plasmids produced (pBBR-orbSΔP, pBBR-orbSΔP2, pBBR-orbSΔP-ptac) contained promoterless *orbS*, placed downstream of a non-native constitutive promoter. As the regulation of *orbS* is mediated by Fur, *orbS* could potentially be constitutively transcribed from its own promoter, if the upstream Fur box were first inactivated. To do this, point mutations could be made within the Fur box of pKAGd4-porbS, to allow identification of mutations that inactivate the Fur box (i.e. result in loss of iron-dependent regulation), without compromising *porbS* activity. These point mutations could be introduced into pBBR-orbS, and should result in constitutive *orbS* expression.

Bioinformatic analysis of the *B. cenocepacia* J2315 genome identified 7 candidate OrbS-dependent promoter sequences outside of the ornibactin gene cluster. The *E. coli* model system for analysing OrbS-dependent promoter sequences (Chapter 6) could be used to determine whether these candidate promoters are recognised by OrbS. These promoters could be synthesised as oligonucleotides containing the 42 bp of DNA sequence corresponding to *porbHds6,* and inserted into pKAGd4 for β-galactosidase assay. Primer extension analysis could then be used to confirm that any of these candidate promoters found to have activity function as promoters in *B. cenocepacia.*

Obtaining pure OrbS protein was attempted during this study but proved unsuccessful, and will be of paramount importance in continuing this work. Other ECF σ factors have been found to be insoluble when overexpressed, for example PvdS and FecI (Angerer *et al.*, 1995; Leoni *et al.*, 2000). Often the key to gaining soluble protein is to grow the *E. coli* cells containing the expression vector at low temperatures. This was attempted unsuccessfully under one set of conditions, and therefore a wider range of conditions must be tested in order to try to obtain soluble protein. Alternatively, another overexpression vector could be used to fuse a His-tag to OrbS, allowing purification under denaturing conditions, as the affinity of histidine residues for nickel and cobalt is generally unaffected by pH.

Once pure OrbS has been obtained, a number of experiments could be carried out to further this study. Firstly, while the evidence supporting the classification of OrbS as a σ factor from *in silico* study and investigation of the ornibactin operon is very strong, OrbS has not yet been proved to be a σ factor. This is generally accomplished by assembly with core RNAP, followed by EMSA or *in vitro* transcription analysis using a promoter fragment specific for the σ factor in question. The genetic evidence presented in this study suggests that OrbS is capable of assembling with *E. coli* core RNAP, which is commercially available. Secondly, OrbS, following removal of the tag used to purify it, could be incubated with Fe^{2+} and subjected to atomic absorption spectroscopy, to determine whether it is capable of binding iron. This would show whether or not the model for direct regulation of OrbS activity via its C-terminal cysteines is plausible. Highly purified OrbS could also potentially be used to solve the crystal structure of OrbS by X-ray crystallography. Furthermore, X-ray crystallography of the $E\sigma^{OrbS}$ holoenzyme-*porbH* complex could be used to determine at which points contact occurs between the recognition domains of an RNAP holoenzyme and a bound promoter, which could further elucidate the functional sequence of the OrbS-dependent promoters, and might also suggest a role for the N-terminal extension of OrbS.

References

Adams, C. W. and Hatfield, G. W. (1984). Effects of promoter strengths and growth conditions on copy number of transcription-fusion vectors. *The Journal of Biological Chemistry* **259**: 7399-403.

Agnoli, K. (2003). M.Sc. Thesis, The University of Sheffield.

Agnoli, K., Lowe, C. A., Farmer, K. L., Husnain, S. I. and Thomas, M. S. (2006). The ornibactin biosynthesis and transport genes of *Burkholderia cenocepacia* are regulated by an extracytoplasmic function sigma factor which is a part of the Fur regulon. *Journal of Bacteriology* **188**: 3631-44.

Aguilar, C., Friscina, A., Devescovi, G., Kojic, M. and Venturi, V. (2003). Identification of quorum-sensing-regulated genes of *Burkholderia cepacia*. *Journal of Bacteriology* **185**: 6456-62.

Ahluwalia, J., Tinker, A., Clapp, L. H., Duchen, M. R., Abramov, A. Y., Pope, S., Nobles, M. and Segal, A. W. (2004). The large-conductance Ca2+-activated K+ channel is essential for innate immunity. *Nature* **427**: 853-8.

Aksoy, S., Squires, C. L. and Squires, C. (1984). Translational coupling of the *trpB* and *trpA* genes in the *Escherichia coli* tryptophan operon. *Journal of Bacteriology* **157**: 363-7.

Alice, A. F., Lopez, C. S., Lowe, C. A., Ledesma, M. A. and Crosa, J. H. (2006). Genetic and transcriptional analysis of the siderophore malleobactin biosynthesis and transport genes in the human pathogen *Burkholderia pseudomallei* K96243. *Journal of Bacteriology* **188**: 1551-66.

Alting-Mees, M. A. and Short, J. M. (1989). pBluescript II: gene mapping vectors. *Nucleic acids research* **17**: 9494.

Amann, E., Ochs, B. and Abel, K. J. (1988). Tightly regulated *tac* promoter vectors useful for the expression of unfused and fused proteins in *Escherichia coli*. *Gene* **69**: 301-15.

Ankenbauer, R. G., Toyokuni, T., Staley, A., Rinehart, K. L., Jr. and Cox, C. D. (1988). Synthesis and biological activity of pyochelin, a siderophore of *Pseudomonas aeruginosa*. *Journal of Bacteriology* **170**: 5344-51.

Asghar, A. H. (2002). Ph.D. Thesis, The University of Sheffield.

Auble, D. T., Allen, T. L. and deHaseth, P. L. (1986). Promoter recognition by *Escherichia coli* RNA polymerase. Effects of substitutions in the spacer DNA separating the -10 and -35 regions. *The Journal of biological chemistry* **261**: 11202-6.

Baichoo, N., Helmann, J.D. (2002). Recognition of DNA by Fur: a reinterpretation of the Fur box consensus sequence. *Journal of Bacteriology* **184**: 5826-5832.

Baldwin, A., Sokol, P. A., Parkhill, J. and Mahenthiralingam, E. (2004). The *Burkholderia cepacia* epidemic strain marker is part of a novel genomic island encoding both virulence and metabolism-associated genes in *Burkholderia cenocepacia*. *Infection and Immunity* **72**: 1537-47.

Bamford, S., Ryley, H. and Jackson, S. K. (2007). Highly purified lipopolysaccharides from *Burkholderia cepacia* complex clinical isolates induce inflammatory cytokine responses via TLR4-mediated MAPK signalling pathways and activation of NFkappaB. *Cell Microbiology* **9**: 532-43.

Barelmann I, M. J.-M., Taraz K, Budzikiewicz H (1996). Cepaciachelin, a new catecholate siderophore from
Burkholderia (Pseudomonas) cepacia. *Zeitschrift für Naturforschung* **51c**: 627–630.

Barton, H. A., Johnson, Z., Cox, C. D., Vasil, A. I. and Vasil, M. L. (1996). Ferric uptake regulator mutants of *Pseudomonas aeruginosa* with distinct alterations in the iron-dependent repression of exotoxin A and siderophores in aerobic and microaerobic environments. *Molecular Microbiology* **21**: 1001-17.

Borukhov, S. and Nudler, E. (2003). RNA polymerase holoenzyme: structure, function and biological implications. *Current Opinion in Microbiology* **6**: 93-100.

Boucher, R. C. (2007). Evidence for airway surface dehydration as the initiating event in CF airway disease. *Journal of Internal Medicine* **261**: 5-16.

Braun, V., Mahren, S. and Ogierman, M. (2003). Regulation of the FecI-type ECF sigma factor by transmembrane signalling. *Current Opinion in Microbiology* **6**: 173-80.

Brzoska, K., Meczynska, S. and Kruszewski, M. (2006). Iron-sulfur cluster proteins: electron transfer and beyond. *Acta Biochimica Polonica* **53**: 685-91.

Buchanan, S. K. (2005). Bacterial metal detectors. *Molecular Microbiology* **58**: 1205-9.

Burkholder, W. H. (1950). Sour skin, a bacterial rot of onion bulbs. *Phytopathology* **40**: 115-117.

Carrillo, N. and Ceccarelli, E. A. (2003). Open questions in ferredoxin-NADP+ reductase catalytic mechanism. *European journal of biochemistry / FEBS* **270**: 1900-15.

Casadaban, M. J. and Cohen, S. N. (1980). Analysis of gene control signals by DNA fusion and cloning in *Escherichia coli*. *Journal of Molecular Biology* **138**: 179-207.

Cash, H. A., Woods, D. E., McCullough, B., Johanson, W. G., Jr. and Bass, J. A. (1979). A rat model of chronic respiratory infection with *Pseudomonas aeruginosa*. *The American Review of Respiratory Disease* **119**: 453-9.

Chimento, D. P., Kadner, R. J. and Wiener, M. C. (2005). Comparative structural analysis of TonB-dependent outer membrane transporters: implications for the transport cycle. *Proteins* **59**: 240-51.

Chipperfield, J. R. and Ratledge, C. (2000). Salicylic acid is not a bacterial siderophore: a theoretical study. *Biometals* **13**: 165-8.

Coenye, T., Vandamme, P., Govan, J. R. and LiPuma, J. J. (2001). Taxonomy and identification of the *Burkholderia cepacia* complex. *Journal of Clinical Microbiology* **39**: 3427-36.

Coenye, T., Vandamme, P., LiPuma, J. J., Govan, J. R. and Mahenthiralingam, E. (2003). Updated version of the *Burkholderia cepacia* complex experimental strain panel. *Journal of Clinical Microbiology* **41**: 2797-8.

Conway, B. A., Chu, K. K., Bylund, J., Altman, E. and Speert, D. P. (2004). Production of exopolysaccharide by *Burkholderia cenocepacia* results in altered cell-surface interactions and altered bacterial clearance in mice. *The Journal of Infectious Diseases* **190**: 957-66.

Corbett, C. R., Burtnick, M.N., Kooi, C., Woods, D.E., Sokol, P.A. (2003). An extracellular zinc metalloprotease gene of *Burkholderia cepacia*. *Microbiology* **149**: 2263-2271.

Cox, C. D. and Graham, R. (1979). Isolation of an iron-binding compound from *Pseudomonas aeruginosa*. *Journal of Bacteriology* **137**: 357-64.

Cox, C. D., Rinehart, K. L., Jr., Moore, M. L. and Cook, J. C., Jr. (1981). Pyochelin: novel structure of an iron-chelating growth promoter for *Pseudomonas aeruginosa*. *Proceedings of the National Academy of Sciences of the United States of America* **78**: 4256-60.

Cunha, M. V., Sousa, S. A., Leitao, J. H., Moreira, L. M., Videira, P. A. and Sa-Correia, I. (2004). Studies on the involvement of the exopolysaccharide produced by cystic fibrosis-associated isolates of the *Burkholderia cepacia* complex in biofilm formation and in persistence of respiratory infections. *Journal of Clinical Microbiology* **42**: 3052-8.

Cunliffe, H. E., Merriman, T. R. and Lamont, I. L. (1995). Cloning and characterization of *pvdS*, a gene required for pyoverdine synthesis in *Pseudomonas aeruginosa*: PvdS is probably an alternative sigma factor. *Journal of Bacteriology* **177**: 2744-50.

Darling, P., Chan, M., Cox, A. D. and Sokol, P. A. (1998). Siderophore production by cystic fibrosis isolates of *Burkholderia cepacia*. *Infection and Immunity* **66**: 874-7.

De Boer, H. A., Comstock, L. J. and Vasser, M. (1983). The *tac* promoter: a functional hybrid derived from the *trp* and *lac* promoters. *Proceedings of the National Academy of Sciences of the United States of America* **80**: 21-5.

de Lorenzo, V., Herrero, M., Jakubzik, U. and Timmis, K. N. (1990). Mini-Tn*5* transposon derivatives for insertion mutagenesis, promoter probing, and chromosomal insertion of cloned DNA in Gram-negative eubacteria. *Journal of Bacteriology* **172**: 6568-72.

DeShazer, D. and Woods, D. E. (1996). Broad-host-range cloning and cassette vectors based on the R388 trimethoprim resistance gene. *Biotechniques* **20**: 762-4.

Donaldson, S. H., Bennett, W. D., Zeman, K. L., Knowles, M. R., Tarran, R. and Boucher, R. C. (2006). Mucus clearance and lung function in cystic fibrosis with hypertonic saline. *The New England Journal of Medicine* **354**: 241-50.

Ebright, R. H. (2000). RNA polymerase: structural similarities between bacterial RNA polymerase and eukaryotic RNA polymerase II. *Journal of Molecular Biology* **304**: 687-98.

Eisenhauer, H. A., Shames, S., Pawelek, P. D. and Coulton, J. W. (2005). Siderophore transport through Escherichia coli outer membrane receptor FhuA with disulfide-tethered cork and barrel domains. *The Journal of Biological Chemistry* **280**: 30574-80.

Enz, S., Mahren, S., Menzel, C. and Braun, V. (2003). Analysis of the ferric citrate transport gene promoter of *Escherichia coli*. *Journal of Bacteriology* **185**: 2387-91.

Escolar, L., Perez-Martin, J. and de Lorenzo, V. (1999). Opening the iron box: transcriptional metalloregulation by the Fur protein. *Journal of Bacteriology* **181**: 6223-9.

Farmer, K. L. (1998). Ph.D. Thesis, The University of Sheffield.

Farmer, K. L. and Thomas, M. S. (2004). Isolation and characterization of *Burkholderia cenocepacia* mutants deficient in pyochelin production: pyochelin biosynthesis is sensitive to sulfur availability. *Journal of Bacteriology* **186**: 270-7.

Fellay, R., Frey, J. and Krisch, H. (1987). Interposon mutagenesis of soil and water bacteria: a family of DNA fragments designed for in vitro insertional mutagenesis of gram-negative bacteria. *Gene* **52**: 147-54.

Ferguson, A. D., Chakraborty, R., Smith, B. S., Esser, L., van der Helm, D. and Deisenhofer, J. (2002). Structural basis of gating by the outer membrane transporter FecA. *Science* **295**: 1715-9.

Friedberg, T., Grassow, M. A. and Oesch, F. (1990). Selective detection of mRNA forms encoding the major phenobarbital inducible cytochromes P450 and other members of the P450IIB family by the RNAse A protection assay. *Archives of Biochemistry and Biophysics* **279**: 167-73.

Fuqua, C., Winans, S. C. and Greenberg, E. P. (1996). Census and consensus in bacterial ecosystems: the LuxR-LuxI family of quorum-sensing transcriptional regulators. *Annual Review of Microbiology* **50**: 727-51.

Gadsby, D. C., Vergani, P. and Csanady, L. (2006). The ABC protein turned chloride channel whose failure causes cystic fibrosis. *Nature* **440**: 477-83.

Garcia-Herrero, A. and Vogel, H. J. (2005). Nuclear magnetic resonance solution structure of the periplasmic signalling domain of the TonB-dependent outer membrane transporter FecA from *Escherichia coli*. *Molecular Microbiology* **58**: 1226-37.

Goldstein, R., Sun, L., Jiang, R. Z., Sajjan, U., Forstner, J. F. and Campanelli, C. (1995). Structurally variant classes of pilus appendage fibers coexpressed from *Burkholderia (Pseudomonas) cepacia*. *Journal of Bacteriology* **177**: 1039-52.

Gotschlich, A., Huber, B., Geisenberger, O., Togl, A., Steidle, A., Riedel, K., Hill, P., Tummler, B., Vandamme, P., Middleton, B., Camara, M., Williams, P., Hardman, A. and Eberl, L. (2001). Synthesis of multiple N-acylhomoserine lactones is wide-spread among the members of the Burkholderia cepacia complex. *Systematic and Applied Microbiology* **24**: 1-14.

Gough, J. A. and Murray, N. E. (1983). Sequence diversity among related genes for recognition of specific targets in DNA molecules. *Journal of Molecular Biology* **166**: 1-19.

Govan, J. R. and Deretic, V. (1996). Microbial pathogenesis in cystic fibrosis: mucoid *Pseudomonas aeruginosa* and *Burkholderia cepacia*. *Microbiology Reviews* **60**: 539-74.

Grass, G. (2006). Iron transport in *Escherichia coli*: all has not been said and done. *Biometals* **19**: 159-72.

Gruber, T. M. and Gross, C. A. (2003). Multiple sigma subunits and the partitioning of bacterial transcription space. *Annual Review of Microbiology* **57**: 441-66.

Gruber, T. M. and Gross, C. A. (2003). Assay of *Escherichia coli* RNA polymerase: sigma-core interactions. *Methods in Enzymology* **370**: 206-12.

Guan, K. L. and Dixon, J. E. (1991). Eukaryotic proteins expressed in *Escherichia coli*: an improved thrombin cleavage and purification procedure of fusion proteins with glutathione S-transferase. *Analytical biochemistry* **192**: 262-7.

Guerinot, M. L. (1994). Microbial iron transport. *Annual Review of Microbiology* **48**: 743-72.

Hanahan, D. (1983). Studies on transformation of *Escherichia coli* with plasmids. *Journal of Molecular Biology* **166**: 557-80.

Hanahan, D. p. (1985). *Techniques for transformation of E. coli*. Oxford. Washington DC., IRL Press.

Hantke, K. (1987). Selection procedure for deregulated iron transport mutants (*fur*) in *Escherichia coli* K 12: *fur* not only affects iron metabolism. *Molecular & General Genetics* **210**: 135-9.

Hantke, K. and Braun, V. (1978). Functional interaction of the *tonA/tonB* receptor system in *Escherichia coli*. *Journal of Bacteriology* **135**: 190-7.

Hausinger, R. P. (2004). FeII/alpha-ketoglutarate-dependent hydroxylases and related enzymes. *Critical Reviews in Biochemistry and Molecular Biology* **39**: 21-68.

Helmann, J. D. (1999). Anti-sigma factors. *Current Opinion in Microbiology* **2**: 135-41.

Helmann, J. D. (2002). The extracytoplasmic function (ECF) sigma factors. *Advances in Microbial Physiology* **46**: 47-110.

Heyworth, P. G., Cross, A. R. and Curnutte, J. T. (2003). Chronic granulomatous disease. *Current Opinion in Immunology* **15**: 578-84.

Hodson, M. E., Geddes, D.M. (2000). *Cystic Fibrosis*, A Hodder Arnold Publication.

Hollenstein, K., Frei, D. C. and Locher, K. P. (2007). Structure of an ABC transporter in complex with its binding protein. *Nature* **446**: 213-6.

Hutchison, M. L., Poxton, I. R. and Govan, J. R. (1998). *Burkholderia cepacia* produces a hemolysin that is capable of inducing apoptosis and degranulation of mammalian phagocytes. *Infection and Immunity* **66**: 2033-9.

Isles, A., Maclusky, I., Corey, M., Gold, R., Prober, C., Fleming, P. and Levison, H. (1984). *Pseudomonas cepacia* infection in cystic fibrosis: an emerging problem. *The Journal of Pediatrics* **104**: 206-10.

Iwanicka-Nowicka, R., Zielak, A., Cook, A. M., Thomas, M. S. and Hryniewicz, M. M. (2007). Regulation of sulfur assimilation pathways in *Burkholderia cenocepacia*: identification of transcription factors CysB and SsuR and their role in control of target genes. *Journal of Bacteriology* **189**: 1675-88.

Kadner, R. J., Heller, K., Coulton, J. W. and Braun, V. (1980). Genetic control of hydroxamate-mediated iron uptake in *Escherichia coli*. *Journal of Bacteriology* **143**: 256-64.

Kiley, P. J. and Beinert, H. (2003). The role of Fe-S proteins in sensing and regulation in bacteria. *Current Opinion in Microbiology* **6**: 181-5.

Klumpp, C., Burger, A., Mislin, G. L. and Abdallah, M. A. (2005). From a total synthesis of cepabactin and its 3:1 ferric complex to the isolation of a 1:1:1 mixed complex between iron (III), cepabactin and pyochelin. *Bioorganic & Medicinal Chemistry letters* **15**: 1721-4.

Koebnik, R. (2005). TonB-dependent trans-envelope signalling: the exception or the rule? *Trends in Microbiology* **13**: 343-7.

Koedam, N., Wittouck, E., Gaballa, A., Gillis, A., Hofte, M. and Cornelis, P. (1994). Detection and differentiation of microbial siderophores by isoelectric focusing and chrome azurol S overlay. *Biometals* **7**: 287-91.

Kooi, C., Subsin, B., Chen, R., Pohorelic, B. and Sokol, P. A. (2006). *Burkholderia cenocepacia* ZmpB is a broad-specificity zinc metalloprotease involved in virulence. *Infection and Immunity* **74**: 4083-93.

Koper, T. E., El-Sheikh, A. F., Norton, J. M. and Klotz, M. G. (2004). Urease-encoding genes in ammonia-oxidizing bacteria. *Applied and environmental microbiology* **70**: 2342-8.

Kovach, M. E., Elzer, P. H., Hill, D. S., Robertson, G. T., Farris, M. A., Roop, R. M., 2nd and Peterson, K. M. (1995). Four new derivatives of the broad-host-range cloning vector pBBR1MCS, carrying different antibiotic-resistance cassettes. *Gene* **166**: 175-6.

Kovach, M. E., Phillips, R. W., Elzer, P. H., Roop, R. M., 2nd and Peterson, K. M. (1994). pBBR1MCS: a broad-host-range cloning vector. *Biotechniques* **16**: 800-2.

Lamont, I. L., Beare, P. A., Ochsner, U., Vasil, A. I. and Vasil, M. L. (2002). Siderophore-mediated signaling regulates virulence factor production in *Pseudomonas aeruginosa*. *Proceedings of the National Academy of Sciences of the United States of America* **99**: 7072-7.

Lamothe, J., Huynh, K. K., Grinstein, S. and Valvano, M. A. (2007). Intracellular survival of *Burkholderia cenocepacia* in macrophages is associated with a delay in the maturation of bacteria-containing vacuoles. *Cell Microbiology* **9**: 40-53.

Lane, W. J. and Darst, S. A. (2006). The structural basis for promoter -35 element recognition by the group IV sigma factors. *PLoS Biology* **4**: e269.

Larsen, R. A., Myers, P. S., Skare, J. T., Seachord, C. L., Darveau, R. P. and Postle, K. (1996). Identification of TonB homologs in the family *Enterobacteriaceae* and evidence for conservation of TonB-dependent energy transduction complexes. *Journal of Bacteriology* **178**: 1363-73.

Lavrrar, J. L. and McIntosh, M. A. (2003). Architecture of a Fur binding site: a comparative analysis. *Journal of Bacteriology* **185**: 2194-202.

Ledson, M. J., Gallagher, M. J., Corkill, J. E., Hart, C. A. and Walshaw, M. J. (1998). Cross infection between cystic fibrosis patients colonised with *Burkholderia cepacia*. *Thorax* **53**: 432-6.

Leoni, L., Ciervo, A., Orsi, N. and Visca, P. (1996). Iron-regulated transcription of the pvdA gene in *Pseudomonas aeruginosa*: effect of Fur and PvdS on promoter activity. *Journal of Bacteriology* **178**: 2299-313.

Leoni, L., Orsi, N., de Lorenzo, V. and Visca, P. (2000). Functional analysis of PvdS, an iron starvation sigma factor of *Pseudomonas aeruginosa*. *Journal of Bacteriology* **182**: 1481-91.

Lewenza, S. and Sokol, P. A. (2001). Regulation of ornibactin biosynthesis and N-acyl-L-homoserine lactone production by CepR in *Burkholderia cepacia*. *Journal of Bacteriology* **183**: 2212-8.

Linn, T. and St Pierre, R. (1990). Improved vector system for constructing transcriptional fusions that ensures independent translation of *lacZ*. *Journal of Bacteriology* **172**: 1077-84.

Locher, K. P., Lee, A. T. and Rees, D. C. (2002). The *E. coli* BtuCD structure: a framework for ABC transporter architecture and mechanism. *Science* **296**: 1091-8.

Lodge, J., Fear, J., Busby, S., Gunasekaran, P. and Kamini, N. R. (1992). Broad host range plasmids carrying the *Escherichia coli* lactose and galactose operons. *FEMS Microbiology Letters* **74**: 271-6.

Lodge, J., Williams, R., Bell, A., Chan, B. and Busby, S. (1990). Comparison of promoter activities in *Escherichia coli* and *Pseudomonas aeruginosa*: use of a new broad-host-range promoter-probe plasmid. *FEMS Microbiology letters* **55**: 221-5.

Lonetto, M., Gribskov, M. and Gross, C. A. (1992). The sigma ^{70} family: sequence conservation and evolutionary relationships. *Journal of Bacteriology* **174**: 3843-9.

Lonetto, M. A., Brown, K. L., Rudd, K. E. and Buttner, M. J. (1994). Analysis of the *Streptomyces coelicolor sigE* gene reveals the existence of a subfamily of eubacterial RNA polymerase sigma factors involved in the regulation of extracytoplasmic functions. *Proceedings of the National Academy of Sciences of the United States of America* **91**: 7573-7.

Loutet, S. A., Flannagan, R. S., Kooi, C., Sokol, P. A. and Valvano, M. A. (2006). A complete lipopolysaccharide inner core oligosaccharide is required for resistance of *Burkholderia cenocepacia* to antimicrobial peptides and bacterial survival *in vivo*. *Journal of Bacteriology* **188**: 2073-80.

Lowe, C. A. (2001). Ph.D. Thesis, The University of Sheffield.

Lowe, C. A., Asghar, A. H., Shalom, G., Shaw, J. G. and Thomas, M. S. (2001). The *Burkholderia cepacia* fur gene: co-localization with omlA and absence of regulation by iron. *Microbiology* **147**: 1303-14.

Mack, D. R., Chiu, T. K. and Dickerson, R. E. (2001). Intrinsic bending and deformability at the T-A step of CCTTTAAAGG: a comparative analysis of T-A and A-T steps within A-tracts. *Journal of Molecular Biology* **312**: 1037-49.

Magalhaes, M., Doherty, C., Govan, J. R. and Vandamme, P. (2003). Polyclonal outbreak of *Burkholderia cepacia* complex bacteraemia in haemodialysis patients. *The Journal of Hospital Infection* **54**: 120-3.

Mahenthiralingam, E., Baldwin, A. and Vandamme, P. (2002). *Burkholderia cepacia* complex infection in patients with cystic fibrosis. *Journal of Medical Microbiology* **51**: 533-8.

Mahenthiralingam, E., Vandamme, P., Campbell, M. E., Henry, D. A., Gravelle, A. M., Wong, L. T., Davidson, A. G., Wilcox, P. G., Nakielna, B. and Speert, D. P. (2001). Infection with *Burkholderia cepacia* complex genomovars in patients with cystic fibrosis: virulent transmissible strains of genomovar III can replace Burkholderia multivorans. *Clinical Infectious Diseases* **33**: 1469-75.

Manno, G., Dalmastri, C., Tabacchioni, S., Vandamme, P., Lorini, R., Minicucci, L., Romano, L., Giannattasio, A., Chiarini, L. and Bevivino, A. (2004). Epidemiology and clinical course of *Burkholderia cepacia* complex infections, particularly those caused by different *Burkholderia cenocepacia* strains, among patients attending an Italian Cystic Fibrosis Center. *Journal of Clinical Microbiology* **42**: 1491-7.

Marolda, C. L., Hauroder, B., John, M. A., Michel, R. and Valvano, M. A. (1999). Intracellular survival and saprophytic growth of isolates from the *Burkholderia cepacia* complex in free-living amoebae. *Microbiology* **145 (Pt 7)**: 1509-17.

Mathew, R. and Chatterji, D. (2006). The evolving story of the omega subunit of bacterial RNA polymerase. *Trends in Microbiology* **14**: 450-5.

McKevitt, A. I., Bajaksouzian, S., Klinger, J. D. and Woods, D. E. (1989). Purification and characterization of an extracellular protease from *Pseudomonas cepacia*. *Infection and Immunity* **57**: 771-8.

McMorran, B. J., Kumara, H. M., Sullivan, K. and Lamont, I. L. (2001). Involvement of a transformylase enzyme in siderophore synthesis in *Pseudomonas aeruginosa*. *Microbiology* **147**: 1517-24.

Meng, W., Savery, N. J., Busby, S. J. and Thomas, M. S. (2000). The *Escherichia coli* RNA polymerase alpha subunit linker: length requirements for transcription activation at CRP-dependent promoters. *The EMBO Journal* **19**: 1555-66.

Meyer, J. M. (2000). Pyoverdines: pigments, siderophores and potential taxonomic markers of fluorescent *Pseudomonas* species. *Archives of Microbiology* **174**: 135-42.

Meyer, J. M., Azelvandre, P. and Georges, C. (1992). Iron metabolism in Pseudomonas: salicylic acid, a siderophore of *Pseudomonas fluorescens* CHAO. *Biofactors* **4**: 23-7.

Meyer, J. M., Hohnadel, D. and Halle, F. (1989). Cepabactin from *Pseudomonas cepacia*, a new type of siderophore. *Journal of General Microbiology* **135**: 1479-87.

Meyer, J. M., Stintzi, A., De Vos, D., Cornelis, P., Tappe, R., Taraz, K. and Budzikiewicz, H. (1997). Use of siderophores to type pseudomonads: the three *Pseudomonas aeruginosa* pyoverdine systems. *Microbiology* **143 (Pt 1)**: 35-43.

Meyer, J. M., Van, V. T., Stintzi, A., Berge, O. and Winkelmann, G. (1995). Ornibactin production and transport properties in strains of *Burkholderia vietnamiensis* and *Burkholderia cepacia* (formerly *Pseudomonas cepacia*). *Biometals* **8**: 309-17.

Miller, J. H. (1972). *Experiments in Molecular Genetics.* Cold Spring Harbor, New York., Cold Spring Harbor Laboratory Press.

Missiakas, D. and Raina, S. (1998). The extracytoplasmic function sigma factors: role and regulation. *Molecular Microbiology* **28**: 1059-66.

Miticka, H., Rezuchova, B., Homerova, D., Roberts, M. and Kormanec, J. (2004). Identification of nucleotides critical for activity of the sigmaE-dependent *rpoEp3* promoter in *Salmonella enterica* serovar *Typhimurium*. *FEMS Microbiology Letters* **238**: 227-33.

Mobley, H. L. and Hausinger, R. P. (1989). Microbial ureases: significance, regulation, and molecular characterization. *Microbiology Reviews* **53**: 85-108.

Muller, K., Matzanke, B. F., Schunemann, V., Trautwein, A. X. and Hantke, K. (1998). FhuF, an iron-regulated protein of *Escherichia coli* with a new type of [2Fe-2S] center. *European journal of biochemistry / FEBS* **258**: 1001-8.

Murakami, K. S. and Darst, S. A. (2003). Bacterial RNA polymerases: the wholo story. *Current Opinion in Structural Biology* **13**: 31-9.

Ochsner, U. A., Johnson, Z., Lamont, I. L., Cunliffe, H. E. and Vasil, M. L. (1996). Exotoxin A production in *Pseudomonas aeruginosa* requires the iron-regulated *pvdS* gene encoding an alternative sigma factor. *Molecular Microbiology* **21**: 1019-28.

Ochsner, U. A., Vasil, A. I. and Vasil, M. L. (1995). Role of the ferric uptake regulator of *Pseudomonas aeruginosa* in the regulation of siderophores and exotoxin A expression: purification and activity on iron-regulated promoters. *Journal of Bacteriology* **177**: 7194-201.

Ochsner, U. A., Wilderman, P. J., Vasil, A. I. and Vasil, M. L. (2002). GeneChip expression analysis of the iron starvation response in *Pseudomonas aeruginosa*: identification of novel pyoverdine biosynthesis genes. *Molecular Microbiology* **45**: 1277-87.

Paget, M. S., Bae, J. B., Hahn, M. Y., Li, W., Kleanthous, C., Roe, J. H. and Buttner, M. J. (2001). Mutational analysis of RsrA, a zinc-binding anti-sigma factor with a thiol-disulphide redox switch. *Molecular Microbiology* **39**: 1036-47.

Paget, M. S. and Buttner, M. J. (2003). Thiol-based regulatory switches. **37**: 91-121.

Paget, M. S. and Helmann, J. D. (2003). The sigma^{70} family of sigma factors. *Genome Biology* **4**: 203.

Parke, J. L. and Gurian-Sherman, D. (2001). Diversity of the *Burkholderia cepacia* complex and implications for risk assessment of biological control strains. *Annual Review of Phytopathology* **39**: 225-58.

Parsek, M. R. and Greenberg, E. P. (2000). Acyl-homoserine lactone quorum sensing in gram-negative bacteria: a signaling mechanism involved in associations with higher organisms. *Proceedings of the National Academy of Sciences of the United States of America* **97**: 8789-93.

Pawelek, P. D., Croteau, N., Ng-Thow-Hing, C., Khursigara, C. M., Moiseeva, N., Allaire, M. and Coulton, J. W. (2006). Structure of TonB in complex with FhuA, *E. coli* outer membrane receptor. *Science* **312**: 1399-402.

Perin, L., Martinez-Aguilar, L., Castro-Gonzalez, R., Estrada-de Los Santos, P., Cabellos-Avelar, T., Guedes, H. V., Reis, V. M. and Caballero-Mellado, J. (2006). Diazotrophic *Burkholderia* species associated with field-grown maize and sugarcane. *Applied and environmental microbiology* **72**: 3103-10.

Pohl, E., Haller, J. C., Mijovilovich, A., Meyer-Klaucke, W., Garman, E. and Vasil, M. L. (2003). Architecture of a protein central to iron homeostasis: crystal structure and spectroscopic analysis of the ferric uptake regulator. *Molecular Microbiology* **47**: 903-15.

Postle, K. and Larsen, R. A. (2007). TonB-dependent energy transduction between outer and cytoplasmic membranes. *Biometals* **20**: 453-65.

Pribnow, D. (1975). Nucleotide sequence of an RNA polymerase binding site at an early T7 promoter. *Proceedings of the National Academy of Sciences of the United States of America* **72**: 784-8.

Quadri, L. E., Sello, J., Keating, T. A., Weinreb, P. H. and Walsh, C. T. (1998). Identification of a *Mycobacterium tuberculosis* gene cluster encoding the biosynthetic enzymes for assembly of the virulence-conferring siderophore mycobactin. *Chemistry & Biology* **5**: 631-45.

Quigley, N. B., Mo, Y. Y. and Gross, D. C. (1993). SyrD is required for syringomycin production by *Pseudomonas syringae* pathovar *syringae* and is related to a family of ATP-binding secretion proteins. *Molecular Microbiology* **9**: 787-801.

Ratledge, C. and Dover, L. G. (2000). Iron metabolism in pathogenic bacteria. *Annual Review of Microbiology* **54**: 881-941.

Ravel, J. and Cornelis, P. (2003). Genomics of pyoverdine-mediated iron uptake in pseudomonads. *Trends in Microbiology* **11**: 195-200.

Redly, G. A. and Poole, K. (2003). Pyoverdine-mediated regulation of FpvA synthesis in *Pseudomonas aeruginosa*: involvement of a probable extracytoplasmic-function sigma factor, FpvI. *Journal of Bacteriology* **185**: 1261-5.

Reeves, E. P., Lu, H., Jacobs, H. L., Messina, C. G., Bolsover, S., Gabella, G., Potma, E. O., Warley, A., Roes, J. and Segal, A. W. (2002). Killing activity of neutrophils is mediated through activation of proteases by K+ flux. *Nature* **416**: 291-7.

Rogers, H. J. (1973). Iron-Binding Catechols and Virulence in *Escherichia coli*. *Infection and Immunity* **7**: 445-456.

Romling, U., Fiedler, B., Bosshammer, J., Grothues, D., Greipel, J., von der Hardt, H. and Tummler, B. (1994). Epidemiology of chronic *Pseudomonas aeruginosa* infections in cystic fibrosis. *The Journal of Infectious Diseases* **170**: 1616-21.

Ross, W., Ernst, A. and Gourse, R. L. (2001). Fine structure of *E. coli* RNA polymerase-promoter interactions: alpha subunit binding to the UP element minor groove. *Genes and Development* **15**: 491-506.

Ross, W., Schneider, D. A., Paul, B. J., Mertens, A. and Gourse, R. L. (2003). An intersubunit contact stimulating transcription initiation by *E. coli* RNA polymerase: interaction of the alpha C-terminal domain and sigma region 4. *Genes and Development* **17**: 1293-307.

Saiman, L., Cacalano, G. and Prince, A. (1990). *Pseudomonas cepacia* adherence to respiratory epithelial cells is enhanced by *Pseudomonas aeruginosa*. *Infection and Immunity* **58**: 2578-84.

Sajjan, U. S., Corey, M., Karmali, M. A. and Forstner, J. F. (1992). Binding of *Pseudomonas cepacia* to normal human intestinal mucin and respiratory mucin from patients with cystic fibrosis. *The Journal of Clinical Investigation* **89**: 648-56.

Santangelo, T. J. and Roberts, J. W. (2004). Forward translocation is the natural pathway of RNA release at an intrinsic terminator. *Molecular Cell* **14**: 117-26.

Santos, P. M., Di Bartolo, I., Blatny, J. M., Zennaro, E. and Valla, S. (2001). New broad-host-range promoter probe vectors based on the plasmid RK2 replicon. *FEMS Microbiology Letters* **195**: 91-6.

Schaffer, S., Hantke, K. and Braun, V. (1985). Nucleotide sequence of the iron regulatory gene *fur*. *Molecular & General Genetics* **200**: 110-3.

Schweizer, H. P. and Chuanchuen, R. (2001). Small broad-host-range *lacZ* operon fusion vector with low background activity. *Biotechniques* **31**: 1258, 1260, 1262.

Schwyn, B. and Neilands, J. B. (1987). Universal chemical assay for the detection and determination of siderophores. *Analytical biochemistry* **160**: 47-56.

Seliger, S. S., Mey, A. R., Valle, A. M. and Payne, S. M. (2001). The two TonB systems of *Vibrio cholerae*: redundant and specific functions. *Molecular Microbiology* **39**: 801-12.

Shalom, G. (2002). Ph.D. Thesis, The University of Sheffield.

Shultzaberger, R. K., Chen, Z., Lewis, K. A. and Schneider, T. D. (2007). Anatomy of *Escherichia coli* sigma^{70} promoters. *Nucleic acids research* **35**: 771-88.

Silipo, A., Molinaro, A., Ierano, T., De Soyza, A., Sturiale, L., Garozzo, D., Aldridge, C., Corris, P. A., Khan, C. M., Lanzetta, R. and Parrilli, M. (2007). The complete structure and pro-inflammatory activity of the lipooligosaccharide of the highly epidemic and virulent gram-negative bacterium *Burkholderia cenocepacia* ET-12 (strain J2315). *Chemistry* **13**: 3501-11.

Simon, R., Priefer, U., Pühler, A. (1983). A broad host range mobilisation system for *in vivo* genetic engineering: transposon mutagenesis in Gram-negative bacteria. *Bio/Technology* **1**: 784-791.

Soberon, X., Covarrubias, L. and Bolivar, F. (1980). Construction and characterization of new cloning vehicles. IV. Deletion derivatives of pBR322 and pBR325. *Gene* **9**: 287-305.

Sokol, P. A. (1986). Production and utilization of pyochelin by clinical isolates of *Pseudomonas cepacia*. *Journal of Clinical Microbiology* **23**: 560-2.

Sokol, P. A., Darling, P., Lewenza, S., Corbett, C. R. and Kooi, C. D. (2000). Identification of a siderophore receptor required for ferric ornibactin uptake in *Burkholderia cepacia*. *Infection and Immunity* **68**: 6554-60.

Sokol, P. A., Darling, P., Woods, D. E., Mahenthiralingam, E. and Kooi, C. (1999). Role of ornibactin biosynthesis in the virulence of *Burkholderia cepacia*: characterization of *pvdA*, the gene encoding L-ornithine N(5)-oxygenase. *Infection and Immunity* **67**: 4443-55.

Sokol, P. A., Sajjan, U., Visser, M. B., Gingues, S., Forstner, J. and Kooi, C. (2003). The CepIR quorum-sensing system contributes to the virulence of *Burkholderia cenocepacia* respiratory infections. *Microbiology* **149**: 3649-58.

Speert, D. P. (2002). Advances in *Burkholderia cepacia* complex. *Paediatric Respiratory Reviews* **3**: 230-5.

Speert, D. P., Henry, D., Vandamme, P., Corey, M. and Mahenthiralingam, E. (2002). Epidemiology of *Burkholderia cepacia* complex in patients with cystic fibrosis, Canada. *Emerging Infectious Diseases* **8**: 181-7.

Steindler, L. and Venturi, V. (2007). Detection of quorum-sensing N-acyl homoserine lactone signal molecules by bacterial biosensors. *FEMS microbiology letters* **266**: 1-9.

Stephan, H., Freund, S., Beck, W., Jung, G., Meyer, J. M. and Winkelmann, G. (1993). Ornibactins--a new family of siderophores from Pseudomonas. *Biometals* **6**: 93-100.

Stewart, P. S. and Costerton, J. W. (2001). Antibiotic resistance of bacteria in biofilms. *Lancet* **358**: 135-8.

Stojiljkovic, I., Baumler, A. J. and Hantke, K. (1994). Fur regulon in gram-negative bacteria. Identification and characterization of new iron-regulated *Escherichia coli* genes by a *fur* titration assay. *Journal of Molecular Biology* **236**: 531-45.

Stover, C. K., Pham, X. Q., Erwin, A. L., Mizoguchi, S. D., Warrener, P., Hickey, M. J., Brinkman, F. S., Hufnagle, W. O., Kowalik, D. J., Lagrou, M., Garber, R. L., Goltry, L., Tolentino, E., Westbrock-Wadman, S., Yuan, Y., Brody, L. L., Coulter, S. N., Folger, K. R., Kas, A., Larbig, K., Lim, R., Smith, K., Spencer, D., Wong, G. K., Wu, Z., Paulsen, I. T., Reizer, J., Saier, M. H., Hancock, R. E., Lory, S. and Olson, M. V. (2000). Complete genome sequence of *Pseudomonas aeruginosa* PA01, an opportunistic pathogen. *Nature* **406**: 959-64.

Sun, L., Jiang, R. Z., Steinbach, S., Holmes, A., Campanelli, C., Forstner, J., Sajjan, U., Tan, Y., Riley, M. and Goldstein, R. (1995). The emergence of a highly transmissible lineage of *cbl+ Pseudomonas (Burkholderia) cepacia* causing CF centre epidemics in North America and Britain. *Nature Medicine* **1**: 661-6.

Thomas, M. S. (2007). Iron acquisition mechanisms of the *Burkholderia cepacia* complex. *Biometals* **20**: 431-52.

Touati, D., Jacques, M., Tardat, B., Bouchard, L. and Despied, S. (1995). Lethal oxidative damage and mutagenesis are generated by iron in delta *fur* mutants of *Escherichia coli*: protective role of superoxide dismutase. *Journal of Bacteriology* **177**: 2305-14.

Tseng, C. F., Burger, A., Mislin, G. L., Schalk, I. J., Yu, S. S., Chan, S. I. and Abdallah, M. A. (2006). Bacterial siderophores: the solution stoichiometry and coordination of the Fe(III) complexes of pyochelin and related compounds. *Journal of Biological Inorganic Chemistry* **11**: 419-32.

Vandamme, P., Holmes, B., Coenye, T., Goris, J., Mahenthiralingam, E., LiPuma, J. J. and Govan, J. R. (2003). Burkholderia cenocepacia sp. nov.--a new twist to an old story. *Res Microbiol* **154**: 91-6.

Vanderpool, C. K. and Armstrong, S. K. (2001). The *Bordetella bhu* locus is required for heme iron utilization. *Journal of Bacteriology* **183**: 4278-87.

Vasil, M. L. and Ochsner, U. A. (1999). The response of *Pseudomonas aeruginosa* to iron: genetics, biochemistry and virulence. *Molecular Microbiology* **34**: 399-413.

Visca, P., Ciervo, A. and Orsi, N. (1994). Cloning and nucleotide sequence of the pvdA gene encoding the pyoverdin biosynthetic enzyme L-ornithine N5-oxygenase in *Pseudomonas aeruginosa*. *Journal of Bacteriology* **176**: 1128-40.

Visca, P., Colotti, G., Serino, L., Verzili, D., Orsi, N. and Chiancone, E. (1992). Metal regulation of siderophore synthesis in *Pseudomonas aeruginosa* and functional effects of siderophore-metal complexes. *Applied and Environmental Microbiology* **58**: 2886-93.

Visca, P., Leoni, L., Wilson, M. J. and Lamont, I. L. (2002). Iron transport and regulation, cell signalling and genomics: lessons from *Escherichia coli* and *Pseudomonas*. *Molecular Microbiology* **45**: 1177-90.

Visser, M. B., Majumdar, S., Hani, E. and Sokol, P. A. (2004). Importance of the ornibactin and pyochelin siderophore transport systems in *Burkholderia cenocepacia* lung infections. *Infection and Immunity* **72**: 2850-7.

West, S. E., Schweizer, H. P., Dall, C., Sample, A. K. and Runyen-Janecky, L. J. (1994). Construction of improved *Escherichia-Pseudomonas* shuttle vectors derived from pUC18/19 and sequence of the region required for their replication in *Pseudomonas aeruginosa*. *Gene* **148**: 81-6.

Whitby, P. W., Vanwagoner, T. M., Springer, J. M., Morton, D. J., Seale, T. W. and Stull, T. L. (2006). *Burkholderia cenocepacia* utilizes ferritin as an iron source. *Journal of Medical Microbiology* **55**: 661-8.

Wiener, M. C. (2005). TonB-dependent outer membrane transport: going for Baroque? *Current Opinion in Structural Biology* **15**: 394-400.

Williams, P., Winzer, K., Chan, W. C. and Camara, M. (2007). Look who's talking: communication and quorum sensing in the bacterial world. *Philosophical Transactions of the Royal Society of London.*

Wilson, K. S. and von Hippel, P. H. (1995). Transcription termination at intrinsic terminators: the role of the RNA hairpin. *Proceedings of the National Academy of Sciences of the United States of America* **92**: 8793-7.

Wilson, M. J., McMorran, B. J. and Lamont, I. L. (2001). Analysis of promoters recognized by PvdS, an extracytoplasmic-function sigma factor protein from *Pseudomonas aeruginosa*. *Journal of Bacteriology* **183**: 2151-5.

Wine, J. J. (1999). The genesis of cystic fibrosis lung disease. *The Journal of Clinical Investigation* **103**: 309-12.

Wirth, C., Meyer-Klaucke, W., Pattus, F. and Cobessi, D. (2007). From the periplasmic signaling domain to the extracellular face of an outer membrane signal transducer of *Pseudomonas aeruginosa*: crystal structure of the ferric pyoverdine outer membrane receptor. *Journal of Molecular Biology* **368**: 398-406.

Wosten, M. M. (1998). Eubacterial sigma-factors. *FEMS Microbiology Reviews* **22**: 127-50.

Xiong, A., Singh, V. K., Cabrera, G. and Jayaswal, R. K. (2000). Molecular characterization of the ferric-uptake regulator, *fur*, from *Staphylococcus aureus*. *Microbiology* **146 (Pt 3)**: 659-68.

Yabuuchi, E., Kosako, Y., Oyaizu, H., Yano, I., Hotta, H., Hashimoto, Y., Ezaki, T. and Arakawa, M. (1992). Proposal of *Burkholderia* gen. nov. and transfer of seven species of the genus *Pseudomonas* homology group II to the new genus, with the type species *Burkholderia cepacia* (Palleroni and Holmes 1981) comb. nov. *Microbiology and Immunology* **36**: 1251-75.

Yang, H. M., Chaowagul, W. and Sokol, P. A. (1991). Siderophore production by *Pseudomonas pseudomallei*. *Infection and Immunity* **59**: 776-80.

Yanisch-Perron, C., Vieira, J. and Messing, J. (1985). Improved M13 phage cloning vectors and host strains: nucleotide sequences of the M13mp18 and pUC19 vectors. *Gene* **33**: 103-19.

Yarnell, W. S. and Roberts, J. W. (1999). Mechanism of intrinsic transcription termination and antitermination. *Science* **284**: 611-5.

Yue, W. W., Grizot, S. and Buchanan, S. K. (2003). Structural evidence for iron-free citrate and ferric citrate binding to the TonB-dependent outer membrane transporter FecA. *Journal of Molecular Biology* **332**: 353-68.

Zamri, A. and Abdallah, M. A. (2000). An improved stereocontrolled synthesis of pyochelin, siderophore of *Pseudomonas aeruginosa* and *Burkholderia cepacia*. *Tetrahedron* **56**: 249-256.

Zenkin, N., Kulbachinskiy, A., Yuzenkova, Y., Mustaev, A., Bass, I., Severinov, K. and Brodolin, K. (2007). Region 1.2 of the RNA polymerase sigma subunit controls recognition of the -10 promoter element. *The EMBO Journal* **26**: 955-64.

Zhang, G., Campbell, E. A., Minakhin, L., Richter, C., Severinov, K. and Darst, S. A. (1999). Crystal structure of *Thermus aquaticus* core RNA polymerase at 3.3 A resolution. *Cell* **98**: 811-24.

Appendix:

Primers used in this study

Appendix: Primers used in this study

Primer name	Primer sequence (5'→3')	Notes
Sequencing primers		
AP2	TCAGGAAGATCGCACTC	Sequencing primer for *lacZ*.
AP3	GCGGTCGGGATAGTTTT	Sequencing primer for *lacZ*.
AP4	TCAGCCTCCAGTACAGCG	Sequencing primer for *lacZ*.
AP5	GCGTGTACCACAGCGGAT	Sequencing primer for *lacZ*.
AP6	CAAGACTGTTACCCATCG	Sequencing primer for *lacZ*.
AP7	CTACGCGTACTGTGAGCC	Sequencing primer for *lacZ*.
AP8	GCGGTCGGGATAGTTTT	Sequencing primer for *lacZ*.
AP9	GATACACTTGCTGATGCG	Sequencing primer for *lacZ*.
AP10	GAACGCTCTCCTGAGTA	For sequencing and clone screening of sequences inserted into the pKAGd4 MCS
AP11	CCTCTATAGTGAGTCGG	For sequencing and clone screening of sequences inserted into the pKAGd4 MCS
M13 universal forward	TGTAAAACGACGGCCAGT	Sequencing primer, anneals to sequences flanking MCS in pUC, pBluescript and pBBR series of plasmids
M13 universal reverse	TCACACAGGAAACAGCTATGAC	Sequencing primer, anneals to sequences flanking MCS in pUC, pBluescript and pBBR series of plasmids
Primers for RT-PCR and primer extension		
fecBpvdEfor	CTGATCGAGCGCAACATCTG	For RT-PCR, to determine whether *orbB* and *orbE* are co-transcribed.
fecBpvdErev	AGCTCGACAACGGACGTATC	For RT-PCR, to determine whether *orbB* and *orbE* are co-transcribed.
fecDfhuFfor	GTCGGCTTCATCGGGCTGAT	For RT-PCR, to determine whether *orbD* and *orbF* are co-transcribed.
fecDfhuFrev	CGCCGTAATGGTCGACCATC	For RT-PCR, to determine whether *orbD* and *orbF* are co-transcribed.
fecEfecDfor	GTGCTGCACGACCTGAACCA	For RT-PCR, to determine whether *orbC* and *orbD* are co-transcribed.

fecEfecDrev	TCCTGTTCGACCTCAATCTGCC	For RT-PCR, to determine whether *orbC* and *orbD* are co-transcribed.
fhuFfecBfor	CTGTTCGGTTCGACCTGCAT	For RT-PCR, to determine whether *orbF* and *orbB* are co-transcribed.
fhuFfecBrev	TCCGCGAACATGAAGTCGAG	For RT-PCR, to determine whether *orbF* and *orbB* are co-transcribed.
mbtHsyrPfor	CGTCTATACGGTCGTCATCAAC	For RT-PCR, to determine whether *orbH* and *orbG* are co-transcribed.
mbtHsyrPrev	CGACGTCGTCGATCGACATC	For RT-PCR, to determine whether *orbH* and *orbG* are co-transcribed.
orbApvdFfor	CGAACCTGTTCAATCGCCACT	For RT-PCR, to determine whether *orbA* and *pvdF* are co-transcribed.
orbApvdFrev	CTTCGTCGTCGTCGACGATC	For RT-PCR, to determine whether *orbA* and *pvdF* are co-transcribed.
orbSmbtHfor	CTGAACGTGTCGCAGACGCT	For RT-PCR, to determine whether *orbS* and *orbH* are co-transcribed.
orbSmbtHrev	GTTGATGACGACCGTATAGACG	For RT-PCR, to determine whether *orbS* and *orbH* are co-transcribed. Determination of *orbH* TSS by primer extension.
pvdAorbAfor	GCATCTACCTGCAAGGCTGCTG	For RT-PCR, to determine whether *pvdA* and *orbA* are co-transcribed.
pvdAorbArev	CGGTCGACGGATTCGTCGTC	For RT-PCR, to determine whether *pvdA* and *orbA* are co-transcribed.
pvdEpvdIfor	CAGCAGCGCAAGGATCAGGC	For RT-PCR, to determine whether *orbE* and *orbI* are co-transcribed. Determination of *orbE* TSS by primer extension.
pvdEpvdIrev	TCGCGGATTCGGTGATGCAGC	For RT-PCR, to determine whether *orbE* and *orbI* are co-transcribed. Determination of *orbI* TSS by primer extension.
pvdFpvdZ2for3	CTGCTCGTGATCCTCGACGA	For RT-PCR, to determine whether *pvdF* and *orbL* are co-transcribed.

pvdFpvdZ2rev3	GTTCTGCCAGAACGTCGTGC	For RT-PCR, to determine whether *pvdF* and *orbL* are co-transcribed.
pvdIpvdDfor	GACATCTGGCAACGCGTGCT	For RT-PCR, to determine whether *orbI* and *orbJ* are co-transcribed.
pvdIpvdDrev	CCGAGTTTGTCGATGAAGACCG	For RT-PCR, to determine whether *orbI* and *orbJ* are co-transcribed.
pvdDpvdZ1for	CCAATGCGGATCTGTTCGAAGC	For RT-PCR, to determine whether *orbJ* and *orbK* are co-transcribed.
pvdDpvdZ1rev	ATGGTTGTAGGCGACGAGGC	For RT-PCR, to determine whether *orbJ* and *orbK* are co-transcribed.
pvdZ1pvdAfor	GTGCGTCGTGCATTACCTGT	For RT-PCR, to determine whether *orbK* and *pvdA* are co-transcribed.
pvdZ1pvdArev	GACGCTCGACGAAGCAATG	For RT-PCR, to determine whether *orbK* and *pvdA* are co-transcribed.
pvdZ2hipOfor	CCGATACGTTCTTCGACACCT	For RT-PCR, to determine whether *orbL* is co-transcribed with the downstream gene, BCAL1703.
pvdZ2hipOrev	AACTGCTCCGCGACGAGATC	For RT-PCR, to determine whether *orbL* is co-transcribed with the downstream gene, BCAL1703.
SKorbSrev	CAGGTCCGGATAACTGCCGA	For determination of *orbS* TSS by primer extension.
SKorbSfor2	GTCGTTCTCCCTTGGAAACG	For RT-PCR, to determine whether *orbS* is co-transcribed with the upstream genes.
SKorbSrev2	GACGAGCTTCACGAACACGT	For RT-PCR, to determine whether *orbS* is co-transcribed with upstream genes.
syrPfecEfor	GCAACGTGTATTACGGCGAC	For RT-PCR, to determine whether *orbG* and *orbC* are co-transcribed.
syrPfecErev	CGGCCGTTCACTTCGACATG	For RT-PCR, to determine whether *orbG* and *orbC* are co-transcribed.

Primers for cloning

altpromfor	GCGCAAGCTTCCTGACAACCGA AAGGGTCAT	For amplification of -69 *orbS* promoter. *Hin*dIII site underlined.
candpromfor	GCGCAAGCTTCGGATTGAGAAT GATTTGCG	For amplification of -40 *orbS* promoter. *Hin*dIII site underlined.
catfor	GCGCCTGCAGGTCGACAATAGG CGTATCACGAG	For amplification of the *cat* gene of pBR328 (Cm^R). *Pst*I and *Sal*I sites underlined.
catrev	GCGCCTGCAGTCGACACCAATA ACTGCATTAA	For amplification of the *cat* gene of pBR328 (Cm^R). *Sal*I and *Pst*I sites underlined.
orbSdeltaX	ATATCCATGGCGGCCGCGCCGC GTGCGCGC	For amplification of *orbS* without its N-terminal extension coding sequence. *Nco*I site underlined.
orbSfor	GCGCAAGCTTCGGTTCGTCAGG AACATGAA	For amplification of *orbS*. *Hin*dIII site underlined.
orbSfor3	GCGCAAGCTTGGAATTTGACGG AGCAGATC	For amplification of +5 *orbS* promoter. *Hin*dIII site underlined.
orbSfor4	GCGCGAATTCGCGGCCGCCGGT TCGTCAGGAACATGAA	For amplification of full-length *orbS* promoter. *Eco*RI and *Not*I sites underlined.
orbSfor6	GCGCGGATCCATGGCCATGGCG GAAGTGCTC	For amplification of *orbS* for insertion into pGEX-KG, for protein purification. *Bam*HI site underlined.
orbSfor7	GCGCCATATGGCCATGGCGGAA GTGCTC	For amplification of *orbS* for insertion into pET-14b, for protein purification. *Nde*I site underlined.
orbSrev2	GCGCGGATCCGGCTTGCGTCAT GATCGGAAA	For amplification of *orbS*, *Bam*HI site underlined.
orbSrev7	CGCGAAGCTTCCATGGCCATCG ATCTGCT	For cloning *orbS* into pRW50, in-frame with *trpBA*.
orbSNTrevGEX	GCGCGGATCCAAGCTTTTAGAC CGGCTGGCGCACCGCGTC	For cloning the DNA encoding the N-terminal region of OrbS into pGEX-KG. *Bam*HI and *Hin*dIII sites underlined.
orbSCTforGEX	GCGCGGATCCATGGCCTATGTG ACGCGGATGGTG	For cloning the DNA encoding the C-terminal region of OrbS into pGEX-KG. *Bam*HI site underlined.

PAppvdEfor	GCGCAAGCTTTCTCAGGGACCA GATATAGG	For amplification of *pvdE* and *pvdF* promoters. *Hin*dIII site underlined.
PAppvdEfor	GCGCAAGCTTTCTCAGGGACCA GATATAGG	For amplification of *pvdE* and *pvdF* promoters. *Hin*dIII site underlined.
PAppvdErev2	GCGCGGATCCAGTGCAAGGCGT TGTTGATG	For amplification of *pvdE* and *pvdF* promoters. *Bam*HI site underlined.
PAppvdErev2	GCGCGGATCCAGTGCAAGGCGT TGTTGATG	For amplification of *pvdE* and *pvdF* promoters. *Bam*HI site underlined.
pbfdrev1	GCGCCTCGAGCACGCAGACGAT CATGAT	For amplification of a 222bp fragment carrying the *bfd* promoter. *Xho*I site underlined.
pbfdrev2	GCGCCTCGAGCTAACGTTAATG CGAATTAT	For amplification of a 192bp fragment carrying the *bfd* promoter. *Xho*I site underlined.
pmbtHfor	GCGCGAATTCGCGGCCGCTATC ACACGGAAGAGGACGA	For amplification of *orbH* promoter. *Eco*RI and *Not*I sites underlined.
pmbtHrev	GCGCAAGCTTTCTAGAGGCTTG CGTCATGATCGGAAA	For amplification of the *orbH* promoter. *Hin*dIII and *Xba*I sites underlined.
pnrpSfor	GCGCGAATTCGCGGCCGCAAAC GGCAAATCTGACGCGA	For amplification of *orbI* promoter. *Eco*RI and *Not*I sites underlined.
pnrpSrev	GGGGAAGCTTTCTAGAAGCAGC GCGACGAACAGTT	For amplification of *orbI* promoter. *Hin*dIII and *Xba*I sites underlined.
porbSrev	GCGCAAGCTTTCTAGATGCGAG ATCAGCACGTCGA	For amplification of the *orbS* promoter fragment. *Hin*dIII and *Xba*I sites underlined.
ppvdEfor	CGCAAGCTTTCTAGAAAACGGC AAATCTGACGCGA	For amplification of *orbE* promoter. *Hin*dIII and *Xba*I sites underlined.
ppvdErev	GGGGGAATTCGCGGCCGCAGCA GCGCGACGAACAGTT	For amplification of *orbE* promoter. *Eco*RI and *Not*I sites underlined.
tacfor	CGGCGGTACCCCGTTCTGGATA ATGTTTTTTG	For amplification of the *tac* promoter.
tacrev	CGCGCTCGAGTGTGTGAAATTG TTATCCGC	For amplification of the *tac* promoter.

Oligonucleotides annealed to make double-stranded DNA fragments

Forward and reverse pairs annealed as described in Chapter 2.

hindfor	AATTCGCAAGCTTCTG	For insertion of a *Hin*dIII site (underlined) into pRW500, to give pKAGc1.
hindrev	GATCCAGAAGCTTGCG	
porbHds1for	AGCTTGCGGTAAAAAAACGCGC	*porbH* fragment, spanning from -38 to -6 relative to TSS. *Bam*HI- and *Hin*dIII-compatible ends underlined.
	CGGCCAACCGTCTATCG	
porbHds1rev	GATCCGATAGACGGTTGGCCGG	
	CGCGTTTTTTTACCGCA	
porbHds2for	AGCTTGCGGCGGTAAAAAAACG	*porbH* fragment, spanning from -41 to +32 relative to TSS. *Bam*HI- and *Hin*dIII-compatible ends underlined.
	CGCCGGCCAACCGTCTATCAGA	
	CAGGAGCGGCCGAATCCGCCGC	
	TTCGCCTCCTTCAG	
porbHds2rev2	GATCCTGAAGGAGGCGAAGCGG	
	CGGATTCGGCCGCTCCTGTCTG	
	ATAGACGGTTGGCCGGCGCGTT	
	TTTTTACCGCCGCA	
porbHds3for	AGCTTGCGGCGGTAAAAAAACG	*porbH* fragment, spanning from -41 to +22 relative to TSS. *Bam*HI and *Hin*dIII compatible ends underlined.
	CGCCGGCCAACCGTCTATCAGA	
	CAGGAGCGGCCGAATCCGCCGC	
	TTCG	
porbHds3rev	GATCCGAAGCGGCGGATTCGGC	
	CGCTCCTGTCTGATAGACGGTT	
	GGCCGGCGCGTTTTTTTACCGC	
	CGCA	
porbHds4for	AGCTTGCGGCGGTAAAAAAACG	*porbH* fragment, spanning from -41 to +13 relative to TSS. *Bam*HI and *Hin*dIII compatible ends underlined.
	CGCCGGCCAACCGTCTATCAGA	
	CAGGAGCGGCCGAATG	
porbHds4rev	GATCCATTCGGCCGCTCCTGTC	
	TGATAGACGGTTGGCCGGCGCG	
	TTTTTTTACCGCCGCA	
porbHds5for	AGCTTGCGGCGGTAAAAAAACG	*porbH* fragment, spanning from -41 to +4 relative to TSS. *Bam*HI and *Hin*dIII compatible ends underlined.
	CGCCGGCCAACCGTCTATCAGA	
	CAGGAG	
porbHds5rev	GATCCTCCTGTCTGATAGACGG	
	TTGGCCGGCGCGTTTTTTTACC	
	GCCGCA	
porbHds6for	AGCTTGCGGTAAAAAAACGCGC	*porbH* fragment, spanning from -38 to +4 relative to TSS. *Bam*HI and *Hin*dIII compatible ends underlined.
	CGGCCAACCGTCTATCAGACAG	
	GAG	
porbHds6rev	GATCCTCCTGTCTGATAGACGG	
	TTGGCCGGCGCGTTTTTTTACC	
	GCA	

porbHds7for	AGCTTGCGGCGGTAAAAAAACG CGCCGGCCAACCGTCTATCCGA CAGGAG	*porbH* fragment containing extreme substitution*, labelled in red. *Bam*HI and *Hin*dIII compatible ends underlined.
porbHds7rev	GATCCTCCTGTCGGATAGACGG TTGGCCGGCGCGTTTTTTTACC GCCGCA	
porbHds8for	AGCTTGCGGCGGTAAAAAAACG CGCCGGCCAACCGTCTATCATA CAGGAG	*porbH* fragment containing extreme substitution*, labelled in red. *Bam*HI and *Hin*dIII compatible ends underlined.
porbHds8rev	GATCCTCCTGTATGATAGACGG TTGGCCGGCGCGTTTTTTTACC GCCGCA	
porbHds9for	AGCTTGCGGCGGTAAAAAAACG CGCCGGCCAACCGTCTATCAGC CAGGAG	*porbH* fragment containing extreme substitution*, labelled in red. *Bam*HI and *Hin*dIII compatible ends underlined.
porbHds9rev	GATCCTCCTGGCTGATAGACGG TTGGCCGGCGCGTTTTTTTACC GCCGCA	
porbHds10for	AGCTTGCGGCGGTAAAAAAACG CGCCGGCCAACCGTCTATCAGA AAGGAG	*porbH* fragment containing extreme substitution*, labelled in red. *Bam*HI and *Hin*dIII compatible ends underlined.
porbHds10rev	GATCCTCCTTCTGATAGACGG TTGGCCGGCGCGTTTTTTTACC GCCGCA	
porbHds11for	AGCTTGCGGCGGTAAAAAAACG CGCCGGCCAACCGTCTATCAGA CCGGAG	*porbH* fragment containing extreme substitution*, labelled in red. *Bam*HI and *Hin*dIII compatible ends underlined.
porbHds11rev	GATCCTCCGGTCTGATAGACGG TTGGCCGGCGCGTTTTTTTACC GCCGCA	
porbHds12for	AGCTTGCGGCGGTAAAAAAACG CGCCGGCCAACCGTCTATCAGA CATGAG	*porbH* fragment containing extreme substitution*, labelled in red. *Bam*HI and *Hin*dIII compatible ends underlined.
porbHds12rev	GATCCTCATGTCTGATAGACGG TTGGCCGGCGCGTTTTTTTACC GCCGCA	
porbHds13for	AGCTTGCGGCGGTAAAAAAACG CGCCGGCCAACCGTCTATCAGA CAGTAG	*porbH* fragment containing extreme substitution*, labelled in red. *Bam*HI and *Hin*dIII compatible ends underlined.
porbHds13rev	GATCCTACTGTCTGATAGACGG TTGGCCGGCGCGTTTTTTTACC GCCGCA	
porbHds14for	AGCTTGCGGCGGTAAAAAAACG CGCCGGCCAACCGTCTATCAGA CAGGCG	*porbH* fragment containing extreme substitution*, labelled in red. *Bam*HI and *Hin*dIII compatible ends underlined.
porbHds14rev	GATCCGCCTGTCTGATAGACGG TTGGCCGGCGCGTTTTTTTACC GCCGCA	

porbHds15for	AGCTTGCGGCGGTAAAAAAACG CGCCGGCCAACCGTATATCAGA CAGGAG	*porbH* fragment containing extreme substitution*, labelled in red. *Bam*HI and *Hin*dIII compatible ends underlined.
porbHds15rev	GATCCTCCTGTCTGATATACGG TTGGCCGGCGCGTTTTTTTACC GCCGCA	
porbHds16for	AGCTTGCGGTAAAAAAACGCGC CGGCCAACCGTCTATCAGACAG GATG	*porbH* fragment containing extreme substitution*, labelled in red. *Bam*HI and *Hin*dIII compatible ends underlined.
porbHds16rev	GATCCATCCTGTCTGATAGACG GTTGGCCGGCGCGTTTTTTTAC CGCA	
porbHds17for	AGCTTGCGGTAAAAAAACGCGC CGGCCAACCGTCTATCCTCACT TCTG	*porbH* fragment containing extreme substitutions*, labelled in red. *Bam*HI and *Hin*dIII compatible ends underlined.
porbHds17rev	GATCCAGAAGTGAGGATAGACG GTTGGCCGGCGCGTTTTTTTAC CGCA	
porbHds18f1	AGCTTGCGGCGGTAAAAAAACG CGCCGGCCAACCGTCTATCAG	All four of these primers were annealed together resulting in *porbH* fragment spanning from -41 to +64 relative to TSS. *Bam*HI and *Hin*dIII compatible ends underlined.
porbHds18f2	ACAGGAGCGGCCGAATCCGCCG CTTCGCCTCCTTCAACCGCCCA GCGATTTCCGATCATGACGCAA GCCG	
porbHds18r1	AAGCGGCGGATTCGGCCGCTCC TGTCTGATAGACGGTTGGCCGG CGCGTTTTTTTACCGCCGCA	
porbHds18r2	GATCCGGCTTGCGTCATGATCG GAAATCGCTGGGCGGTTGAAGG AGGCG	
porbHds19for	AGCTTGCGGTAAAAAAACGCGC CGGCCAACCGTCTATAAGACAG GAG	*porbH* fragment containing extreme substitution*, labelled in red. *Bam*HI and *Hin*dIII compatible ends underlined.
porbHds19rev	GATCCTCCTGTCTTATAGACGG TTGGCCGGCGCGTTTTTTTACC GCA	
porbHds20for	AGCTTGCGGTAAAAAAACGCGC CGGCCAACCGTCTAGCAGACAG GAG	*porbH* fragment containing extreme substitution*, labelled in red. *Bam*HI and *Hin*dIII compatible ends underlined.
porbHds20rev	GATCCTCCTGTCTGCTAGACGG TTGGCCGGCGCGTTTTTTTACC GCA	
porbHds21for	AGCTTGCGGTAAAAAAACGCGC CGGCCAACCGTCTCTCAGACAG GAG	*porbH* fragment containing extreme substitution*, labelled in red. *Bam*HI and *Hin*dIII compatible ends underlined.
porbHds21rev	GATCCTCCTGTCTGAGAGACGG TTGGCCGGCGCGTTTTTTTACC GCA	

porbHds22for	AGCTTGCGGTAAAAAAACGCGC CGGCCAACCGTCGATCAGACAG GAG	*porbH* fragment containing extreme substitution*, labelled in red. *Bam*HI and *Hin*dIII compatible ends underlined.
porbHds22rev	GATCCTCCTGTCTGATCGACGG TTGGCCGGCGCGTTTTTTTACC GCA	
porbHds23for	AGCTTGCGGTAAAAAAACGCGC CGGCCAACCGGCTATCAGACAG GAG	*porbH* fragment containing extreme substitution*, labelled in red. *Bam*HI and *Hin*dIII compatible ends underlined.
porbHds23rev	GATCCTCCTGTCTGATAGCCGG TTGGCCGGCGCGTTTTTTTACC GCA	
porbHds24for	AGCTTGCGGTAAAAAAACGCGC CGGCCAACCTTCTATCAGACAG GAG	*porbH* fragment containing extreme substitution*, labelled in red. *Bam*HI and *Hin*dIII compatible ends underlined.
porbHds24rev	GATCCTCCTGTCTGATAGAAGG TTGGCCGGCGCGTTTTTTTACC GCA	
porbHds25for	AGCTTGCGGTAAAAAAACGCGC CGGCCAACAGTCTATCAGACAG GAG	*porbH* fragment containing extreme substitution*, labelled in red. *Bam*HI and *Hin*dIII compatible ends underlined.
porbHds25rev	GATCCTCCTGTCTGATAGACTG TTGGCCGGCGCGTTTTTTTACC GCA	
porbHds26for	AGCTTGCGGTAAAAAAACGCGC CGGCCAAACGTCTATCAGACAG GAG	*porbH* fragment containing extreme substitution*, labelled in red. *Bam*HI and *Hin*dIII compatible ends underlined.
porbHds26rev	GATCCTCCTGTCTGATAGACGT TTGGCCGGCGCGTTTTTTTACC GCA	
porbHds27for	AGCTTGCGGTAAAAAAACGCGC CGGCCACCCGTCTATCAGACAG GAG	*porbH* fragment containing extreme substitution*, labelled in red. *Bam*HI and *Hin*dIII compatible ends underlined.
porbHds27rev	GATCCTCCTGTCTGATAGACGG GTGGCCGGCGCGTTTTTTTACC GCA	
porbHds28for	AGCTTGCGGTAAAAACACGCGC CGGCCAACCGTCTATCAGACAG GAG	*porbH* fragment containing extreme substitution*, labelled in red. *Bam*HI and *Hin*dIII compatible ends underlined.
porbHds28rev	GATCCTCCTGTCTGATAGACGG TTGGCCGGCGCGTGTTTTTACC GCA	
porbHds29for	AGCTTGCGGTAAAACAACGCGC CGGCCAACCGTCTATCAGACAG GAG	*porbH* fragment containing extreme substitution*, labelled in red. *Bam*HI and *Hin*dIII compatible ends underlined.
porbHds29rev	GATCCTCCTGTCTGATAGACGG TTGGCCGGCGCGTTGTTTTACC GCA	

porbHds30for	AGCTTGCGGTAAACAAACGCGC CGGCCAACCGTCTATCAGACAG GAG	*porbH* fragment containing extreme substitution*, labelled in red. *Bam*HI and *Hin*dIII compatible ends underlined.
porbHds30rev	GATCCTCCTGTCTGATAGACGG TTGGCCGGCGCGTTTGTTTACC GCA	
porbHds31for	AGCTTGCGGTAAATAAACGCGC CGGCCAACCGTCTATCAGACAG GAG	*porbH* fragment containing extreme substitution*, labelled in red. *Bam*HI and *Hin*dIII compatible ends underlined.
porbHds31rev	GATCCTCCTGTCTGATAGACGG TTGGCCGGCGCGTTTATTTACC GCA	
porbHds32for	AGCTTGCGGTAACAAAACGCGC CGGCCAACCGTCTATCAGACAG GAG	*porbH* fragment containing extreme substitution*, labelled in red. *Bam*HI and *Hin*dIII compatible ends underlined.
porbHds32rev	GATCCTCCTGTCTGATAGACGG TTGGCCGGCGCGTTTTGTTACC GCA	
porbHds33for	AGCTTGCGGTACAAAAACGCGC CGGCCAACCGTCTATCAGACAG GAG	*porbH* fragment containing extreme substitution*, labelled in red. *Bam*HI and *Hin*dIII compatible ends underlined.
porbHds33rev	GATCCTCCTGTCTGATAGACGG TTGGCCGGCGCGTTTTTGTACC GCA	
porbHds34for	AGCTTGCGGTCAAAAAACGCGC CGGCCAACCGTCTATCAGACAG GAG	*porbH* fragment containing extreme substitution*, labelled in red. *Bam*HI and *Hin*dIII compatible ends underlined.
porbHds34rev	GATCCTCCTGTCTGATAGACGG TTGGCCGGCGCGTTTTTTGACC GCA	
porbHds35for	AGCTTGCGGGAAAAAAACGCGC CGGCCAACCGTCTATCAGACAG GAG	*porbH* fragment containing extreme substitution*, labelled in red. *Bam*HI and *Hin*dIII compatible ends underlined.
porbHds35rev	GATCCTCCTGTCTGATAGACGG TTGGCCGGCGCGTTTTTTTCCC GCA	
porbHds36for	AGCTTGCGTTAAAAAAACGCGC CGGCCAACCGTCTATCAGACAG GAG	*porbH* fragment containing extreme substitution*, labelled in red. *Bam*HI and *Hin*dIII compatible ends underlined.
porbHds36rev	GATCCTCCTGTCTGATAGACGG TTGGCCGGCGCGTTTTTTTAAC GCA	
porbHds37for	AGCTTGCTGTAAAAAAACGCGC CGGCCAACCGTCTATCAGACAG GAG	*porbH* fragment containing extreme substitution*, labelled in red. *Bam*HI and *Hin*dIII compatible ends underlined.
porbHds37rev	GATCCTCCTGTCTGATAGACGG TTGGCCGGCGCGTTTTTTTACA GCA	

porbHds38for	AGCTTGAGGTAAAAAAACGCGC	*porbH* fragment containing extreme substitution*, labelled in red. *Bam*HI and *Hin*dIII compatible ends underlined.
	CGGCCAACCGTCTATCAGACAG	
	GAG	
porbHds38rev	GATCCTCCTGTCTGATAGACGG	
	TTGGCCGGCGCGTTTTTTTACC	
	TCA	
porbHds39for	AGCTTTCGGTAAAAAAACGCGC	*porbH* fragment containing extreme substitution*, labelled in red. *Bam*HI and *Hin*dIII compatible ends underlined.
	CGGCCAACCGTCTATCAGACAG	
	GAG	
porbHds39rev	GATCCTCCTGTCTGATAGACGG	
	TTGGCCGGCGCGTTTTTTTACC	
	GAA	
porbHds40for	AGCTTGCGGTAAAAAAACTATA	*porbH* fragment containing extreme substitution*, labelled in red. *Bam*HI and *Hin*dIII compatible ends underlined.
	ATTAAAACCGTCTATCAGACAG	
	GAG	
porbHds40rev	GATCCTCCTGTCTGATAGACGG	
	TTTTAATTATAGTTTTTTTACC	
	GCA	
porbHds41for	AGCTTGCGGTAAAAAAACGAGA	*porbH* fragment containing extreme substitution*, labelled in red. *Bam*HI and *Hin*dIII compatible ends underlined.
	CTGACAACCGTCTATCAGACAG	
	GAG	
porbHds41rev	GATCCTCCTGTCTGATAGACGG	
	TTGTCAGTCTCGTTTTTTTACC	
	GCA	
porbHds42for	AGCTTGCGGTAAAAAACCGCGC	*porbH* fragment containing extreme substitution*, labelled in red. *Bam*HI and *Hin*dIII compatible ends underlined.
	CGGCCAACCGTCTATCAGACAG	
	GAG	
porbHds42rev	GATCCTCCTGTCTGATAGACGG	
	TTGGCCGGCGCGGTTTTTTACC	
	GCA	
porbHds43for	AGCTTGCGGTAAAAAAACGCGC	*porbH* fragment containing extreme substitutions*, labelled in red. *Bam*HI and *Hin*dIII compatible ends underlined.
	CGGCCAACCGTCTATCCTCAAT	
	GCTG	
porbHds43rev	GATCCAGCATTGAGGATAGACG	
	GTTGGCCGGCGCGTTTTTTTAC	
	CGCA	
porbHds44for	AGCTTGCGGTAAAAAAACGCGC	*porbH* fragment containing extreme substitutions*, labelled in red. *Bam*HI and *Hin*dIII compatible ends underlined.
	CGGCCAACCGTCTATCCTCCAG	
	GAGG	
porbHds44rev	GATCCCTCCTGGAGGATAGACG	
	GTTGGCCGGCGCGTTTTTTTAC	
	CGCA	
porbHds45for	AGCTTGCGGTAAAAAAACGCGC	*porbH* fragment containing extreme substitutions*, labelled in red. *Bam*HI and *Hin*dIII compatible ends underlined.
	CGGCCAACCGTCTATCAGAACT	
	GAGG	
porbHds45rev	GATCCCTCAGTTCTGATAGACG	
	GTTGGCCGGCGCGTTTTTTTAC	
	CGCA	

porbHds46for	AGCTTGCGGTAAAAAAACGCGC CGGCCAACCGTCTATCAGACAG TCTG	*porbH* fragment containing extreme substitutions*, labelled in red. *Bam*HI and *Hin*dIII compatible ends underlined.
porbHds46rev	GATCCAGACTGTCTGATAGACG GTTGGCCGGCGCGTTTTTTTAC CGCA	
porbHds47for	AGCTTGCGGTAAAAAAAAGCGC CGGCCAACCGTCTATCAGACAG GAG	*porbH* fragment containing extreme substitution*, labelled in red. *Bam*HI and *Hin*dIII compatible ends *underlined.*
porbHds6rev	GATCCTCCTGTCTGATAGACGG TTGGCCGGCGCTTTTTTTTACC GCA	
porbHds48for	AGCTTGCGGTAAAAAAACGCGC CGGCCCACCGTCTATCAGACAG GAG	*porbH* fragment containing extreme substitution*, labelled in red. *Bam*HI and *Hin*dIII compatible ends underlined.
porbHds48rev	GATCCTCCTGTCTGATAGACGG TGGGCCGGCGCGTTTTTTTACC GCA	
porbHds49for	AGCTTGCGGTAACCAAACGCGC CGGCCAACCGTCTATCAGACAG GAG	*porbH* fragment containing extreme substitutions*, labelled in red. *Bam*HI and *Hin*dIII compatible ends underlined.
porbHds49rev	GATCCTCCTGTCTGATAGACGG TTGGCCGGCGCGTTTGGTTACC GCA	
porbHds50for	AGCTTGCGGTAAAAACCCGCGC CGGCCAACCGTCTATCAGACAG GAG	*porbH* fragment containing extreme substitutions*, labelled in red. *Bam*HI and *Hin*dIII compatible ends underlined.
porbHds50rev	GATCCTCCTGTCTGATAGACGG TTGGCCGGCGCGGGTTTTTACC GCA	
porbHds51for	AGCTTGCGGTAAACCAACGCGC CGGCCAACCGTCTATCAGACAG GAG	*porbH* fragment containing extreme substitutions*, labelled in red. *Bam*HI and *Hin*dIII compatible ends underlined.
porbHds51rev	GATCCTCCTGTCTGATAGACGG TTGGCCGGCGCGTTGGTTTACC GCA	
ppvdEds1bfor	AGCTTCCGCTAAATACCGGGCA TCCTGCTTCGTCTGTCTGCAAG GAG	*ppvdE* fragment spanning equivalent bases to porbHds6. *Bam*HI and *Hin*dIII compatible ends underlined.
ppvdEds1brev	GATCCTCCTTGCAGACAGACGA AGCAGGATGCCCGGTATTTAGC GGA	
ppvdEds3for	AGCTTCCGCTAAATAAACGCGC CGGCCAACCGTCTGTCTGCAAG GAG	*ppvdE* fragment, red bases are *porbH* sequence substituted for the WT *ppvdE* ones. *Bam*HI and *Hin*dIII compatible ends underlined.
ppvdEds3rev	GATCCTCCTTGCAGACAGACGG TTGGCCGGCGCGTTTATTTAGC GGA	

ppvdEds4for	AGCTTCCGCTAAATACCGGGCA TCCTGCTTCGTCTATCAGACAG GAG	*ppvdE* fragment, red bases are *porbH* sequence substituted for the WT *ppvdE* ones. *Bam*HI and *Hin*dIII compatible ends underlined.
ppvdEds4rev	GATCCTCCTGTCTGATAGACGA AGCAGGATGCCCGGTATTTAGC GGA	
ppvdEds5for	AGCTTCCGCTAAATAAACGCGC CGGCCAACCGTCTGTCAGACAG GAG	*ppvdE* fragment, red bases are *porbH* sequence substituted for the WT *ppvdE* ones. *Bam*HI and *Hin*dIII compatible ends underlined.
ppvdEds5rev	GATCCTCCTGTCTGACAGACGG TTGGCCGGCGCGTTTATTTAGC GGA	
ppvdEds6for	AGCTTGCGGTAAAAACCGGGCA TCCTGCTTCGTCTGTCTGCAAG GAG	*ppvdE* fragment, red bases are *porbH* sequence substituted for the WT *ppvdE* ones. *Bam*HI and *Hin*dIII compatible ends underlined.
ppvdEds6rev	GATCCTCCTGTCTGATAGACGA AGCAGGATGCCCGGTTTTTACC GCA	
ppvdEds7for	AGCTTCCGCTAAAAAAAGGGCA TCCTGCTTCGTCTGTCTGCAAG GAG	*ppvdE* fragment, red bases are *porbH* sequence substituted for the WT *ppvdE* ones. *Bam*HI and *Hin*dIII compatible ends underlined.
ppvdEds7rev	GATCCTCCTTGCAGACAGACGA AGCAGGATGCCCTTTTTTTAGC GGA	
pPR9TTfor	AGCTTGATATCCTGCAGAATCC CGGGTAAGTAAGTAAGGAGAAA AAAATGGC	For insertion of Shine-Dalgarno site and ATG start codon for *lacZ* (underlined) into pPR9TT.
pPR9TTrev	GCCATTTTTTTCTCCTTACTTA CTTACCCGGGATTCTGCAGGAT ATCA	

Primers for mutagenesis

cysala3for	TGCCTCGACGCGGCCCATCGCG GCGTC	For SOE mutagenesis. C203A codon substitution underlined.
cysala4for	CGCGGCGTCGCCGCTCCGGTGT TCCTG	For SOE mutagenesis. C209A codon substitution underlined.
cysalaall	CGCCGCGGAAGCCCTCGACGCG GCCCATCGCGGCGTCGCCGCTC CGGTGTTCC	For SOE mutagenesis. C196A, C199A, C203A and C209A Codon substitutions underlined.
orbSstart2-ala	GAGCACTTCCGCGGCGGCCATC GATCTG	For introduction of alanine codon (underlined) at second *orbS* ATG codon.
orbSstart2-stop	GAGCACTTCCGCTTAGGCCATC GATCTG	For introduction of stop codon (underlined) at second *orbS* ATG codon.

orbSstart3-stop	CGGTCGGTCGAGTTATTCCGCC ATGGC	For introduction of stop codon (underlined) at *orbS* GTG codon.
orbSstart3-val	CGGTCGGTCGAGGACTTCCGCC ATGGC	For introduction of non-initiating valine codon (underlined) at *orbS* GTG codon.
orbSstart-stop	TTCCGCCATGGCTTACGATCTG CTCCG	For introduction of stop codon (underlined) at first *orbS* ATG codon. *Nco*I site underlined.

Primers for ribonuclease protection assay

To amplify fragments bearing a T7 RNAP promoter for *in vitro* transcription of RNA probes for RPA.

IVTorbEorbIr	**GGAAATTAATACGACTCACTAT AGGGAG**ATCAAGCTCGGATCGC GGATTCGGTGATGCAGC	T7 RNAP promoter emboldened, *B. cenocepacia* homologous region underlined.
IVTorbEorbIf	GTATCAGACGCTGCAGACATTA TACTGCAACTACACTAAGCCAG CAGCGCAAGGATCAGGC	*B. cenocepacia* homologous region underlined.
IVTorbJorbKf	TGGGCTACAGCAATCACTTGCA TAGCTGCCTGTGGTCTGACACG TTCGC	*B. cenocepacia* homologous region underlined.
IVTorbJorbKr	**GGAAATTAATACGACTCACTAT AGGGAG**CCAAACAGGCCGTCCG CGAAT	T7 RNAP promoter emboldened, *B. cenocepacia* homologous region underlined.
IVTorbIorbJf	CCTTACTTAACCGGATACAGTG ACTTTGACAGGTTTGGACATCT GGCAACGCGTGCT	*B. cenocepacia* homologous region underlined.
IVTorbIorbJr	**GGAAATTAATACGACTCACTAT AGGGAG**GTACCAGCCGAGTTTG TCGATGAAGACCG	T7 RNAP promoter emboldened, *B. cenocepacia* homologous region underlined.

Abbreviations used within this table

MCS, multiple cloning site; ds, double-stranded; TSS, transcriptional start site.

* 'Extreme' base substitutions were as follows: purine bases were substituted for non-complementary pyrimidines and *vice versa*, that is T, C, G and A were substituted for G, A, T and C, respectively. Substituted bases are emboldened and shown in red font.